FUNCTIONAL AND MORPHOLOGICAL STUDIES OF THE PRIMATE OUTFLOW APPARATUS

A thesis submitted to the University of Glasgow for the degree of Doctor of Philosophy in the Faculty of Medicine.

Paul G. McMenamin
Tennent Institute of Ophthalmology
University of Glasgow and Western Infirmary
38 Church Street
Glasgow, G11 6NT

NOVEMBER 1981

CONTENTS

LIST OF TABLES

LIST OF FIGURES

Figure 16a: Diagram to show how serial micrographs were taken along the inner wall of Schlemm's canal.

Figure 16b: Orientation of field for image analysis of 'empty space'.

Figure 17: Diagram of outer meshwork showing seven sites at which intensity of colloidal iron staining was scored.

Figure 18: Diagram of results of flow rates at 18 mm Hg.

Figure 19: Diagram of results of flow rates at 22 mm Hg.

Figure 20: Results of aqueous outflow facility measurements.

Figure 21: Results of total flows.

Figure 22: Light micrograph of normal pig tailed macaque tissue. (x 160)

Figure 23: Scanning electron micrograph of uveal trabeculae and operculum in normal pig tailed macaque tissue. (x 170)

Figure 24: Light micrograph of normal pig tailed macaque outflow apparatus. (x 370)

Figure 25: Scanning electron micrograph of normal pig tailed macaque outflow apparatus (x 1600)

Figure 26: Transmission electron micrograph of normal trabecular meshwork in the pig tailed macaque. (x 1600)

Figure 27: Transmission electron micrograph of normal pig tailed macaque tissue. (x 14500)

Figure 28: Transmission electron micrograph of smooth muscle in Mn 2. (x 3000)

Figure 29: Transmission electron micrograph of smooth muscle in the pig tailed macaque outflow apparatus. (x 4500)

Figure 30: Transmission electron micrograph of smooth muscle as in Fig. 29. (x 10000)

Figure 31: Transmission electron micrograph of nerve bundle in trabecular meshwork. (x 24700)

Figure 32: Transmission electron micrograph of normal pig tailed macaque outflow apparatus. (x 4600)

Figure 33: Transmission electron micrograph of the cribriform layer in normal tissue. (x 5900)

Figure 34: High power transmission electron micrograph of ground substance and 10 nm microfilaments in the cribriform layer. (x 60000)

Figure 35: Transmission electron micrograph of normal pig tailed macaque tissue (colloidal iron converted to Prussion blue). (x 15200)

Figure 36: Transmission electron micrograph of ground substance and cell membranes in normal pig tailed macaque tissue. (x 96000)

Figure 37: Scanning electron micrograph of lining endothelium of Schlemm's canal. (x 3100)

Figure 38: Scanning electron micrograph of cut surface of outflow apparatus. (x 560)

Figure 39: Transmission electron micrograph to show tissue histiocyte in normal pig tailed macaque tissue. (x 7600)

Figure 40: Transmission electron micrograph to show erythrocytes in the cribriform layer and lumen of a 'giant vacuole'. (x 4100)

Figure 41: Light micrograph of control tissue. (x 150)

Figure 42: Scanning electron micrograph of Schlemm's canal and control tissue (Mn 10). (x 280)

Figure 43: Transmission electron micrograph of control pig tailed macaque tissue. (x 1300)

Figure 44: Scanning electron micrograph of outer meshwork in control pig tailed macaque tissue. (x 930)

Figure 45: Transmission electron micrograph of control pig tailed macaque tissue. (x 8800)

Figure 46: Transmission electron micrograph of control pig tailed macaque tissue.

Figure 47: Transmission electron micrograph of colloidal iron stained control tissue. (x 9100)

Figure 48: Scanning electron micrograph of a 'giant vacuole' in control tissue. (x 4300)

Figure 49: Scanning electron micrograph of inner wall lining endothelium of control tissue. (x 3800)

Figure 50: Transmission electron micrograph of cribriform layer and Schlemm's canal in control tissue. (x 1400)

Figure 51: Transmission electron micrograph of a 'blow-out' in control tissue. (x 4500)

Figure 52: Scanning electron micrograph of inner wall of Schlemm's canal in control tissue. (x 1000)

Figure 53: Scanning electron micrograph, side view of 'blow-out' in control tissue. (x 1100)

Figure 54: Transmission electron micrograph showing herniation of inner wall of Schlemm's canal into collector channel opening. (x 1200)

Figure 55: Light micrograph of outflow apparatus in control tissue. (x 340)

Figure 56: Transmission electron micrograph to show plasma cell in control tissue. (x 20000)

Figure 57: Scanning electron micrograph of platelet aggregation in control tissue. (x 2500)

Figure 58: Light micrograph of experimental pig tailed macaque tissue. (x 150)

Figure 59: Light micrograph of experimental pig tailed macaque tissue. (x 150)

Figure 60: Transmission electron micrograph of experimental pig tailed macaque tissue. (x 1300)

Figure 61: Transmission electron micrograph of experimental tissue (colloidal iron). (x 13800)

Figure 62: Light micrograph of outflow apparatus in experimental tissue. (x 340)

Figure 63: Transmission electron micrograph showing a 'blow-out' in Mn 4. (x 1700)

Figure 64: Scanning electron micrograph of experimental tissue. (x 500)

Figure 65: Transmission electron micrograph of experimental tissue. (x 1100)

Figure 66: Transmission electron micrograph of distended area of cribriform layer in experimental tissue. (x 1400)

Figure 67: Transmission electron micrograph to show 'giant vacuoles' in experimental tissue. (x 4700)

Figure 68: Transmission electron micrograph in experimental tissue showing intense staining of ground substance. (x 7600)

Figure 69: Higher power transmission electron micrograph of area A in Fig. 68. (x 117000)

Figure 98: Higher power transmission electron micrograph of tissue in Fig. 97 (264/78) (x 6300)

Figure 99: Transmission electron micrograph of the cribriform layer in a 22 year old human eye. (476/80) (x 8200)

Figure 100: Transmission electron micrograph of trabecular meshwork in a 46 year old human eye. (435/79) (x 1300), (inset x 3000)

Figure 101: Transmission electron micrograph of corneoscleral trabeculae in a 43 year old human eye. (188/78) (x 11000)

Figure 102: Transmission electron micrograph of outer meshwork in a 43 year old human eye. (188/78) (x 4200)

Figure 103: Transmission electron micrograph of the cribriform layer in a 38 year old human eye (76/75) (x 6800)

Figure 104: Transmission electron micrograph of colloidal iron stained human tissue. (232/79 - 45 years) (x 45000)

Figure 105: Light micrograph of outflow apparatus in a 51 year old human eye. (211/80) (x 180)

Figure 106: Transmission electron micrograph of the cribriform layer in a 54 year old human eye. (03/71) (x 9800)

Figure 107: Light micrograph of outflow apparatus in a 72 year old human eye. (408/79) (x 190)

Figure 108: Light micrograph of outflow apparatus in an 83 year old human eye. (19/79) (x 350)

Figure 109: Light micrograph of another region in the same 83 year old human eye. (19/79) (x 350)

Figure 110: Transmission electron micrograph of trabecular meshwork of a 72 year old human eye. (32/75) (x 1700)

Figure 111: Transmission electron micrograph of the trabecular meshwork in a 76 year old human eye. (264/78) (x 1300)

Figure 112: Transmission electron micrograph of an 80 year old human eye. (185/76) (x 1300)

Figure 113: Transmission electron micrograph of the outer meshwork in a 73 year old human eye. (111/78) (x40000)

Figure 114: Transmission electron micrograph of colloidal iron stained tissue from an 83 year old human eye. (19/79) (x 34000)

Figure 115: Histogram of age frequency distribution of the 25 human eyes used in the trabecular thickness study.

Figure 116: Graph showing results of trabecular thickness study.

Figure 117: Histogram of age frequency distribution of the 20 human eyes in the study of vacuolar incidence.

Figure 118: Graph showing results of vacuolar incidence study.

Figure 119: Graph of mean number of 'giant vacuoles' plotted against age.

Figure 120: Graph showing coefficient of variation of total number of vacuoles in each eye plotted against age.

Figure 121: Histogram of age frequency distribution of the 36 human eyes used in the study of the components of the cribriform layer.

Figure 122: Histogram of age frequency distribution of the numbers of prints used in the study of the components of the cribriform layer.

Figure 123: Graph of the results of the percentage area occupied by ground substance component in the 36 human eyes of various ages.

Figure 124: Graph of the results of the percentage area occupied by electron dense plaques plotted against age.

Figure 125: Graph of the percentage area of basement membrane component in the cribriform layer plotted against age.

Figure 126: Graph of the results of the percentage area occupied by the cellular component plotted against age.

Figure 127: Graph of the relationship between the percentage area occupied by ground substance and electron dense plaques in the cribriform layer.

Figure 128: Schematic diagram of the human outflow apparatus in an infant and in old age.

Figure 129: Diagram to summarise the important age-related changes and factors which may contribute to these changes.

ACKNOWLEDGEMENTS

I would like to express my thanks to my supervisor Professor W.R. Lee for allowing me to undertake this project and for his advice, encouragement, patience and criticism over the past three years, which were greatly appreciated.

I am indebted to Professor W.S. Foulds for the privilege of carrying out this research in the Tennent Institute of Ophthalmology and for his kindness in supporting my attendance at conferences.

I would also like to thank my colleagues in the Department and I would like to thank Dr Ian Grierson and Dr John V. Forrester for their intellectual stimulation.

I am very grateful to Mrs Dorothy Aitken and Mrs Sam Cameron for their technical assistance. I am also grateful to Miss Fiona Maitland for typing this thesis with such care.

I would like to express my gratitude to Dr Murray Harper of the Wellcome Surgical Research Unit for generously allowing the use of the facilities during the experimental work. I am indebted to my supervisor Professor W.R. Lee for his surgical assistance and to the animal nurses for the help they kindly provided.

I am also grateful for receiving the Isaac Schlar Scholarship for two years. I am grateful to the MRC for providing the studentship which enabled me to carry out this project. I am also very grateful to the Wellcome

Trust who provided a grant for the experimental work (Grant Number 1.5/7181).

I am particularly grateful to my friends and relatives, especially my mum, for tolerating my long months of apparent inattentive behaviour towards them.

Finally, I would like to express my deep gratitude to my wife, Christine, for tolerating my long absences and for her help and encouragement in preparing this thesis.

Declaration

The work described in this thesis was performed entirely by the author apart from the help acknowledged.

SUMMARY

The present investigation of the primate outflow apparatus comprises of two parts. Part I is concerned with the physiological and morphological effects of hyaluronidase on the outflow apparatus of the pig tailed macaque. Part II is a study of age-related changes in the human outflow apparatus.

The aim of the first part of the investigation was to discover whether glycosaminoglycans in the trabecular meshwork, particularly the cribriform layer, contributed towards the resistance to aqueous outflow through this pathway. Nine pig tailed macaques (Macaca nemestrina) received an intracameral injection of 300 I.U. of testicular hyaluronidase (in 100 µl of Bárány's fluid) in one eye and the fellow eye served as a control, receiving Bárány's fluid alone. One hour after the injections the flow rates at 18 mm Hg and 22 mm Hg from a perfusion system were determined in order to calculate outflow facility. The eyes were perfuse fixed in situ at 18 mm Hg, half an hour after the physiological determinations.

Four eyes, two controls and two experimentals, were excluded from the study due to manipulative failures during the experiment. There was a great deal of variation in the results between animals. Despite this it was found that the flow rates in the hyaluronidase-treated eyes were significantly greater than the controls in three of five pairs at 18 mm Hg and in all five pairs at 22 mm Hg. Due

to the variation between animals the group results did not prove to be statistically significant. There was no gross morphological difference between control and hyaluronidase-treated eyes, with the exception of slightly greater distension and fewer 'giant vacuoles' in the enzyme treated eyes. The outflow apparatus in both groups of eyes showed marked alterations in configuration compared with the normal unperfused tissue. These changes included : rounding up of trabecular endothelial cells; disruption of the cribriform layer; "blow-outs" or focal ballooning of the lining endothelium of Schlemm's canal and herniation of cribriform tissue into collector channel openings. These changes were more severe than would have been predicted on the basis of pressure effects alone and may in fact have been due to physiological manipulation and over perfusion with mock aqueous.

In Part II, a wide age range of human eyes, which had been immerse fixed after enucleation in the treatment of various ocular and orbital disorders of the posterior pole, were morphologically investigated. There was a great deal of variation in the morphological appearance of the outflow tissues not only between eyes of similar ages but also within one eye. Despite the variation, several age-related changes were qualitatively and quantitatively described. These included : the thickening of the trabeculae due to increased deposition of connective tissue elements; the trabeculae in older eyes often appeared denuded of their cell cover which seemed to cause focal degeneration and the

release of connective tissue materials which appeared to accumulate in the outer meshwork; there was an increase with age in the electron dense plaques in the cribriform layer and a decrease in the ground substance; 'giant vacuoles' in the lining endothelium of Schlemm's canal were rare in older eyes (over 50 years); the incidence of localised canal closure due to apposition of the inner and outer walls was greater in older eyes.

The present study of age-related changes in the human outflow apparatus will hopefully contribute to future morphological studies of the outflow apparatus from patients suffering from primary open angle glaucoma.

ABBREVIATIONS

Glycosaminoglycans	GAGs
Transmission electron microscopy	TEM
Scanning electron microscopy	SEM

Key to figures : see back inside cover.

GENERAL INTRODUCTION

THE PRESENT INVESTIGATION

The tissues which comprise the outflow system of the primate eye serve to drain the aqueous humour from the anterior chamber and return it to the venous system. The aqueous humour before reaching the episcleral venous plexus must pass through the outflow tissues comprising the trabecular meshwork, Schlemm's canal, a series of collector channels and aqueous veins.

The present investigation of the outflow apparatus in the primate eye can be divided into two main parts. The first (Part I) concerns the physiological and morphological effects of hyaluronidase on the outflow tissues of the pig-tailed macacque (Macaca nemestrina). The second (Part II) describes the age-related changes in the morphology of the human outflow apparatus.

It is necessary to the understanding of both parts of this thesis that a general introduction be given to the structure and function of the normal primate outflow apparatus. Particular attention will be paid to the pathways of aqueous outflow and the site of resistance to this flow.

THE AQUEOUS HUMOUR

a) Functions

The aqueous humour is a transparent colourless fluid contained mainly within the anterior and posterior chambers

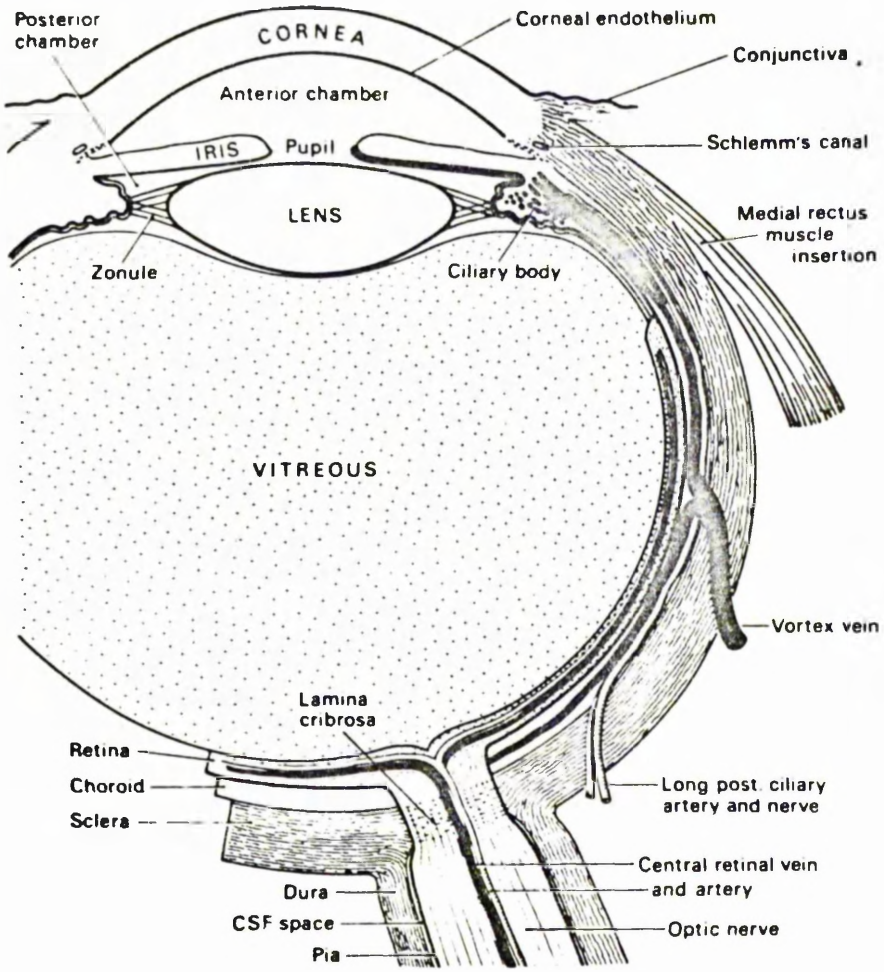

Figure 1: Schematic diagram showing the structural features of the primate eye.

of the vertebrate eye (Fig 1). It is formed continuously in the ciliary processes from where the fluid flows through the posterior chamber, around the pupil and into the anterior chamber (Fig 2). Aqueous humour has two principle functions: firstly it is the medium which provides the necessary nutrients for the metabolic function of the lens and cornea which are avascular, it also removes toxic waste from these tissues and the iris, second, and equally important, the function of the aqueous is hydro-mechanical, ie maintainance of intraocular pressure. The intraocular pressure depends on the balance between the rate of aqueous production and the resistance to outflow, within the intact corneoscleral coat of the eye. Both functions of the aqueous in addition to its optical transparency are of primary importance to the normal functioning of the eye.

b) Composition

The aqueous has a volume of about 250 µl in primates. The most obvious difference between the composition of aqueous humour and blood plasma is in the protein content. In plasma the protein concentration is 6-7 g/100 ml, in human aqueous in man it is only 5-15 mg/100 ml. The sodium and potassium ion content of aqueous are similar to those of plasma, the chloride ion content is lower in the posterior chamber but rises as the fluid passes through the anterior chamber, and is balanced by an excess of bicarbonate ions. Other inorganic constituents include calcium, magnesium, phosphate, sulphate and hydrogen ions. The pH is 0.2 units greater than that of plasma (Kinsey and

Reddy 1964). The organic constituents are numerous, however the most important seems to be the high levels of ascorbic acid and lower levels of glucose. The subject is covered more fully by Kinsey and Reddy (1964).

c) Production

The first step in aqueous production appears to be the formation of a plasma filtrate in the stroma of the ciliary processes, which have a very rich capillary bed. The production of aqueous seems to be by two means. Firstly, active secretion: an active sodium pump is located in the non-pigmented ciliary epithelium. Carbonic anhydrase also seems to be involved in this process of secretion (Maren 1976). Cole's hypothesis (1977) is based on the understanding of the ultrastructure of the blood-aqueous barrier, ie vascular endothelium, its basement membrane, stromal tissue and two layers of epithelial cells with a tight junction in a junctional complex at the apices of the non-pigmented ciliary epithelium (reviewed by Raviola 1977). The intercellular spaces of the non-pigmented cells are thus open to the posterior chamber. The hypothesis states that solutes (chiefly sodium) are pumped into this cleft, making it hypertonic and thus establishing a gradient across which water moves, creating a standing gradient osmotic flow. The water then passes out into the posterior chamber (Cole 1977).

The second means of aqueous production is by ultrafiltration, which unlike the previous process is believed to be dependent on intraocular pressure and rates

of blood flow, and not energy driven. The tight junctions in non-pigmented ciliary epithelium may be 'leaky' allowing some pressure dependent flow of salt and water (Green and Pederson 1972, Pederson and Green 1975). Of the two means of production the active component seems the more important. The subject of aqueous humour formation has been reviewed by Cole (1974, 1977). The subject of amino acid transport across the blood aqueous barrier is reviewed by Reddy (1979).

d) Drainage

It is generally accepted that the bulk of the aqueous leaves the anterior chamber by the structures in the iridocorneal angle (Fig 2). Small but negligible amounts of aqueous are lost through the vitreous body and optic nerve head (Hayreh 1966), the iris stroma and cornea (Svedbergh 1974, Bill 1974). The conventional route of aqueous drainage is by way of the trabecular meshwork, Schlemm's canal, collector channels and into the general circulation via the episcleral and conjunctival veins (Fig 2). Aqueous may also leave the anterior chamber by the 'unconventional' or uveoscleral route (Bill 1965, 1977b), through the meshwork and iris root, then posteriorly between the ciliary muscle fibres into the supraciliary and suprachoroidal spaces. From here it probably leaves the eye through the loose connective tissues around nerves and blood vessels which pass through the sclera (Inomata, Bill and Smelser 1972b, Inomata and Bill 1977, Sherman, Green and Laties 1978). Estimations of the contribution of this

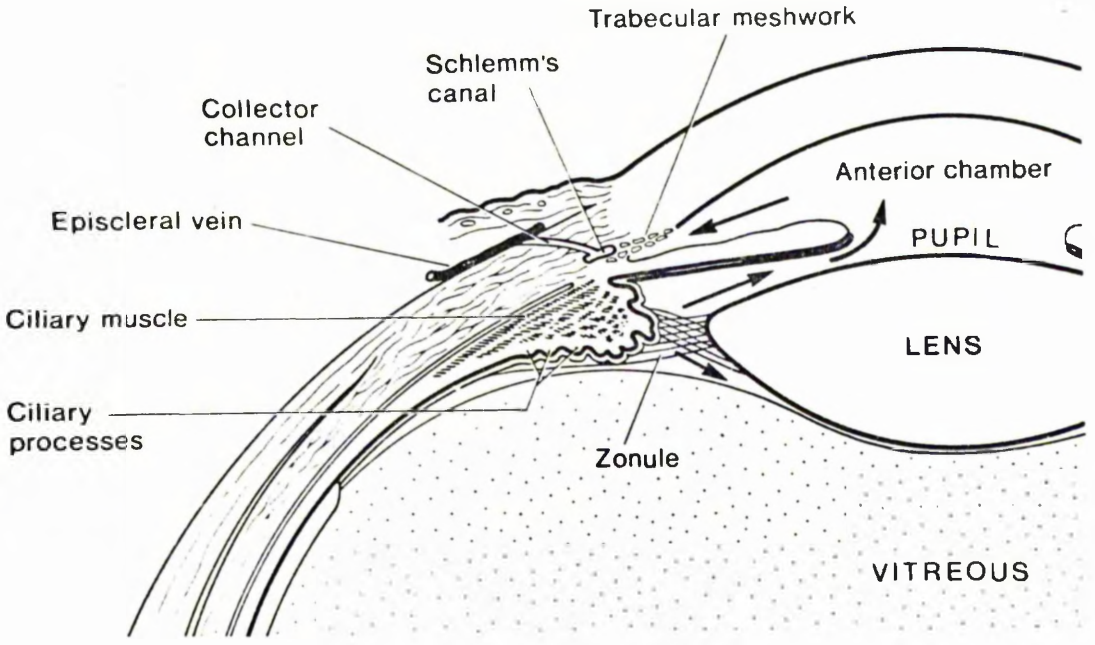

Figure 2: Schematic diagram to show the major route of aqueous movement (arrows) in the anterior segment of the primate eye.

route to the aqueous drainage vary from about 3% in rabbits (Cole and Munro 1976) to 35-55% in monkeys (Bill 1971) and around 5-15% in humans (Bill and Phillips 1971).

e) Aqueous Dynamics

As previously mentioned the intraocular pressure is determined by the balance between the rate of aqueous production and ease of outflow. It can be measured by manometry in the experimental situation by the introduction of a cannula attached to a pressure measuring device. This is obviously not feasible for the human eye and non-invasive tonometric devices which rely on corneal or scleral indentation have been developed to measure intraocular pressure. The two types of tonometers in current clinical use are those developed by Schiotz and Goldmann.

The intraocular pressure in 95.5% of normal human eyes in the first five decades of life lies in the range 10.5-20.5 mm Hg, with a mean of 15-16 mm Hg (Leydecker, Akiyama, Neumann 1958). The pressure has a diurnal fluctuation of 2-5 mm Hg, and is highest in the early morning and lowest at midnight. The intraocular pressure in a free ranging colony of Rhesus monkeys was 14.9 ± 2.1 mm Hg (Bito, Merrit, De Rousseau 1979), which is remarkably similar to humans.

The outflow of aqueous humour, depends on several factors and can be expressed as

$$F = \frac{P_i - P_e}{R}$$

Equation 1.

where F is the flow rate (µl/min), Pi is the intraocular pressure in mm Hg and Pe is the episcleral venous pressure in mm Hg. Assuming that flow follows Poiseuille's Law, R is the resistance within the outflow system.

In the experimental situation, where episcleral venous pressure is rarely known, it is convenient to measure resistance in terms of facility (C), which is the inverse of resistance ($\frac{1}{R}$) and is expressed in units of µl/min/mm Hg.

$$C = \frac{\Delta F}{\Delta P_i}$$

Equation 2.

that is, the change in flow rate for a given rise in pressure. This is a well established method for the determination of facility of aqueous outflow (Bárány 1964). Two variations in technique are employed in the experimental situation.

i) To maintain perfusion or flow at a constant rate and to measure the rise in pressure produced by an increase in the perfusion rate (Sears 1960).

ii) To measure flow into the eye at incremental pressure rises (Becker and Constant 1956a, Bárány 1964).

In humans the outflow facility is measured by the non invasive techniques of tonography (Kolker and Hetherington 1976) and fluophotometry. The former of these techniques have provided most data concerning outflow facility in humans, and estimates have been made by several authors, 0.31 (Becker and Constant 1956b), 0.33-0.23 (Becker 1958, Grant 1963), 0.285 (Kupfer and Ross 1971) and 0.28 (Kolker and Hetherington 1976). The facility seems to be generally higher in sub-human primates, but varies from species to species.

There are several factors which affect intraocular pressure as a result of equation 1.

i) The first of these is episcleral venous pressure. This has been shown to be between 9-11 mm Hg in the normal human eye (Brubaker 1967, Kupfer and Ross 1971). When episcleral venous pressure is increased the intraocular pressure also rises (Macri 1961).

ii) Variations in the rate of blood flow through the capillary bed of the ciliary body affects aqueous production. For example, in experimental situations in which the common carotid artery is ligated there is a drop in intraocular pressure (Bárány 1947) which is probably caused by a decrease in ultrafiltration (Bárány 1947, Bill 1970B, Tokoro 1972, Masuda 1974). Ultrafiltration itself is also sensitive to changes in intraocular pressure. A rise in intraocular pressure causes a decrease in this method of aqueous production, which in the experimental situation occurs when the reservoir is raised to a new

higher level in facility determinations. Consequently the drop in inflow allows more fluid to enter the eye from the perfusion system than may have been expected, giving a falsely high reading for facility, the pseudofacility (Bill and Bárány 1966).

iii) The blood osmolality also effects the intraocular pressure, and is easily demonstrated during the 'water drinking test' (Armaly 1970) which is used to provoke a raised intraocular pressure, and detect glaucoma suspects.

iv) The third part of the equation to have an effect on intraocular pressure is the resistance to aqueous outflow (R). Increased resistance will result in raised intraocular pressure.

Since the relationship between resistance and intraocular pressure is the principal theme of this thesis, the potential sites for resistance within the outflow system will be discussed in more detail later.

THE MORPHOLOGY AND NOMENCLATURE OF THE PRIMATE OUTFLOW APPARATUS

The following description applies in a general way to the primate outflow apparatus. There are considerable variations between species and these have been documented by previous authors (Tripathi 1974, 1977a, Grierson 1976). A more detailed consideration of the pig tailed macaque (Macaca nemestrina) and human outflow systems will be discussed in Part I and Part II respectively. Table 1

Structure	Human	Pig tailed macaque
Iris processes	Rare	Rare
Operculum	Absent	Present
Uveal meshwork	Cord-like trabeculae	Flat broader trabeculae
Scleral spur	Present	Absent
Collagenous septae in Schlemm's canal	Occasional	Frequent
Distinct uveal and corneoscleral meshwork layers	Obvious	Less obvious

Table 1: Table outlining the major differences in anatomy of the human and pig tailed macaque outflow systems.

summarises some of the major differences in these two species.

The limbal region of the eye is the zone of transition between the transparent cornea and the opaque sclera. On the inner surface of the limbus there is a circumferential recess, the scleral sulcus, which accomodates the canal of Schlemm and the outer components of the trabecular meshwork. In man, where the corneal diameter is 11.7 mm horizontally and 10.6 mm vertically, the circumference of Schlemm's canal is about 36 mm.

The trabecular meshwork is a three sided prismatic wedge shaped band of tissue, whose apex unites anteriorly with the corneal lamellae at Schwalbe's line, which is the termination of Descemet's membrane (Fig 3). Posteriorly the broad base of the meshwork is connected in part to the scleral spur, if developed as in the human eye to the anterior limit of the ciliary muscle fibres and to the connective tissue of the iris root (Fig 3). The inner surface of the trabecular tissue is in direct communication with the aqueous humour in the anterior chamber, while the outer aspect forms the inner wall of Schlemm's canal. The trabecular meshwork, as the name implies, consists of flat lamellae or sheets which are separated by fluid filled intertrabecular spaces. These lamellae are incomplete in nature and have large perforations, known as intratrabecular spaces. The labyrinth of inter and intratrabecular spaces, which allows the outward movement of aqueous, becomes more tortuous in the outer part of the meshwork

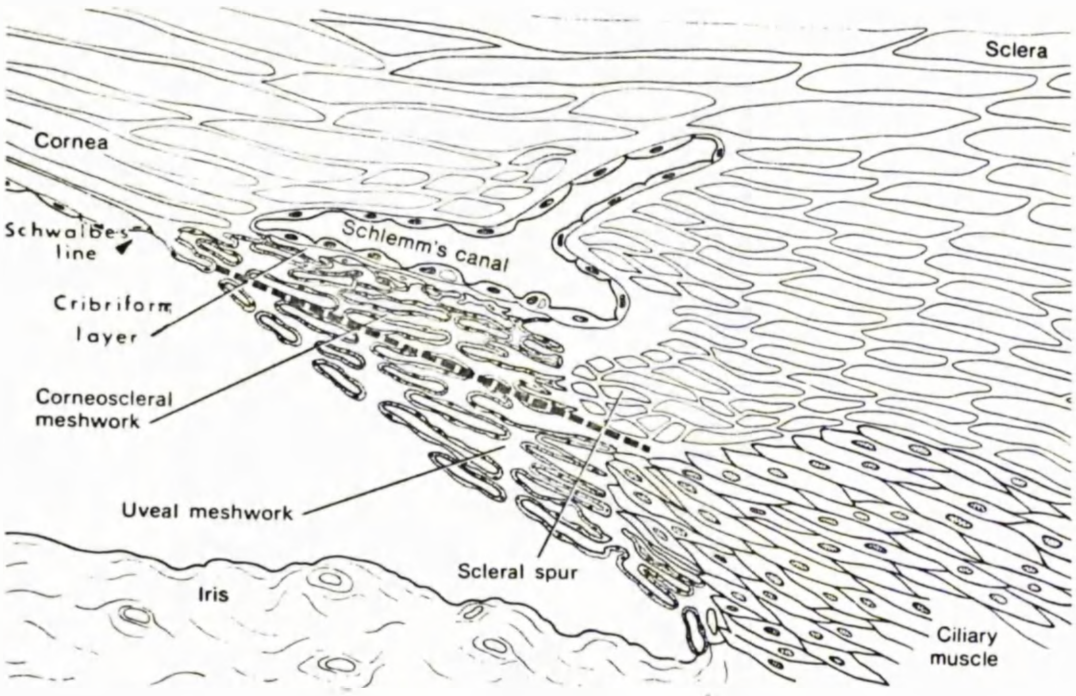

Figure 3: Diagram of the primate outflow apparatus to show the general configuration and terminology of the trabecular meshwork.

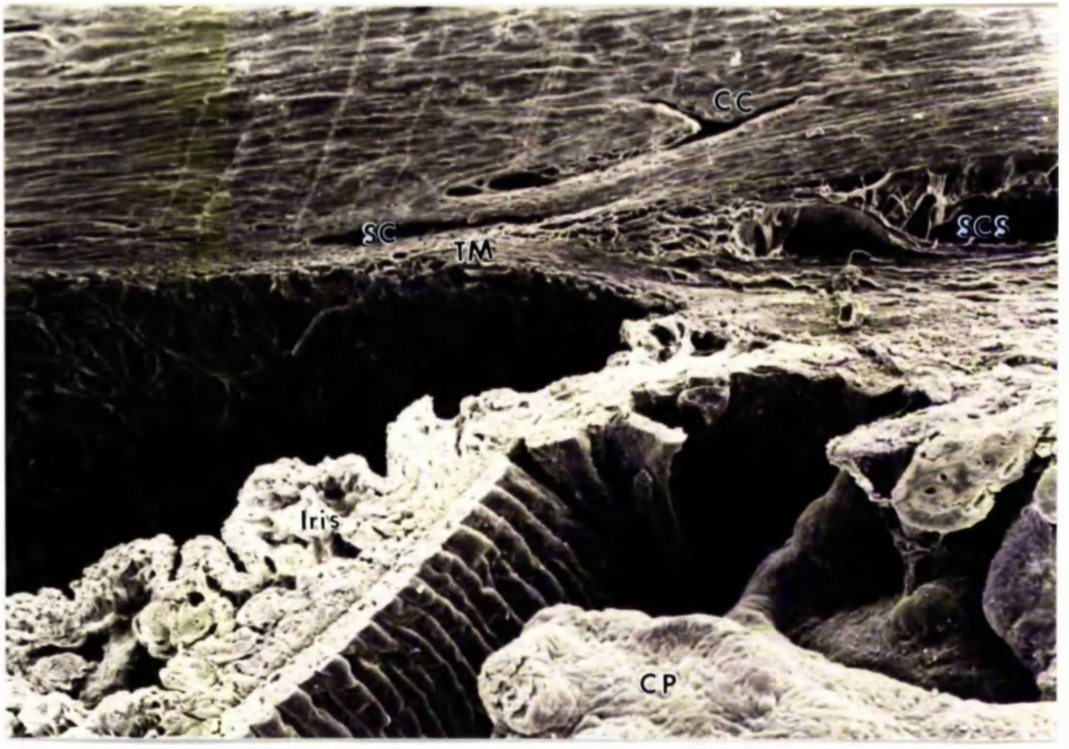

Figure 4: a) Scanning electron micrograph of the cut surface of a meridional slice of limbal tissue from a human eye. Low magnification to show the appearance of the iris, ciliary processes (CP), supraciliary space(SCS), trabecular meshwork, Schlemm's canal and collector channels. (X 110).

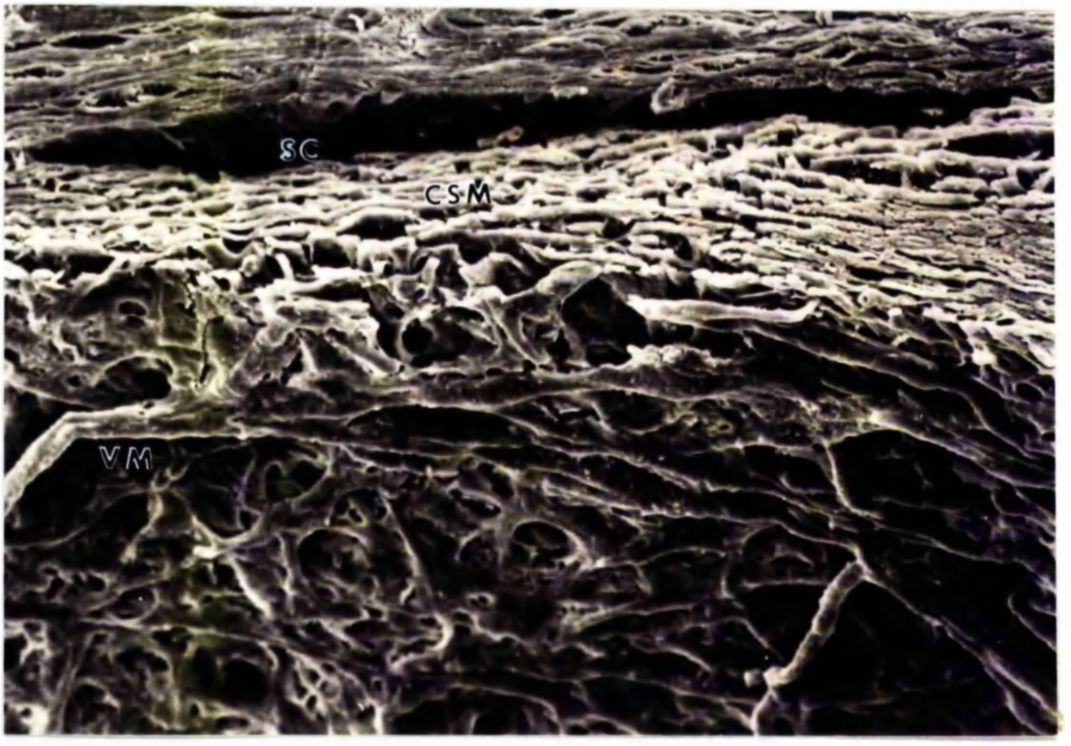

b) Higher magnification of the trabecular meshwork and Sclemm's canal to show in particular the rope-like uveal trabeculae and the sheets of the corneoscleral meshwork. (X 430).

adjacent to Schlemm's canal (Fig 3 and 4a and b).

This general description of the location limits and general shape of the outflow system is similar to previous descriptions (Salzmann 1912, Hogan, Alvorado and Weddell 1971, Rohen and Lütjen-Drecoll 1971, Tripathi 1974, 1977a).

In sections taken in the meridional plane (Fig 5 a and b) the trabecular meshwork appears as a series of short collageneous rods lined by endothelial cells, orientated in the antero-posterior plane (relative to the axis of the eye), fanning out toward the posterior limit. Thus there are some 3-7 layers of trabeculae in the anterior part and 10-25 in the posterior part. The trabecular meshwork can be divided into three main regions, the uveal meshwork, the corneoscleral meshwork and the cribriform layer (Fig 3 and Fig 5). The meshwork is divided into an inner uveal portion and an outer corneoscleral portion by a line drawn from the tip of the scleral spur to the edge of the cornea (Fig 3). This distinction is less obvious in some species of sub-human primates which lack a scleral spur (Table 1).

The thickness of the individual trabeculae varies with age, species and morphometry and has been quoted as being 2-4 μ (Tripathi 1974) and 5 μ (Hogan, Alvorado and Weddell 1971). The ultrastructure of the trabeculae has been debated since Saltzmann (1912) described the four layers by light microscopy. Subsequent workers who mostly agree on the basic organisation, disagree in the interpretation of the morphology and nature of the components (Garron and Feeney 1959, Leeson and Speakman 1961, Spelsberg and

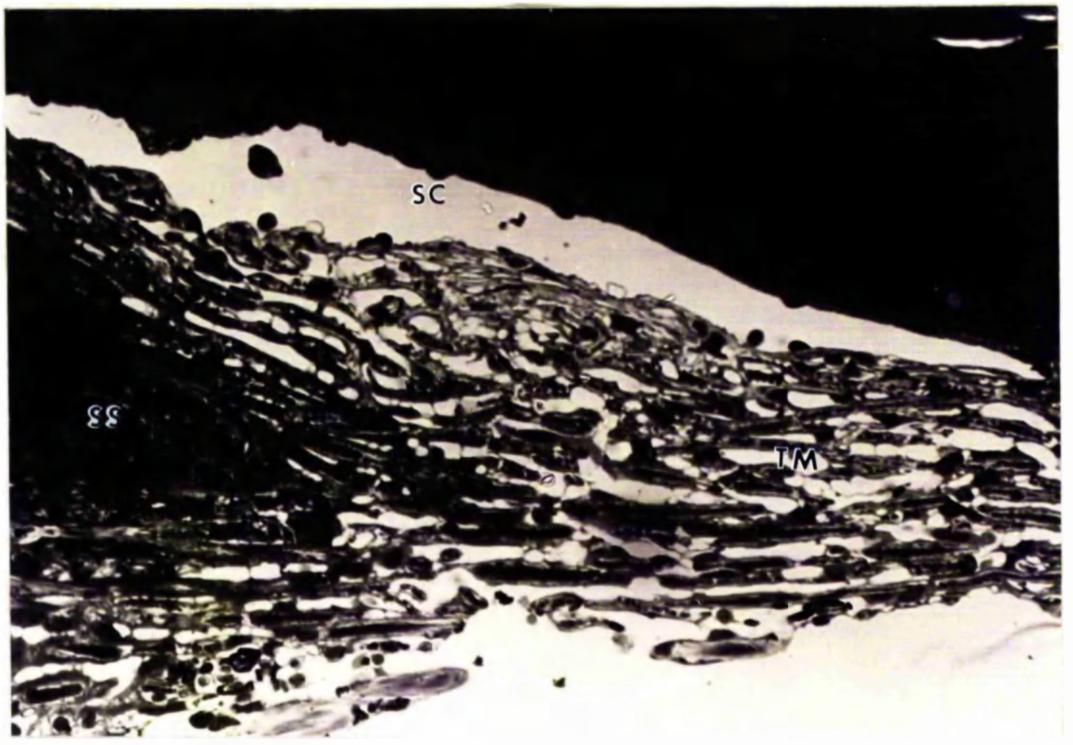

Figure 5: a) Light micrograph of human outflow apparatus to show the appearance of the trabecular meshwork, the scleral spur and the canal of Schlemm. (X 160).

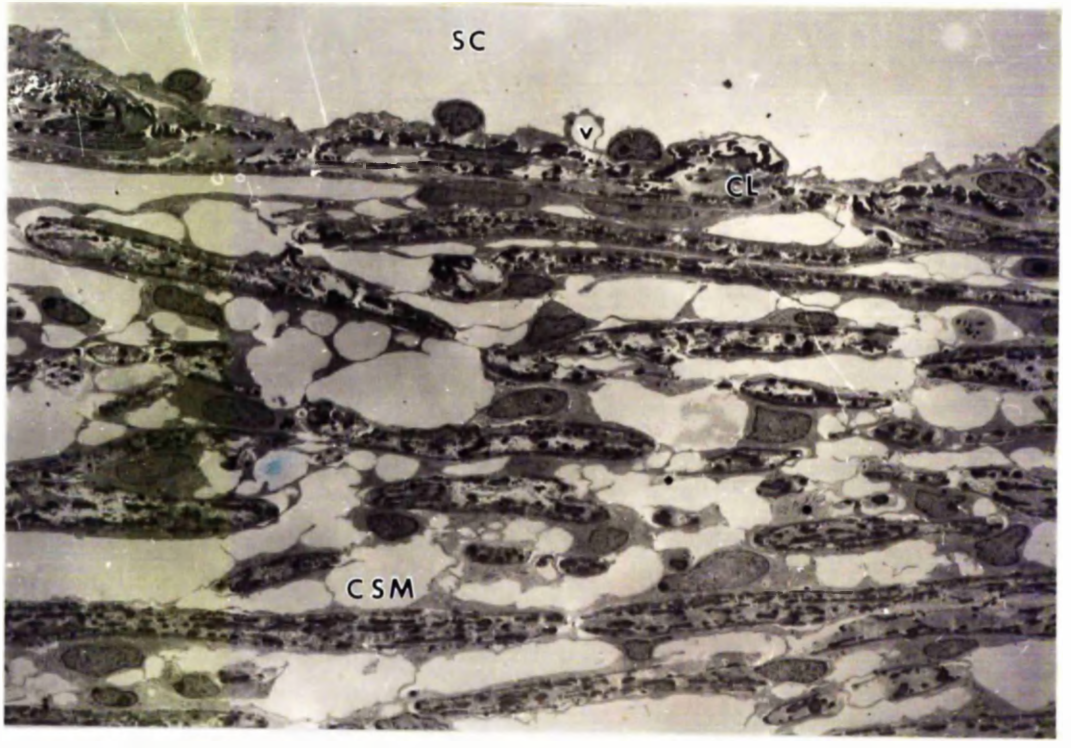

b) Transmission electron micrograph of the trabecular meshwork (human) to show the arrangement of the corneoscleral trabeculae and the cribriform layer. (X 1300).

Chapman 1962, Fine 1964, Iwamoto 1964, Tripathi 1969, 1974, Vegge and Ringvold 1971, Hogan, Alvorado and Weddell 1971, Rohen and Lütjen-Drecoll 1971, Agarwal, Singh, Mishra and Khosla 1972). Each trabeculae can be divided into four layers; central collagenous core, elastic-like fibres, cortical region and endothelial cell cover.

Central collagenous core consists of collagen fibres (64 nm periodicity, 30-50 nm diameter), generally orientated parallel to the long axis of each trabeculae, but may be more random in nature (Fig 6). The core may also contain some 'curly collagen' and elastic-like material (Fig 6).

Elastic-like fibres appear in meridional sections by light microscopy on toluidine blue stained sections as small black dots around a core, and in coronal sections as bands, suggesting they are circumferentially orientated. They are more common in the corneoscleral than the uveal meshwork (Fig 5). By transmission electron microscopy of meridional sections they are seen to have two distinct zones, a core which may be either electron lucent or electron dense depending on several factors such as age and staining techniques (Fig 6) and a sheath which appears granular or fibrillar in nature, and may show some periodicity.

These elastic-like fibres stained as dark purple dots by Weigert's stain, and greenish dots by Giemsa similar to elastic fibres of guinea pig aorta, in a light microscopic study by Iwamoto (1964). The elastic-like fibres are

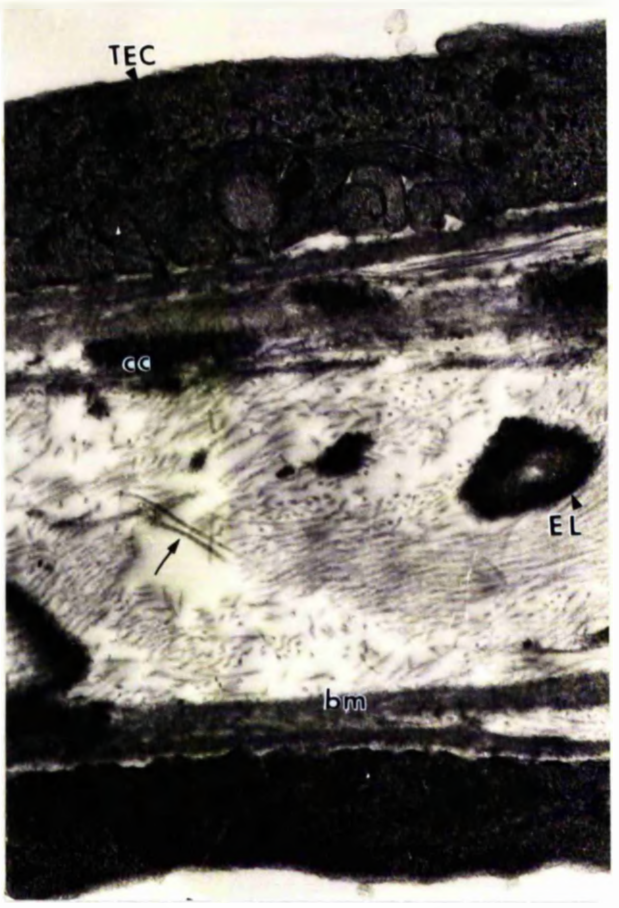

Figure 6: Transmission electron micrograph to show the ultrastructural organisation of the connective tissue elements (collagen (arrow), elastic-like fibres, curly collagen and basement membrane) of the trabeculae and the covering endothe lial cells. Pig tailed macaque tissue. (X 6300).

embedded in randomly orientated collagen fibres and an amorphous ground substance.

Cortical region is composed of a basement membrane or 'glass membrane' which has a variable thickness, and may appear granular or fibrillar but is more usually amorphous. Embedded in this material, or in close association with it, are the clumps of wide banded collagen or 'curly collagen', with its distinctive 100 nm periodicity (Fig 6).

Endothelial cell cover is the final layer of the trabeculae, and in most areas it completely surrounds the connective tissue core. The cells rest on the basement membrane region and have a series of surface specialisations which are presumably important in adhesion of the cell to the trabeculae. The first of these are the numerous hemidesmosome-like cytoplasmic condensations, which occur along the undulating cell margin (Fig 6 and Fig 7). The second form of specialisation are the small cytoplasmic pegs (Fig 7) and lastly there are more rarely invaginations in the cell cytoplasm (Fig7).

Neighbouring cells are attached by macula adhaerentes and gap junctions (Grierson and Lee 1974a). Extensions of the cells cross the intertrabecular spaces, and also form a fine incomplete 'membrane' over the intratrabecular spaces, which effectively reduces the diameter of the aperture (Fig 7).

The trabecular endothelial cells have a large ovoid nucleus, and the cytoplasm is richly endowed with organelles, the more frequent of which are golgi apparatus,

rough endoplasmic reticulum, free ribosomes and microfilaments. The mitochondria are usually small and dense. Other organelles include smooth endoplasmic reticulum, primary lysosomes, lysosomal complexes, lipid vesicles, melanin granules, glycogen and occasionally cilia and centrioles. The organelles seem to suggest the cell is active in carbohydrate and protein synthesis.

The microfilaments in these cells have been identified as two types, the small diameter actin-like filaments (5-7 nm) and the larger intermediate or tonofilaments (10 nm diameter). Gipson and Anderson (1979) using anti actin histochemical markers noted plaques of staining product in the endothelial cells, which appeared to be associated with cell to cell and cell to trabeculae adhesion. The larger intermediate filaments although maybe having some contractile properties are thought to be mainly cytoskeletal in function. Several authors have speculated as to the function of the microfilaments in trabecular tissues (Spelsberg and Chapman 1962, Vegge 1963, Holmberg 1965, Inomata, Bill and Smelser 1972a, Tripathi 1974, Ringvold 1978, Grierson and Rahi 1979, Gipson and Anderson 1979). The organisation of the trabeculae is summarised diagramatically in Fig 7. The third region of the trabecular meshwork, the cribriform layer, has in the past received a lot of attention and consequently there has been some confusion as to nomenclature. It has been called "cell rich tissue" (Saltzmann 1912), "cotton-wool tissue" (Wolff 1954), "pore-tissue" (Flocks 1956), "trabeculum

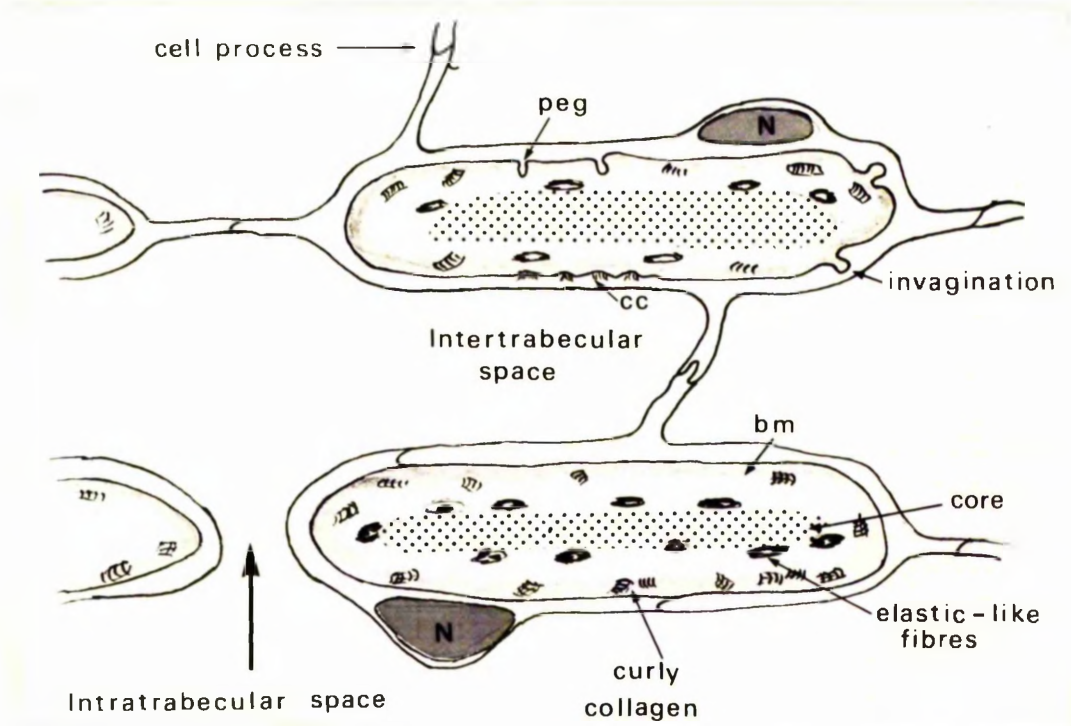

Figure 7: Schematic diagram to summarise the arrangement of the trabeculae and the cell to trabeculae specialisations. Note also the inter and intratrabecular spaces. (cc - cytoplasmic condensations)

cribriforme" (Rohen and Lütjen Drecoll 1971), "filtration tissue" (Garron 1959), "juxtacanalicular connective tissue" (Fine 1964), "trabecular wall of Schlemm's canal" (Tripathi 1969) and finally the "endothelial meshwork" (Speakman 1960).

The nomenclature which is used in this thesis, cribriform layer has been arrived at after much debate with other workers in this field. The most accepted term 'endothelial meshwork' led to confusion, since one often has to refer to "endothelial lining of the endothelial meshwork" or "endothelial cells in the endothelial meshwork". "Juxtacanalicular" is not an ideal term since it does not exclude the outer wall of the canal.

The anatomical boundaries of the "trabeculum cribriforme" described by Rohen and Lütjen-Drecoll (1971) were applied in the present investigation, ie the lining endothelium of Schlemm's canal on the outer aspect and the first distinct intertrabecular space of the corneoscleral meshwork on the inner aspect. This area lacks the trabecular organisation and consists of several layers of flat fibroblast-like cells, which lie in sheets parallel to the lining endothelium of Schlemm's canal, embedded in extracellular components. The endothelial cells in this tissue are similar in appearance to those covering the trabeculae, but they have many long cytoplasmic extensions which are attached to neighbouring cells forming a net-like arrangement (hence the term cribriform). These cells also have associations with both the lining endothelium of

Schlemm's canal and the trabecular endothelial cells of the corneoscleral meshwork. The microfilaments in the endothelial cells of the cribriform layer are more evenly distributed throughout the cytoplasm than in trabecular endothelial cells (Gipson and Anderson 1979, Grierson and Rahi 1979).

The extracellular matrix of the cribriform layer contains the following: loose collagen fibrils; 'curly collagen'; elastic-like material, electron dense plaques and fine granular ground substance. The ground substance is particularly apparent just beneath the lining endothelium of the canal (Fig 8). Glycosaminoglycans, probably both free (hyaluronate) and in proteoglycan complexes, are a major component of this tissue (vide infra).

The lining endothelium of the inner wall of Schlemm's canal is characterised by the presence of 'giant vacuoles' (Fig 8). These are not vacuoles in the strict scientific sense, namely intracytoplasmic, since when examined by serial sections they are found to communicate with the underlying cribriform layer. Less frequently the vacuoles are found to have an opening or pore on the canal aspect, thus a small percentage function as through and through transcellular channels. They are membrane bound ovoid structures which mostly appear to be 'empty' (Fig 8), but occasionally fragments of cellular and extracellular debris are found within the cavity. A more detailed description of 'giant vacuoles' will be given later when describing

Figure 8: Transmission electron micrograph to show the cribriform layer and a 'giant vacuole' in the lining endothelium of Schlemm's canal. Pig tailed macaque tissue (Mn 1) (X 3800).

their quantification.

The cells of the lining endothelium form an uninterrupted monolayer in the normal outflow apparatus. The individual cells of the monolayer are elongate spindle shaped cells with their long axis orientated circumferentially. The nuclei are prominent ovoid structure which, like the 'giant vacuoles', bulge into the canal lumen. By scanning electron microscopy the lining endothelium is seen to contain openings of 1-2 μm in diameter and these are located on the swellings or bulges and also in flat regions of the cells. Such openings are referred to as vacuolar and non-vacuolar pores, and were first described by Bill (1970) and subsequently by many other workers.

Schlemm's canal is an elliptical shaped vessel lined by endothelium. The relative dimensions of the canal depends to some extent on species. The canal is drained by a series of collector channels which are distributed evenly around the circumference, and number about 25-35 in the human eye (Ashton 1951, Hogan, Alvorado and Weddell 1971). Some pass directly to the surface of the sclera as aqueous veins (Asher 1942), others join the deep scleral plexus to merge ultimately with the episcleral and conjunctival venules. These collector channels are relatively large, 20-90 μm in diameter (Rohen 1969, Bill and Svedbergh 1972, Tripathi 1974).

THE TRABECULAR MESHWORK AS A FILTER

The trabecular meshwork functions very effectively as a self-cleansing filter. Any material such as debris from the iris stroma which is carried with the aqueous into the meshwork is either extruded into the canal (via 'giant vacuoles') or else is dealt with by phagocytosis either by active tissue histiocytes or by the native trabecular endothelial cells. Whether the monocytic macrophage-like histiocytes stay in the meshwork for any length of time is unknown, but they do appear to play an important role in the meshwork. The trabecular endothelial cells appear to be capable, given the proper stimulus, of detaching from the trabeculae to take up a more active phagocytic role. Examples of this have been shown in experimental stituations (Rohen and van der Zypen 1968, Lee 1971) in pseudoexfoliation (Ringvold and Vegge 1971), and in traumatic hyphaema (Grierson and Lee 1973).

CURRENT CONCEPTS ON THE ROUTE OF AQUEOUS OUTFLOW

It is generally accepted by morphologists and physiologists that the bulk of aqueous drainage is by the conventional route of the trabecular meshwork and Schlemm's canal. The actual mechanism by which aqueous passes through the lining endothelium has been the topic of research and discussion for more than fifty years. The detailed history of the debate is beyond the scope of this presentation and has been reviewed comprehensively by

Holmberg (1965) and Tripathi (1974, 1977a). The concept which has emerged over the last 15 years is that the 'giant vacuoles' are responsible for bulk movement of aqueous humour into the lumen of Schlemm's canal. In serial sections of these structures, the majority have been shown to have a meshwork pore, a few have a lumen pore and a few will possess both thus acting as transcellular channels, allowing the passage of aqueous across the pressure differential (Holmberg 1959, 1965, Grierson and Lee 1975a, 1975b, 1978, Tripathi 1968, 1969, 1971, 1974, 1977a, Kayes 1967, Inomato, Bill and Smelser 1972a). Scanning electron microscopical studies have confirmed the presence of lumen pores (Bill 1970a, Lee 1971, Bill and Svedbergh 1972, Segawa 1973). Non-vacuolar pores have also been seen in ultrastructural (Segawa 1973, Bill and Svedbergh 1972, Fink, Felix and Fletcher 1972) and topographical investigations (Segawa 1973, Bill and Svedbergh 1972).

Tracers introduced into the anterior chamber very quickly find their way into the 'giant vacuoles' (Feeney and Wissig 1966, Rohen and van der Zypen 1968, Bill 1970, Lee 1971, Inomata, Bill and Smelser 1972a). Tripathi introduced the hypothesis of the 'vacuolation cycle' to explain the mechanism of aqueous transfer by the vacuoles (Tripathi 1971). He proposed that a vacuole formed initially as an invagination on the trabecular aspect of the lining endothelial cell which enlarged to form a blind outpouching. A pore on the lumen aspect was formed probably at a weak point in the cytoplasm, such as a

fenestration or minipore, thus creating the transcellular channel. Since only a small percentage of vacuoles were transcellular channels (approximately 2%) it was proposed that this was a cyclical event, with each vacuole having a short life-span. It has been pointed out by Grierson and Lee (1978) that not all invaginations need ever become transcellular channels, and that once formed a channel may stay functional as long as is necessary.

Some authors have disputed the existence of 'giant vacuoles' and have argued that they are autolytic or post-mortem artefacts (Ashton 1960, Shabo, Reese and Gaasterland 1973), while others have found higher incidence in eyes in which fixation was delayed (Fine 1966, Segawa 1971, Grierson and Johns on 1981). However, it has been clearly shown that post-mortem vacuoles are morphologically distinct from true 'giant vacuoles', which do not increase in incidence post-mortem (Grierson and Johns one 1981).

Several studies have shown that 'giant vacuoles' increase in number and size with incremental increase in intraocular pressure (Johnstone and Grant 1973, Grierson and Lee 1975a, 1975b, 1977a, 1978, Kayes 1975) as do the numbers of vacuolar and non-vacuolar pores (Lee and Grierson 1975, Grierson and Lee 1978). No vacuoles or pores are found when the intraocular pressure is maintained at 0 mm Hg for one hour, which is in conflict with the suggestion that they are autolytic in nature. The linear increase in 'giant vacuole' incidence and intraocular pressure is true within the physiological range of 8-30 mm

Hg, at 50 mm Hg there are fewer than at 22 or 30 mm Hg probably due to occlusion of Schlemm's canal by the distended outer meshwork (Grierson and Lee 1975a).

The relationship between physiologically measured flow rates and vacuolar incidence has not been investigated as thoroughly as that of vacuoles and pressure, although a general agreement was found by Grierson, Lee and Abraham (1979b) in a study of the physiological and morphological effects of pilocarpine on control and pilocarpine treated baboon eyes.

The trabecular tissues demonstrate remarkable pliability in response to altered intraocular pressure, particularly in the outer or cribriform layer. In the hypotensive situation (Fig 9a) the cells of the cribriform layer lie parallel to the lining endothelium, in the horizontal plane, with most of the intercellular spaces being occupied by extracellular materials with very little 'empty space' for the passage of aqueous. There are few bulges (due to nuclei and vacuoles) in the flat lining endothelium. In the hypertensive situation (Fig 9b) the tissue becomes distended with a greatly increased amount of free space for fluid passage (Grierson and Lee 1974b, 1975, Johnstone and Grant 1973, Kayes 1975, Svedbergh 1976). The endothelial cells of the cribriform layer take on a more perpendicular arrangement and bulges due to both nuclei and 'giant vacuoles' are more noticeable in the lining endothelium. Cell to cell contact was maintained within the range of 8-30 mmHg after one hour of maintained

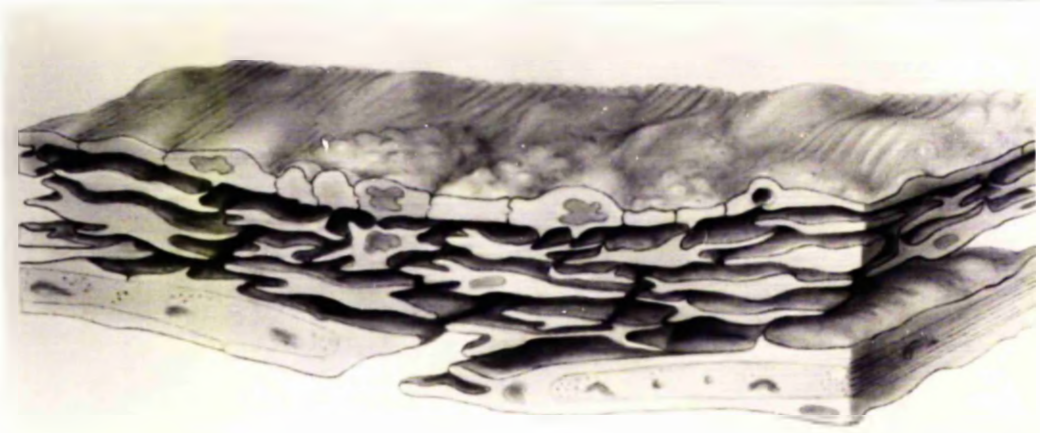

HYPOTENSIVE OUTFLOW APPARATUS

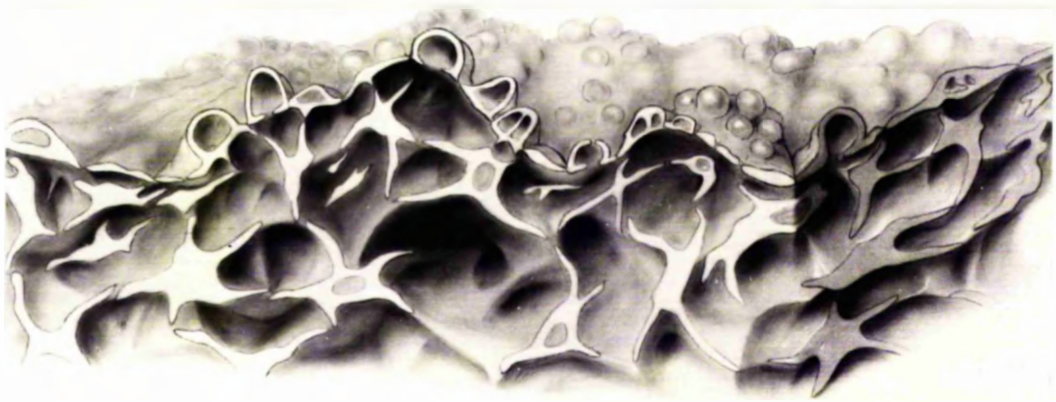

HYPERTENSIVE OUTFLOW APPARATUS

Figure 9: a) and b) Schematic diagrams to show the differences in configuration between the a) hypotensive and b) hypertensive primate outflow apparatus.

intraocular pressure in rhesus monkeys (Grierson and Lee 1974b, 1975a) and in human eyes fixed almost immediately after enucleation due to malignant melanoma (Johnstone and Grant 1973). The attachments of the lining endothelium to the underlying cellular and extracellular elements of the cribriform layer may function as an anchorage and be necessary for vacuolation (Johnstone 1979). In the absence of a true basement membrane, cytoplasmic microfilaments and cell to cell junctions may play a very important role in maintaining tissue integrity and elasticity (Grierson and Lee 1975a, Grierson, Lee and McMenamin 1981). Others have suggested that elastic elements in the tissue may also be important (Inomata, Bill and Smelser 1972a).

This change in configuration of the trabecular tissues at high intraocular pressures is also characterised by the loss of extracellular elements, which are assumed to be 'washed out' through transcellular channels (Grierson and Lee 1975a, 1977b, Kayes 1975).

Grierson and Lee (1975a) could find no increase in organelles associated with energy production or protein synthesis in eyes maintained at higher pressures. Metabolic inhibitors (Bárány 1953) and changes in temperature (van Buskirk and Grant 1974) do not effect outflow facility. This evidence would suggest that the change in configuration of the tissue is not energy dependent but merely a passive response to an increased pressure gradient.

The disappearance of transcellular channels in the

hypotensive state is very important to the value-like function of the meshwork, thus preventing blood from refluxing into the anterior chamber (Johnstone and Grant 1973, Grierson and Lee 1974b, Kayes 1975). Some workers found that plasma and red blood cells did reflux into the anterior chamber (Bartels, Pederson, Gaasterland and Armaly 1979) in monkey eyes in which the eye was depressurised in 5 seconds, which may be too rapid for any existing transcellular channels to close.

In monkey eyes maintained at high intraocular pressures (> 30 mm Hg), Schlemm's canal may become occluded, the inner wall in some areas herniates into the openings of collector channels and disruptions of the lining endothelium also occur (Grierson and Lee 1975a, Svedbergh 1976).

Other routes of aqueous movement into Schlemm's canal have been proposed, but few have the supportive evidence of 'giant vacuoles'.

Sonderman's canals (internal collector channels)

These channels have been suggested as providing a route between the trabecular meshwork and Schlemm's canal (Sonderman 1933, Ashton, Brini and Smith 1956, Iwamoto 1967, Hogan, Alvorado and Weddell 1971). Although diverticulae of Schlemm's canal have been seen by other authors, on serial sectioning they have been endothelial lined blind outpouchings, which are not in free communication with the trabecular meshwork (Holmberg 1965, Kayes 1967, Tripathi 1974a). It has been stressed that

Sonderman's canals would be too large to obey the laws of aqueous dynamics (Hamberg 1965).

Micropinocytosis

The evidence against this being an important mechanism of aqueous movement as suggested by some workers (Fine 1964, Feeney and Wissig 1966, Rohen 1969) are that they not only decrease with raised intraocular pressure (Grierson and Lee 1975a, 1975b) but they would also be energy dependent, which does not seem to be true for aqueous outflow (vide supra).

Intercellular drainage

Fluid movement between the lining endothelial cells has also been proposed as a mechanism of aqueous movement into the canal (Feeney and Wissig 1966, Fine 1966, Rohen 1969, Shabo, Reese and Gaasterland 1973). The intercellular junctions of the monolayer appear to be zonulae occludentes, ie continuous bands of membrane fusion (Feeney and Wissig 1966, Tripathi 1968, Hogan, Alvorado and Weddell 1971, Inomata, Bill and Smelser 1972a, Grierson and Lee 1975a), but definitive proof is still lacking, and in fact others have claimed that the junctions were indeed focal (Shabo, Reese and Gaasterland 1973). The lack of penetration of particulate tracers through the intercellular clefts; the theoretical calculations of Bill (1975); and the fact that the cells do not separate when overperfused, all seem to suggest that intercellular clefts do not serve as a major route in the transfer of aqueous into Schlemm's canal.

THE LOCUS OF RESISTANCE TO AQUEOUS OUTFLOW

On the accumulated evidence of both morphologists and physiologists it seems that the bulk of the resistance to aqueous outflow lies in the trabecular meshwork. In vitro studies on enucleated human eyes (Grant 1958, Ellingsen and Grant 1971a) suggested that the trabecular tissues accounted for 75% of the total resistance, while similar studies in enucleated rhesus monkey eyes provided estimates of 83-97% (Ellingsen and Grant 1971b) and 68% (Peterson and Jocson 1974).

It has been suggested that the main resistance to outflow may lie between Schlemm's canal and the episcleral venous system (Perkins 1955, Sears 1966). It may certainly be the case that increased resistance at higher intraocular pressures may be explained on the basis of closure of Schlemm's canal (reviewed by Moses 1977). If the main site of resistance in the normal primate eye did lie external to the trabecular meshwork it would be very difficult to reconcile the changes in morphological configuration within the trabecular meshwork with altered intraocular pressures or after treatment with drugs which are known to increase aqueous outflow (pilocarpine). The changes include quantitative increases in 'giant vacuoles' and transcellular channels. It seems difficult to ignore therefore that resistance is localised in the trabecular meshwork, the next question which arises is where exactly is the

resistance situated?

Many morphologists find it difficult to accept that the large inter and intratrabecular spaces could account for a significant proportion of the resistance to aqueous outflow (Tripathi 1974, Svedbergh 1976, Watson and Grierson 1981, Grierson, Lee and McMenamin 1981). It seems more likely that the cribriform layer with its narrow and tortuous free spaces and abundant extracellular materials or the uninterrupted monolayer of the lining endothelium of Schlemm's canal could be the major source of resistance to aqueous movement. Tripathi (1968) suggested that the resistance lay in the lumen pores of the 'giant vacuoles' and later Cole and Tripathi (1971) calculated on theoretical grounds and on recent ultrastructural evidence, that only 2% of vacuoles had lumen pores, that the pores could explain the pressure dependency of aqueous outflow.

Other authors have more recently re-examined the morphological evidence and with the use of mathematical models derived from the dimensions and shape of the 'giant vacuoles' and pores have concluded that these structures could not account for more than a small proportion (5-10%) of the total resistance to aqueous outflow (Bill and Svedbergh 1972, Grierson, Lee, Moseley and Abraham 1979, Eriksson and Svedbergh 1980). These studies led the authors to conclude that the main site of resistance was localised in the cribriform layer. This is supported by the following evidence, some of which is derived from experimental work and some from pathological situations in

the human eye:

i) When particulate material is introduced into the anterior chamber, the particles tend to accumulate in the cribriform layer (Inomata, Bill and Smelser 1972a). Although this fact in itself reveals little about the nature of aqueous movement, it does show that larger particles are impeded in their progress by this layer of tissue.

ii) Underperfusion

In eyes which have undergone trabeculectomy drainage procedures and the remainder of the trabecular meshwork is by-passed and thus underperfused (Lütjen-Drecoll and Bárány 1974). In this situation there is abundant extracellular materials and little free or 'empty space' in the cribriform layer.

iii) Overperfusion

This may be due to the action of drugs such as pilocarpine (Grierson, Lee and Abraham 1978) or else as a result of raised intraocular pressure (Johnstone and Grant 1973, Grierson and Lee 1974b, 1975a, Kayes 1975). Overperfusion is characterised by distension of the outer meshwork, 'wash-out' of extracellular elements and increased vacuolar incidence, which all suggest a decrease in resistance. Other agents known to have a physiological resistance lowering effects have also been shown to change the configuration of the outer meshwork, for example, cytochalasin B (Svedbergh, Lütjen-Drecoll, Ober and Kaufman 1978, Johnstone, Tanner, Chau and Kopecky 1980) and Na_2

EDTA (Bill, Lütjen-Drecoll and Svedbergh 1980).

iv) Glycosaminoglycans

These substances are an important component of the cribriform layer and may play a role in altering resistance to aqueous outflow (see introduction to Part I of this thesis for full consideration of this topic).

v) Morphological studies of primary open angle glaucoma have shown an accumulation of extracellular elements in the drainage wall (Rohen and Witmer 1972, Rodrigues, Spaeth, Silalingam and Weinreb 1976, Segawa 1975, 1979). It has been suggested that these may be the primary cause of increased resistance in this disease.

vi) Aggregations of fibrillar material in the cribriform region have been observed in corticosteroid glaucoma (Rohen, Limmer and Witmer 1973, Grierson, Lee and McMenamin 1981).

PRIMARY OPEN ANGLE GLAUCOMA

Primary open angle glaucoma (chronic simple glaucoma) is a disease which is characterised by raised levels of intraocular pressure which are sufficient to cause damage to the optic nerve and nerve fibre layer of the retina, producing field loss (Kolker and Hetherington 1976). This disease occurs predominantly in older individuals and is the commonest of all of the glaucomas. The disease occurs in approximately 2% of the population over 40 years of age.

The cause of the raised intraocular pressure is

abnormally high resistance in the aqueous outflow pathways. It is only by studying aqueous dynamics and the functional morphology of the primate outflow apparatus, particularly those factors which affect resistance, that advances will be made in the understanding of the aetiology and pathogenesis of primary open angle glaucoma.

THE AIMS AND APPROACH TO THE CURRENT INVESTIGATION

This thesis consists of two main parts. Part I is the study of the physiological and morphological effects of hyaluronidase on the outflow apparatus of the pig tailed macaque. Part II is a morphological study of aging changes in the human eye.

Although both Parts I and II have their own main introductory and discussion chapters (see contents) and could be read separately, it is hoped that this main introductory chapter will help in the understanding of both Parts I and II.

The overall aim of this thesis is to improve the understanding of the function and morphology of the primate outflow apparatus, with particular reference to factors which may play a role in resistance to aqueous outflow. To this end the approach has been multifaceted, with the emphasis on the quantitation of the morphological appearance of the outflow system as seen by light microscopy, scanning and transmission elecron microscopy.

A more detailed guide to the aims and approach to each

of the two parts will be given in their respective introductory chapters (see contents).

PART I

THE PHYSIOLOGICAL AND MORPHOLOGICAL EFFECTS OF HYALURONIDASE ON THE OUTFLOW APPARATUS IN THE EYE OF THE PIG TAILED MACAQUE (*Macaca nemestrina*)

INTRODUCTION TO PART I

THE PRESENCE OF GLYCOSAMINOGLYCANS IN THE TRABECULAR MESHWORK

An important component of the extracellular matrix in vertebrate connective tissues are the polysaccharides formaly called mucopolysaccharides but now generally referred to as glycosaminoglycans (GAGs). With the exception of hyaluronate, they do not normally occur as free polymers in vivo but as proteoglycans in which many glycosaminoglycan chains are linked to a protein core. Glycosaminoglycans are linear polymers of repeating disaccharide units which consist of hexosamine and hexuronic acid (except keratan sulphate which contains glucosamine and galactose). The molecules rarely contain only a single type of disaccharide unit. The dominant type of disaccharide unit for the more important GAGs of extracellular matrices are shown in Fig 10a. The GAGs are characterised by their charged anionic groups : the carboxylate group ($-COO^-$) the sulphate ester group ($-O-SO_3-$) and the sulphamino group ($-N-SO_3^-$).

Proteoglycans consist of a protein core (molecular weight 2×10^5) to which chondroitin sulphate chains (mol wt $4-8 \times 10^3$) are attached in clusters of about 4 chains (Fig 10b). There may be up to 20-30 clusters on the protein core. Keratan sulphate may also be bound to this core. The protein core possesses a globular region at its end by which it may bind to the large hyaluronate molecules

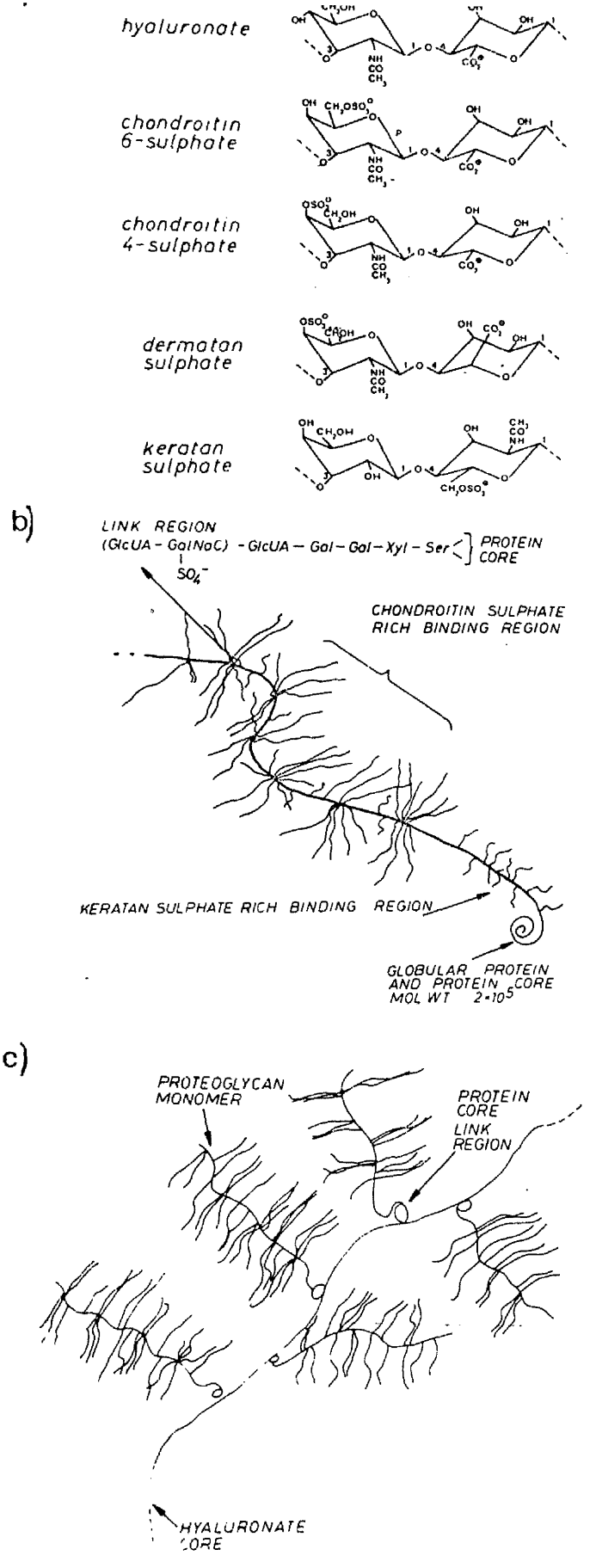

Figure 10: a) Diagrams of the disaccharide units in the major extracellular GAGS.

b) Diagram of a cartilage proteoglycan unit showing the the relationship between the protein core and GAGs.

c) A hyaluronate core with attached proteoglycan monomers. Diagrams from Couper and Laurent (1978).

(Fig 10c) forming large aggregates (mol wt 50 x 10^5). Most knowledge of proteoglycans is based on cartilage proteoglycans. They can also interact with other proteins for example collagen, in which case 2-4 proteoglycans link to each collagen molecule. Proteoglycans are synthesised intracellularly and secreted into the extracellular matrix.

Water may be bound by hydrogen bonds and polar bonds to the hydroxyl groups and charged groups on the polysaccharide chains (1-2.5 water molecules per disaccharide unit depending on which GAGs are present -Fig 10a). The highly entangled gel-like nature of the polysaccharides tend to retain water by osmotic forces and resist water movement through areas where they occur (Ogson 1970, Comper and Laurent 1978). They have many roles in connective tissues, affecting the movement of electrolytes, their viscoelastic properties are important to their functioning as a lubricant in synovial fluid and as a shock absorber in intervertebral discs.

Hyaluronate was first isolated from the vitreous humour of the eye by Meyer and Palmer (1934). In man the hyaluronate concentration in the vitreous is $140^{\pm}338$ µg/ml (Balazs 1965) and in aqueous humour is 1.1±0.1 µg/ml (Laurent 1980).

The earliest evidence of glycosaminoglycans in the outflow system (Vrabec 1957, Zimmerman 1957) revealed that these substances were present in the intertrabecular spaces of both sheep and human eyes. Zimmerman (1957), studying human eyes enucleated in the treatment of malignant

melanoma of the choroid, reported that the GAGs were more concentrated in the outer meshwork. Ashton (1960) could not support this finding and suggested that the staining reaction was dependent on fixation techniques. Duke and Siegelman (1961) also disputed Zimmerman's findings and said that the finding of mucopolysaccharides in the intertrabecular spaces and cribriform layer was a feature peculiar to eyes containing choroidal melanomas which by the nature of their expansion cause compression of the vitreous. Ashton (1960) did, however, show metachromatic staining within the trabecular cores.

Segawa (1970) using both light and electron microscopy provided ultrastructural evidence of GAGs in the trabecular meshwork. Using a cationic dye, colloidal iron which stains GAGs, and is sufficiently electron dense to be visualised in the electron microscope, he described staining of the surfaces of all the endothelial cells, including the lining of the 'giant vacuoles'; the extracellular matrix was also filled with stained material. Stained areas all exhibited sensitivity to pre-incubation with testicular hyaluronidase, with the possible exception of the trabecular cores and the luminal aspect of the lining endothelium of Schlemm's canal. Armaly and Wang (1975) who studied the outflow apparatus of the rhesus monkey found that the staining reaction of GAGs and their subsequent sensitivity to pre and postincubation with testicular hyaluronidase was variable. They could not unequivocably demonstrate GAGs in the tissue by light microscopy using

Authors	Stain employed	Species investigated	Sensitivity to enzymes	Results
Segawa (1970)	Colloidal iron (P.b.)	Human	Testicular hyaluronidase	+ve
Armaly and Wang (1975)	Colloidal iron	Rhesus monkey	Testicular hyaluronidase	+ve
Grierson and Lee (1975)c.	Colloidal thorium Colloidal iron (with & without P.B.)	Human, baboon, rhesus monkey, rabbit.	Testicular hyaluronidase	+ve
Segawa (1975)	Ruthenium red Phosphotungstic acid	Human (P.O.A.G.)	Papain Human plasmin Streptomyces hyaluronidase Chondroitinase ABC	+ve +ve -ve +ve
Harnish (1976)	Ruthenium red	Human (P.O.A.G.)	-	
Grierson and Lee (1977)b.	Colloidal iron Colloidal thorium	Rhesus monkey	Testicular hyaluronidase	+ve
Grierson, Lee Abraham (1977)c.	Ruthenium red	Baboon, rabbit.	Testicular hyaluronidase	equi-vocal
Mizokami (1977)	Ruthenium red	Human	Detailed enzymatic identification	

Table 2: Table to summarise the results obtained in previous electron microscopic investigations of GAGs in the outflow system, the techniques used and the effects of enzymatic identification.

P.b. - Conversion to prussion blue.

P.O.A.G. - Primary open angle glaucoma.

two modes of fixation and stained with either colloidal iron (counter stained with Van Gieson), alcian blue or toluidine blue. However, electron microscopy proved more successful and the localisation of the GAGs using colloidal iron and their sensitivity to hyaluronidase was similar to that demonstrated by Segawa (1970).

The ultrastructural evidence for the presence of GAGs in the outflow apparatus of several mammalian species are summarised in Table 2. In this literature the location of GAGs was found to be similar in all the species studied. Several authors using the cationic dyes, colloidal iron and colloidal thorium (Armaly and Wang 1975, Grierson and Lee 1975c, Grierson and Lee 1977b) have found a reduction in staining after long incubations in testicular hyaluronidase. Since testicular hyaluronidase, one of three main types of hyaluronidase, is not specific to hyaluronic acid in its action but also degrades chondroitin-4-sulphate and chondroitin-6-sulphate then one must conclude from these studies that all of these GAGs may be present to some extent in the trabecular meshwork.

More detailed enzymatic digestion studies have been carried out recently (Segawa 1975, Mizokami 1977), which have shed more light on the character of the GAGs. Segawa (1975) studied trabeculectomy specimens from thirty cases of primary open angle glaucoma. Utilising both ruthenium red and phosphotungstic acid he found almost complete disappearance of the staining in the thick basement membrane ("glass membrane") of the trabeculae and the

elastic fibre sheath as well as the amorphous material in the cribriform layer, after exposure to human plasmin, papain and chondroitinase ABC. There was only a slight reduction in staining after exposure to streptomyces hyaluronidase which specifically degrades hyaluronic acid. This evidence led the author to conclude that the non-fibrillar components of the trabecular meshwork in these glaucomatous eyes were "chondroitin sulphate-protein complexes".

Mizokami (1977) carried out histochemical studies of the GAGs in the normal human trabecular meshwork. He demonstrated that GAGs which are masked by electrostatic binding to proteins can be visualised after treatment with 2-mercaptoethanol (2-ME). This substance attacks the disulphide bonds in high molecular weight proteins by a reducing process and is one way of "demasking" GAGs. The GAGs were identified before and after treatment with 2-ME by enzyme digestion. From the results he concluded that the amorphous material in the cribriform layer was composed mainly of chondroitin-4-sulphate, chondroitin-6-sulphate and "masked" hyaluronic acid. The basement membrane material in the trabeculae contained both hyaluronic acid and dermatan sulphate. Knepper, Farbman and Telser (1981) have recently identified, by zone electrophoresis, and subsequent enzyme digestion the glycosaminoglycans in the rabbit "aqueous outflow pathways and iris-ciliary body" as being hyaluronic acid, keratan sulphate, heparan sulphate and hybrid dermatan sulphate-chondroitin sulphate.

The basement membrane material in the trabeculae and cribriform layer in the human eye has also been shown recently by immunofluorescence and immunoperoxidase (Rodriques, Katz, Foidart and Spaeth 1980) to contain type IV collagen, fibronectin and laminin.

On the basis of the evidence from previous work it can be concluded beyond reasonable doubt that GAGs are important constituents of the extracellular matrix in the primate outflow apparatus. The fact that cultured trabecular endothelial cells are able to produce GAGs provides evidence that these materials may be synthesised locally (Schachtschabel, Bigalke and Rohen 1977, Polansky, Gospodarowicz, Weinreb and Alvorado 1978). This has been supported by in vitro studies of the biochemistry of calf trabecular meshwork (Anderson, Wang and Epstein 1980). Biochemical studies of the angular tissues in the rabbit eye (Hayasaka and Sears 1978) have shown high lysosomal enzyme activities particularly lysosomal hyaluronidase and β-glucuronidase. Similar studies on human eyes enucleated due to tumours of the orbit and maxillary sinus have also shown the concentration of lysosomal hyaluronidase to be high in the "inner region of the corneoscleral junction" (Hayasaka, Hara, Shiono and Mizuno 1980). These lysosomal enzymes play an important role in the catobolism of glycosaminoglycans (Barret 1969, Tappel 1969). It therefore seems likely that GAGs are synthesised and degraded locally by the trabecular endothelial cells.

THE ROLE OF GLYCOSAMINOGLYCANS IN THE RESISTANCE TO AQUEOUS OUTFLOW

Interest in the possibility that the GAG content of the outflow system might be important in primary open angle glaucoma was initiated by Meyer in 1947. He tentatively suggested, on the basis that he had found both hyaluronic acid and hyaluronidase in the aqueous humour of cattle eyes, that glaucoma - which even then was suspected as being due to increased resistance in the outflow pathways - was due to the presence of a hyaluronidase inhibitor in the aqueous. The obvious corollary was that hyaluronidase, by reducing the abnormally high resistance, could be used in the treatment of ocular hypertension.

Perfusion of the anterior chamber (Linn and Ozment 1950, Weekers, Watillon and de Rudder 1956) or sub-conjunctival injection (Stanworth 1966) of hyaluronidase preparations in glaucomatous eyes had only mixed success in temporarily reducing the intraocular pressure but this was far outweighed by the side-effects of the treatment which produced an unacceptable inflammatory reaction.

The first experimental attempts to investigate the physiological effects of hyaluronidase on aqueous dynamics were carried out by Bárány and his associates (Bárány and Scotchbrook 1953, Bárány and Woodin 1954, Bárány 1956a, Bárány 1956b - seen Table 3). Perfusion of bovine eyes in vitro with hyaluronidase resulted in a very rapid 50% reduction in resistance. The concentration of the enzyme

Table 3: A summary of previous experiments which have studied the effects of hyaluronidase on aqueous outflow dynamics in the mammalian eye.

Author	Species		Concentration of hyaluronidase	Physiological Effects	Notes
Linn & Ozment (1950)	Rabbit	(vivo)	10 TRU	No change in IOP	Inflamma response
	Human	(vivo)	1 TRU	Decrease in IOP	Temporar beneficia
Bárány & Scotchbrook (1953)	Bovine	(vitro)	0.25 - 4 VRU	50% decrease in R	
Bárány & Woodin (1954)	Bovine	(vitro)	0.05 - 5 VRU	50% decrease in R	
Bárány (1956)a.	Bovine	(vitro)	0.075 VRU	50% decrease in R	Differen
	Rabbit	(vitro)	2.5 VRU	" " " "	and diff
	Horse	(vitro)	5 VRU	" " " "	concentra
	Pigs	(vitro)	-	" " " "	have same
Bárány (1956)b.	Bovine	(vitro)	5 VRU	50% decrease in R	
			Bacterial	" " " "	
			Bee venom	" " " "	
			Testicular	" " " "	
			Snake venom	" " " "	
François, Rabaey & Neetens (1956)	Rabbit	(vitro)	20 VRU	50% decrease in R	
	Human	(vitro)	20 VRU	25-30% decrease in R	
Pedlar (1956)	Bovine	(vitro)	4 VRU	17% decrease in R	After on perfusio
				47% decrease in R	After 30 perfusio
	Human	(vitro)	8 VRU	46% decrease in R	In paire only
Weekers, Watillon & de Rudder (1956)	Human	(vivo)	-	-	Acute in reactio
	Bovine	(vitro)	250 VRU	50% decrease in R	
Berggren & Vrabec (1957)	Bovine	(vitro)	3 VRU	50% decrease in R	
	Sheep	(vitro)	3 VRU	?	
	Rabbit	(vitro)	2.5 & 25 VRU	30% decrease in R	
Melton & De Ville (1960)	Cats	(vitro)	10 units	Negligible effect	"Washout
	Dogs	(vitro)	10 units	" "	"
	Rabbit	(vitro)	10 units	30% decrease in R	No "wash
	Guinea pigs	(vitro)	10 units	50% decrease in R	" "
Grant (1963)	Human	(vitro)	50 TRU	Variable effect	Effect i eyes but in post-r
Stanworth (1966)	Human	(vivo)	1500 I.U.	Decrease in IOP	Subconju in glauc Inflamma and alte
Peterson & Jocson (1974)	Rhesus monkey	(vitro)	150 I.U.	40% decrease in R	Variable (24-65%)
Van Buskirk & Brett (1978)	Canine	(vitro)	150 I.U.	80% decrease in R	"Washout important
	"		300 I.U.	85% decrease in R	No diffe effect b concentra

PLEASE UNFOLD

did not alter the magnitude of the decrease and the authors stated that 0.05 VRU (viscosity reducing units) was the minimum concentration required for an effect (Bárány and Woodin 1954). Different types of hyaluronidase (Bárány 1956b -Table 3) all produced a similar effect, which in retrospect is surprising since different types of hyaluronidase have different activities (vide supra) (Buddeche and Kresse 1974, Barret 1969, Morton 1976). Even different species of non-primates (horse, bovine and rabbit) all showed a similar 50% decrease in resistance (Bárány 1956a). On the evidence it was suggested that a hyaluronidase sensitive barrier existed in the aqueous outflow pathways. Similar results have been found by other workers using non-primates (François, Rabaey and Naetens 1956, Pedlar 1956, Bergφen and Vrabeç 1957, Melton and de Ville 1960, Van Buskirk and Brett 1978). However, many authors noted that prolonged perfusions with control solutions with mock aqueous alone led to a gradual decrease in resistance. This was called the "washout effect" and it was considered that hyaluronidase accelerated this effect by the removal of resistance producing substances from the outflow pathways of non-primates. Melton and de Ville (1960) found that rabbits and guinea pigs did not show a "washout effect" on prolonged perfusion but did show a decrease in resistance after hyaluronidase perfusion: cats and dogs on the other hand did show a "washout effect", but only a marginal hyaluronidase effect (see Table 3). However, Van Buskirk and Brett (1978) demonstrated a very

significant hyaluronidase effect in dogs. This conflict in results has never adequately been explained but may be due to some genetic difference in the dogs used in the respective studies, or in the mode of hyaluronidase perfusion.

The effects of hyaluronidase on resistance to aqueous outflow in vitro in primate eyes have been extremely variable (see Table 3). François, Rabaey and Neetens (1956) using fresh post-mortem eyes found very variable results with a mean decrease in resistance of between 25-30% and two eyes of the twenty four studied showed increased resistance. Pedlar (1956) reported similar variability in the effects of hyaluronidase. Grant (1963) reported that an effect could only be detected in freshly enucleated normal eyes and in some eyes containing malignant melanoma which he suggested may have been due to the presence of episcleral blood or "some other factor in fresh eyes". The suggestion that hyaluronidase may be acting on sites other than the trabecular meshwork, eg episcleral venous system was supported by the work of Peterson and Jocson (1974). The authors studied the effects of hyaluronidase alone and in conjunction with 360° trabeculectomy in rhesus monkey eyes in vitro. As well as describing the variable effect of the enzyme, in agreement with previous studies, they also found that the enzyme further decreases resistance after the 360° trabeculectomy procedure. Finding no evidence of increased flow through the unconventional routes (ciliary

body, suprachoroid, vitreous) the authors concluded that the enzyme as well as acting on resistance in the trabecular meshwork (total of about 75% of which enzyme accounted for 40%) was capable of reducing the remaining 25% of the resistance to almost zero, suggesting it was acting external to Schlemm's canal.

The first morphological study of the effects of hyaluronidase *in vivo* in primates has recently been provided by Grierson, Lee and Abraham (1979a). The authors found that an intracameral injection of testicular hyaluronidase, in baboons (*Papio anubis*), into one eye and a control solution into the other produced a detectable morphological effect. In the hyaluronidase treated eyes there seemed a greater degree of distension of the cribriform layer and a higher incidence of 'giant vacuoles' in the lining endothelium of Schlemm's canal.

From this morphological evidence Grierson and co-workers surmised that perfusion with hyaluronidase had increased conductance through the trabecular meshwork. In the absence of physiological confirmation of increased flow the authors concluded by saying "A combined ultrastructural and physiological study of hyaluronidase effects on the drainage tissues would be a reasonable extension of this initial report".

THE AIMS OF PART I

i) To study the effects of testicular hyaluronidase on

the resistance to aqueous outflow *in vivo* in the primate eye.

ii) To study the morphological effects of perfusion alone and perfusion with testicular hyaluronidase.

iii) To correlate the physiological and morphological results and discuss the findings in relation to the functional anatomy of the primate outflow system.

APPROACH TO PART I

The species of monkey used in the current investigation, the pig tailed macaque (*Macaca nemestrina*), was chosen due to the limited availability of other species of primates which would have been more desirable for example baboons such as *Papio anubis* or *Papio cynocephalus*. They would have had the advantage that they have been used previously in investigations of this nature. Since there seemed to be no immediate signs of improvement in the situation, a colony of ten pig tailed macaques were chosen as the experimental animal.

The reasons for carrying out this experiment *in vivo* were twofold. Firstly it was one of the main aims of this project to investigate whether hyaluronidase had any resistance lowering effect *in vivo* in the primate eye, which had never been previously investigated. The possibility that an "enzyme cocktail" might be a means of reducing the resistance to aqueous outflow in patients with primary open angle glaucoma and thus returning the

intraocular pressure to a more clinically acceptable level has been proposed (Grierson, Lee and McMenamin 1981). As a means of assessing the feasibility of such a procedure it was necessary to carry out a preliminary study of the physiological effects of hyaluronidase *in vivo* in the primate eye.

The second main reason that the experiment be carried out *in vivo* was that the other major aims of the project were to study the morphological effects of the enzyme perfusion (vide infra) which demands that the eyes be perfuse fixed *in vivo* at a predetermined pressure.

The type of enzyme, testicular hyaluronidase, was chosen on the basis of the morphological, physiological and biochemical evidence that GAGs such as hyaluronic acid and chondroitin sulphates were present in the aqueous outflow pathways (vide supra) and that this enzyme would be capable of degrading these GAGs. Testicular hyaluronidase also has a higher pH optimum than for example streptomyces hyaluronidase (Buddecke and Kresse 1974).

Although past workers had found very little dose related response *in vitro* (Bárány and Woodin 1954, Van Buskirk and Brett 1978) the present concentration was chosen for the following reason. In preliminary experiments on baboons 150 I.U. of testicular hyaluronidase did not produce a marked physiological effect although this concentration was that used previously by Grierson, Lee and Abraham (1979a) in the morphological study, and also by Peterson and Jocson (1974) who had some success *in vitro*.

It was decided therefore that 300 I.U. may be required in these older and larger pig tailed macaques, to produce a detectable effect.

A two step pressure technique was chosen for the measurement of facility of aqueous outflow due to its simplicity as a technique and also because it has been successfully applied by previous workers (Bárány 1964, Lamble 1974).

In preliminary experiments with baboons it was found that assessing the facility of aqueous outflow before and after the introduction of the enzyme involved excessive manipulations and perfusion. It had not only been reported that a physiological "washout effect" could be achieved by perfusion alone (vide supra) but there were also reports that excessive perfusions had adverse effects on the trabecular tissues (Grierson, Lee and Abraham 1979b). Therefore it was decided that it would be more advisable to limit the measurement of facility to after the enzyme injection. The control eyes (receiving only Bárány's fluid) and the experimental eyes (hyaluronidase in Bárány's fluid) would both be treated in exactly the same fashion, which it was hoped would allow comparisons in both physiological and morphological results.

In the morphological investigation emphasis was placed on the quantitation of structures which might indicate a decreased resistance and increased flow. The 'giant vacuoles' which change in numbers in a pressure/flow dependent manner (vide supra) can be easily quantified by

light microscopy (Grierson and Lee 1977a). The quantification of the size and incidence of pores in the lining endothelium as seen by scanning electron microscopy gives an indication of the numbers of transcellular channels and therefore flow through the trabecular tissues (Bill and Svedbergh 1972, Lee and Grierson 1975).

Transmission electron microscopy was used in the conventional fashion to study the ultrastructural changes in the trabecular meshwork and to quantify the degree of distension in the cribriform layer. The use of cationic dyes in conjunction with transmission electron microscopy would hopefully allow a study of the changes in distribution in quantity of glycosaminoglycans in control and experimental eyes.

It was hoped that the use of a wide variety of techniques would not only maximise the information obtained from the study without dependence on any one mode of investigation but also; should hyaluronidase change the resistance to aqueous outflow by its action on the extracellular elements of the trabecular meshwork then this would be detected by the detailed morphological investigation.

MATERIALS AND METHODS FOR PART I

EXPERIMENTAL ANIMALS

Ten male pig tailed macaques (Macaca nemestrina) weighing between 10.5-14 kilograms (mean weight = 11.9 kg) were used in the present investigation. The animals were all healthy adults which were kept in quarantine at the Wellcome Surgical Research Centre. Although the ages of the animals were unavailable, the data reported by Napier and Napier (1967) that males of this species weighed between 6.2-14.5 kilograms suggests the animals used in this study were mature adult males. In addition, the secondary sexual characteristics, eg the mane and the large canines were well developed.

In a preliminary experiment, one animal was anaesthetised and both eyes were immediately enucleated and immerse fixed in order to study the morphology of the normal unperfused outflow apparatus in this species as this information was not available in the literature. The remaining nine animals were used to study the physiological and morphological effects of hyaluronidase.

EXPERIMENTAL DETAILS

Anaesthetics

The anaesthetic technique was similar to that described by Strang, Wilson and Mackenzie (1977). The animals were tranquilised with ketamine hydrochloride (Ketalar, 22-44

mg/kg body weight) and anaesthetised with thiopentone (Pentothal, 7.5 mg/kg) via a leg vein to the level at which the corneal reflex was suppressed.

The anaesthesia was maintained, after endotracheal intubation, by a mixture of Halothane (0.5-1.5% depending on requirements) and a gas mixture ratio of oxygen: nitrous oxide (2,000:6,000cc /min). The animals received an intramuscular injection of suxamethonium (50 mg Scoline) every 30 minutes.

Preparation for experiment

The animals were lying in the supine position to allow maximum access to the eyes. The head and shoulders were slightly elevated to prevent kinking of the endotracheal tube. The head was fixed by placing a metal bar through the mouth behind the large canine teeth, and was tilted slightly backwards. This species of macaques had deep sockets and pronounced orbital rims which made cannulation procedures difficult. To facilitate cannulation the eyes were exposed by an incision into the lateral canthus to the orbital margin. Care was taken to avoid cutting the large orbital vein. The eyelids were loosely sutured to widen the interpalbebral fissure. The soft tissue was divided to the periosteum. A cut was made 1.5 cm into the nasal skin and the plica semilunaris was divided. The deep nasal orbital vein was clamped and tied if necessary. The upper lid was sutured to the eyebrow (Mersilk sutures 4/0). A double loop of suture was placed in the superior fornix tissue and secured to the eyebrow (Mersilk 5/0). The same

procedure was repeated for the lower lid which was attached to the cheek skin. These sutures were slackened after the cannulation. A triple loop of suture was put through the temporal bulbar conjunctiva (Mersilk 5/0) and gripped with a pair of Spencer-Wells forceps in order to stabilise the eye during cannulation.

Throughout the experiment the eyes were covered with swabs soaked in saline after Hypromellose had been applied to the eyes to prevent corneal drying which occurred very rapidly in the absence of the blink reflex. Applanation tonometry (using Perkins hand held tonometer) was found to be unreliable due to the rapid loss of the tear film and also due to the difficulty in calibrating the instrument.

Monitoring of systemic physiological parameters

A catheter in the femoral artery was connected to a pressure transducer (Bell and Howell) which was linked to a pen recorder (Devices) in order to monitor blood pressure. Blood pressure was kept relatively low and steady by adjustment of the gas mixtures, but did of course vary depending on the blood gas levels (pO_2, pCO_2, bicarbonate, [HCO_3^-] and base excess [B/Ex]) which were recorded at regular intervals by analysis of 2 ml arterial blood samples in an Astrup Blood Gas Analyser. Body temperature was monitored with rectal and oral thermometers and was maintained at 37.5^oC using heat lamps and a heating blanket.

The blood gas levels were maintained within normal limits by adjustment of the volume of the respirator and

the O_2/CO_2 ratios. The intubation tube had a connection to a capnograph (Godart-Statham) which continuously monitored the concentration of exhaled CO_2; the values were displayed on a pen recorder (Devices). This provided a useful indicator of any change in the respiratory exchange of the animal or in the anaesthetic system which might have led to alterations of blood gases, eg hypoxia, pulmonary oedema or incorrect placement of the intubation tube.

Cannulation procedure

Previous experiments had shown that insertion of two conventional 25-gauge needles into the anterior chamber provided an unstable system unsuitable for long experiments and also entailed the risk of trauma to the iris or lens. The specially adapted needle of Nagasubramanian (1977) was modified by the author. The 2.5 cm shank was filed by hand under the dissecting microscope, 1.5 cm from the tip, creating a small recess on one side of the needle which opened into the lumen. The holes were checked with a dissecting microscope to make sure there were no rough edges which might tear into the corneal stroma during cannulation. Each needle was tested to ensure the lumen was patent. The needles were then sterilised in ethylene oxide and stored in sterile packets until required. The metal blade of the needle was separated from the plastic base and was attached to soft plastic tubing (Technicon 0.5 mm internal diameter) at one end before the cannulation procedure (Fig 11a). The hole in the shank was covered during the cannulation by a small plastic sheath to prevent

Cannulation Procedure

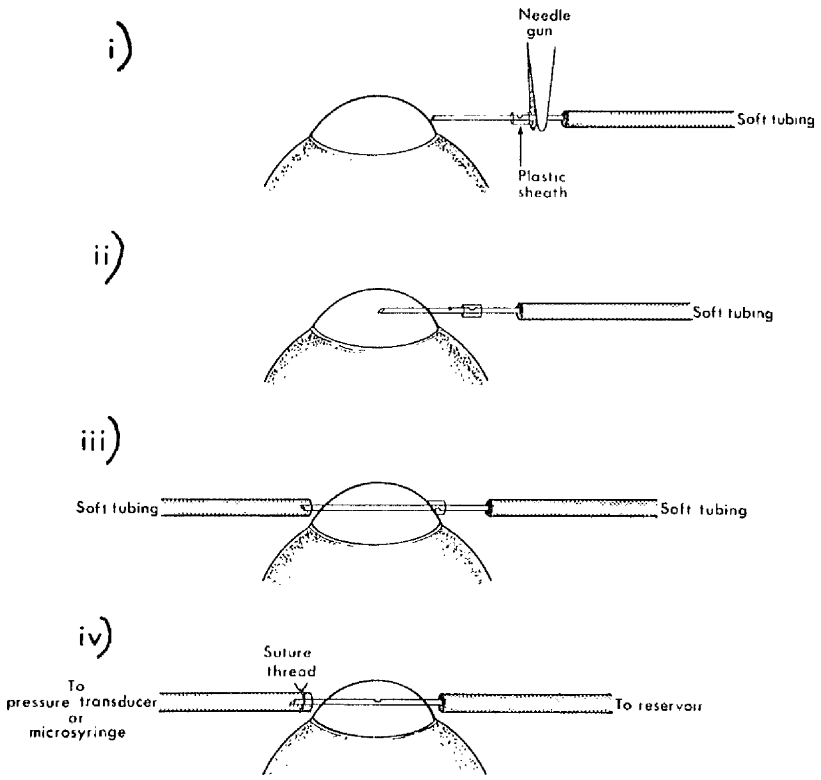

Figure 11: a) Diagram showing the procedure used to cannulate the anterior chamber of the pig tailed macaque eye.

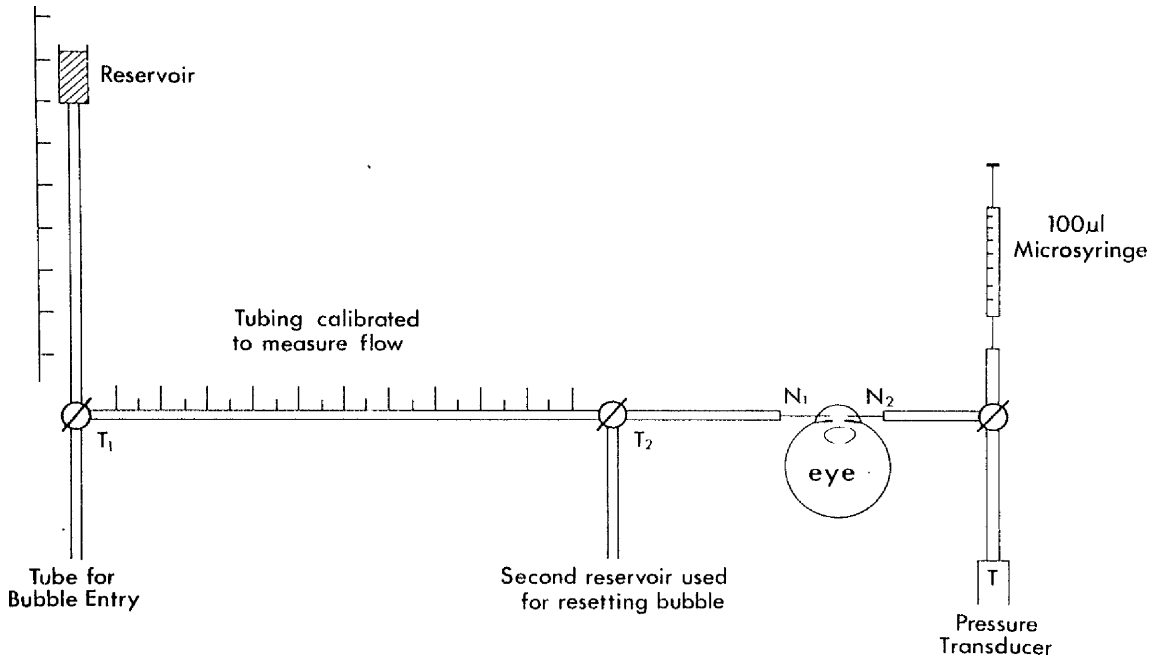

Figure 11: b) Diagram showing the experimental system in the pig tailed macaque hyaluronidase study. ∅ - three way tap.

the collapse of the anterior chamber (Fig 11a (i)).

The needle was inserted at the temporal periphery of the cornea using a needle gun (Yarlett). It was then pushed through the anterior chamber and out through the nasal peripheral cornea against counter tension from the sutures on the temporal bulbus. When the tip of the needle emerged it was attached to soft tubing which was then secured by a small loop of suture. The distance of 1.5 cm from the tip to the hole in the shank was necessary to prevent the loss of aqueous during this procedure (summarised in Fig 11a). Transfixation of the cornea prevented trauma to the iris and lens.

One side of the needle was attached via tubing to a reservoir, set to a height which maintained 18 mm Hg in the anterior chamber during the cannulation procedure. This was closed off at the end of the cannulation. The nasal end of the needle was connected via tubing to a 3-way tap system, further connected to either a pressure transducer or a microsyringe (Fig 11b).

Experimental design

The experimental system (Fig 11b) was filled with Bárány's fluid (Bárány 1964) which was washed through until any air bubbles had been removed. The Bárány's fluid was sterilised by filtration under negative pressure which had the added advantage of simultaneously degassing the fluid. The fluid was prepared the day before the experiment from stock solutions and was stored in a sealed container at 4°C. Bárány's fluid has a pH of 7.2-7.4.

The pressure transducer (Bell and Howell) was calibrated in mm Hg at the beginning of each experiment by adjusting the height of the reservoir (100 mm H_2O = 7.6 mm Hg). The internal diameter of most of the tubing was 0.8 mm with the exception of the soft polythene tubing between T_2-N_1 and N_2-O (see Fig 11b); and the length of tubing between T_1-T_2 which was of a smaller bore (0.33 mm) and placed beside a meter rule, to achieve maximum measurement accuracy. The volume of fluid contained in 100 mm of small bore tubing was found to be 125 µl. During experimental procedures the distance moved in one minute by a small bubble along this tubing was measured; from this the volume of fluid which entered the eye was calculated (Conversion factor 1 mm = 1.25 µl). It was assumed that the resistance to fluid movement in this tubing was not prejudicial to flow through the perfusion system.

Two 100 µl microsyringes (Terumo) were used to introduce fluid into the anterior chamber. One contained 100 µl of Bárány's fluid (control eye); the other contained 300 I.U. of bovine testicular hyaluronidase (Sigma chemicals, product no 1628), dissolved in 100 µl of Bárány's fluid (experimental eye).

A small operating microscope was used to examine the eyes at regular intervals during the 4-5 hour period of the experiment. In none of the experiments was there blood or flare in the anterior chamber.

Experimental protocol

The following experimental protocol was strictly

adhered to in the nine pig tailed macaques.

i) The eyes were prepared and cannulated after which they were left to settle for 10 minutes.

ii) The intraocular pressure was measured in both eyes.

iii) After a further 10-15 minutes the contents of both microsyringes were injected slowly into the anterior chamber at 2 µl/minute, total injection time was 50 minutes. The reservoir was open to the eye to maintain a pressure of 18 mm Hg during the injection, thereby dampening fluctuations in pressure.

iv) On completion of the injections the pressure transducer was reconnected and T_2 closed off. The eyes were left undisturbed for one hour, monitoring intraocular pressure throughout this period.

v) After the introduction of a small bubble into the system (achieved by producing a negative pressure from a second reservoir), the tap T_2 was opened to the eye with the meniscus of the reservoir set at 23.5 cm above the eye ($\simeq$ 18 mm Hg).

vi) The flow rate, as measured by the distance travelled by the bubble, was recorded at minute intervals for 10 minutes.

vii) The tap T_2 was closed and the eyes left undisturbed for 15 minutes.

viii) The second flow rate at a pressure head of 28.5 cm H_2O ($\simeq$ 22 mm Hg) was measured for 10 minutes.

ix) T_2 was closed and the eyes left for 30 minutes.

x) Two reservoirs of fixative (2-4% gluteraldehyde in

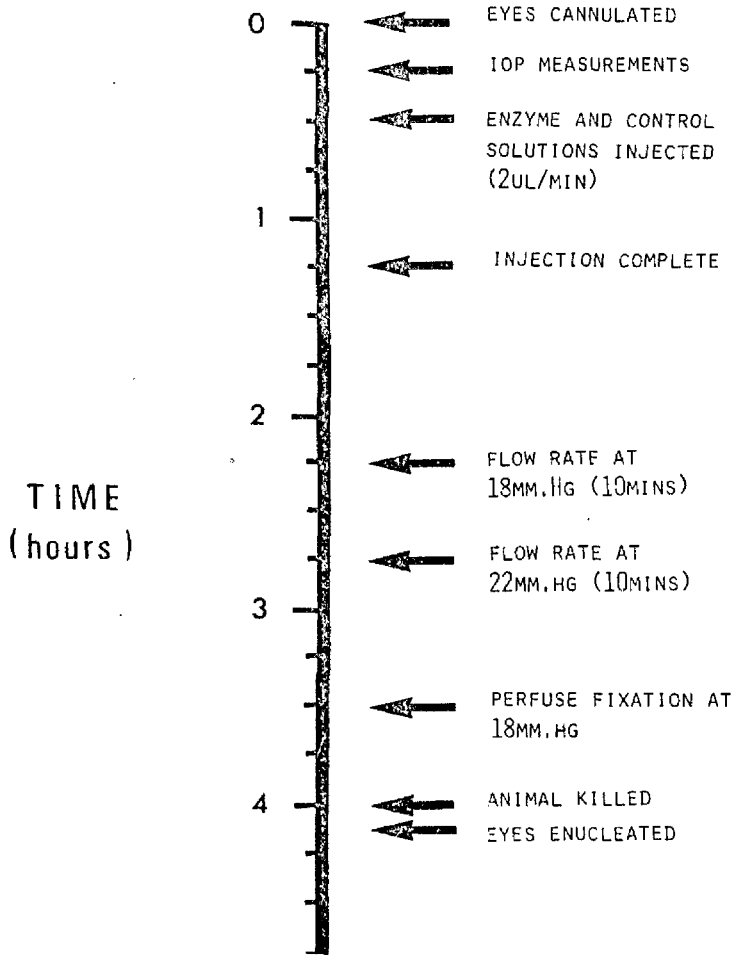

Figure 12: Summary of the experimental protocol in hyaluronidase study.

cocodylate buffer pH 7.2-7.4), which contained a few drops of fluorescein to act as a marker dye, were connected to the tubing at N_2 in each eye and set to a height of 23.5 cm H_2O (18 mm Hg). Fixation was allowed to take place for 30 minutes or more until it was established that the anterior chamber was filled with fixative and the cornea was firm. Fluorescein generally entered the anterior chamber and moved downwards into the superior half, which was lower than the inferior half due to the tilt of the head.

xi) The animal was killed by an overdose of sodium pentobarbitone (Euthatal). Having established adequate fixative penetration into the episcleral and conjunctival vessels the tubing to the needle was tied off and divided. The eyes were then enucleated and immerse fixed in gluteraldehyde and stored at 4°C.

The experimental protocol is summarised in Fig 12.

Calculation of outflow facility

A mean value for the flow rate at each of the pressure levels (18 and 22 mm Hg) was obtained from the results of the last nine minutes. The first minute is excluded from the results since very high flow rates are often recorded during the rapid expansion phase when the eye is opened to the reservoir due to the volume of the eye increasing as the sclera expands slightly (Lamble 1974).

The facility of aqueous outflow, as described in the general introduction, can be calculated as the difference in inflow rates produced by a change in pressure. It is calculated after Bárány (1964) as

$$C = \frac{F_1 - F_2}{P_1 - P_2}$$

C = facility of aqueous outflow (µl/min/mm Hg)

F_1 = first flow rate (µl/min)

F_2 = second flow rate (µl/min)

P_1 = first pressure (mm Hg)

P_2 = second pressure (mm Hg)

The total volume of fluid entering the eye throughout the experiment was also calculated.

The details of each of the nine experimental animals are given in appendices 2-10. These include the animal's number, body weight, starting blood pressure, resting intraocular pressure, blood gas analysis results and general comments on each experiment.

TISSUE PREPARATION FOR LIGHT MICROSCOPY AND TRANSMISSION ELECTRON MICROSCOPY

Tissue dissection

Within 2-24 hours of each experiment the eye was bisected at the equator. The front of the eye was dissected as follows: the lens was removed after division of the zonula fibres; the anterior segment was then divided into quadrants (Fig 13). Each quadrant was coded, and seven meridional slices or blocks of limbal tissue were

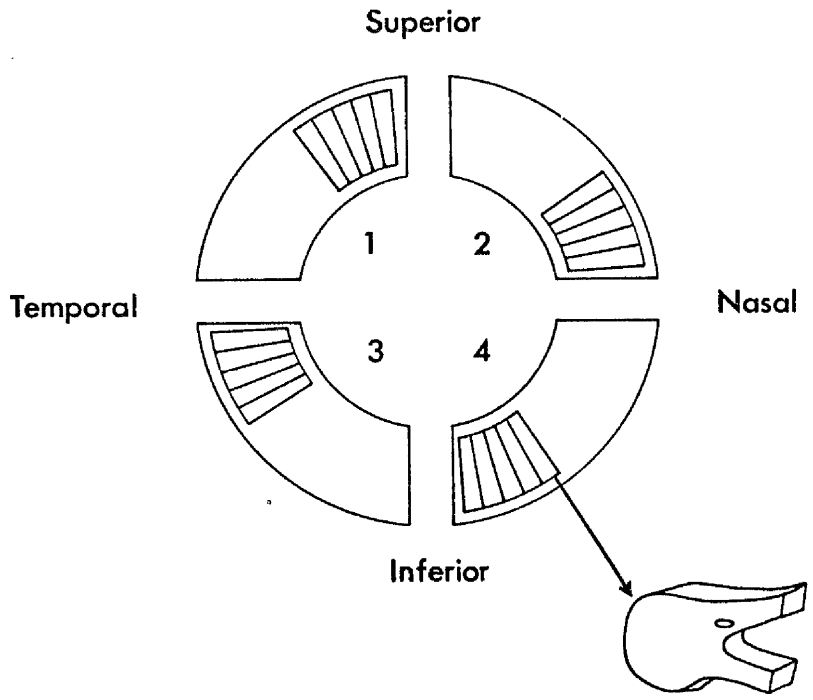

Figure 13: Diagram to show the dissection and sampling of limbal tissue from the various quadrants (1-4) of the pig tailed macaque anterior chamber.

cut from each quadrant. Four pieces per quadrant were for conventional transmission electron microscopy and three pieces for "en bloc" cationic dye treatment. Samples of the remaining tissue were used for scanning electron microscopy (vide infra).

The tissue was stored at 4°C until the termination of all the physiological experiments - a period of about two weeks.

Tissue preparation for light microscopy and transmission electron microscopy

The tissue from the eyes of the nine experimental animals was processed and embedded in one batch (16 blocks per eye - total - 300 pieces). Although it was appreciated that there was a risk involved, it was felt that this ensured uniformity in the osmication, dehydration, impregnation and curing. This was mandatory for the quantitative studies which were an integral part of the investigation. Although some tissue was stored for about two weeks there did not seem to be any deleterious morphological effect, eg when comparing Mn 2 to Mn 10.

The following stages were used in processing the tissue blocks.

i) The tissue blocks were washed no less than three times in cacodylate buffer (10 minutes each).

ii) Post-fixed in 1% buffered osmium tetroxide for one hour.

iii) Rewashed several times in buffer (10 minutes each).

iv) Dehydrated through graded alcohols

25% alcohol	10 minutes
50% alcohol	10 minutes
75% alcohol	10 minutes
Absolute alcohol (Repeated 4 times)	10 minutes

v) Tissue is then cleared in propylene oxide (2 changes of 10 minutes each).

vi) An equal volume of araldite is added to the second change of propylene oxide; this was gently rotated overnight.

vii) The tissue was placed in a 3:1 mixture of propylene oxide and araldite (see appendix) for 6 hours.

viii) The tissue was then blocked out into freshly prepared araldite in labelled rubber moulds; curing took place at 60°C for 24-48 hours.

Colloidal iron technique

To demonstrate the complex polysaccharides in the outflow system the technique described by Gasic and Berwick (1964) was employed. Colloidal iron is regarded as being more specific than other stains, eg ruthenium red and colloidal thorium (Serafini-Fracassini and Smith 1974). The slices of limbal tissue were stained "en bloc" after post-fixation with osmium tetroxide. The technique was as follows:

i) Washed with cacodylate buffer.

ii) Briefly rinsed in 12% acetic acid.

iii) Exposed to dialysed colloidal iron (BDH chemicals Ltd) in 12% acetic acid (pH 1.1-1.3 at room temperature) for 60-90 minutes.

iv) Briefly rinsed in 12% acetic acid.

If conversion to prussian blue was required the procedure continued as follows:

v) The tissue blocks were exposed to a mixture of 2% potassium ferrocyanide and 2% hydrochloric acid for 20 minutes.

vi) Finally washed in distilled water.

The procedure then followed the described technique for araldite embedding.

Sectioning and staining for light and transmission electron microscopy

The araldite blocks were trimmed using a scalpel blade to the desired trapezoid shape and orientation shown in Fig 14. Semi-thin sections (1-2 μ) and ultrathin sections (600-900A°) were cut on an LKB Ultrotome III, using glass knives for the former and a diamond knife (Du Pont) for the latter. Semithin sections were stained with toluidine blue (1:1, 1% toluidine blue : 2.5% sodium carbonate solutions) and mounted in canada balsam. Light photomicrography was carried out using an Orthoplan photomicrographic unit, with either Panatomic X (32 ASA) black and white film or Kodachrome colour film (25 ASA).

Ultrathin sections were mounted on 150 mesh copper grids (Polaron) and stored in grid boxes (LKB). All ultrathin sections with the exception of "en bloc" stained tissue, were counterstained with a saturated solution of uranyl acetate in 50% ethanol (30 minutes) and subsequently exposed to Reynold's lead citrate solution (15 minutes).

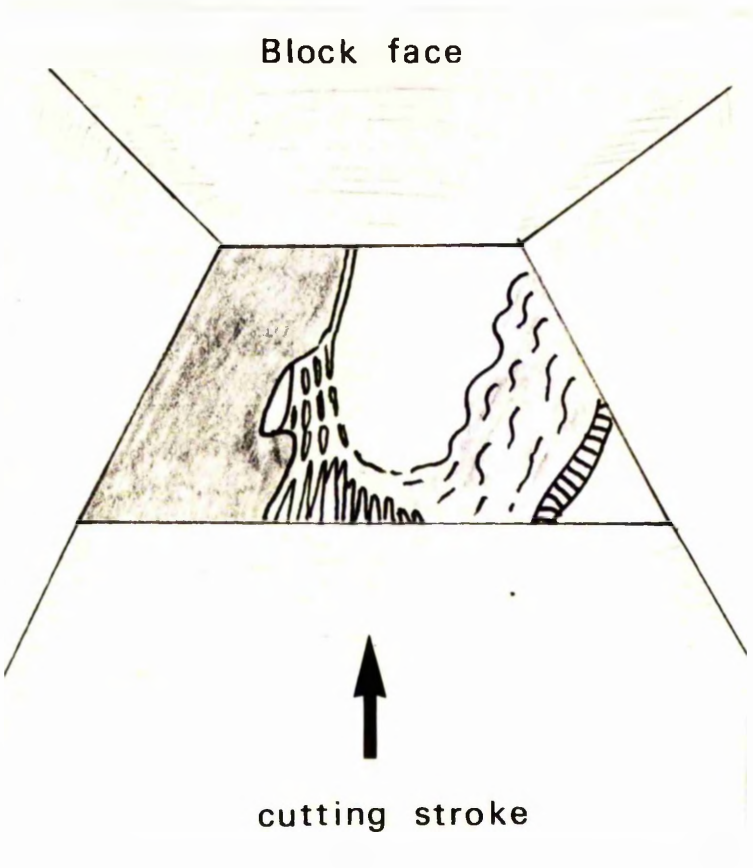

Figure 14: Diagram to show the orientation of the tissue in the block face for optimum section quality.

The sections were examined in a Philips 301 electron microscope and photographed on Kodak electron microscope film 4489 (8.3 x 10.2 cm).

PREPARATION FOR SCANNING ELECTRON MICROSCOPY

Samples of tissue from each quadrant were studied by scanning electron microscopy (SEM). Eight or more meridional slices of limbal tissue were taken from each of the 20 pig tailed macaque eyes.

The tissue was washed several times in buffer, post-fixed in 1% osmium tetroxide for one hour and rewashed with buffer. A few pieces from each eye were not dissected any further and were used to study the meridional cut surface. To investigate the transcellular channels or 'giant vacuole' lumen pores in the lining endothelium of Schlemm's canal, the canal was dissected in the manner shown in Fig 15 (Lee 1971). Dissections of the pig tailed macaque tissue was often difficult due to the numerous septae and cords which were present within the canal and also the narrowing of the canal lumen in tissue where the meshwork was distended.

The majority of the tissue was critical point dried while only a few pieces were freeze dried. Most recent studies which have carried out quantitative studies of the pores in the lining endothelium have used freeze drying (Bill 1970a, Bill and Svedbergh 1972, Lee and Grierson 1975, Grierson, Lee, Moseley and Abraham 1979). In a

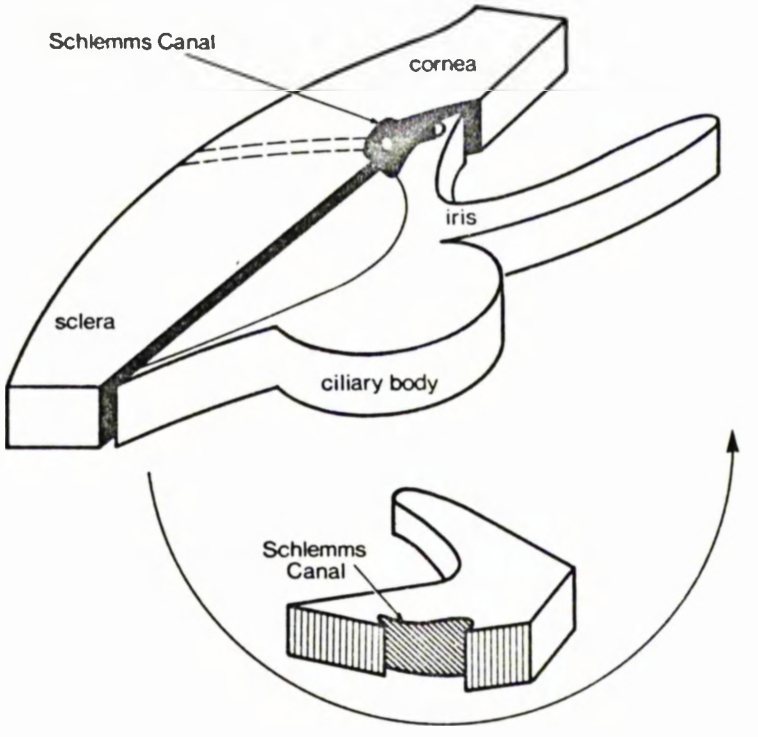

Figure 15: Diagram showing the dissection technique used to expose the trabecular wall of Schlemm's canal for investigation by SEM (from Lee (1971)).

preliminary comparison of both critical point drying (CPD) and freeze drying (FD) it was found that the architecture of the lining endothelium was better preserved in CPD tissue. Although the shrinkage with CPD is greater, 30-50%, than FD, $\simeq$ 5% (Boyde 1978, Jensen, Prause and Laursen 1981) it was decided to use CPD for the present investigation. The procedure for CPD (Wells 1974) was as follows:-

i) The tissue was dehydrated by passing through graded alcohols (30, 50, 70, 80, 90, 100%, repeat 100%) at 15 minute intervals.

ii) Amyl acetate was substituted for alcohol by transfer through the following amyl acetate/alcohol ratios - 25/75, 50/50, 75/25 to 100% amyl acetate.

iii) The tissue was carefully placed along with the appropriate label in the transfer port, containing amyl acetate, and placed in the critical point drying apparatus (Polaron E 3000). The chamber was closed and the inlet valve was opened to allow liquid carbon dioxide to fill the chamber. The vent valve was opened to allow amyl acetate vapour to escape. After flushing the chamber in this fashion the amyl acetate in the tissue was substituted by liquid CO_2 (completed when no smell of amyl acetate could be detected - within about 10 minutes). Once this was achieved the valves were closed and the CO_2 was allowed to penetrate the tissue for one hour.

iv) The flushing procedure was then repeated and the valves closed again.

v) The temperature in the chamber was raised to 36-38°C which is above the critical point of CO_2 liquid/gas phase at 31°C at 1300 psi.

vi) The CO_2 gas was slowly vented from the chamber over a period of 5 minutes and once the pressure was reduced the tissue was removed. Control and experimental tissue from each animal were processed in parallel.

vii) The tissue was then mounted on aluminium stubs using silver conductive paint. The dissected tissue to be used in the quantitative study was mounted with the exposed trabecular wall uppermost. The stubs were coated with gold in an SEM sputter coater (Polaron SEM coating unit E 5000) and examined in a JEOL JSM T200 scanning electron microscope.

The few pieces of tissue which were freeze dried were treated in essentially the same fashion as that described by Lee (1971), and was performed in a Balzars Micro BA_3 freeze drying unit which maintained a vacuum of 10^{-5} Torr. Before water extraction the tissue was passed through liquid arcton and frozen in liquid nitrogen. After freeze drying the tissue was mounted, coated and examined as previously described.

QUANTITATIVE TECHNIQUES USED TO STUDY THE MORPHOLOGICAL EFFECTS OF HYALURONIDASE ON THE OUTFLOW APPARATUS

Quantitative assessment of vacuolar incidence in the lining

endothelium of Schlemm's canal

The technique used to count 'giant vacuoles' has previously been described by Grierson and Lee (1977a). It has been shown to be a quick and reliable method of quantifying vacuolar incidence. Semithin sections (1 μ) were cut from 10 tissue blocks in each eye and were examined using a x100 oil immersion objective. The following features were counted on one section from each block.

i) Inner wall nuclei : This count was performed as a control for the number of cells in the monolayer.

ii) Inner wall 'giant vacuoles' : These structures (see results for definition) were counted and expressed as mean count per section.

iii) Other 'giant vacuoles' : ie, on the outer wall, the septae, the anterior and posterior walls. These results were also expressed as mean count per section.

The mean and standard deviation was calculated for each of these features in each eye. All the counts were carried out on coded sections. Repeatability for the author showed a less than 9% variation. Interobserver differences (PG McMenamin and WR Lee) showed a variation of between 13 and 25% and depended a great deal on the quality of the sections.

Image analysis of the 'empty space' component in the cribriform layer

Several methods were considered for the assessment of distension of the cribriform layer and the 'washout' of

extracellular elements. Irregularities in staining of toluidine blue sections and the limited resolution of light microscopy made this material unsuitable for image analysis. This part of the investigation was therefore performed at the ultrastructural level (TEM). Although the time and effort required to achieve adequate samples is much greater by this method, it was hoped that this would be outweighed by the benefits of high resolution and accuracy. The next step was to decide on a suitable system of area measurement. The technique used for the study of human material (see materials and methods in Part II) was inappropriate for this investigation mainly due to the large numbers of electron micrographs to be studied. Automated image analysis has developed in recent years due to the advances in TV scanning systems and electronics. These techniques are used by many morphologists to quantify ultrastructural changes in many varied types of tissue (Bradbury 1979).

The basic concept of the system of image analysis used in the present study (Optomax - Micromeasurements LTD) was to present an image, in this case a TEM negative, to a television camera (scanner) and analyse the resulting video signal to obtain quantitative data from the specimen. The features selected for analysis are detected by grey level discrimination (contrast). Several parameters can then be measured, eg area, length and total counts of the selected features. In the present study the area of 'empty space' under the lining endothelium was of interest and could be

detected by adjusting Selectors A and B, the former of which detects the darkest features, which "bright up" on the video screen, selector B can be used to detect intermediate grey levels. The area of detection can be read off as units of picture points of the total field.

The system performs best on high contrast images, thus any image, eg negatives, micrographs or sections should be produced in high contrast, eg by using electron-dense stains for TEM. Image analysis has the advantage that many samples can be tested in a short period of time. They are more accurate than manual systems because there is less boredom and fatigue in the observer. The technique used in the present study was as follows:-

i) Ultrathin sections were cut from 8 blocks in each eye and counterstained in the conventional fashion.

ii) Serial photomicrographs were taken along the inner wall of Schlemm's canal (Fig 16a) at a magnification of x1900. The reasons for failure to photograph the whole inner wall was due to the presence of grid bars (Fig 16a) and to some extent the convolutions in the canal.

iii) The negatives were placed on the illuminated base of the Optomax below the TV camera and a black mask was placed around the negative to exclude an extraneous light. The camera system was set up in precisely the same manner before each session, to produce a total magnification on the viewing screen of x 5396. The frame size was 250 x 40 picture units which was equivalent to 72.25 μm^2. The area of electron lucent spaces within this frame ($\simeq$ 20 μm under

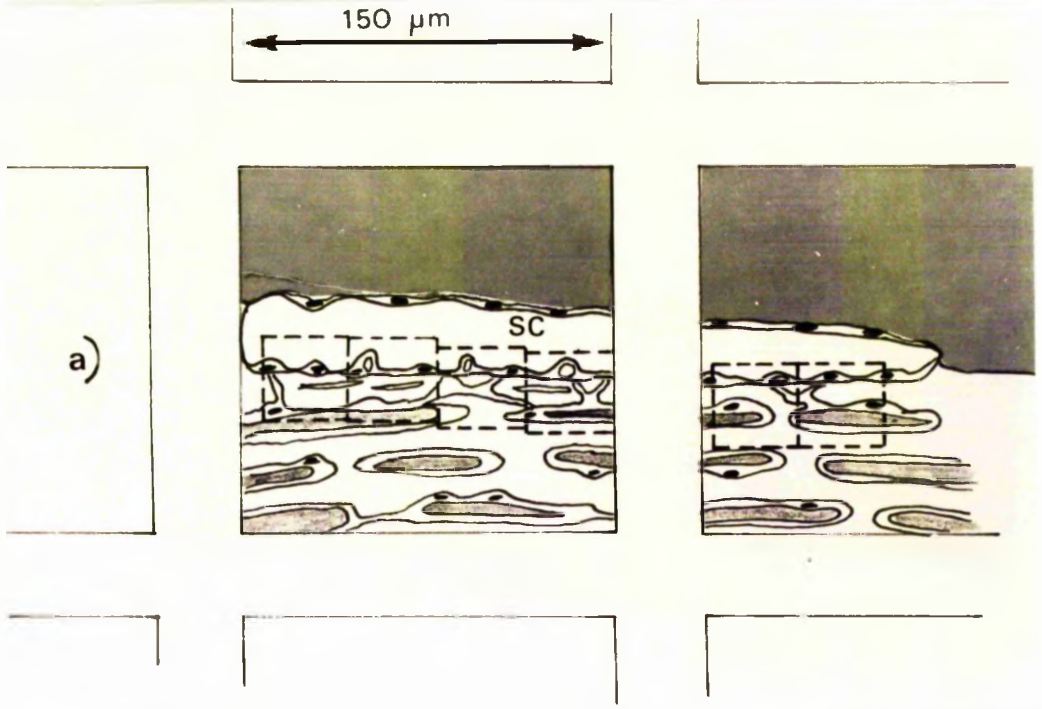

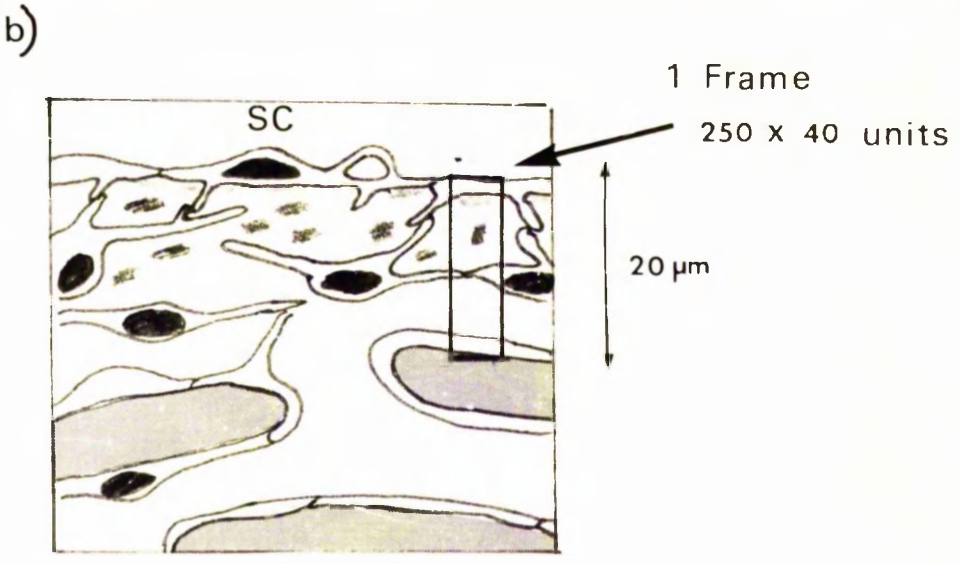

Figure 16: a) Diagram to show how serial photomicrographs were taken along the areas of inner wall of Schlemm's canal which are not covered by the grid bars.

b) Orientation of the field or frame below the lining endothelium in the image analysis of the 'empty space' component of the cribriform layer.

the lining endothelium - Fig 16b) was detected by adjusting selectors A and B. Fifteen sequential frames were measured on each negative and repeated for all the negatives from each section. The data was fed into a Hewlett-Packard desktop computer (9815A) which is interfaced with the Optomax. The mean and standard deviation for the percentage area of 'empty space' in the cribriform layer was calculated for each section.

Groups of coded negatives were examined in this fashion, care was taken that within one day's work both eyes from the same animal were analysed. When the study was complete, the code was broken and pooled means and standard deviations were calculated for each eye.

At the start of each day's session a repeatability test was carried out on the same group of negatives (randomised to prevent over familiarity). The mean percentage area (± SD) of 'empty space' from the five sessions was 58.1 ± 1.6, a standard error of 0.72. A second observer carried out the procedures in one eye. The values obtained were:

	Mean	SD
PG McM	50.2	±17.3
WRL	63.0	±15.3

The second observer consistantly detected 25% more 'empty space' than the author. It is accepted that detection is to some extent subjective, however, as all the observations were made by one observer the comparison of results between control and experimental tissue is considered valid.

Incidence of 'breaks' in the lining endothelium of Schlemm's canal

During the course of the investigation it became apparent that the vacuole counts did not conform fully to the physiological data. One possible explanation was that excess flow through the trebecular meshwork could cause disruption in the lining endothelium thus bypassing the more conventional route of 'giant vacuoles'. In order to investigate this possibility the following procedure was carried out.

The serial micrographs used in the analysis of 'empty space' in the cribriform layer were enlarged to a total magnification of x 5160 (20 x 25 cm format). The number and nature of the disruptions in the lining endothelium were recorded in the following categories:

i) Artefactual disruptions

The edges of these breaks were ragged in appearance and the cytoplasm exposed, suggesting their artefactual nature.

ii) Experimentally induced disruptions

This category was similar in size to artefactual breaks but were considered real if the separated ends of the cells were rounded and bound by a continuous plasma membrane. If the gap in the monolayer was greater than 2 μm it came under this category, if it was smaller it was either of the next two categories.

iii) Non-vacuolar pores

These were pores in the lining endothelium generally

under 2 μm but not associated with a 'giant vacuole'.

iv) Vacuolar pores

These were openings on the canal aspect of the 'giant vacuoles', providing communication between the contents of the vacuole and the lumen of Schlemm's canal.

All measurements were made from the print with a calibrated x 7 magnifier, the values expressed in micrometers.

Scanning electron microscopic study of size and incidence of vacuolar and non- vacuolar pores in the lining endothelium of Schlemm's canal

Tissue from normal, control and experimental eyes was dissected, critical point dried, mounted and coated as previously described. Mapping photographs were taken of the intact areas of lining endothelium, which were often smaller than would have been desired due to damage produced during dissections (vide supra), at a screen magnification of x 2000, using a T20-CSI-1 camera and 70 mm Ilford roll film. Prints (20 x 25 cm format) corresponding to an area of 3000 μ^2 and total magnification of x 4100 were produced.

The following features were counted on each print; cellular bulges, pores on bulges and pores not on bulges. The maximum width of all pores was measured on each print with the use of a calibrated x 7 magnifier and converted to microns. The pore diameters were grouped into size categories of 0.5 μm intervals, from 0-2.5 μm.

The area sampled in each eye varied from 36,000 μm^2 to 105,000 μm^2 (mean 55,000 μm^2).

Quantitative assessment of collector channel incidence by light microscopy

During the course of the investigation it became apparent that in some eyes the distended outer meshwork often occluded the entrance to collector channels. Since the obstruction of collector channels openings could have altered the resistance to aqueous outflow it was decided to undertake the following investigation.

Coded semithin sections were examined by light microscopy and the presence or absence of a collector channel draining Schlemm's canal was noted, as was occlusion by prolapse of the cribriform layer.

Examination of colloidal iron stained tissue : an attempt to quantify glycosaminoglycans

Colloidal iron has been used successfully in previous studies of GAGs in the trabecular meshwork (Table 2). Although both ruthenium red and colloidal thorium were investigated they both proved unsuitable due to the variability in staining quality and inadequate penetration, therefore they were not used in the quantitative investigation. Initially it had been hoped that image analysis and cationic dye preparations could have been used in conjunction to investigate whether 'washout' had taken place in the hyaluronidase treated eyes. However, the colloidal iron particles which appear as fine rod structures (50Å wide and over 100Å in length) lacked sufficient electron density and contrast for image analysis (vide supra).

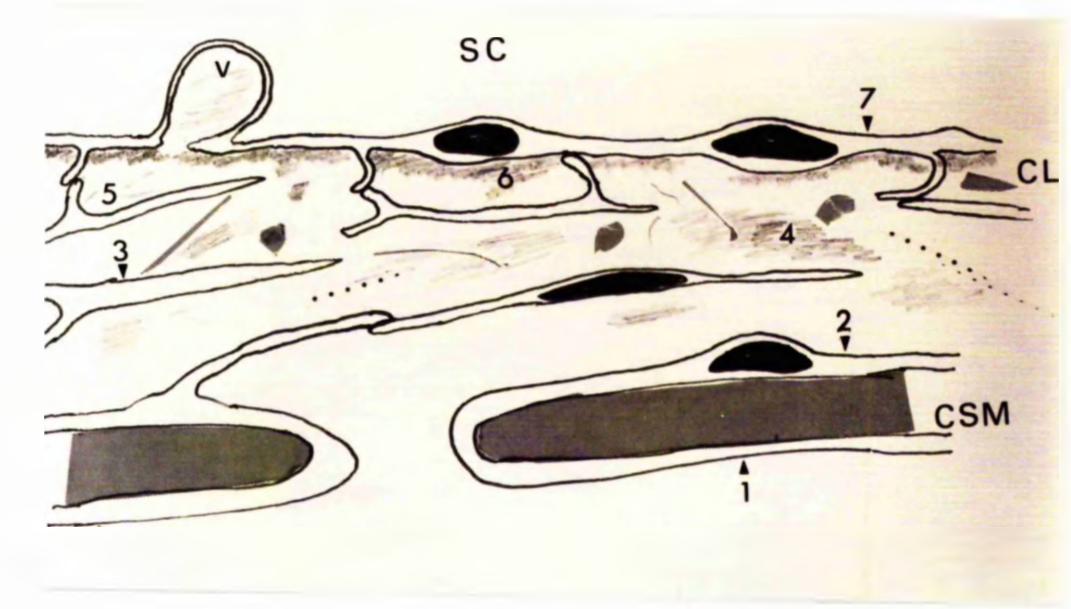

Figure 17: Diagram of the outer meshwork showing the seven sites at which the intensity of colloidal iron staining was scored.

1. Inner aspect of the trabecular endothelial cells.
2. Outer aspect of the trabecular endothelial cells.
3. Cell membranes in the cribriform layer.
4. Extracellular materials in the cribriform layer.
5. 'Empty space' - which in colloidal iron stained normal tissue contained fine strands of stain particles.
6. Sub-endothelial ground substance.
7. Lumen aspect of the lining epithelium of Schlemm's canal.

The only convenient way to assess the staining of GAGs in the tissue was to develop a scoring system for the area and degree of stain present in the extracellular tissue. Coded sections from colloidal iron treated blocks from each eye investigated were examined in the transmission electron microscope without further section staining. The intensity of staining reaction at seven sites (Fig 17) was judged and awarded a score of 0, absent; +, poor; ++, moderate; +++, intense. The staining reaction was judged in comparison to that present in the normal pig-tailed macaque outflow apparatus (Mn 1), which meant a maximum possible score of 21.

A separate count was made for the total vacuoles in the lining endothelium and the differences in the content of staining reaction was noted.

After all sections from a particular eye had been examined and scored, a guess was made as to whether or not it was control or experimental. At the end of this investigation the code was broken and the guess compared to the actual status of the eyes.

Quantitative assessment of inflammatory cell infiltration - by light microscopy

Inflammatory cell infiltration was a feature of many eyes investigated. Although this was not usually very marked it was considered necessary to assess as far as possible the degree of infiltration. It was hoped to elucidate whether the infiltration was as a consequence of the enzyme or whether it was part of a more general

response to the release of prostoglandins and leukotrines due to the invasive technique.

Semithin section stained with toluidine blue were examined by light microscopy and the number of inflammatory cells in the trabecular meshwork was recorded. Ten sections were studied in each eye. The types of cells were categorised by either polymorphonuclear leukocytes or 'other cells' (lymphocytes, tissue histiocytes and monocytes). Polymorphonuclear leukocytes were the most numerous and easily distinguished type of cell in these toluidine blue sections, but distinction between the other cells, which were less common, was more difficult.

Statistical analysis

All the data from quantative studies (Parts I and II) was stored in an ICL 2976 computer and retrieved at will for analysis using the MINITAB statistical package.

RESULTS

For the purposes of brevity the following terms will be used henceforth.

Normal; ie Mn 1, immersion fixed.

Control; those control eyes in Mn 2 to Mn 10 which received only Bárány's fluid.

Experimental; the hyaluronidase-treated eyes in Mn 2 to Mn 10.

Owing to unfortunate circumstances and manipulative failures which occurred in some experiments, the following eyes were excluded from the study henceforth and therefore are not considered in the statistical analysis. The main criteria which was used for exclusion of the following eyes were that the fellow eye was not subject to similar unfortunate circumstances, eg acute paracentesis, severe scleral compression, which therefore prohibited paired comparisons. The eyes excluded were Mn 2 right eye (control); Mn 5 left eye (experimental); Mn 8 right eye (experimental), Mn 9 left eye (control).

In some animals the general condition was less than statisfactory owing to unstable blood pressure or blood pH levels (due to CO_2 retention). These animals are retained in the study on the assumption that both eyes would be equally affected and that comparison of control and experimental eyes would be valid and indeed might provide

useful information.

The reasons for excluding specific eyes are as follows:

i) Mn 2, control eye:

The anterior chamber of this eye collapsed during cannulation and intraocular pressure remained low throughout the experiment. The excessively high flow rates observed in this eye wre probably a result of reconstitution of the corneoscleral envelope.

ii) Mn 5, experimental eye:

The anterior chamber of this eye collapsed both during cannulation and immediately prior to the physiological measurements. One consequence of this may have been the loss of enzyme from the anterior chamber. High flow rates in this eye were again probably a result of reconstitution of the intraocular fluid.

iii) Mn 8, experimental eye:

This eye also collapsed and remained flaccid before a separation in the tubing was discovered to be the cause of the leakage.

iv) Mn 9, control eye:

This eye suffered an unusual form of insult. A pair of Spencer-Wells forceps attached to the suture on the temporal bulbus had become trapped and the animal's head had slipped down, causing tension to be exerted on the eye. Flow rates wre negligible in this eye, presumably because the intraocular pressure was high.

The results of the physiological study are summarised in Table 4 and represented diagramatically in Figures 18 to

	Mn 2		Mn 3		Mn 4		Mn 5		Mn 6		Mn 7		Mn 8		Mn 9		Mn 10	
	CON	EXP	CON	EXP	CON	EXP	CON	EXP	CON	EXP	CON	EXP	CON	EXP	CON	EXP	CON	EXP
Flow rate at 18 mm Hg (µl/min)				***								***						***
$\bar{x}$	–	1.90	0	3.81	1.73	0	1.87	–	1.57	1.39	0	0.68	0.15	–	–	0.64	4.85	11.85
± S.D.	–	1.90	0	0.44	1.37	0	1.00	–	0.10	0.36	0	0.08	0.10	–	–	0.36	3.45	6.19
Flow rate at 22 mm Hg (µl/min)				**		***				***		**						*
$\bar{x}$	–	2.96	0.04	0.65	2.20	5.20	4.16	–	1.47	3.20	0.13	0.71	3.07	–	–	3.28	8.69	14.65
± S.D.	–	1.31	0.06	0.48	2.50	1.46	1.24	–	0.44	0.49	0.11	0.40	2.90	–	–	0.52	2.84	5.27
Outflow facility (µl/min/ mm Hg)	–	0.27	0.01	–0.79	0.12	1.30	0.57	–	–0.03	0.45	0.03	0.01	0.73	–	–	0.66	0.96	0.70
Total flow (µl)	–	61.10	1.10	46.60	46.70	44.90	76.00	–	41.4	69.8	1.90	13.80	36.50	–	–	50.60	171.50	348.60

Table 4: Table showing the results obtained for the physiological parameters in the nine pig tailed macaques.
* $p < 0.05$, ** $p < 0.01$, *** $p < 0.001$.

21. Of the seven control and seven experimental eyes only five are matched pairs. It can be seen that there is a great deal of variation between eyes in all parameters in both control and experimental groups.

At 18 mm Hg flow was not recorded in two control eyes (Mn 3, Mn 7) and one experimental eye (Mn 4). Paired t-tests on the differences in flow rates over the nine minutes, between control and experimental eyes showed that in three of the five pairs the values were significantly higher in the enzyme treated eyes (Mn 3, Mn 7, Mn 10). This is diagramatically represented in Fig 18. There was no difference in Mn 6 and in Mn 4 the flow rates were higher in the control eye.

The flow rate at 22 mm Hg was higher in most of the eyes than at 18 mm Hg but in three eyes there was little or no increase (Mn 3 control, Mn 7 control and experiment) and in two cases the flow rates were lower than at 18 mm Hg (Mn 3 experimental, Mn 6 control) which accounts for the negative facility of outflow. Paired t-tests on the differences in flow rates over the nine minute period between control and experimental eyes showed that in each of the five pairs there was a statistical difference (Fig 9).

The group results for each of the four parameters is summarised in Table 5. The group results of flow rates at 18 and 22 mm Hg in control and experimental groups were not statistically significant using a two-sample t-test and paired t-test due to the large variation between eyes and

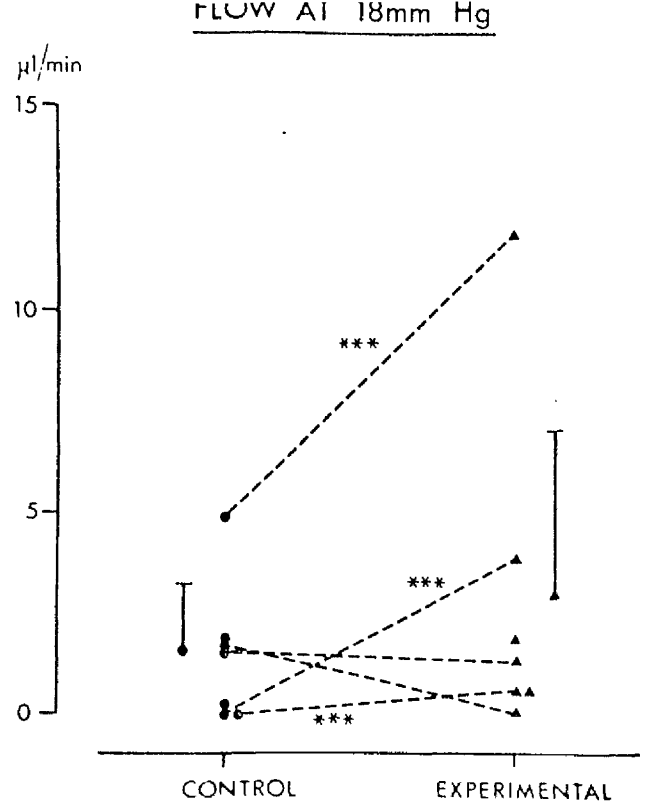

Figure 18: Diagrammatic representation of the results of the flow rates at 18mm Hg, showing individual results (five pairs) and the group mean ± S.D. * $p < 0.05$ ** $p < 0.01$ *** $p < 0.001$

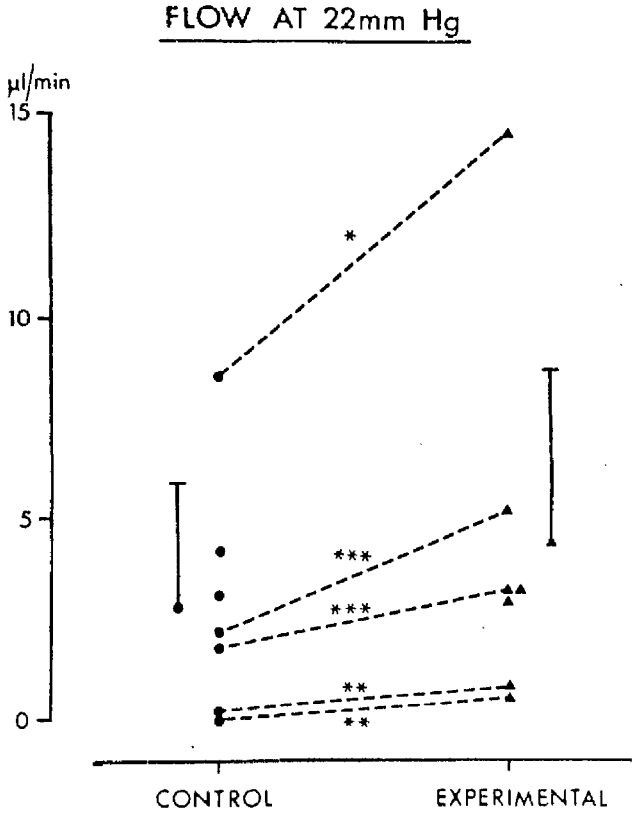

Figure 19: Diagrammatic representation of the results of the flow rates at 22mm Hg, showing individual results and group mean± S.D. Levels and significance as in Fig. 18.

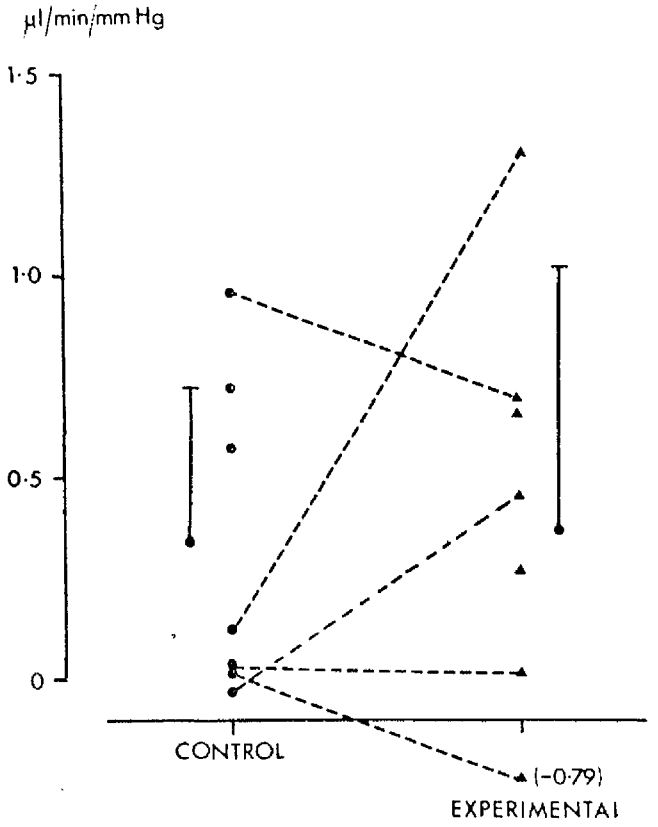

Figure 20: Results of aqueous outflow facility measurements in control and experimental eyes (5 pairs). Group mean ± S.D. are indicated.

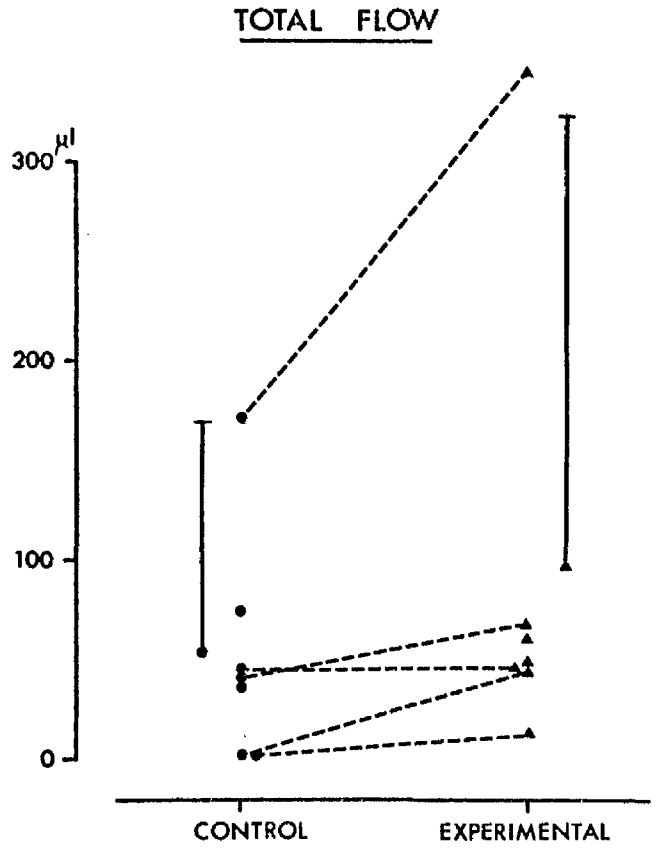

Figure 21: Results of the total amount of fluid which entered the eye during the experiment. Individual results and group results ± S.D. are indicated.

		Flow at 18 mm Hg	Flow at 22 mm Hg	Outflow Facility	Total Flow
Group mean (+ S.D.) n = 7	Control	1.42 ± 1.72	2.82 ± 2.99	0.34 ± 0.4	53.5 ± 58.2
	Exp.	2.89 ± 4.14	4.34 ± 4.8	0.37 ± 0.65	90.7 ± 115
	F-TEST F value	5.79 *	2.57	2.60	38.60 *
	TWO-SAMPLE t-TEST t value	- 0.86	-0.73	-0.10	0.76
	PAIRED t-TEST t value	1.27	2.37	0.34	1.60

Table 5: Table to show the group results for each of the four main physiological parameters and the results of the statistical analysis.

* $p < 0.05$

the small sample size. An F-test showed the the variation in the experimental eyes was significantly greater at 18 mm Hg flow rates.

The facility of aqueous outflow results were extremely variable (Fig 20) in only two of the five pairs was facility higher in the hyaluronidase treated eyes (Mn 4, Mn 6), in one case there was no real difference (Mn 7), and in two animals it was lower in the experimental eye (Mn 3, Mn 10). The group means appeared to be almost identical (Table 5, Fig 20).

The values for total flow, the volume of fluid entering the eye throughout the experiment were greater in the experimental eye in four of the five matched pairs (Table 4, Fig 21). Statistical analysis of the group results showed no statistical difference using two-sample t-test or paired t-test, however, there was a significant increase in the variance in the experimental group as indicated by the F-test (Table 5, Fig 21).

Despite the fact that the experimental group mean was higher in each of the four parameters, there was no statistically significant difference.

Summary

Hyaluronidase altered flow rates in the five matched pairs of eyes particularly at 22 mm Hg; facility of aqueous outflow was not affected. However, due to the small sample size and the great deal of variation between the values from different animals, analysis of the group results showed no significant difference between control and

hyaluronidase treated eyes.

THE MORPHOLOGY OF THE OUTFLOW APPARATUS IN THE PIG TAILED MACAQUE, NORMAL; CONTROL; AND EXPERIMENTAL EYES

The normal morphology of the pig tailed macaque outflow apparatus

The pig tailed macaque has so far never been used in this particular field of ophthalmic research and the normal anatomy of the outflow system is undocumented. In order to remedy this situation and to be fully conversant with the anatomy in the normal undisturbed state it was decided to investigate the morphology of the outflow system in two immerse fixed eyes (Mn 1).

The anatomic configuration of the angular tissues was essentially similar to that of other primates (Fig 22). The major differences between the pig tailed macaque and human outflow systems have been summarised in Table I in the general introduction. The description which follows will therefore emphasise features peculiar to this species of sub-human primate especially those which may have some effect on aqueous outflow dynamics.

The operculum or "operculum trabeculi" (Rohen, Lütjen and Bárány 1967) was not as prominent as in other sub-human primates, eg Cercopithecus aethiops, Macacae irus (Rohen, Lütjen and Bárány 1967), Papio cynocephalus (Grierson, Lee and Abraham 1979a, 1979b). This structure was situated on the inner surface of the meshwork. It extended from the

Figure 22: Light micrograph of the normal pig tailed macaque outflow system. (X 160).

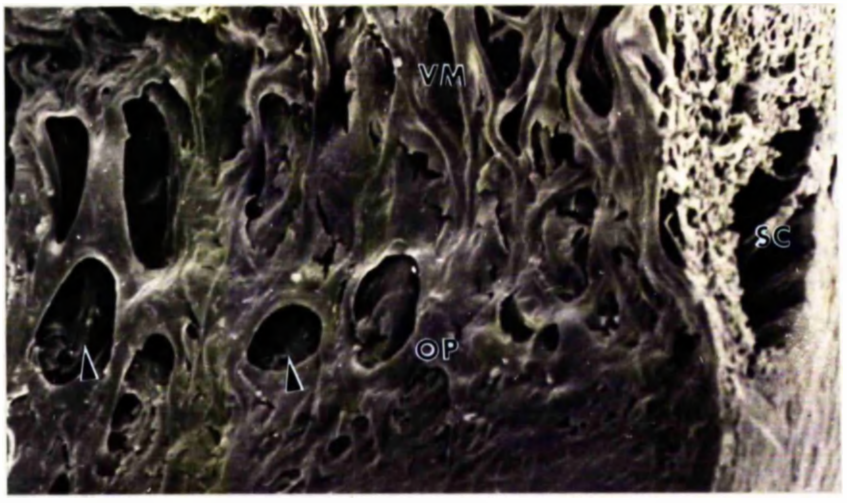

Figure 23: Scanning electron micrograph of the uveal trabeculae and operculum in the pig tailed macaque showing the large perforations (arrows). (X 170).

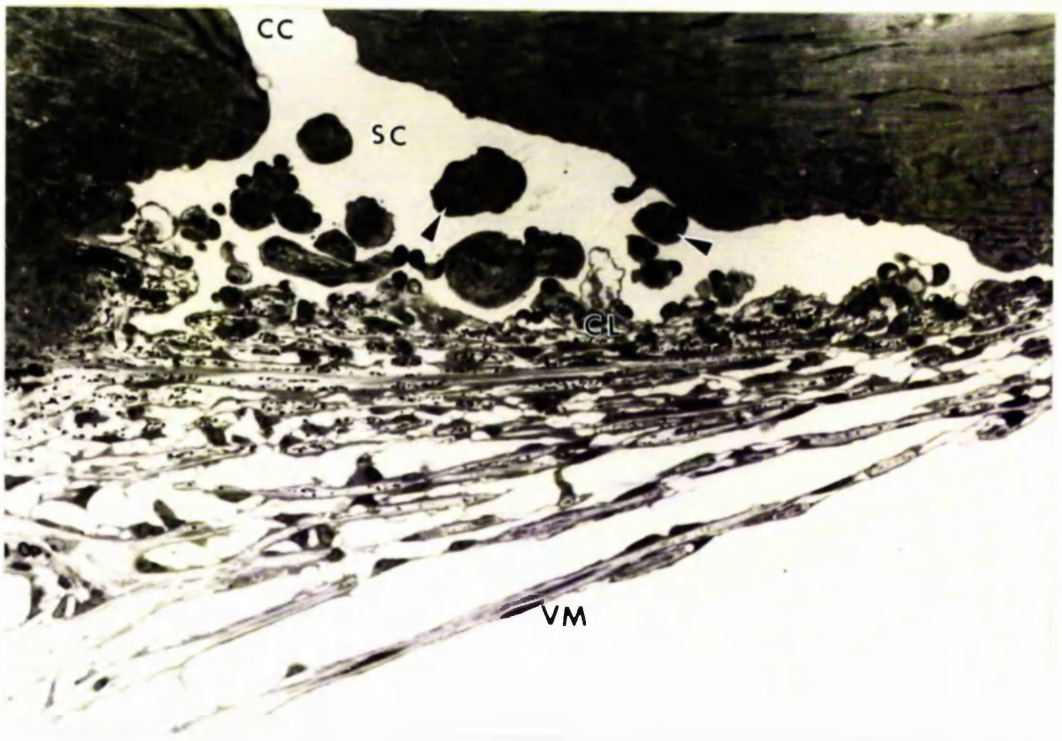

Figure 24: Light micrograph of the normal pig tailed macaque outflow apparatus. Note the numerous collagenous cords (arrows) in Schlemm's canal and the sheet-like uveal trabeculae. (x 370).

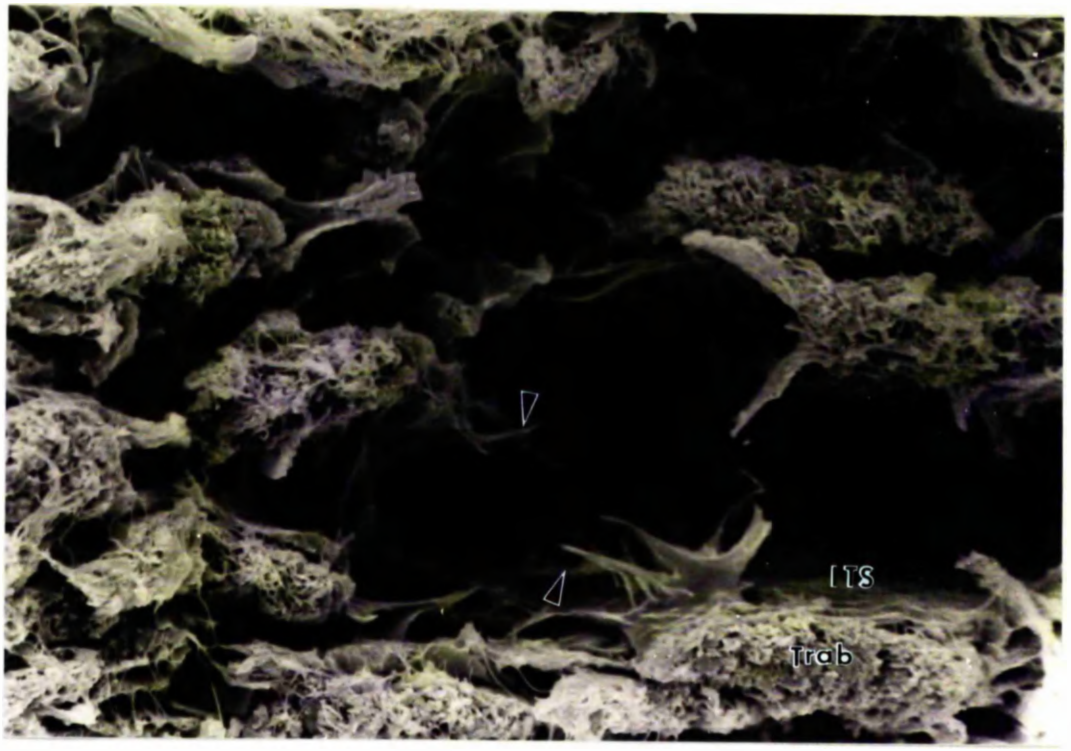

Figure 25: Scanning electron micrograph of the cut surface of the corneoscleral meshwork in the normal pig tailed macaque outflow apparatus to show inter and intratrabecular spaces and the numerous cytoplasmic processes of the trabecular endothelial cells(arrows). (X 1600).

corneal lamellae and Descemet's membrane to cover the anterior part of the meshwork, and merge with the often robust uveal trabeculae. It appeared to be totally absent in some isolated meridional sections (Fig 22) but scanning electron microscopy revealed that it was in fact present but was frequently interrupted by large perforations (20-150 μm).

This structure was of interest because if it had been well developed it may have protected the anterior half of the meshwork from aqueous flow and serve to direct flow more into the posterior half of the meshwork, however, this did not appear to be the case in this species.

Due to the diminuitive nature of the scleral spur, the trabeculae merged posteriorly with the ciliary muscle fibres and the loose connective tissue of the iris base (Fig 22). The intertrabecular spaces were largest in the inner or uveal meshwork (Fig 24), becoming more complex in the outer layers where they were traversed by numerous cytoplasmic processes from the trabecular endothelial cells (Fig 25). These fine projections contained very few organelles, the junctions with which they formed associations with other cells being their most characteristic feature (Fig 26 and 27). Trabecular endothelial cells were also seen to cross the intratrabecular spaces, forming incomplete 'membranes' over the perforations (Fig 26), which could possibly hinder fluid movement through these layers. The intertrabecular spaces which in conventional preparations appeared devoid

Figure 26: Transmission electron micrograph of the normal trabecular meshwork in the pig tailed macaque. Note the cytoplasmic 'membranes' over the intratrabecular spaces (arrows), the compact cribriform layer and the 'giant vacuoles' (X 1600).

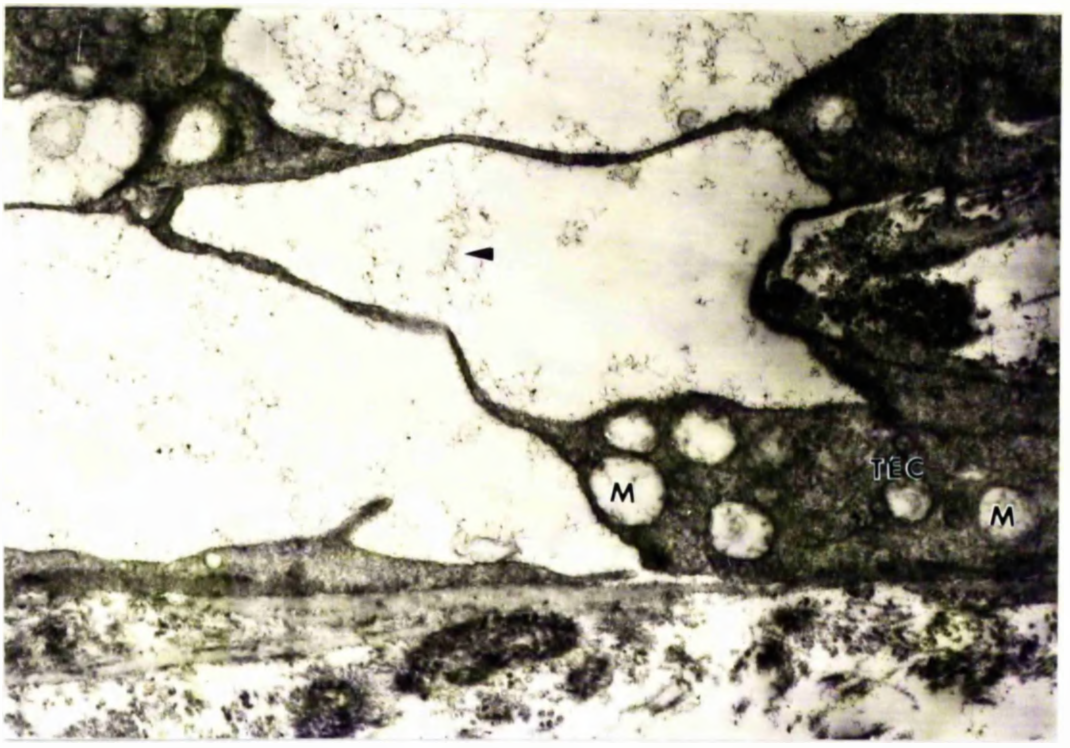

Figure 27: Transmission electron micrograph (colloidal iron preparation) showing the stained particles in the intratrabecular spaces (arrow), cell membranes and in the trabeculae of the normal pig tailed macaque (X 14,500). Note the distended mitochondria.

of any material, were seen in colloidal iron stained tissue to contain fine networks or strands of stain (Fig 27). The surfaces of the trabecular endothelial cells lining the spaces also had a rich coating of iron particles, suggesting the presence of glycosaminoglycans.

The arrangement of the trabeculae was identical to that described in the general introduction. Colloidal iron stain was found within the trabeculae in association with the ground substance, and collagen fibrils but did not penetrate the elastic-like fibres, curly collagen or basement membrane material (Fig 27). Most of the cells in the outflow system in both normal eyes (Mn 1) contained swollen and distended mitochondria with disrupted cristae, probably as a result of delayed fixation (immersion).

One of the more unusual features of this species was that extensions of the ciliary muscle appeared to penetrate more anteriorly than in other species and were more circumferentially orientated than the longitudinal muscle fibres. The groups of smooth muscle cells were not found in many sections in each eye, therefore did not run round the complete circumference. However, they were found in 11 of the 20 eyes (normal, controls and experimentals), which was consistent enough to suggest they were a real entity and deserved further investigation.

The bundles of smooth muscle cells (5-20 cells, Figs 28 and 29) were located at the posterior end of the meshwork, adjacent to the diminu tive scleral spur. The cell ultrastructure was characteristic of smooth muscle:

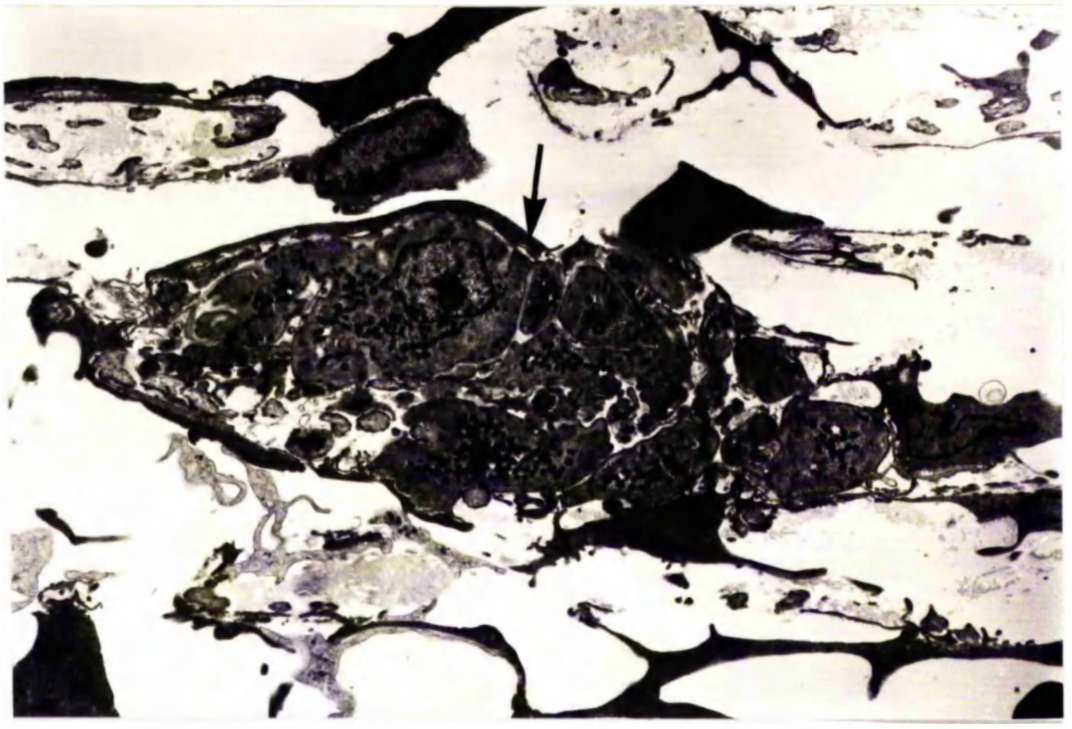

Figure 28: Transmission electron micrograph to show a bundle of smooth muscle cells (arrow) in the trabecular meshwork (Mn 2), (X 3000).

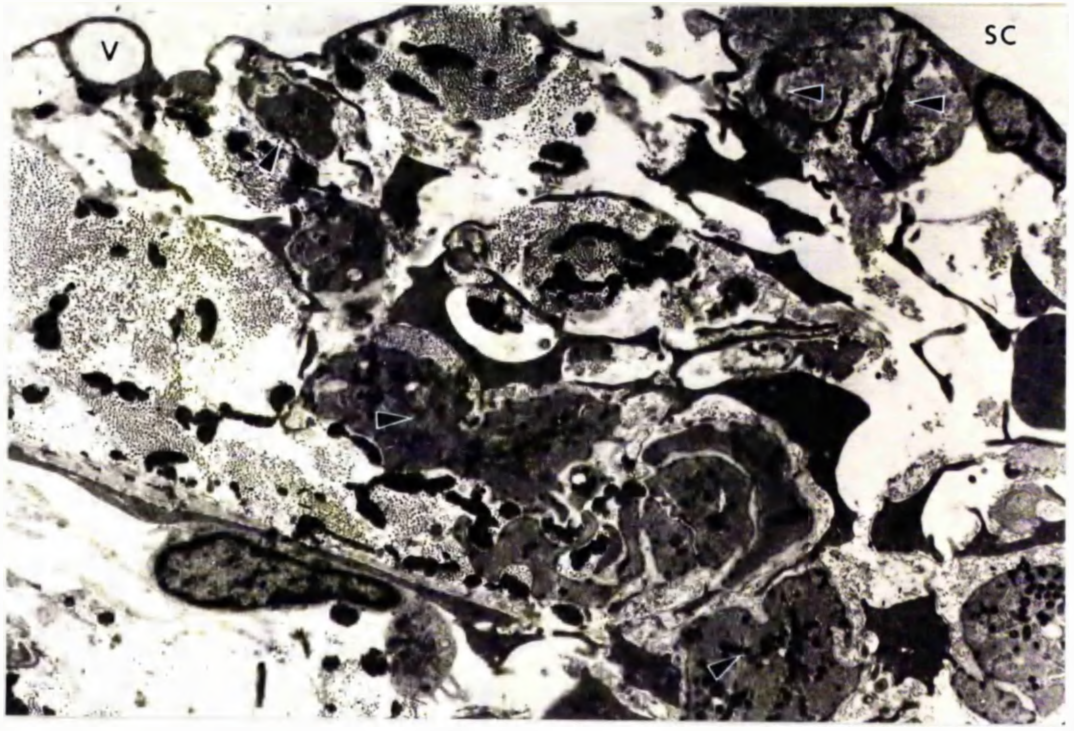

Figure 29: Transmission electron micrograph to show smooth muscle cells (arrow) in the cribriform layer in the pig tailed macaque outflow apparatus (Mn 8), (X 4500).

Figure 30: Transmission electron micrograph showing higher magnification of area in Fig. 29. Note the smooth muscle cells coming into contact with the cells in the cribriform layer (small arrow) and in close association with the lining endothelium (large arrow). N - nerve bundle (X 10,000).

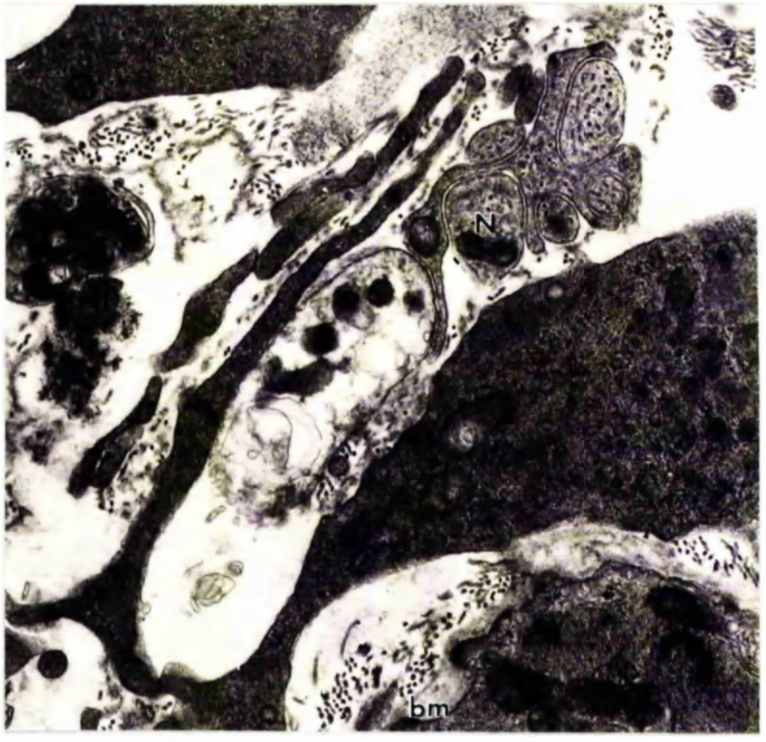

Figure 31: Transmission electron micrograph. Higher magnification of nerve bundle in Fig. 30, lying in intercellular space in the trabecular meshwork, near smooth muscle cells (arrow), (X 24, 700).

small compact mitochondria; microfilament rich cytoplasm with condensations adjacent to the cell membrane; and a thick basement membrane surrounding the cell only interrupted in regions of cell-to-cell junctions (gap junctions and macula adhaerentes) (Figs 28, 29, 30 and 31). Small bundles of unmyelinated nerve fibres were often seen in the loose connective tissue in close proximity to these muscle cells (Figs 29, 30, and 31), but no neuromuscular junctions were observed. In some areas the smoooth muscle cells were seen in association with the trabecular endothelial cells, the native endothelial cells of the cribriform layer and the endothelial monolayer of Schlemm's canal (Figs 29 and 30).

The cribriform layer of the trabecular meshwork was similar to that of other primates in the sense that it lacked the organisation of the inner layers of the meshwork, consisting instead of cells loosely arranged in an extracellular matrix (Fig 32). However, there were cells in the cribriform layer which appeared larger and more specialised than the flat fibrocyte-like cells (Fig 32). They were up to 15 µm in both vertical and horizontal directions within one section and probably sent ramifications over much greater distances in the cribriform layer. They were connected by junctions not only to each other but to endothelial cells of the corneoscleral meshwork and most importantly to the lining endothelium of Schlemm's canal. The cells are very rich in cytoplasmic microfilaments (10 nm diameter) which as well as being

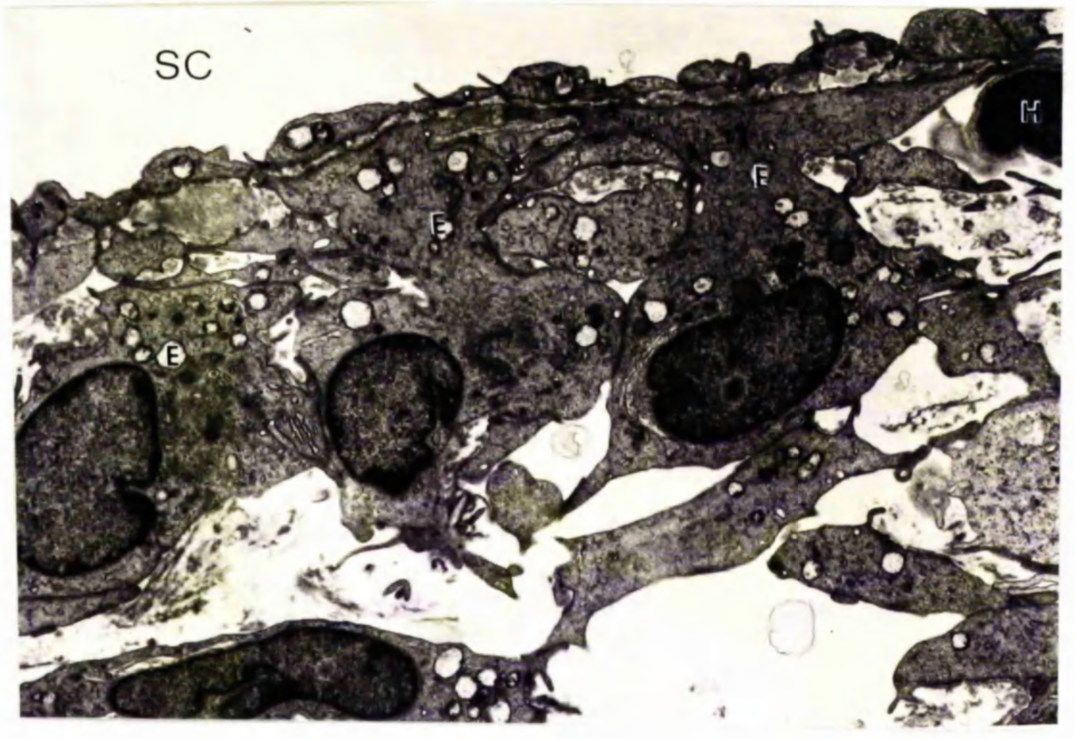

Figure 32: Transmission electron micrograph of the cribriform layer in the normal pig tailed macaque outflow apparatus. Note large endothelial cells (E) which are attached to the lining endothelium. (X 4600).

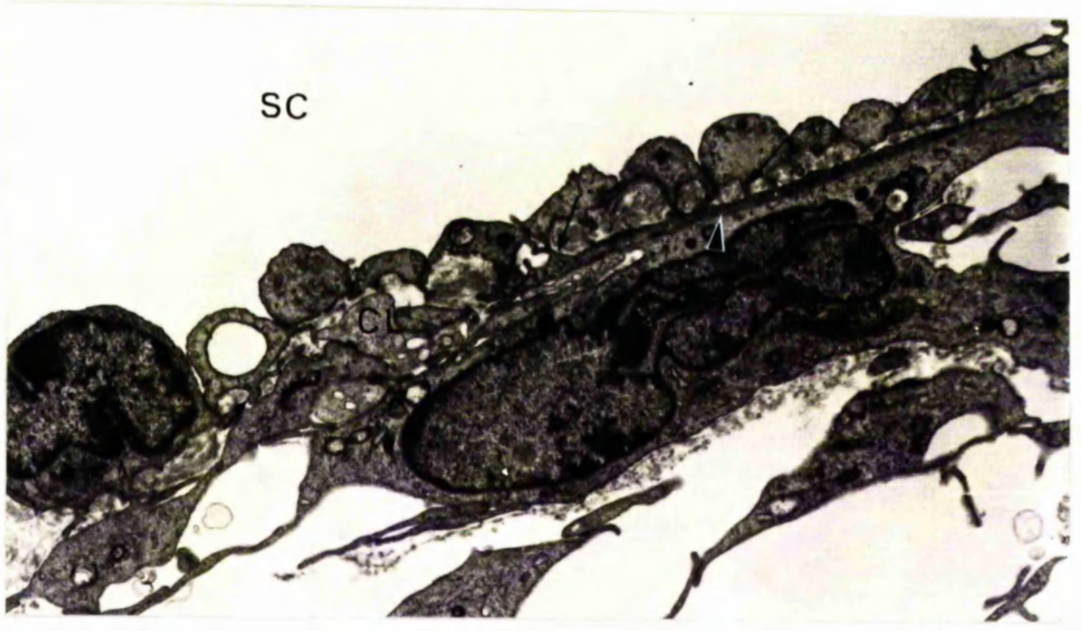

Figure 33: Transmission electron micrograph of cribriform layer showing a large endothelial cell in the cribriform layer of normal tissue. Note condensation of microfilaments in these cells (large arrow) and 'pegs' (small arrows) in the lining endothelium. (X 5900).

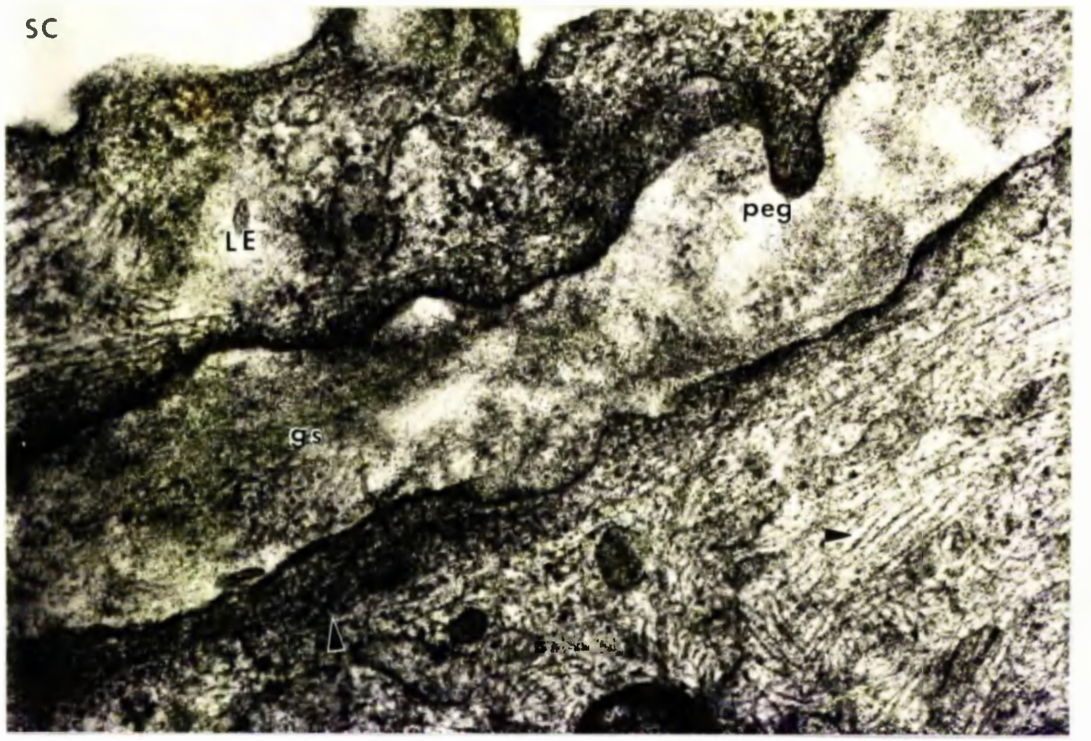

Figure 34: High power transmission electron micrograph to show lining endothelium, sub-endothelial ground substance, and 10 nm microfilaments (arrows) in cells of the cribriform layer. (X 60,000).

loosely dispersed in the cytoplasm are found in bundles near junctions and most noticeably at the cell margin directly under the lining endothelium (Figs 33 and 34). In this latter site the monolayer and the specialised cells had numerous connections in the form of small cytoplasmic 'pegs'. The 'pegs' were more frequent on the lining endothelium (Fig 33).

The extracellular elements in the cribriform layer consisted of a mixture of materials: the ground substance which was particularly abundant under the lining endothelium (Figs 32, 33, 35 and 36); collagen fibrils, often 'lost' in processing to leave only the 'ghosts' (Fig 35); and electron dense plaques (Fig 35). In colloidal iron stained material (with and without conversion to prussian blue) staining reaction was noted around collagen 'ghosts'; at the periphery of electron dense plaques; on all cell surfaces; but was most intense in areas where ground substance was abundant. Colloidal iron particles were also seen in loose strands in the few 'empty spaces' of the cribriform layer.

The 'giant vacuoles' in the lining endothelium of Schlemm's canal were identical to the description in the general introduction (vide supra). Openings on the trabecular aspect of 'giant vacuoles' were noted, but pores on the canal aspect were not seen in either of the two normal eyes in the sections studied (no serial sectioning was carried out). In conventional TEM sections it was evident that a large proportion of the vacuoles contained

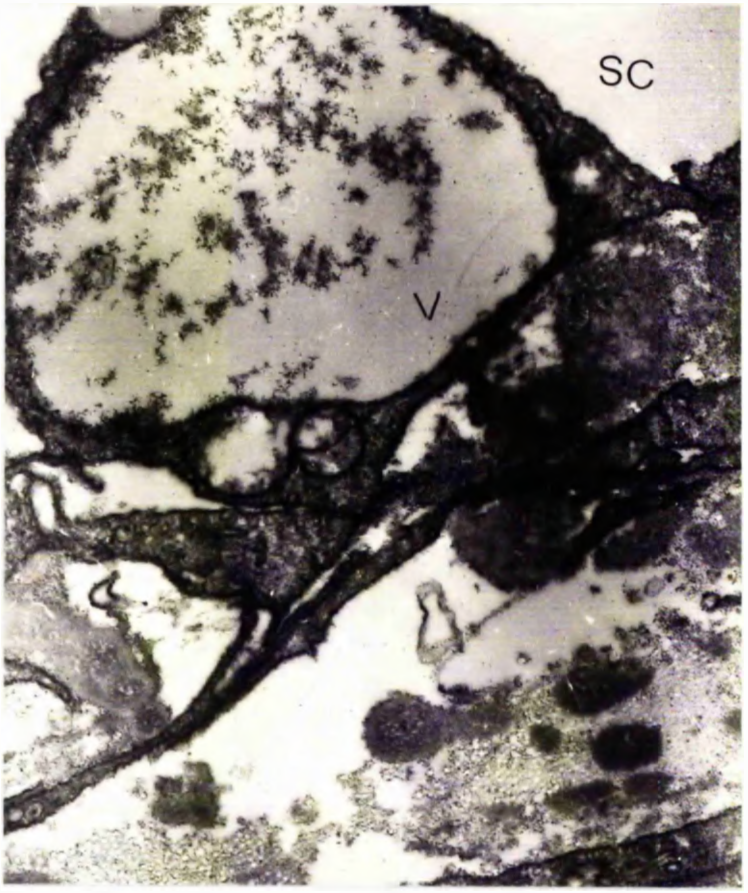

Figure 35: Transmission electron micrograph of colloidal iron stained normal pig tailed macaque tissue (converted to prussian blue), to show distribution of stain on all membranes, extracellular materials and in the lumen of the 'giant vacuole'. (X 15,200).

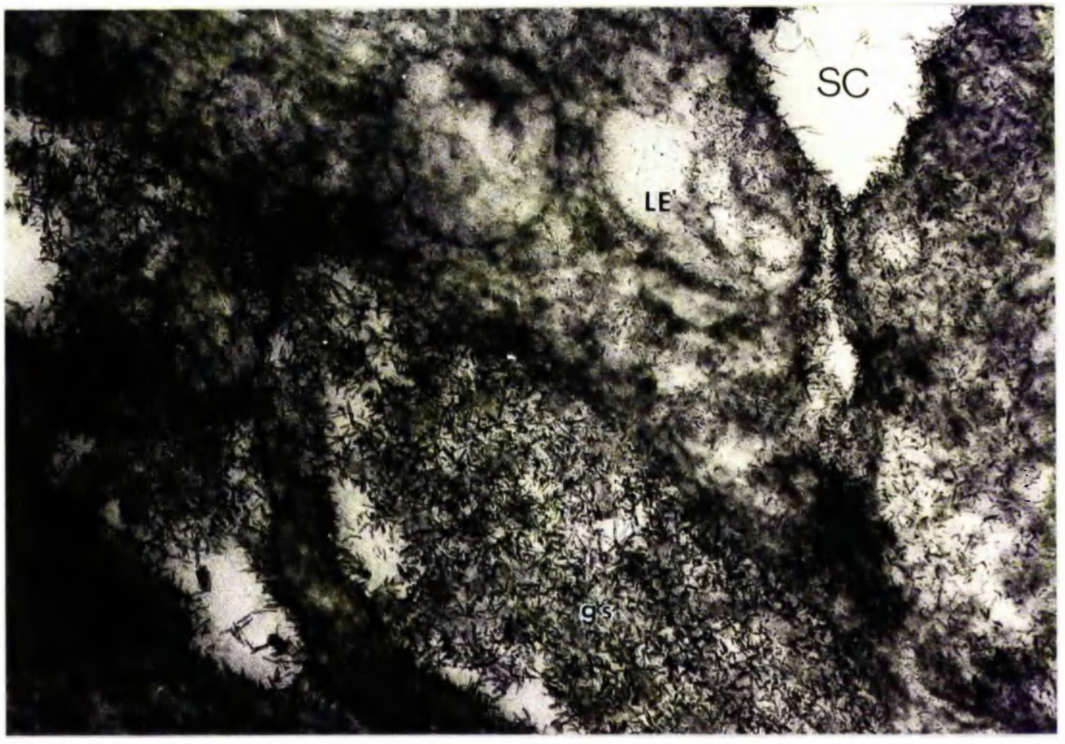

Figure 36: Transmission electron micrograph of colloidal iron stained normal pig tailed macaque tissue. Rich staining of sub-endothelial ground substance and cell membranes. (X 96,000).

loose ground substance within their lumens (Fig 26). This was confirmed in colloidal iron treated tissue (Fig 35), where the stain commonly appeared clumped but was also seen to be evenly dispersed in other cases. 'Giant vacuoles' also frequently contained fine delicate membranous structures or 'cell profiles'.

The topography of the trabecular wall of Schlemm's canal was very complex in this species (Fig 24 and 38). In the few reasonably flat areas the topography was similar to that of other primates (Fig 37). The long narrow cells which make up the monolayer of the inner wall were orientated parallel to the long axis of the canal (circumferential) and bulges protruded into the canal lumen. These bulges comprised of both nuclei and 'giant vacuoles' and it was only when the vacuoles showed signs of collapse (Fig 37) (artefactually produced during preparation) that one could with certainty differentiate between the two. Real vacuolar and non-vacuolar pores were rarely encountered in the samples of tissue studied, however, artefactual pores with their distinctive ragged edges were more frequent.

The convoluted nature of the trabecular or inner wall of Schlemm's canal and the numerous collagenous 'islands' and septae in the canal lumen were frequently noted in meridional sections (Fig 24). The true nature of these features was, however, best illustrated by scanning electron microscopy (Fig 38). The collagenous 'islands' were in fact cord or rope-like structures which ran

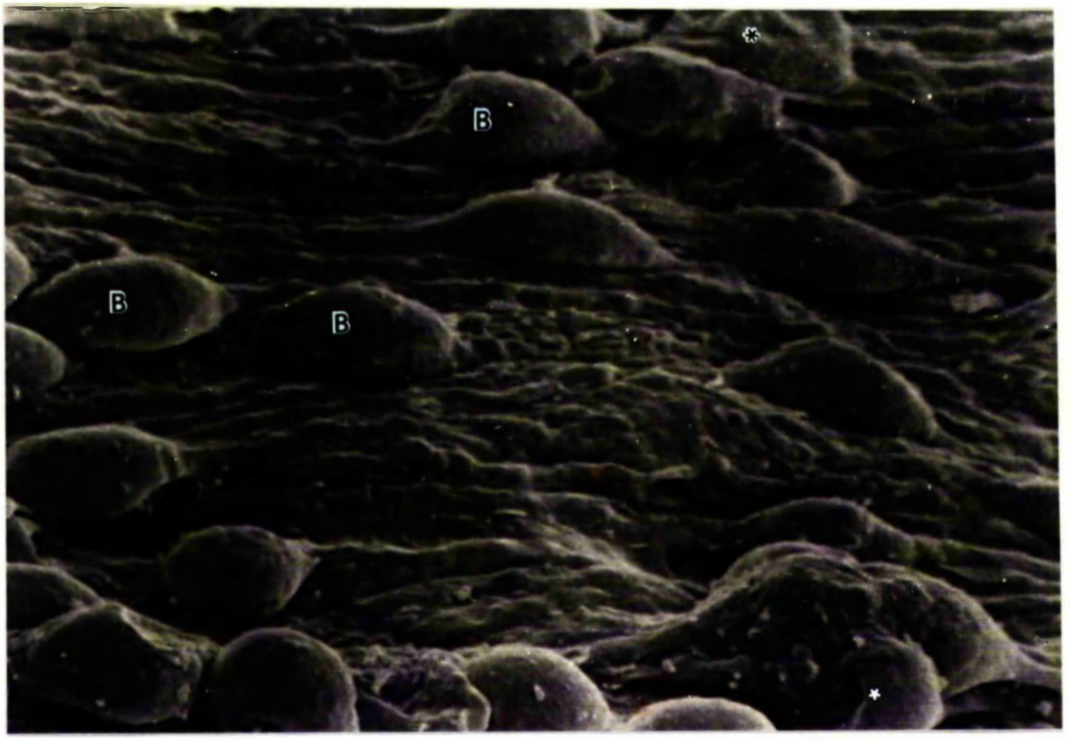

Figure 37: Scanning electron micrograph of the lining endothelium of the trabecular wall of Schlemm's canal. Note bulges (B) those which are collapsed (*) are probably 'giant vacuoles'. (X 3100).

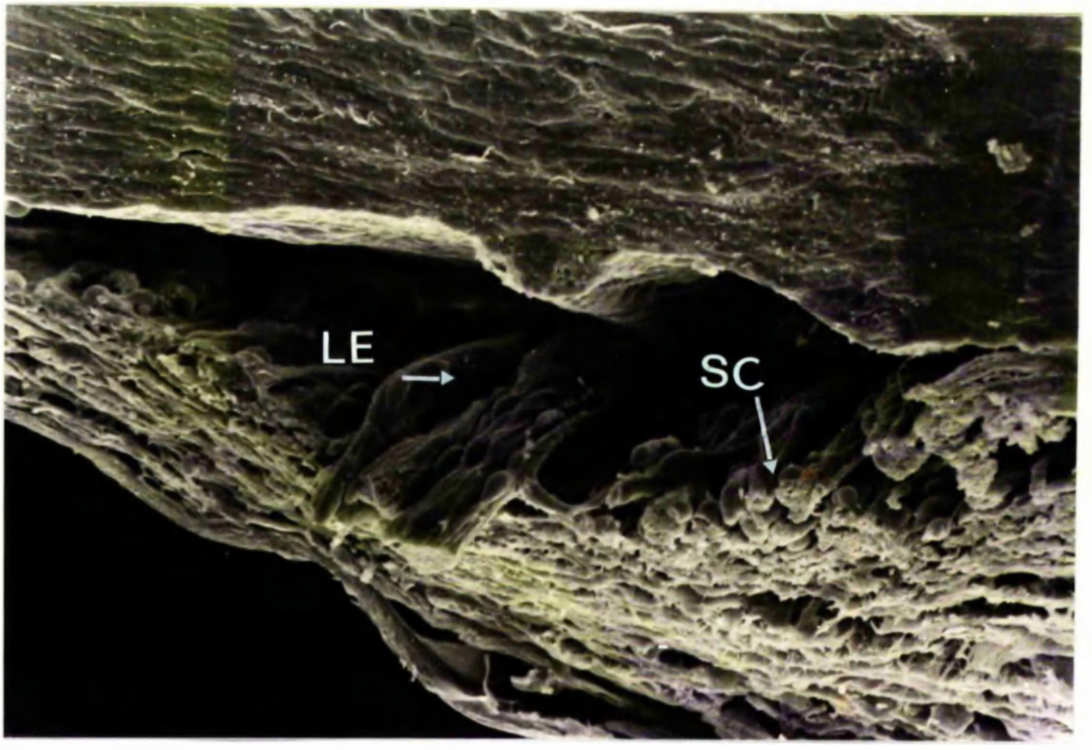

Figure 38: Scanning electron micrograph of the cut surface of outflow apparatus in normal tissue to show the collageneous cords (arrows) in Schlemm's canal. (X 560).

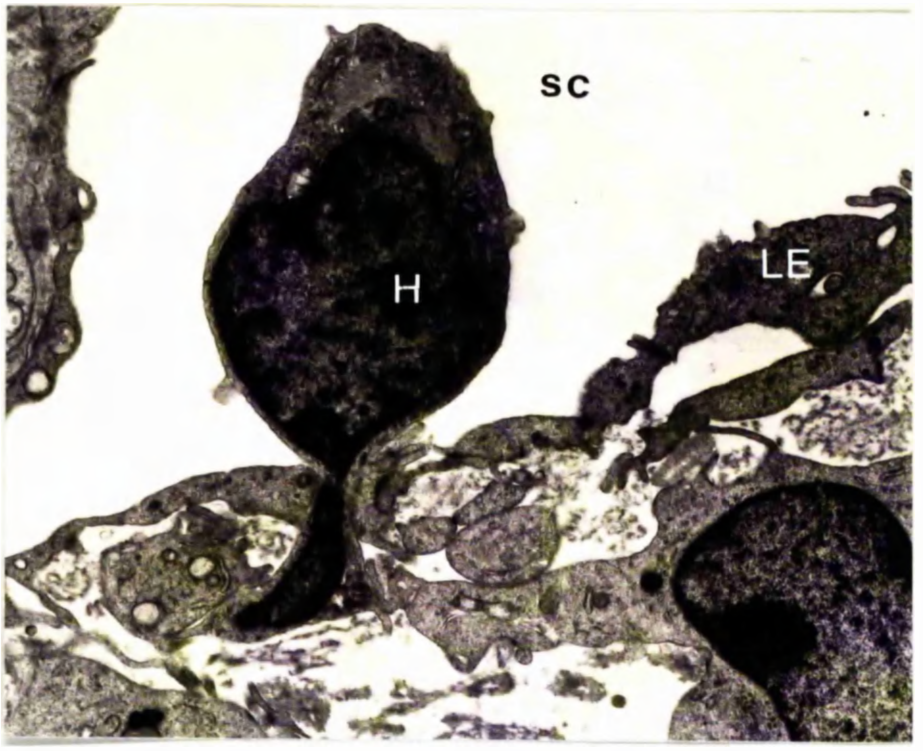

Figure 39: Transmission electron micrograph to show tissue histiocyte migrating through the lining endothelium in normal pig tailed macaque. (X 7600).

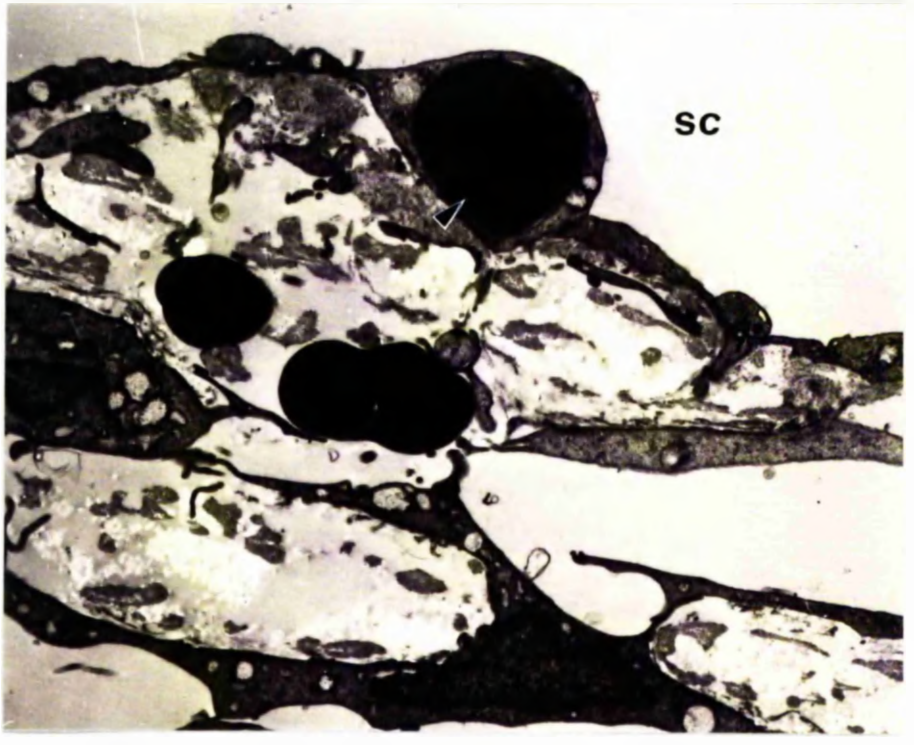

Figure 40: Transmission electron micrograph to show erythrocytes both in the cribriform layer and contained within the lumen of a 'giant vacuole', normal tissue. (X 4100).

parallel to the long axis of the canal, and occasionally seen to merge with both the inner and outer walls (also seen in meridional sections). These cords varied in diameter from a few micrometers to 50-60 μm, and had a complete covering of endothelial cells, whose nuclei bulged into the canal lumen (Fig 24 and 38). More obvious septae which bifurated Schlemm's canal were rare in this species of primate. These cords may serve as support for the inner wall of Schlemm's canal.

Cells other than endothelial cells were relatively common in the normal outflow apparatus of the pig tailed macaque. Which of these cells were native tissue histiocytes-macrophages and which were blood borne cells only passing through the tissue was in most cases impossible to distinguish. The cells which were adherent to the trabeculae and in some cases within the connective tissue core, appeared to be phagocytosing debris and were therefore considered to be native tissue histiocytes. Other cells were seen in the cribriform layer (Fig 32) or within the lining endothelium, 'in transit' (Fig 39). These cells were usually lymphocytes or monocytes. Polymorphonuclear leucocytes, plasma cells and mast cells were not present in any of the sections examined in these normal eyes. A few erythrocytes were seen in some sections within the cribriform layer, and in one case within the lumen of a 'giant vacuole' (Fig 40).

The morphology of the outflow apparatus after prolonged perfusion with Bárány's fluid

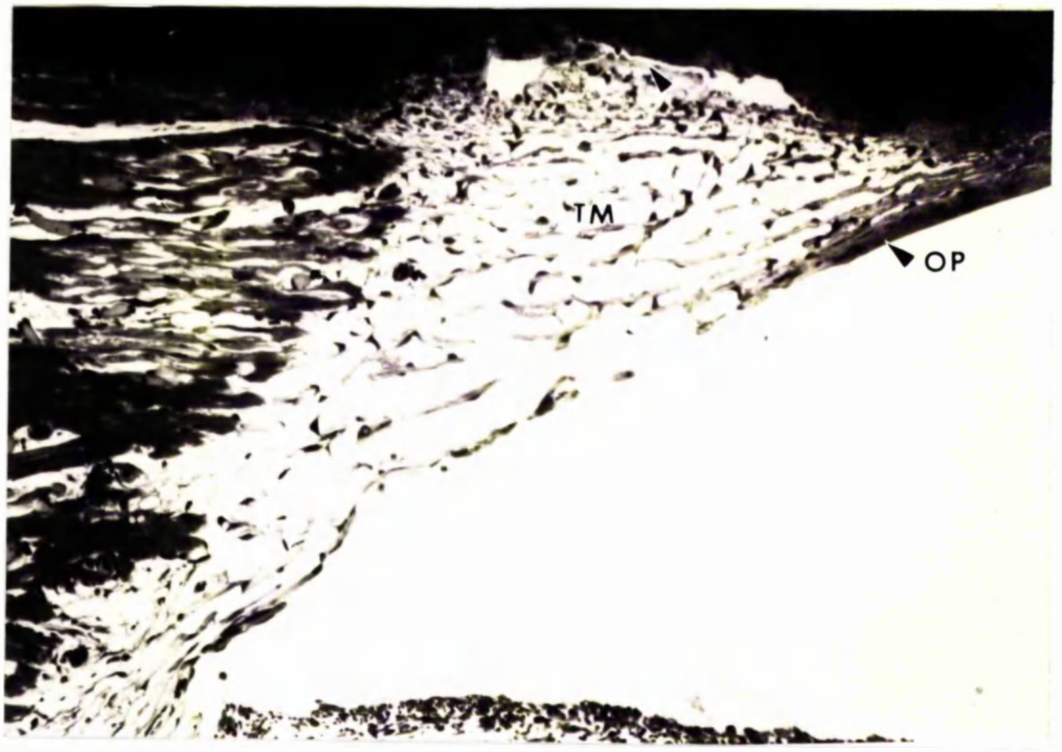

Figure 41: Light micrograph of control tissue to show the distension of the trabecular meshwork, particularly the outer meshwork, and narrowing of Schlemm's canal. (Mn3), (X 150).

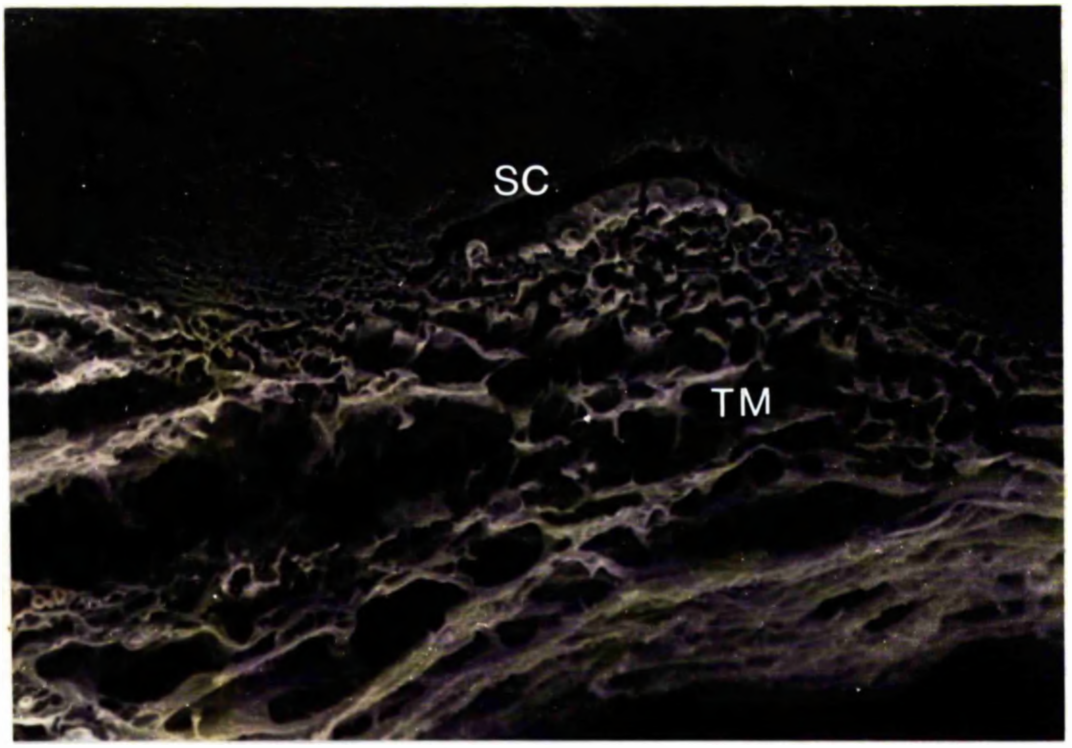

Figure 42: Scanning electron micrograph to show the distension of the meshwork and narrowing of Schlemm's canal in control tissue (Mn10) (X 280).

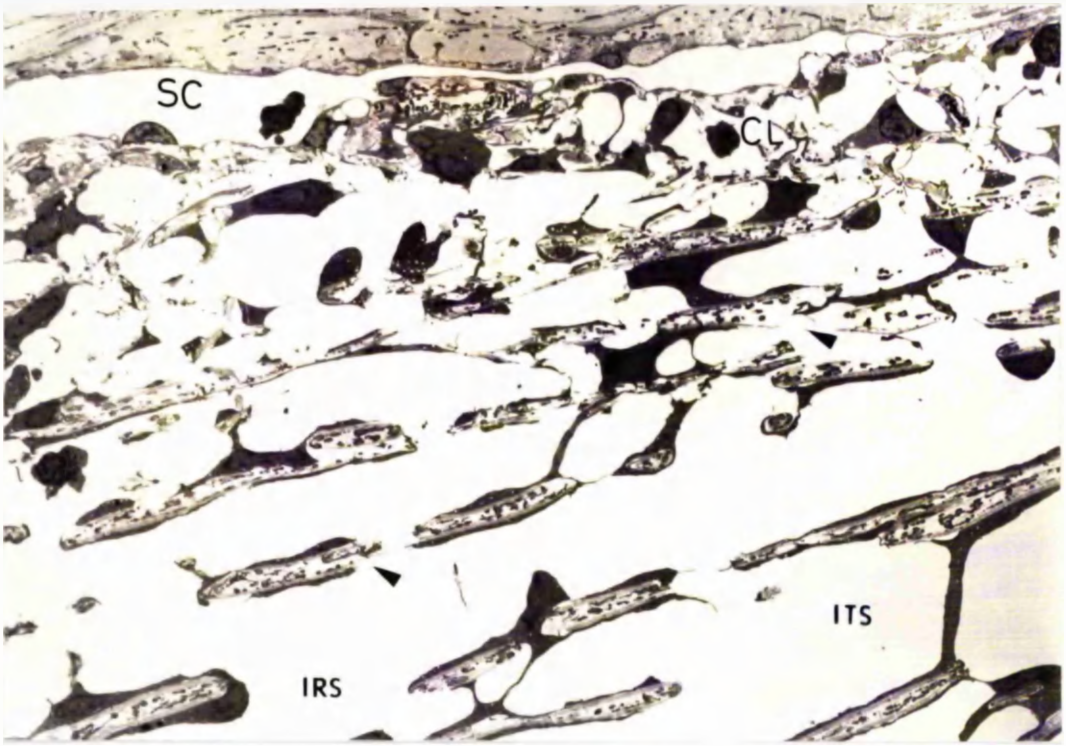

Figure 43: Transmission electron micrograph of the pig tailed macaque outflow apparatus, control tissue (Mn3). Note the large inter and intratrabecular spaces in the corneoscleral meshwork, denuded trabeculae (arrows) and distension of the cribriform layer. (X 1300).

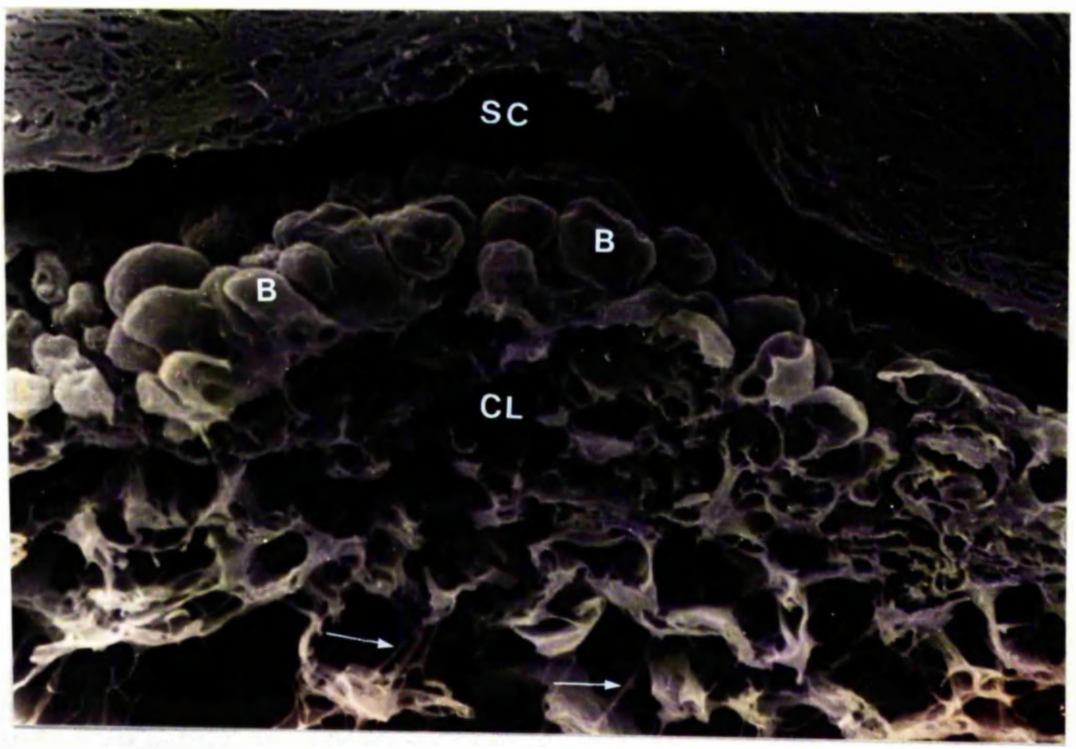

Figure 44: Scanning electron micrograph of the outer meshwork. Note the stretched cytoplasmic processes (arrows), and the lining endothelium with abundant vacuolar bulges(B), control tissue(Mn 10). (X 930).

Tissue from control eyes was studied to investigate the morphological effects of prolonged perfusion with Bárány's fluid on the pig tailed macaque outflow system. Attention was paid to those features which differed from the normal unperfused eyes.

The longitudinal ciliary muscle fibres, which are normally compact, in some regions had excessively wide clefts between the fibre bundles (Figs 41 and 42). The trabecular meshwork had wide inter and intratrabecular spaces giving the tissue a dilated or distended appearance, with a narrowed canal of Schlemm.

The large inter and intratrabecular spaces in the uveal and corneoscleral meshwork were a consequence of changes in the trabecular endothelial cells. The delicate cytoplasmic projections which crossed the intertrabecular spaces were lost or stretched into very fine thread-like processes (Figs 43 and 44). The membrane-like extensions of the cells which crossed the intratrabecular spaces in normal eyes were also lost (Fig 26 and Fig 43). In some regions the connective tissue core was disturbed where there was incomplete cell cover. The widened intertrabecular spaces did not contain a network of colloidal iron particles (Fig 45) as seen in normals. The staining of cell surfaces lining the spaces was also poor in comparison to normal tissue, however, the trabecular cores showed normal affinity for the colloidal iron particles.

In the cribriform layer there was often a great deal of distension (Figs 43, 44 and 46), although there was some

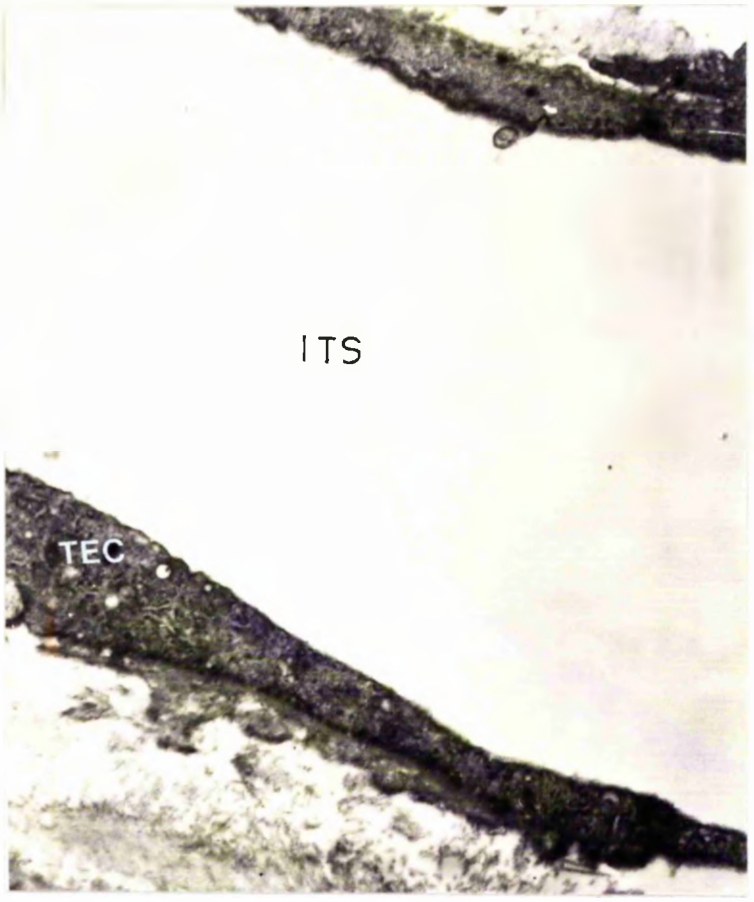

Figure 45: Transmission electron micrograph of control tissue (Mn10) stained with colloidal iron to show absence of stain particles in the intertrabecular spaces and on the cell membranes. (X 8800).

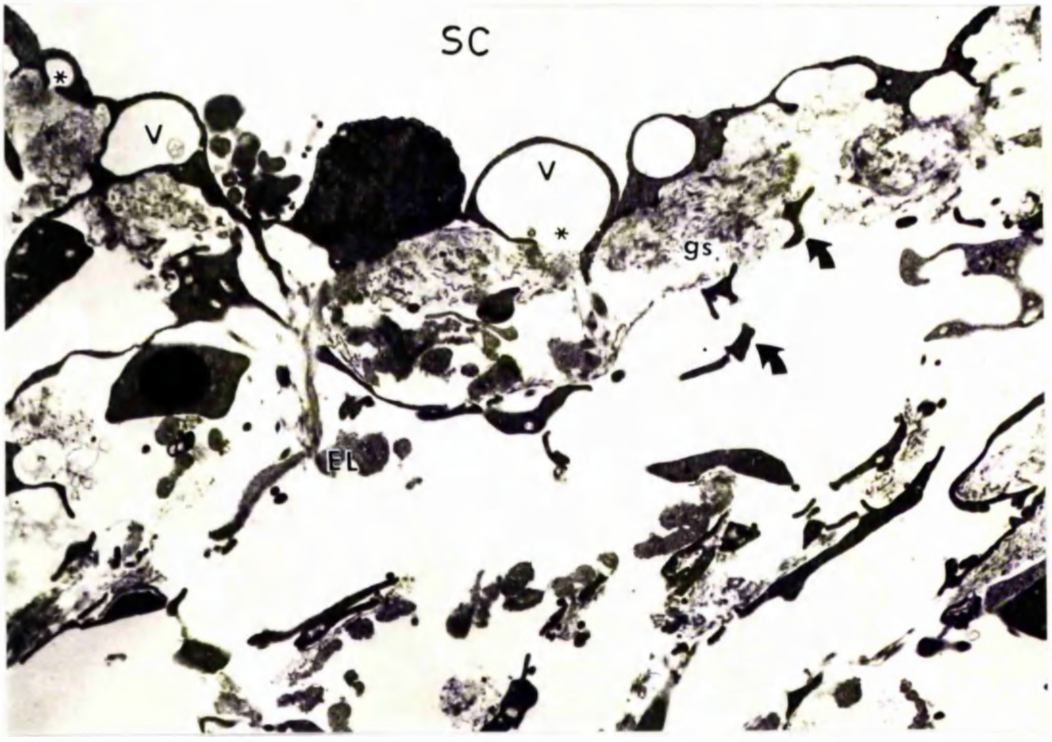

Figure 46: Transmission electron micrograph of control tissue (Mn7). Note the distended cribriform layer, containing ground substance, elastic-like material and isolated pieces of cell cytoplasm (arrows). 'Giant vacuoles' are abundant some of which have an opening on the trabecular aspect (*).

variation from region to region within the one eye. There were large electron lucent spaces and the endothelial cells were orientated more at right angles to the lining endothelium than in normal eyes (Fig 26 and Fig 46). The large specialised cells seen in this layer in the normal tissue, were unrecognisable in these control eyes since they were probably stretched into fine processes, in a similar fashion to the other endothelial cells. The ultrastructure of the cells in this layer seemed normal, the cytoplasm of the fine processes contained few organelles with the exception of microfilaments.

In some regions of the cribriform layer there was undoubtedly a 'washout' of extracellular materials (Fig 54), which usually coincided with areas of high vacuolar incidence, suggesting high flow pathways. In other regions, however, it was more difficult to ascertain if there had been a genuine loss of extracellular material or whether the normal amount of material was still present but was surrounded by a greatly increased area of electron lucent spaces, thus appearing as a loss (Fig 46 and 50). The ground substance under the lining endothelium was seen to persist even in apparent high flow areas (Fig 50) and in some cases was clearly seen to plug the trabecular openings of 'giant vacuoles' (Fig 46 and 54). This ground substance, as in normal eyes, stained intensely with colloidal iron. The large electron lucent spaces in the cribriform layer were devoid of fine strands of colloidal iron particles and the cell surfaces in this layer were in

general also less intensely stained than normals.

By conventional TEM the lumen of most vacuoles were electron lucent (Fig 43, 46, 50 and 54), however, in colloidal iron preparations about half of the vacuole population contained some staining reaction, on the internal membrane and in the lumen as either a diffuse staining reaction or as a fine network of strands of iron particles (Fig 47). Other vacuoles were devoid of stain.

The 'giant vacuoles' had a patchy distribution within each eye, ranging from being very abundant (Fig 44, 50 and 54) to being relatively scarce (Fig 43). Some of the greatly distended regions had fewer vacuoles. The lining endothelium had fewer connections with both the cells and the extracellular elements of the underlying cribriform layer, ie the 'pegs' described in the normal tissue.

The 'giant vacuoles' were often of a greater diameter (up to 15 μm) than in normal eyes. Figure 48 shows an unusual view of 'giant vacuole' which was opened during tissue preparation. The vacuole was a thin walled structure which was crossed internally by delicate cellular membranes, partly subdividing the lumen. The opening shown on the canal aspect could represent the outer part of a transcellular channel.

Vacuolar pores and non-vacuolar pores in the lining endothelium of Schlemm's canal were more easily seen by examining the dissected trabecular wall by SEM (Fig 49). Non-vacuolar pores were also occasionally seen by TEM (Fig 56) as membrane bound interruptions in the endothelial

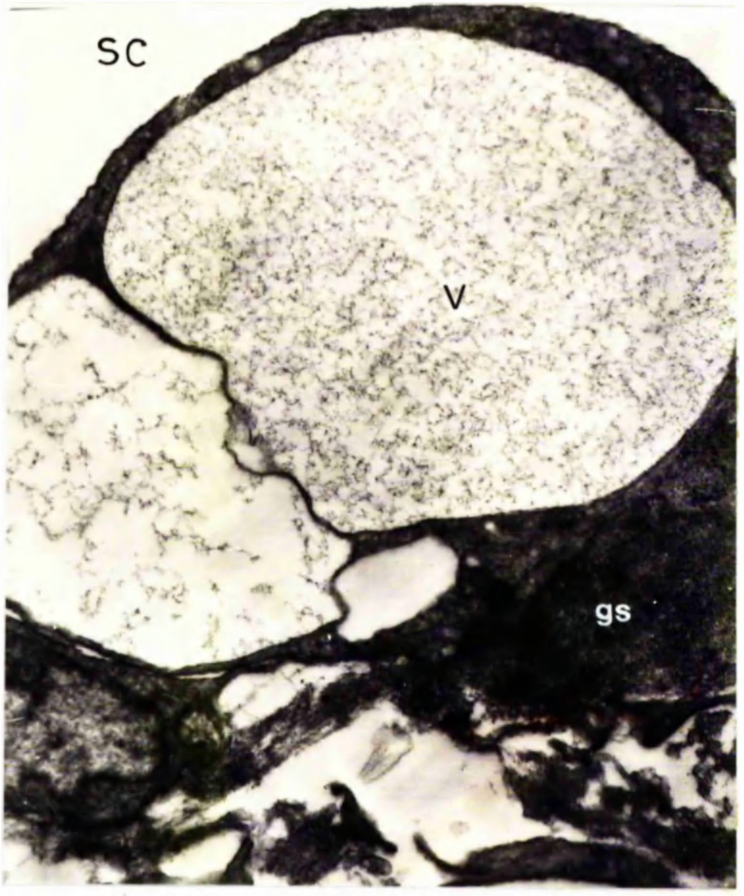

Figure 47: Transmission electron micrograph of colloidal iron stained control tissue (Mn10) in which two compartments of a 'giant vacuole' contain stain particles. The stain is most dense in one of the compartments. (X 9100).

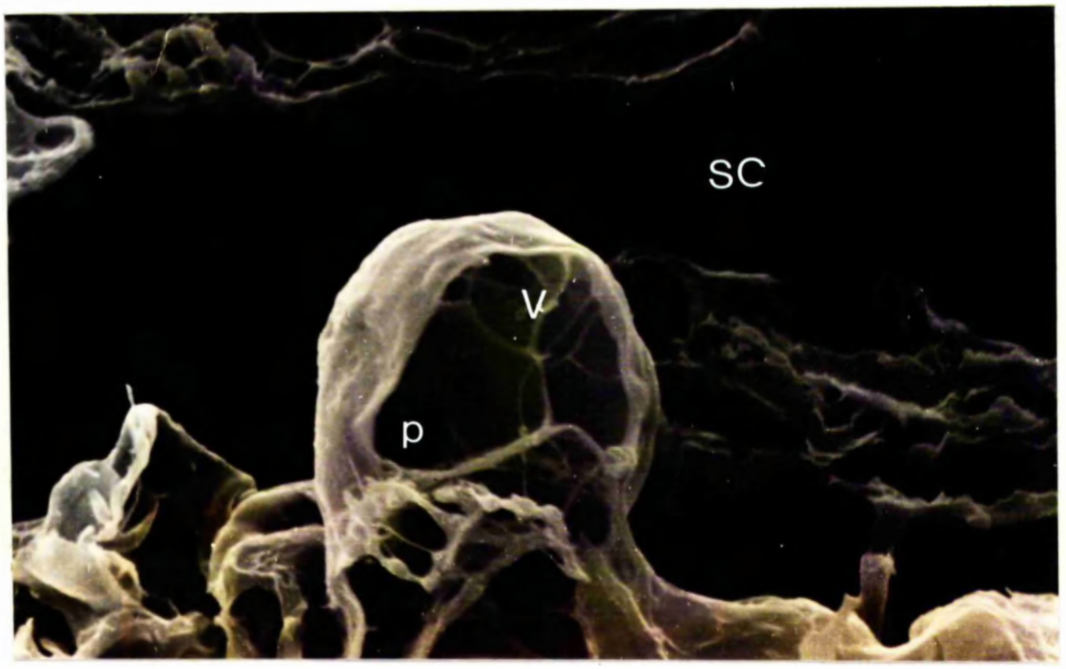

Figure 48: Scanning electron micrograph of a 'giant vacuole' in the lining of Schlemm's canal which has been cut open during dissection to show a possible lumen pore (p). Control tissue (Mn10) (X4300).

monolayer. Breaks in the lining endothelium which were considered to be artefactually produced were rare, but when present had a ragged cell border which was not membrane bound. These were usually associated with areas of inner-outer wall apposition which are presumably disturbed during processing to create artefactual breaks in both monolayers.

The lining endothelium of the control eyes was also characterised by focal ballooning or 'blow-outs' (Fig 50, 51, 52 and 53). These structures consisted of large areas of the lining endothelium, involving more than one cell, and were up to 70 μm in diameter. The endothelial monolayer, and in some cases also the sub-endothelial layer, was detached from the underlying tissue and protruded into Schlemm's canal. All attachments to the underlying tissue were lost. The 'blow-outs' contained very little contents, except perhaps a few disorganised cell processes and a little loosely dispersed ground substance (Fig 50, 51, 52 and 53). They are usually smooth surfaced with only a few nuclear bulges and perhaps a few vacuoles mostly confined to the sides of the structure (Fig 52 and 53).

The openings of collector channels where they entered Schlemm's canal were frequently occluded by prolapsed trabecular tissue (Fig 54). Although the tissue which blocked the entrance resembled the 'blow-outs' described previously they may be much more extensive, involving large areas of the inner wall, and commonly involved not only the endothelial monolayer but also the cellular and extracellular elements of the cribriform layer (Fig 54).

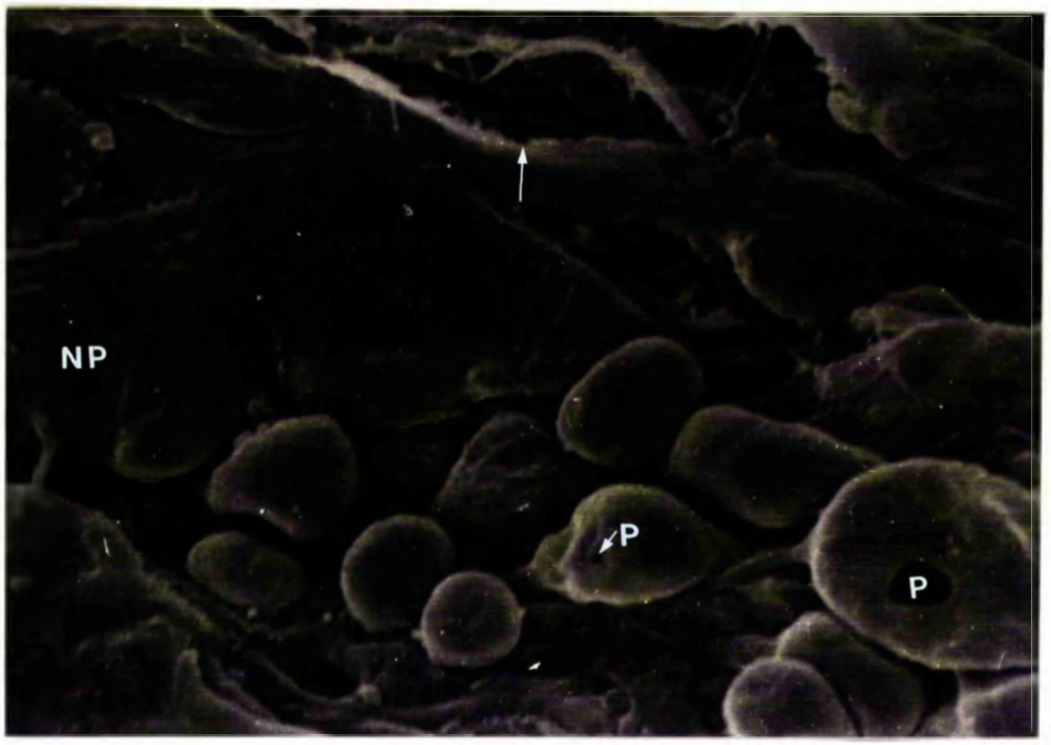

Figure 49: Scanning electron micrograph of the inner wall lining endothelium of control tissue (Mn10), to show an area where pores are abundant, both bulge pores (P) and non-bulge pores (NP). Note areas where lining endothelium is disrupted (arrow), (X 3800).

Figure 50: Transmission electron micrograph of the cribriform layer and Schlemm's canal in control tissue (Mn5). Note sub-endothelial ground substance and large 'blow-outs' in the lining endothelium (arrows) (X 1400).

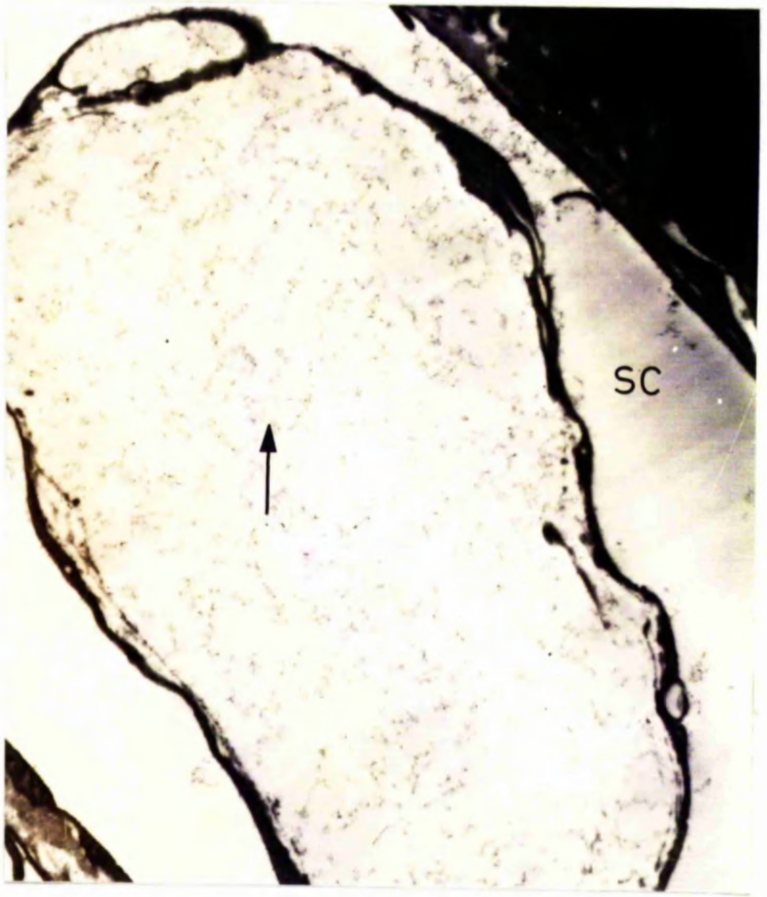

Figure 51: Transmission electron micrograph of a 'blow-out' containing colloidal iron particles (arrow) in control tissue (Mn6) (X 4500).

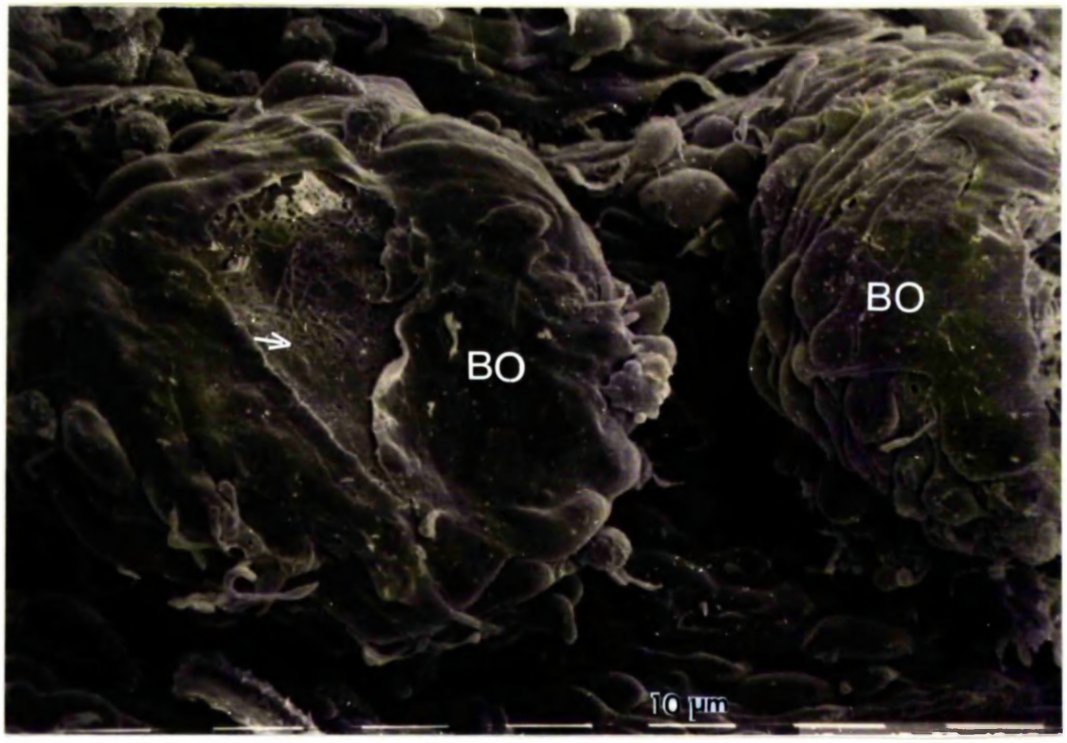

Figure 52: Scanning electron micrograph of the inner wall of Schlemm's canal from dissected control tissue (Mn4). Plan view. Note large 'blow-outs' in the lining endothelium and some areas where lining endothelium has been artefactually removed (arrow) (X 1000).

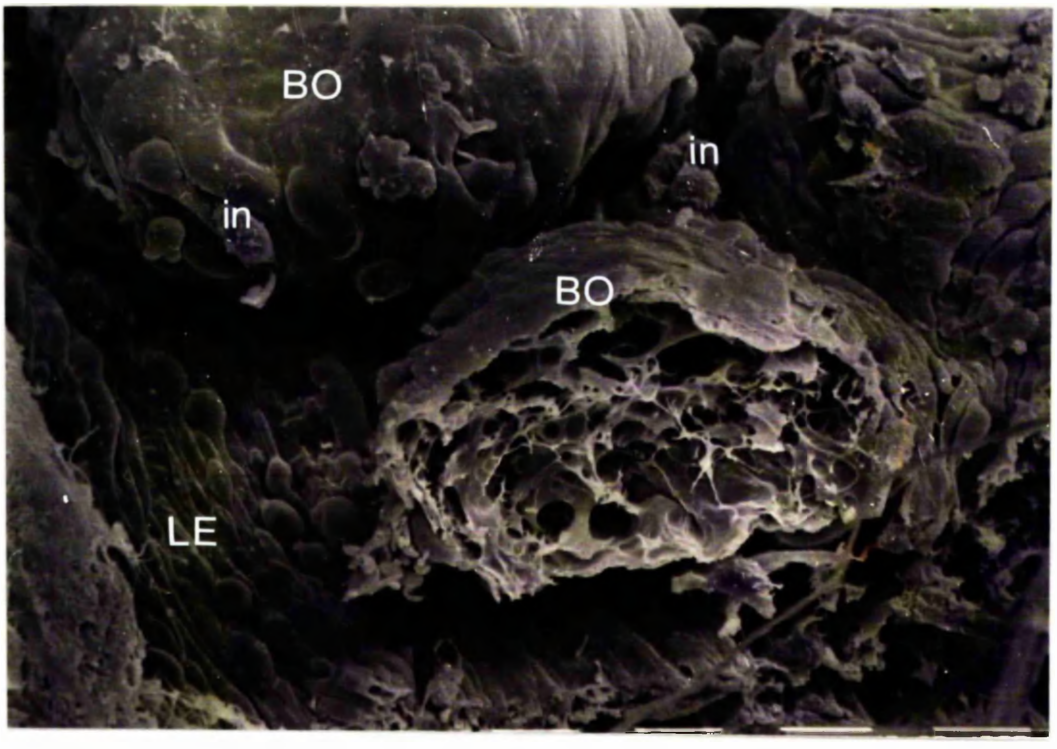

Figure 53: The same tissue as in Figure 52, showing a side view of the 'blow-outs' in the lining endothelium. (X 1100).

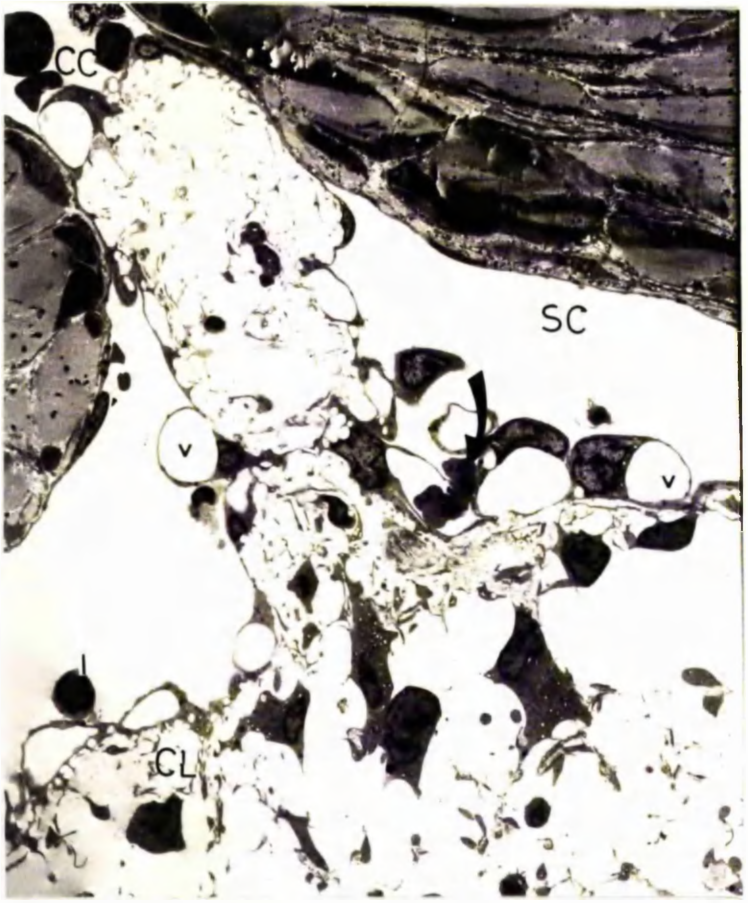

Figure 54: Transmission electron micrograph showing the herniation of the inner wall of Schlemm's canal into the opening of a collector channel. Note 'wash out ' of extracellular materials from the cribriform layer and polymorph migrating through the lumen pore of the 'giant vacuole' (arrow). (X 1200).

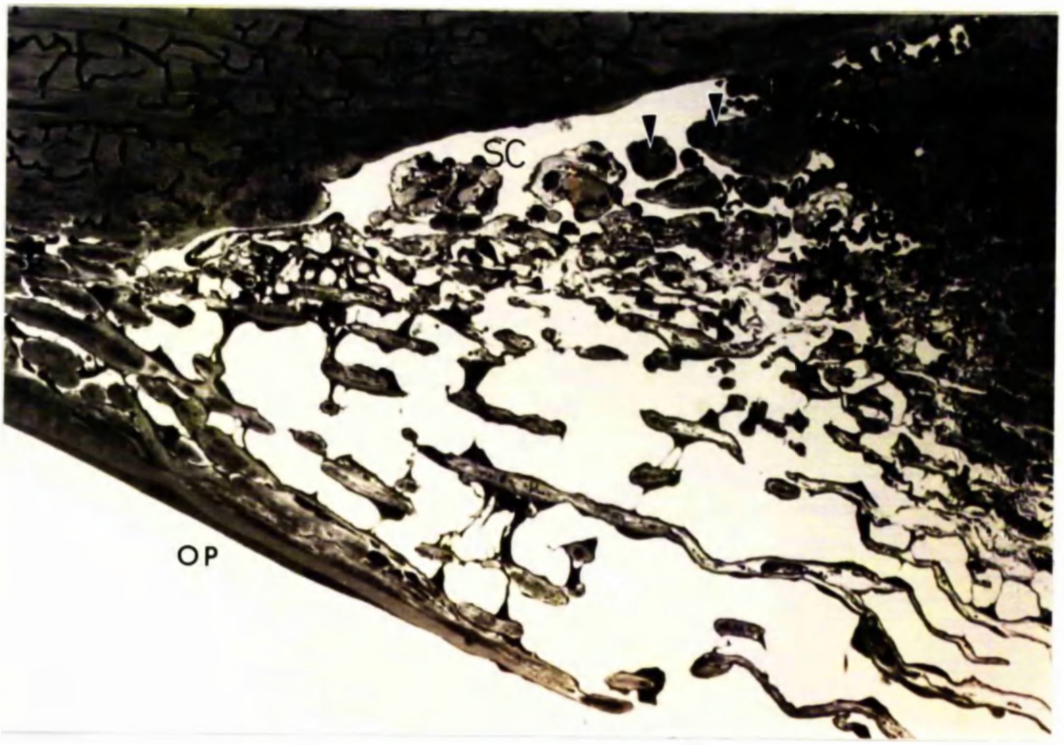

Figure 55: Light micrograph of outflow apparatus in control tissue (Mn8) which shows the collageneous cords in Schlemm's canal (arrows) which prevent canal closure and blockage of collector channels in some areas. Note also large operculum, (X 340)

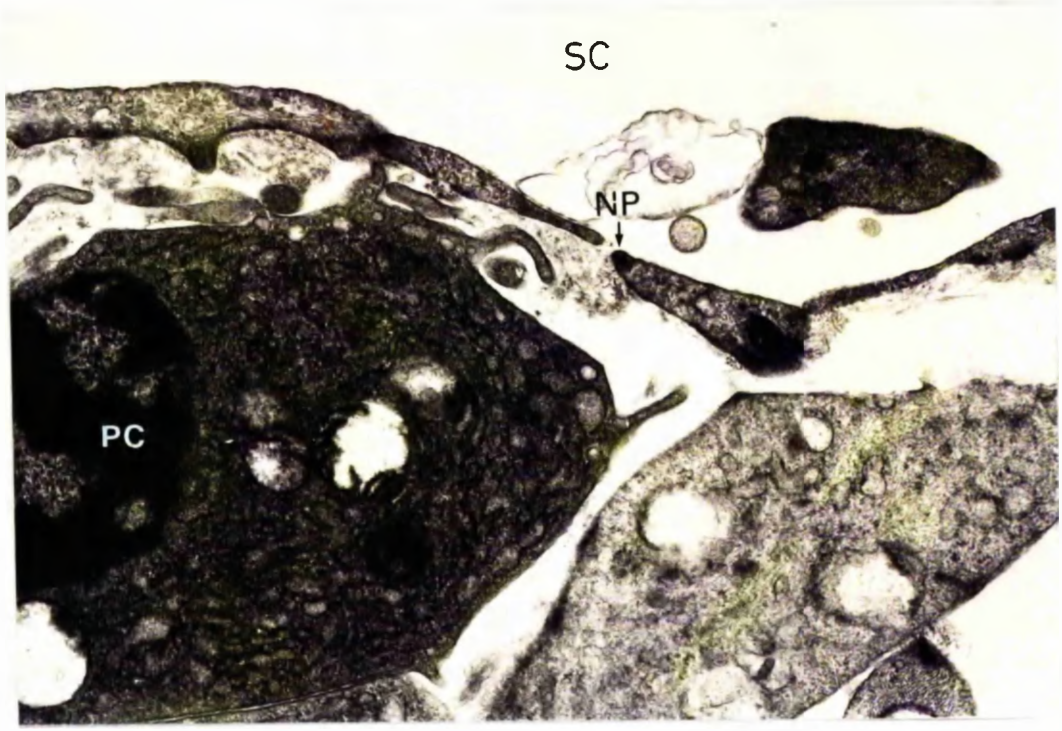

Figure 56: Transmission electron micrograph to show a plasma cell (PC) directly under the lining endothelium which is interrupted by a non-vacuolar pore (NP), control tissue (Mn 5). (X 20,000).

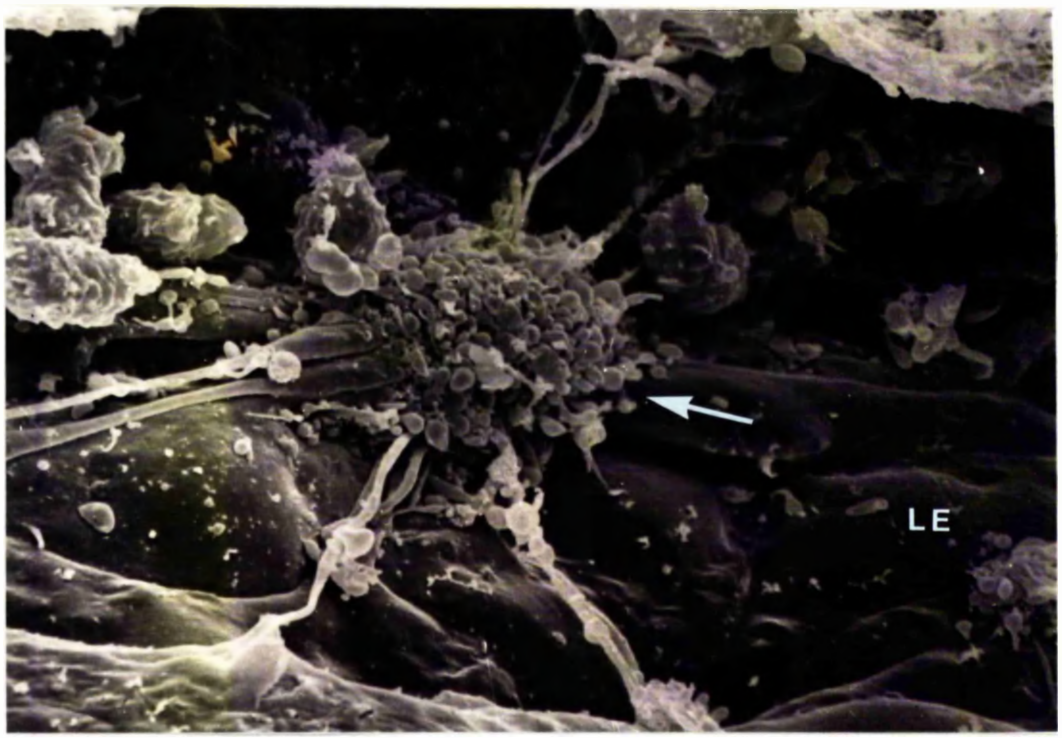

Figure 57: Scanning electron micrograph of a platelet aggregation (arrow) on the surface of the lining endothelium of Schlemm's canal in control tissue (Mn 3), (X 2500).

In some sections the opening to the collector channel appeared completely blocked, however, this was not always the case, and even when it was, serial sectioning would be required to confirm that the orifice was completely occluded.

Areas of canal closure due to inner-outer wall apposition were frequently seen in control eyes. In these regions there were very few 'giant vacuoles'. Complete canal closure was often prevented by the presence of the collagenous cords in the canal lumen, which served to restrain the outward bowing of the inner wall (Fig 55).

Inflammatory cell infiltration in the outflow apparatus was mild, the chief cell type being polymorphonuclear leukocytes (Fig 43, 54 and 55). Other types of cell which were noted occasionally were erythrocytes, lymphocytes, monocytes and plasma cells (Fig 56). More cells were present in the canal of Schlemm and collector channels than in the trabecular meshwork. Cells were also frequently seen passing through the lining endothelium via both non-vacuolar and vacuolar pores. Small platelet aggregates were seen on the luminal surface of Schlemm's canal in a few eyes, but were not sufficiently frequent to suggest that any damage had been suffered by the tissue.

The morphology of the outflow apparatus in hyaluronidase treated eyes

Examples of the outflow system from two different experimental eyes (Fig 58 and 59) illustrate the general appearance of the tissue and also the variation in the

ciliary muscle configuration. In Fig 59 the longitudinal ciliary muscle bundles are widely separated, in the other eye (Fig 58) they are more tightly arranged.

The trabecular meshwork in experimental eyes showed similar changes to those observed in the control eyes. There were large inter and intratrabecular spaces in the uveal and corneoscleral meshwork due to the changes in configuration of the trabecular endothelial cells (Fig 56, 59 and 60). In colloidal iron preparations the intertrabecular spaces were devoid of stain, the cell surfaces lining these spaces were also poorly stained, however, the staining within the trabecular cores was comparable to that in normal eyes (Fig 61).

The 'blow-outs' in the inner wall of the canal were identical to those described in control eyes, involving either the monolayer alone or two to three layers of cells and extracellular elements of the cribriform layer (Fig 62 and 63). In the latter cases a few 'giant vacuoles' were seen on the otherwise smooth lining endothelium which enclosed the 'blow-outs'.

In regions where a collector channel drained Schlemm's canal there was often a greater degree of distension in the outer meshwork than in adjacent areas. This often resulted in apparent blockage of the collector channel opening by prolapsed trabecular tissue (Fig 64 and 65) identical to that noted in control eyes.

In some regions of the experimental eyes, increased vacuolar incidence was accompanied by a great deal of

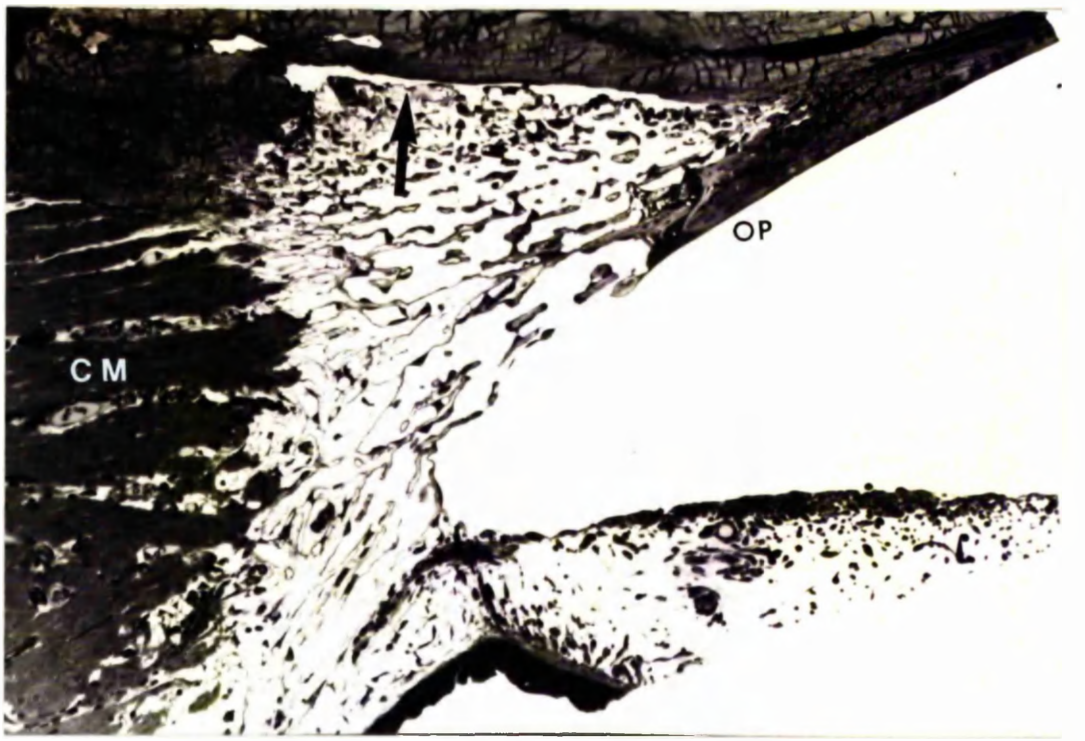

Figure 58: Light micrograph of experimental pig tailed macaque tissue (Mn 2). Note large operculum, compact ciliary muscle and narrowed canal of Schlemm due to distension of the outer meshwork (arrow), (X 150).

Figure 59: Light micrograph of experimental tissue from another eye (Mn 9) showing diminuitive operculum, dilated clefts between the ciliary muscle fibres and narrowing of Schlemm's canal. (X 150).

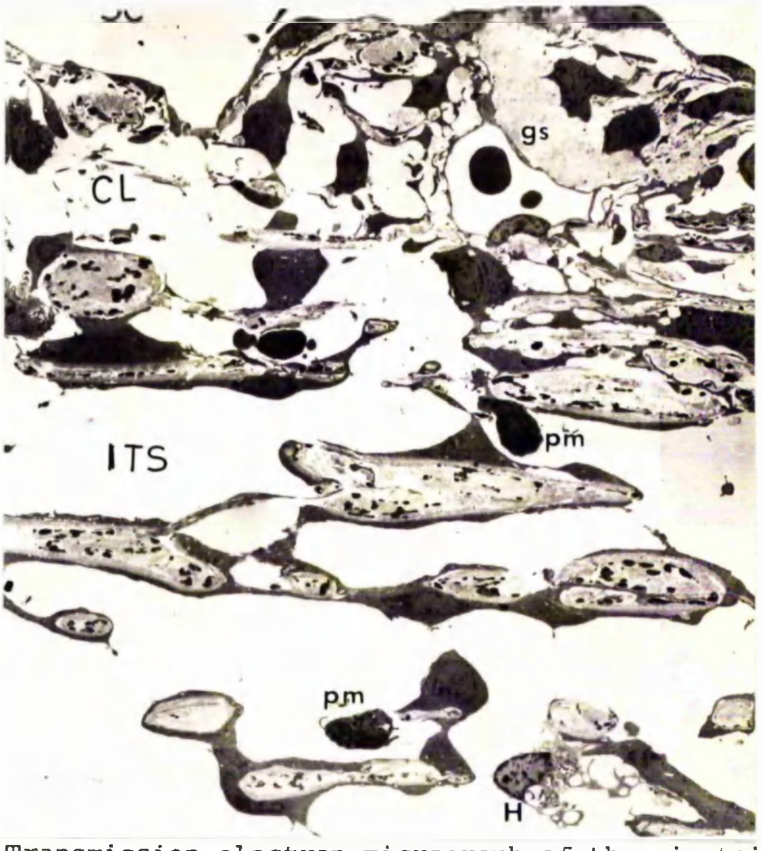

Figure 60: Transmission electron micrograph of the pig tailed macaque outflow apparatus in an experimental eye (Mn 5). Note the 'rounded up' trabecular endothelial cells, large inter and intratrabecular spaces and inflammatory cells. The ground substance persisted in a few areas of the cribriform layer, (x 1300).

Figure 61: Transmission electron micrograph of colloidal iron stained experimental tissue (Mn 10). The intertrabecular spaces are devoid of stain. The connective tissue elements of the trabeculae are rich in staining reaction (arrows). (X 13,800).

distension and disruption of the cells in the cribriform layer, and a loss of the extracellular materials (Fig 66). The cells of the cribriform layer in these areas appeared as isolated pieces of cytoplasm rather than the fine processes seen in areas of milder distension (Fig 60). In some greatly distended areas there was also a great deal of damage to the outermost corneoscleral trabeculae (Fig 65 and 66). Other regions which suffered less disruptive effects had fewer vacuoles, abundant extra-cellular materials (Fig 60), and the arrangement of the cells in the cribriform layer was a more normal appearance with perhaps the cell organelles being confined to a smaller perinuclear zone of cytoplasm than in the more normotensive state.

It was expected that in the hyaluronidase-treated eyes there would have been a dispersion or 'washout' of the ground substance in the cribriform layer, however, the impression from qualitative observations was that this material was as abundant, particularly under the lining endothelium, as in control eyes (Fig 60, 65, 67 and 70). Openings on the trabecular aspect of 'giant vacuoles' were sometimes accompanied by a depletion of the ground substance in their vicinity (Fig 67), however, it was equally as likely to find these openings blocked by ground substance with a high affinity for colloidal iron (Fig 68). The appearance of the extracellular materials in the cribriform layer by conventional TEM, and the staining pattern and intensity in colloidal iron preparations were analogous to control eyes.

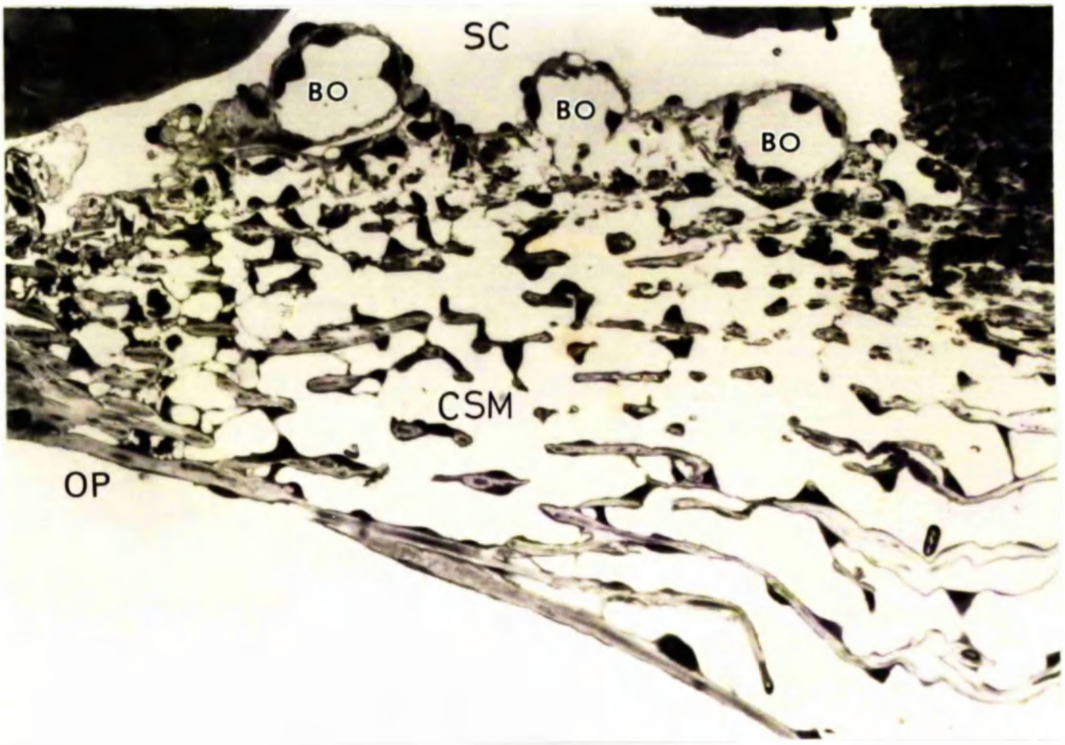

Figure 62: Light micrograph of outflow apparatus in experimental tissue (Mn 4). Note rounding up of cells and large spaces in corneoscleral meshwork. The lining endothelium shows three large focal 'blow outs'. (X 340).

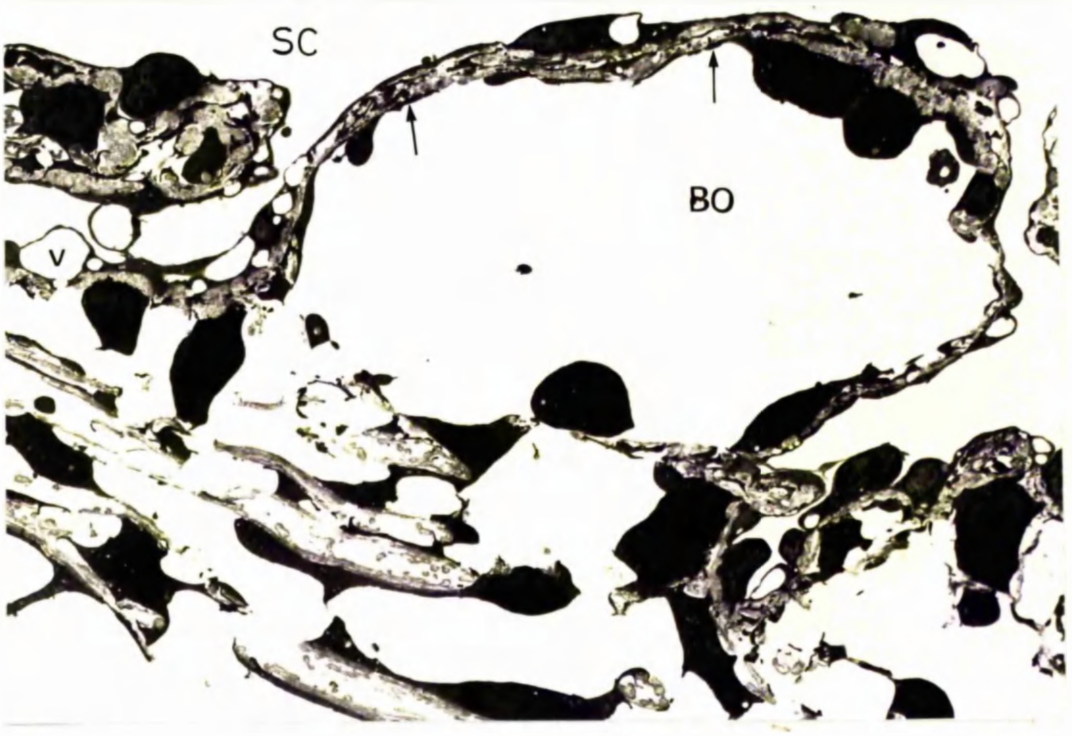

Figure 63: Transmission electron micrograph showing a 'blow out' in more detail (Mn 4). Note that two or three layers of cells directly under the lining endothelium (arrows) have also become detached in the region of the 'blow out', otherwise these structures are 'empty'. (X 1700).

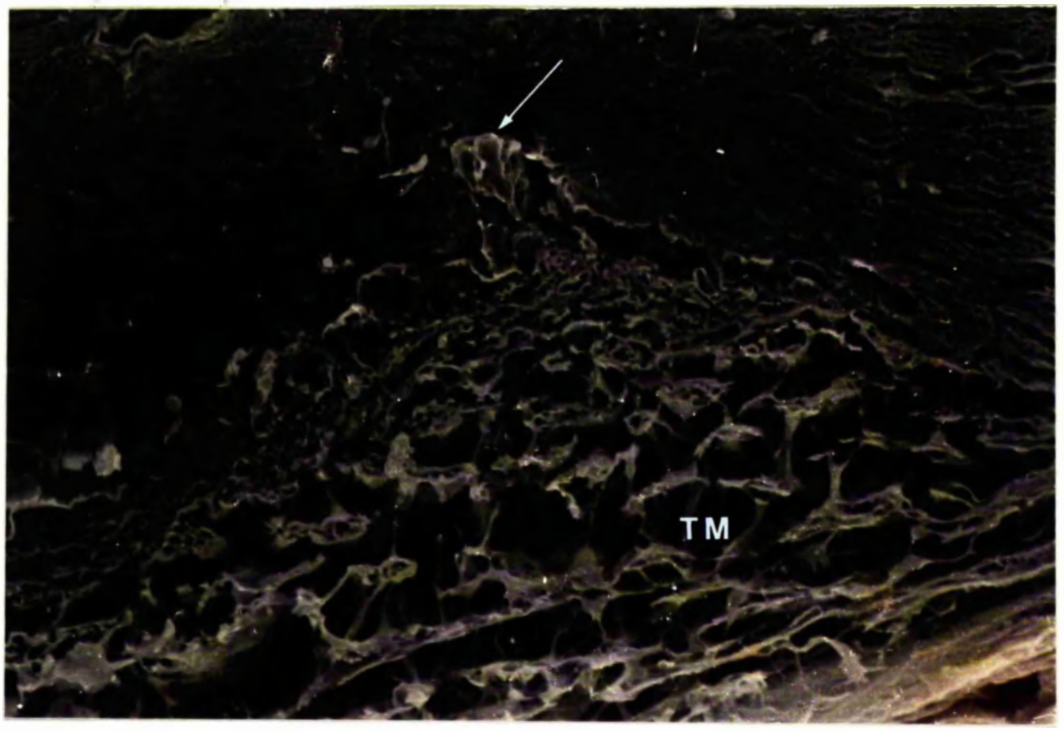

Figure 64: Scanning electron micrograph of experimental tissue (Mn 10) to show the distended trabecular meshwork (particularly the stretched cells), and the outer meshwork which had herniated into the opening of a collector channel, (arrow). (X 500).

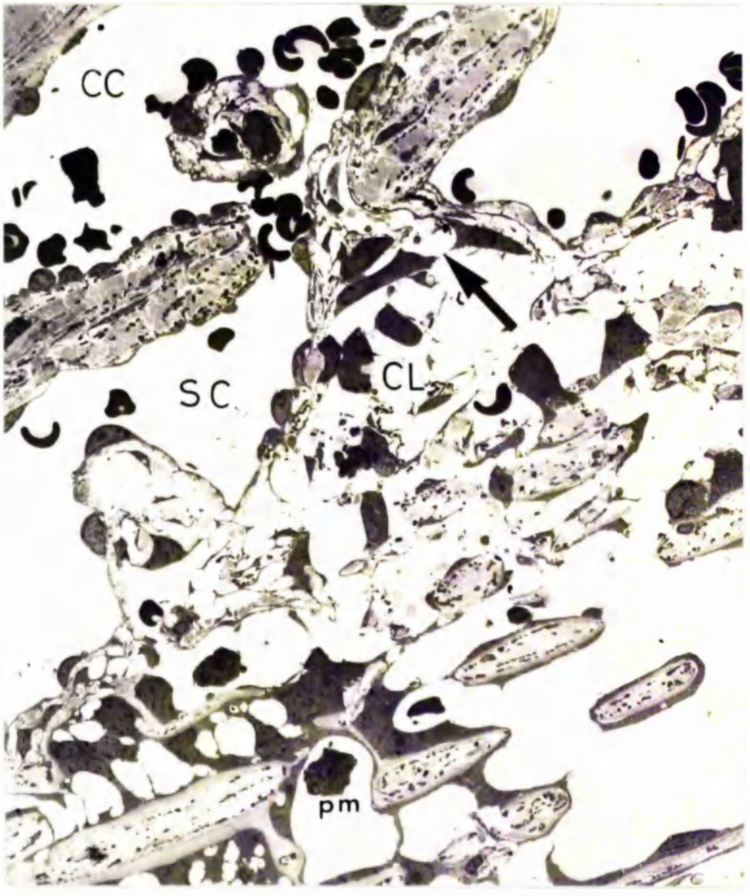

Figure 65: Transmission electron micrograph of experimental tissue (Mn 6), to show as in Fig. 64 the herniation of outer meshwork into the collector channel opening, this consisted of not only the lining endothelium but also the disorganised cells and extracellular elements of the cribriform layer (arrow). (X 1100).

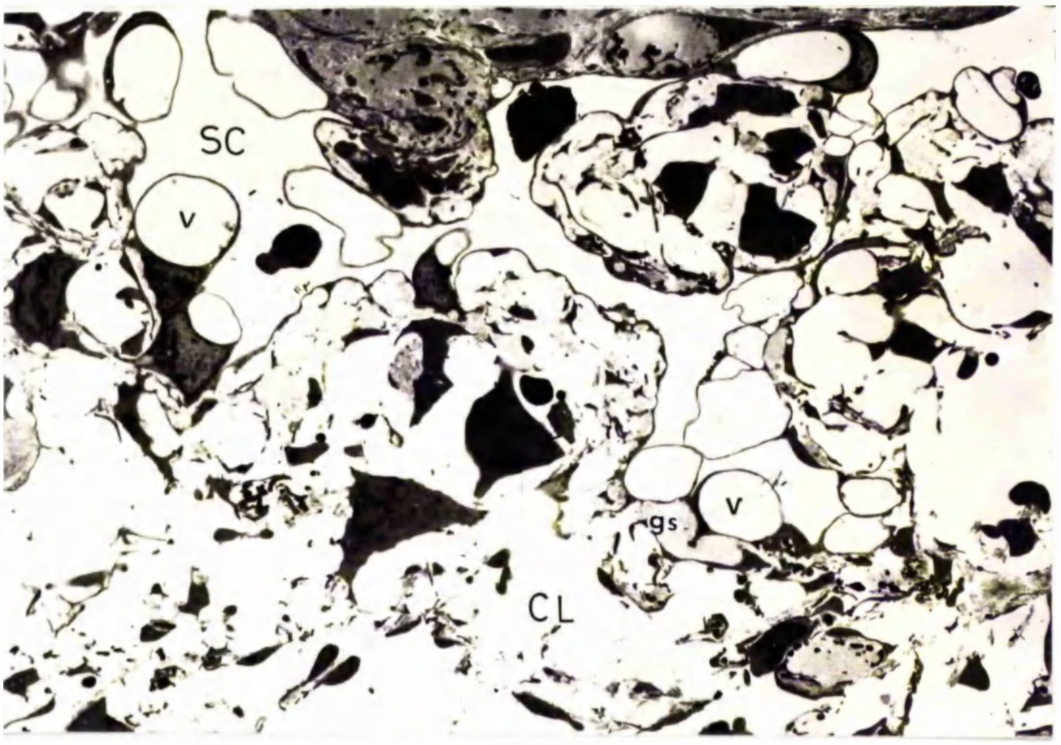

Figure 66: Transmission electron micrograph of an extremely distended area of the cribriform layer in experimental tissue (Mn 4). 'Giant vacuoles' are abundant in the lining endothelium. The cribriform layer is disorganised with the depletion of the extracellular materials and isolated fragments of cells. (X 1400).

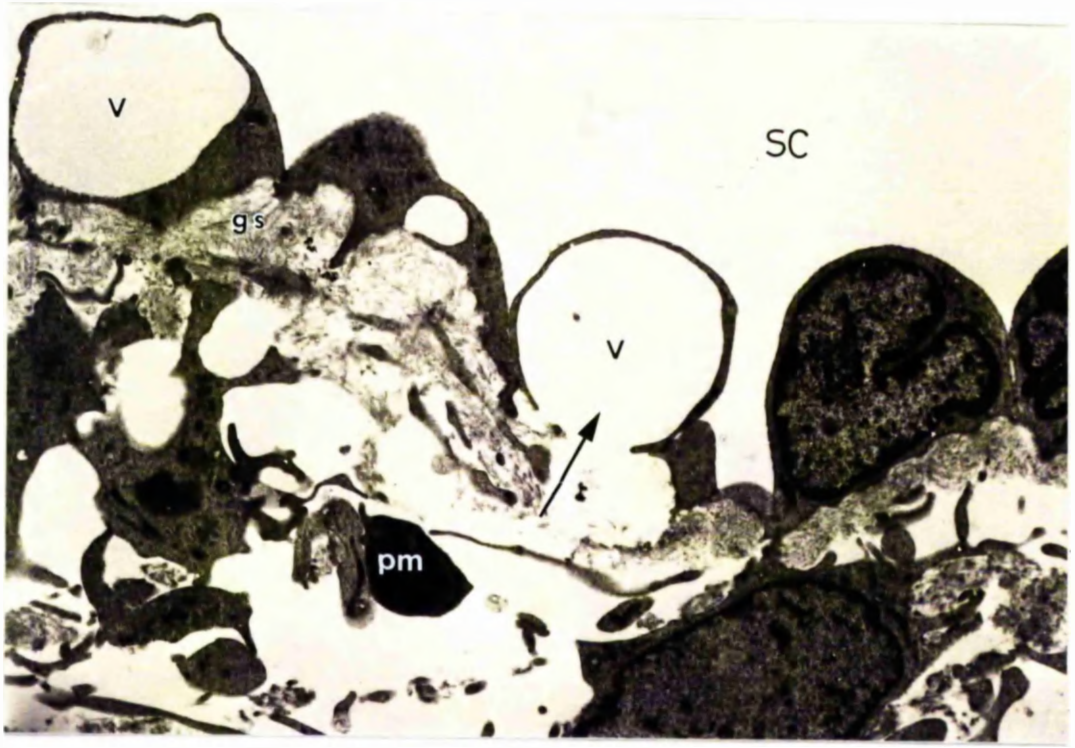

Figure 67: Transmission electron micrograph to show 'giant vacuoles' in the lining endothelium of experimental tissue (Mn 3). There was a depletion of the ground substance at the trabecular pore of one of these vacuoles (arrow). (X 4700).

The majority of the 'giant vacuoles' in experimental eyes were electron lucent in conventional TEM preparations, while in colloidal iron preparations about half of the vacuole population contained some sparse staining of their internal membrane (Fig 68) and about a quarter of the population contained a more widespread staining reaction in the lumen (Fig 68). The pattern of the stain was either diffuse, clumped or in chains of colloidal iron particles forming a loose network (Fig 69). Similar patterns were noted in control eyes.

Large breaks or disruptions in the lining endothelium were rarely noted in these eyes, even in greatly distended areas, and whenever such breaks did occur their origin was more than likely of an artefactual nature since they were usually associated with regions of inner-outer wall apposition as in control eyes.

Vacuolar and non-vacuolar pores were observed by both TEM (Fig 70) and SEM (Fig 71). The non-vacuolar pores were generally smaller (<1 µm) than vacuolar pores (0.5-2.5 µm) but seemed to be present in greater numbers. Due to the complex nature of the lining endothelium it seemed very likely that a great many pores would not be visible when examining the topography of the dissected trabecular wall of Schlemm's canal.

In common with control eyes there was an apparent decrease in the numbers of tissue histiocytes in the experimental eyes. The inflammatory cell infiltrate was of a similar nature and intensity to that in controls (Fig 60,

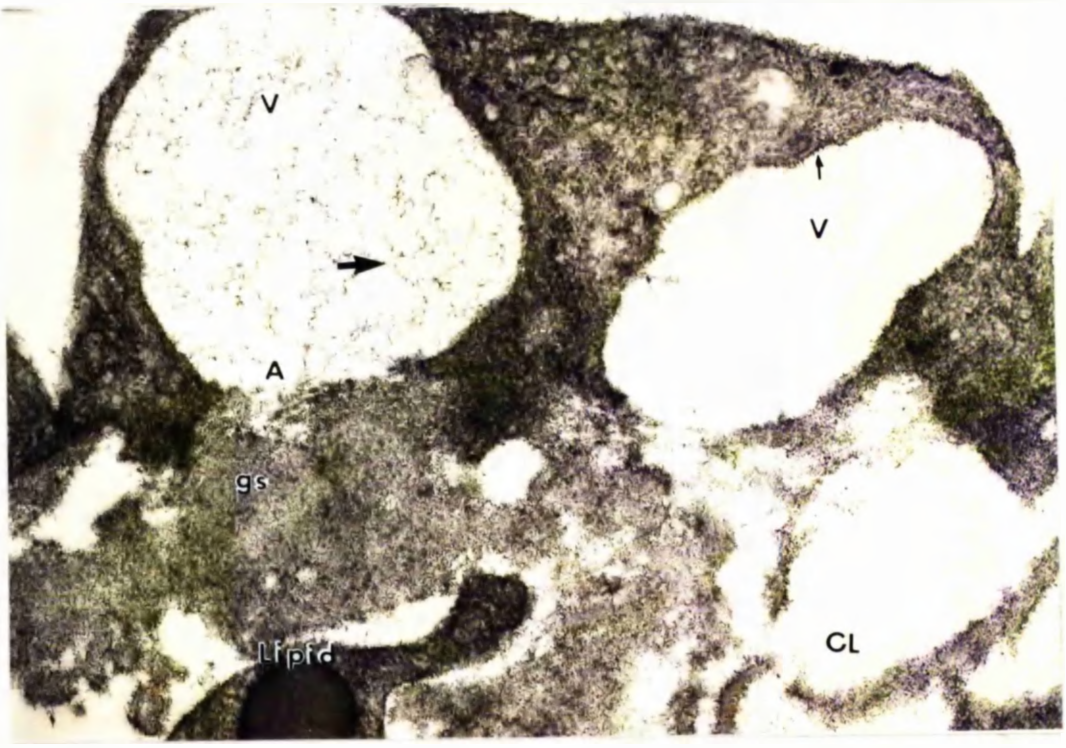

Figure 68: Transmission electron micrograph in experimental tissue (Mn 10) to show intense staining of the ground substance. One 'giant vacuole' contains some loosely dispersed stain particles (large arrow) while the other only shows some staining on the membrane (small arrow). (X 7600).

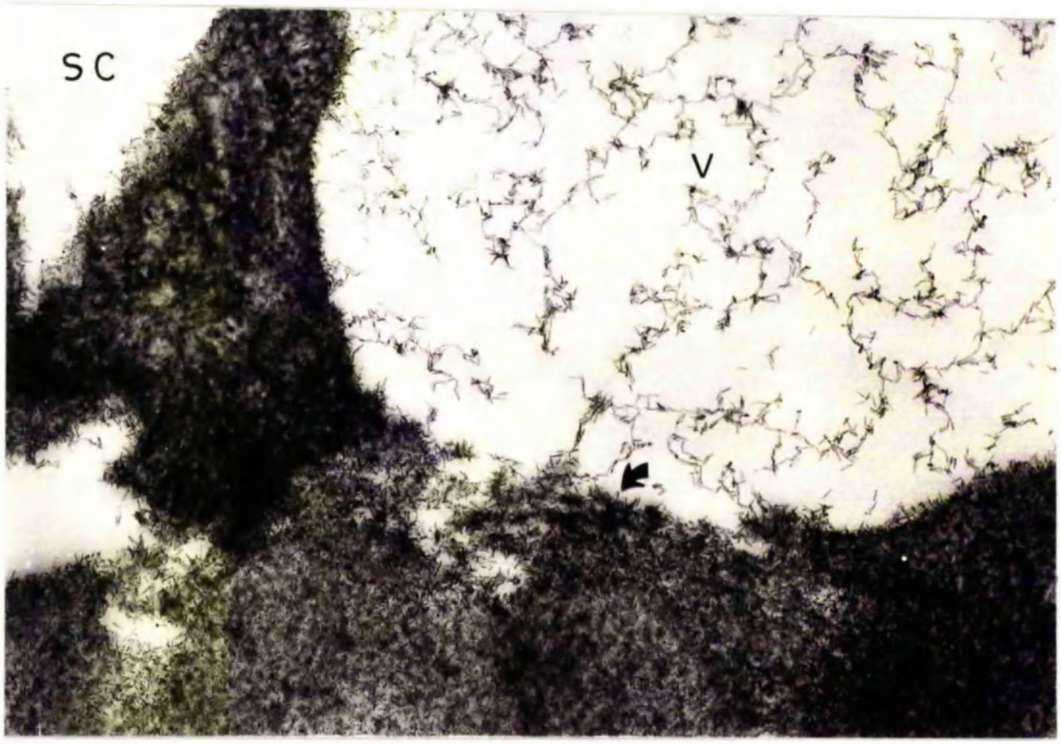

Figure 69: Higher power transmission electron of area A in Fig. 68. Note the plugging of the trabecular opening to the 'giant vacuole' by richly stained material (arrow). Also note the fine structure of the colloidal iron particles. (X 117,000).

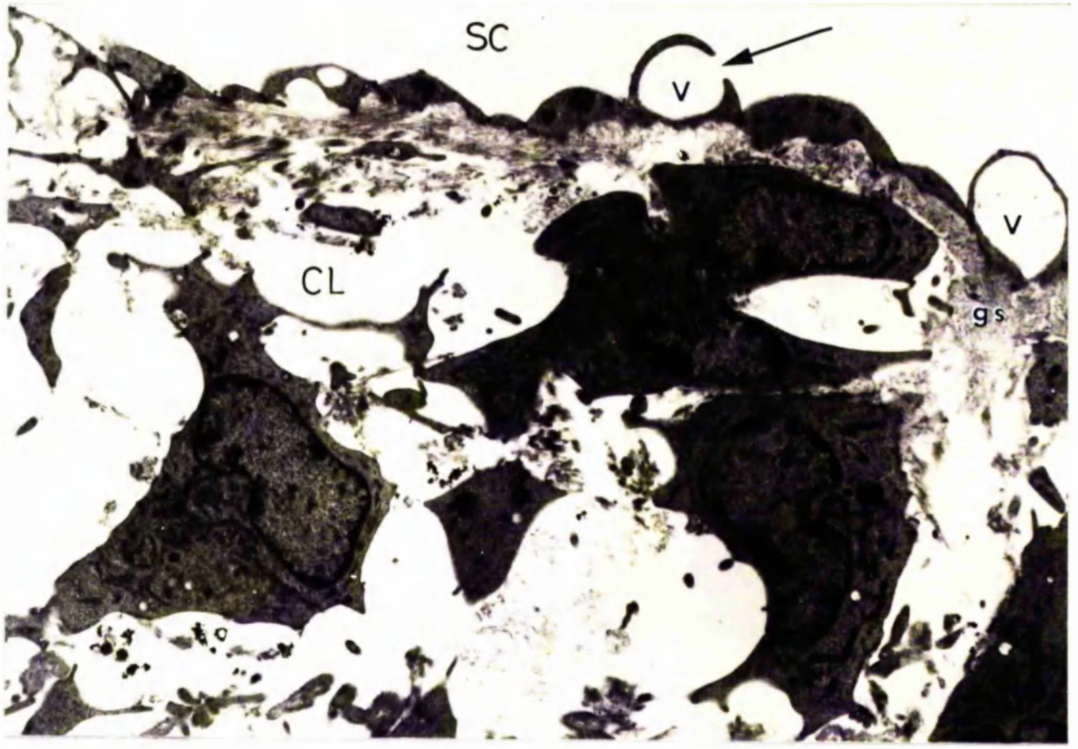

Figure 70: Transmission electron micrograph of the cribriform layer and lining endothelium in an experimental eye (Mn3). Note the abundance of ground substance, the large cells rich in organelles and the vacuolar-pore (arrow). (X 8000).

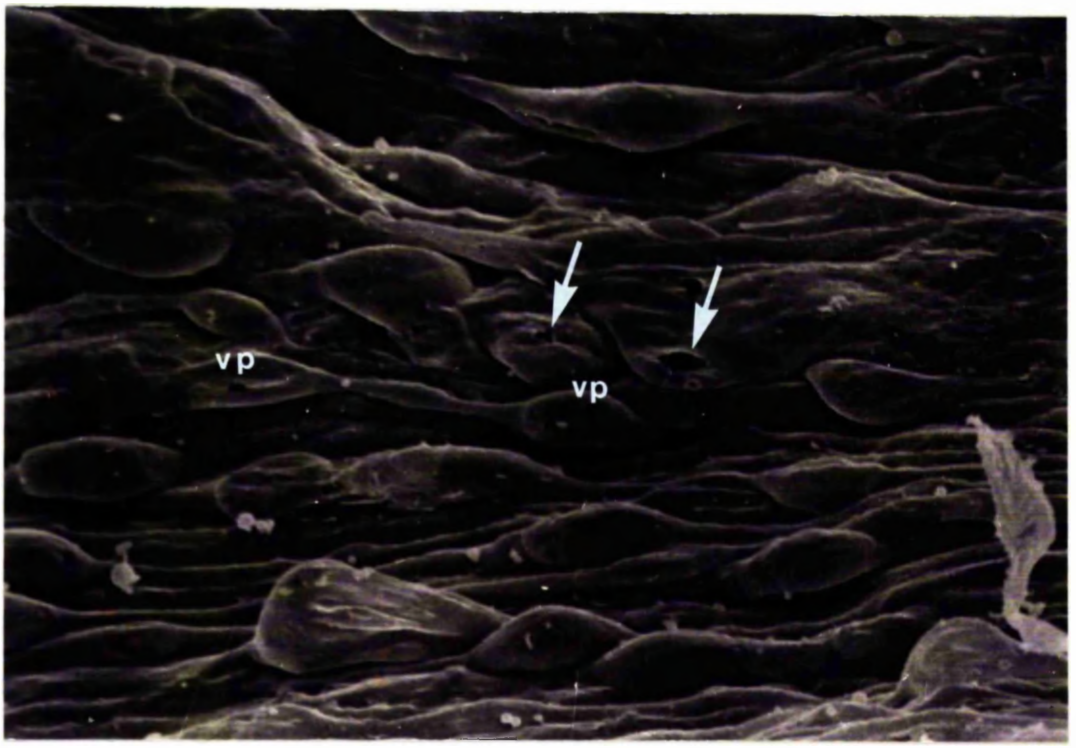

Figure 71: Scanning electron micrograph of the inner wall of Schlemm's canal in an experimental eye (Mn9) to show the arrangement of the cells and bulges some of which are collapsed (*) and others have pores (vp). Two artefactual pores are indicated by arrows. (X 2600).

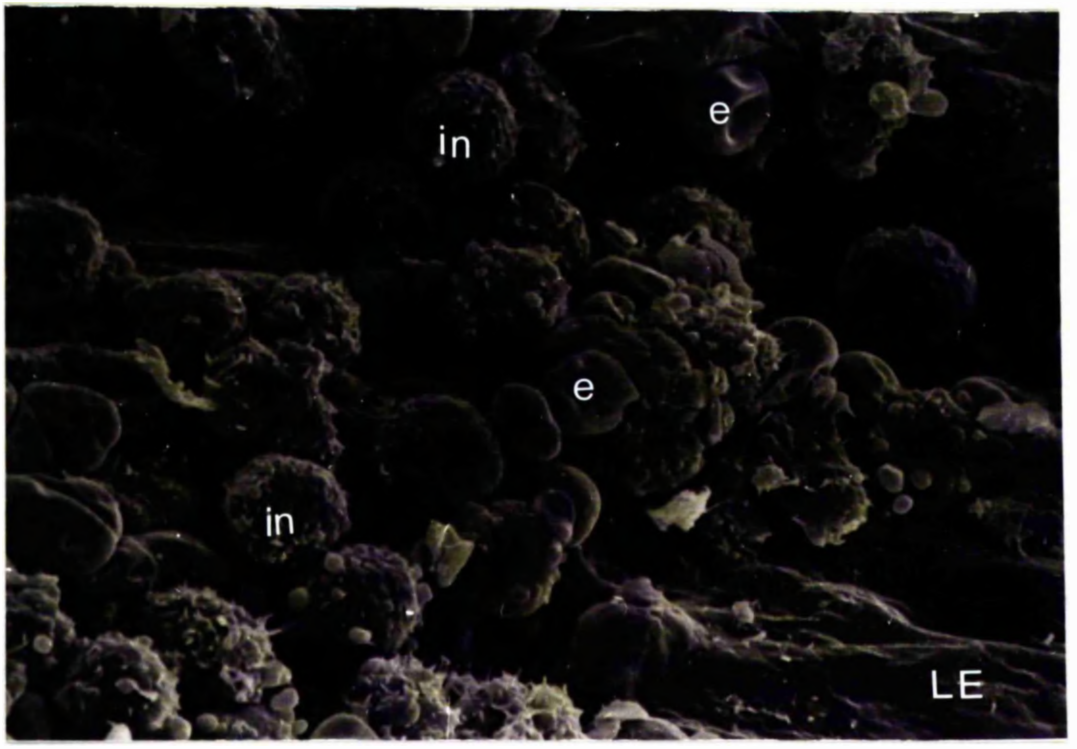

Figure 72: Scanning electron micrograph of an area of the lining endothelium in an experimental eye (Mn7) which is covered by a mixture of erythrocytes and inflammatory cells. (X 2600).

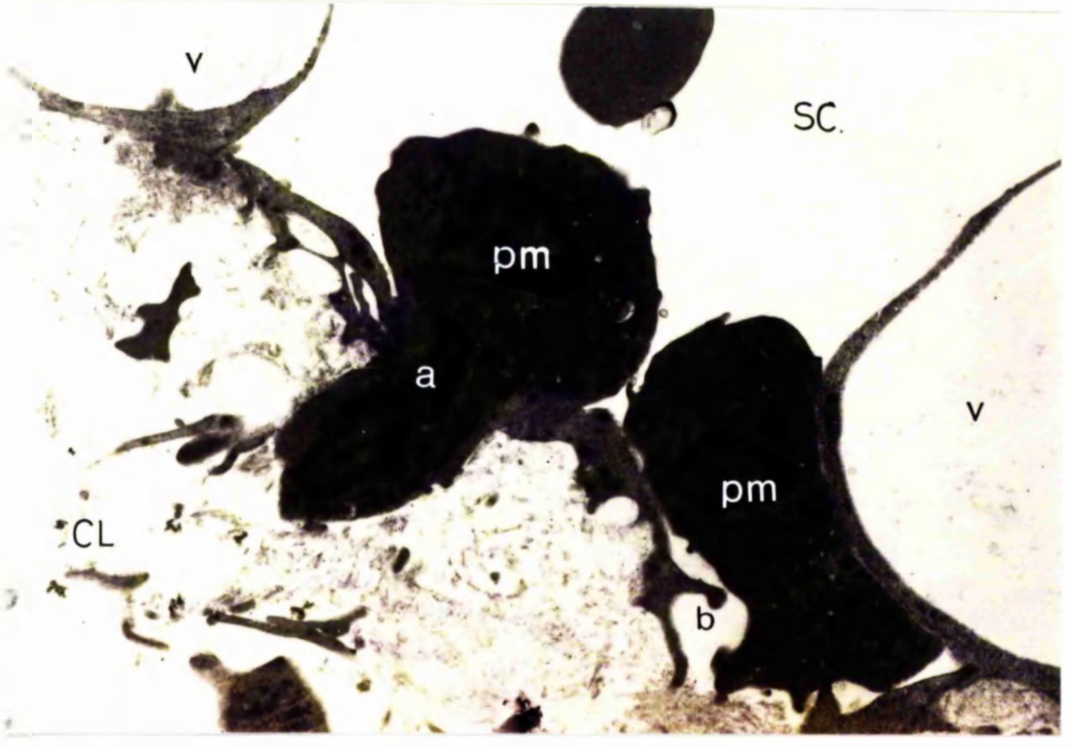

Figure 73: Transmission electron micrograph to show polymorphonuclear leucocytes migrating through the lining endothelium via a) a non-vacuolar pore and b) what may be a vacuolar pore. Experimental tissue (Mn3). (X 6300).

65, 66, 67, 72 and 73).

QUANTITATIVE MORPHOLOGICAL STUDY OF THE EFFECTS OF HYALURONIDASE

The incidence of 'giant vacuoles' in the lining endothelium of Schlemm's canal

As described in the general introduction 'giant vacuoles' have been strongly implicated in the role of aqueous movement across the lining endothelium. Their numbers have been shown to correlate with intraocular pressure and flow at the time of fixation. It was therefore considered an important part of this study to investigate vacuolar incidence in normal, control and experimental eyes.

The assessment of the incidence of 'giant vacuoles' by light microscopy was limited by the resolution of the oil immersion lens and errors in counting were inevitable, however, since the analysis was performed on coded sections the error was equal for all eyes investigated. Structures which might have been mistakenly counted as vacuoles (although care was taken not to) were as follows:

i) Pseudovacuoles (Rohen 1969), ie those structures enclosed by more than one endothelial cell (Fig 74a).

ii) Intracytoplasmic swellings, which may be the result of distended mitochondria or endoplasmic reticulum, in poorly fixed material, eg Mn 1 in present study (Fig 74b).

iii) Small folds in the lining endothelium (Fig 74c).

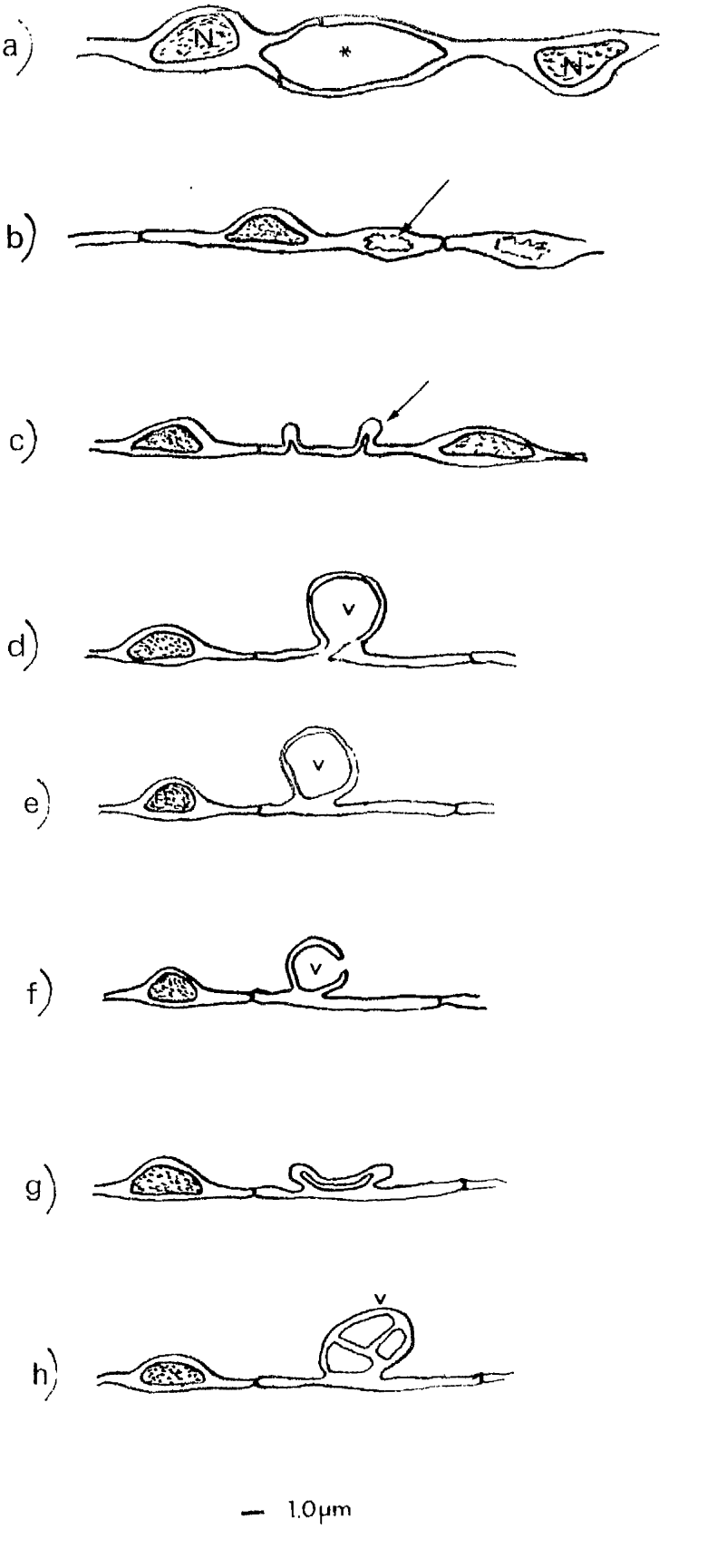

Figure 74:
a) Pseudovacuole
b) Distended mitochondria
c) Folds in lining endothelium
d) 'Giant vacuole' with meshwork pore
e) 'Giant vacuole' totally intracytoplasmic
f) 'Giant vacuole' with canal or lumen pore
g) Collapsed 'giant vacuole'
h) Multilobed 'giant vacuole' (counted as one)

Structures which were counted as one 'giant vacuole' are shown in Fig 74d-h. In order to reduce the error in counting false vacuoles any structure below 2 μm was not counted. Although this may have excluded smaller vacuoles, or those cut off-centre, this was considered an acceptable error which would be equal in all eyes studied. These criteria were also applied to the study of the human outflow system (Part II). The result of the 'giant vacuole' counts are shown in Table 6.

Inner wall nuclei

The main number of nuclei in the inner wall, expressed as a count per section, was between 7.7-14.9, with an overall group mean and standard deviation of 10.6±2.2. There was a slight but insignificant variation in the nuclei counts between control and experimental eyes (Fig 75b). The count was carried out to ensure that the length of endothelium studied was comparable, and possibly as a correction factor if the difference was significant. It can be seen from Table 6 that the counts in the majority of animals was very similar in both eyes.

'Giant vacuoles'

In the normal eyes (Mn 1) which were immerse fixed the counts in the left and right eye were surprisingly different (Table 6, Fig 75a) with the count in the left eye being double that of the right. This may be attributed to the loss of intraocular pressure which occurred when the sclera was perforated during enucleation of the right eye prior to immerse fixation.

	Mn 1 (Normal)		Mn 2		Mn 3		Mn 4		Mn 5		Mn 6		Mn 7		Mn 8		Mn 9		Mn 10	
	L	R	CON	EXP	CON	EXP	CON	EXP	CON	EXP	CON	EXP	CON	EXP	CON	EXP	CON	EXP	CON	EXP
nner wall uclei																				
$\bar{x}$	12.5	12.5	-	9.2	7.9	9.1	10.2	10.5	9.9	-	10.4	11.4	12.4	14.9	8.3	-	-	14.1	9.0	7.7
± S.D.	3.7	3.7	-	3.6	1.9	3.4	3.7	4.8	2.6	-	3.3	3.8	4.1	4.7	2.8	-	-	5.6	3.9	2.3
nner wall giant vacuoles'																				
$\bar{x}$	14.2	7.1	-	18.8	5.8	8.0	21.0	12.8	20.7	-	25.4	19.9	12.9	4.0	9.0	-	-	15.4	15.5	7.4
± S.D.	3.6	4.2	-	8.6	3.6	4.8	9.4	7.4	7.6	-	7.5	5.9	5.7	2.6	5.4	-	-	3.9	3.6	3.0
ther 'giant acuoles'																				
$\bar{x}$	1.0	0.3	-	4.1	0.9	0.6	3.6	1.9	3.8	-	5.5	3.7	3.0	0.9	2.4	-	-	2.2	4.5	1.7
± S.D.	1.7	0.7	-	4.0	1.4	0.9	4.2	1.5	3.0	-	4.6	4.2	3.3	2.4	2.9	-	-	2.6	4.2	3.1
otal 'giant acuoles'																				
$\bar{x}$	16.1	7.7	-	27.0	7.6	9.1	28.1	*16.5	28.3	-	36.4	*27.9	18.9	**6.0	13.8	-	-	19.8	24.4	**10.8
± S.D.	4.2	3.9	-	13.3	4.1	5.5	10.2	8.6	10.3	-	8.9	7.9	6.7	3.5	8.8	-	-	4.8	4.5	5.2

able 6: Table to summarise the results of the study of vacuolar incidence in the pig tailed macaques. Levels of significance are indicated - * $p<0.05$, ** $p<0.01$ (t-test).

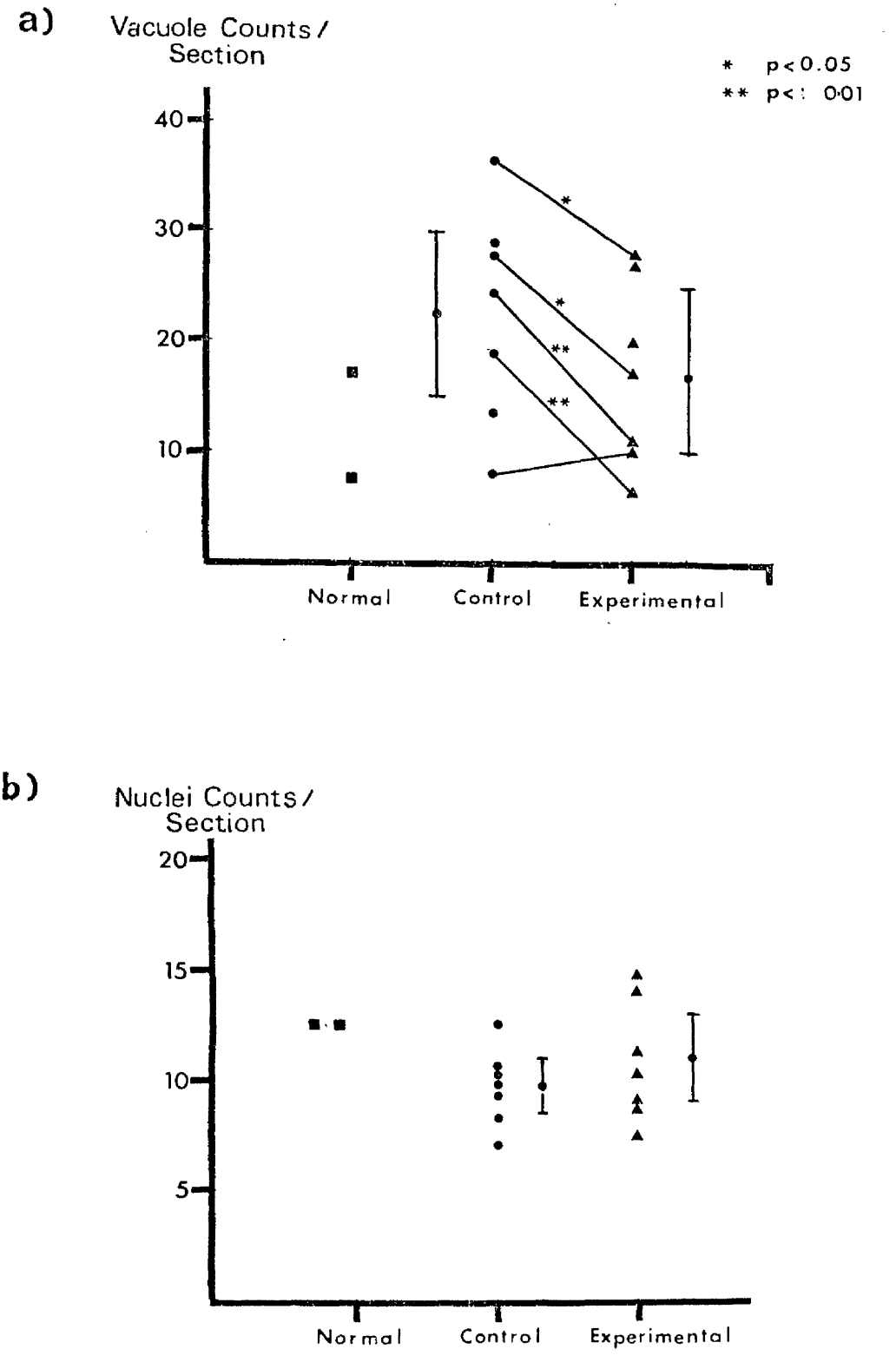

Figure 75: a) Results of the assessment of vacuolar incidence in the lining endothelium of Schlemm's canal in the three groups of pig tailed macaques, normal, control, and experimental. In four of the five pairs of eyes there were significantly fewer vacuoles in the experimental eye (t-test). Group means (±SD) are also indicated.
b) Results of the nuclei counts in the three groups of eyes. Group means ±SD are indicated.

The results in the control group varied between 7.6 to 36.4 total 'giant vacuoles' per section, with a group mean and standard deviation of 22.5±8.0 (Fig 75a). The counts per section in the experimental eyes varied from 6.0 to 27.9 with a group mean and standard deviation of 16.7±7.6 (Fig 75a). A t-test carried out on the group data indicated that there were significantly fewer 'giant vacuoles' in the experimental eyes ($t=4.36$, $p < 0.001$). If the slightly higher nuclei counts in experimental eyes were taken into account it indicated that there was an even more significant decrease in the numbers of 'giant vacuoles' in the available length of endothelial monolayer. A paired t-test on the differences in the mean counts per eye in the five matched pairs also indicated there were significantly fewer vacuoles in experimental eyes ($t=3.25$, $p < 0.05$).

Of the five pairs of eyes there was a lower vacuolar incidence in the experimental eyes in four pairs which were of varying statistical significance using a t-test on the mean and standard deviation of the counts from the ten sections in each eye (Fig 75a : Mn 4; $t = 2.75$, $0.01 < p < 0.02$: Mn 6; $t=2.25$, $0.02 < p < 0.05$: Mn 7; $t=5.4$, $p < 0.001$: Mn 10; $t=6.25$ $p < 0.001$). In the other pair of eyes (Mn 3) there was no statistical difference in vacuole counts.

The distribution of the vacuole counts in each quadrant in normal, control and experimental groups of eyes is shown in Table 7. Chi-squared tests were carried out to discover whether the counts in each quadrant varied, suggesting an uneven distribution. However, it was found that there was

Quadrants / Group	Sup. Temp.	Sup. Nasal	Inf. Temp.	Inf. Nasal	Overall group result
Normals (2) Vacuoles/section	12.6	8.6	13.6	12.6	11.9
Controls (7) Vacuoles/Section	22.5	21.6	22.1	23.7	22.5
Experimentals (7) Vacuoles/Section	18.4	16.6	14.5	17.5	16.7

Table 7: Table showing the distribution of vacuole counts in each quadrant in normal; control and experimental groups. Number in parentheses = number of eyes used.

no difference although experimental eyes seemed a bit more unevenly distributed than controls.

In summary the quantitation of vacuolar incidence revealed that fewer 'giant vacuoles' were present in hyaluronidase treated eyes compared to the controls. This was established in four of the five matched pairs of eyes and was also true of the group data.

The state of distension in the cribriform layer

As described in the general introduction the trabecular meshwork changes configuration in passive response to increased intraocular pressure and flow. One of the noticeable changes is in the cribriform layer which becomes more distended with increased free or 'empty space' available for aqueous movement. Glycosaminoglycans may act as a biological cement helping to hold this tissue together. It was postulated therefore that in those eyes exposed to hyaluronidase there would be a 'washout' of extracellular materials and a resulting greater degree of distension.

A total of 671 negatives from 112 ultrathin sections were assessed. Fifteen fields were measured on each negative therefore a total of 10,065 measurements were made in this investigation. Approximately equal samples were taken from each eye (Table 8). Pooled estimates of the mean and standard deviation for each eye were calculated from the results of the eight sections (Table 8).

In the normal eyes (Mn 1) approximately 36% of the area beneath the lining endothelium was occupied by 'empty

	Mn 1		Mn2		Mn3		Mn4		Mn5	
	L	R	CON	EXP	CON	EXP	CON	EXP	CON	EXP
No. of fields per eye	705	660	-	600	600	675	555	615	675	-
Mean % area 'empty space' per eye	36.9	35.5	-	57.9	52.2*	45.5	50.1	53.8*	53.5	-
Pooled S.D.	11.3	10.4	-	15.7	14.3	17.8	17.5	16.4	18.6	-

	Mn 6		Mn 7		Mn 8		Mn 9		Mn 10	
	L	R	CON	EXP	CON	EXP	CON	EXP	CON	EXP
No. of fields per eye	645	705	540	570	540	-	-	735	555	585
Mean % area 'empty space' per eye	51.0	52.4	50.2*	45.8	39.8	-	-	51.1	52.7*	49.6
Pooled S.D.	18.4	15.5	17.3	15.8	17.6	-	-	16.6	15.2	15.0

Table 8: Table to show the results of the quantitative assessment of distension in the cribriform layer in the pig tailed macaques.

* $p < 0.001$ (t-test)

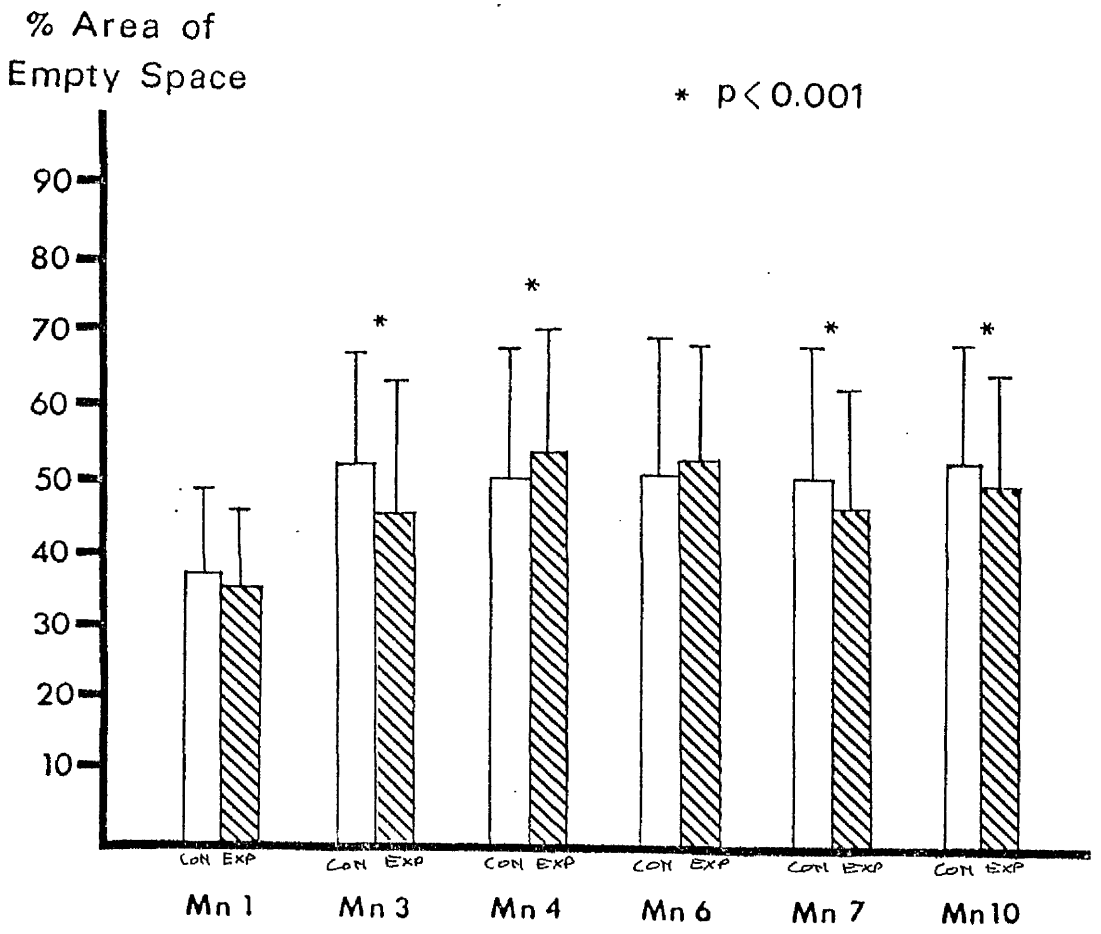

Figure 76: Diagrammatic representation of the results (in five pairs of eyes) of the qualitative assessment of the percentage area of 'empty space' in the cribriform layer. Levels of significance (t-test) are indicated.

Quadrant / Group (n)	Sup. Temp.	Sup. Nasal	Inf. Temp.	Inf. Nasal	Total
NORMALS (2)					
No. of sections	4	4	4	4	16
Mean % 'empty space'	34.48	35.75	39.2	35.4	
'Expected % 'empty space'	36.2	36.2	36.2	36.2	
$\frac{(Obs - Exp)^2}{Exp}$	0.08	0.005	0.24	0.017	$\chi^2 = \underline{0.342}$ NS
CONTROLS (7)					
No. of sections	13	15	18	10	56
Mean % 'empty space'	49.63	53.12	47.14	48.1	
Expected % 'empty space'	49.9	49.9	49.9	49.9	
$\frac{(Obs - Exp)^2}{Exp}$	0.001	0.21	0.15	0.06	$\chi^2 = \underline{0.421}$ NS
EXPERIMENTAL (7)					
No. of sections	16	13	16	11	56
Mean % 'empty space'	50.08	53.64	50.19	52.0	
Expected % 'empty space'	50.9	50.9	50.9	50.9	
$\frac{(Obs - Exp)^2}{Exp}$	0.01	0.14	0.001	0.02	$\chi^2 = \underline{0.171}$ NS

Table 9: Table to show the variation in the results of the quantitative assessment of distension between quadrants.
The results of Chi squared tests are shown.
NS - not significant.
Number in parantheses = number of eyes in group.

space'. The means and standard deviations of the two eyes were similar although there was slightly less distension in the right eye.

All the results in control and experimental eyes are shown in Table 8, however, only the results in paired eyes are diagrammatically represented in Fig 76. Of these five matched pairs, distension was significantly less in the experimental eye in three, as indicated by a t-test (Mn 3, t=7.4; Mn 7, t=4.4; Mn 10, t=3.4). In one pair there was no difference (Mn 6) and in another it was greater in the experimental eye (Mn 4, t=3.7).

The overall group results were as follows:

control:- 49.9 ± 17.1, n=4,110

experimental:- 50.9 ± 16.2, n=4,415

A t-test indicated that this difference was statistically significant ($t=2.83$, $0.001 < p < 0.01$). This was of course due to the very large sample sizes, hence very small standard errors and confidence intervals.

The distension data was broken down into quadrants as in the vacuole study (Table 9). Chi-squared tests were carried out and the low values indicated that the degree of distension was evenly distributed between the quadrants in normal, control and experimental eyes.

There was a great deal of variation in the amount of 'empty space' in the cribriform layer within one eye, this was true of both control and experimental eyes.

In summary, the use of image analysis revealed a slightly greater degree of distension in the cribriform

layer of the hyaluronidase treated eyes.

The incidence of 'breaks' in the lining endothelium of Schlemm's canal (as seen by TEM)

The qualitative examination of the tissue showed that there were areas of marked distension in the cribriform layer, and that there were some tears or 'breaks' in the lining endothelium (vide supra). Since it was feasible that the lower incidence of 'giant vacuoles' in experimental eyes might be the result of drainage through this less conventional route a quantitative ultrastructural study of the incidence, nature and size of any breaks in the lining endothelium was undertaken.

A total of 274 electron micrographs from control eyes and 299 from experimental eyes were assessed. There were three major disruptions in the control eye of Mn 4, which were considered to be preparation artefacts judged on the criteria previously described (see materials and methods).

A total of five non-vacuolar pores were noted in the seven control eyes, and three in the seven experimental eyes, all of which were under 0.5 μm in size. Only one vacuolar pore (ie, on the lumen aspect of a 'giant vacuole') was noted in the control eyes, and six were noted in experimental eyes, all were about 1 μm or less in size. There were twelve small disruptions which were identified as artefacts in control eyes, and six similar disruptions in experimental eyes.

In summary, although large areas of lining endothelium were studied at the ultrastructural level, only a few

breaks in the lining endothelium were found, the majority of which were considered to be artefacts. The small numbers involved were unsuitable for a valid analysis, however, it did not appear that there was any difference between control and experimental eyes. Admittedly a study of this nature, without serial sections, is of limited value but it was considered important to exclude the possibility that hyaluronidase treated eyes had suffered major disruptions to the lining endothelium.

Quantitative study of the bulges and pores in the lining endothelium of Schlemm's canal by scanning electron microscopy

In conjunction with the other quantitative studies it was considered essential that the pores in the trabecular wall of Schlemm's canal be studied, since these structures represent transcellular channels, and as such they would be expected to vary in accordance with the physiological measurements. This study was carried out by SEM in order to investigate larger areas of lining endothelium in both control and experimental eyes.

The criteria used in the present investigation were similar to previous authors who have carried out quantitative studies of this nature (Bill 1970, Lee 1971, Bill and Svedbergh 1972, Lee and Grierson 1975, Grierson, Lee, Mosely and Abraham 1979). The following features were counted on each print of intact areas of lining endothelium (and diameter measured in the case of pores):

i) Bulges; by SEM it was unclear whether these were

Animal	Mn 1		Mn 2		Mn 3		Mn 4		Mn 5	
	LEFT	RIGHT	Con	Exp	Con	Exp	Con	Exp	Con	Exp
Total area examined (n x 3000) μ^2	72,000	105,000		60,000	57,000	42,000	102,000	48,000	57,000	
Bulges	4,902	5,476		6,383	4,421	5,857	5,107	4,583	5,315	
Pores on bulges	69	19		499	228	309	186	187	491	
% Bulges with pores	1.4	0.35		7.8	5.2	5.3	3.6	4.1	9.2	
Other pores	138	57		333	280	190	264	238	298	
Total pores	207	86		832	508	499	450	425	789	

Animal	Mn 6		Mn 7		Mn 8		Mn 9		Mn 10	
	Con	Exp	Con	Exp	Con	Exp	Con	Exp	Con	Exp
Total area examined (n x 3000) μ^2	63,000	63,000	84,000	36,000	51,000			93,000	81,000	42,000
Bulges	4,777	6,333	5,249	4,694	6,235			5,333	5,407	6,548
Pores on bulges	635	492	166	194	0			333	358	48
% Bulges with pores	13.2	7.8	3.2	4.1	0			6.2	6.6	0.7
Other pores	730	825	416	333	294			440	395	523
Total pores	1,365	1,317	582	527	294			773	753	571

Table 10: Table summarising the results of the quantitative SEM study of the lining endothelium of Schlemm's canal. Results expressed as features/mm^2.

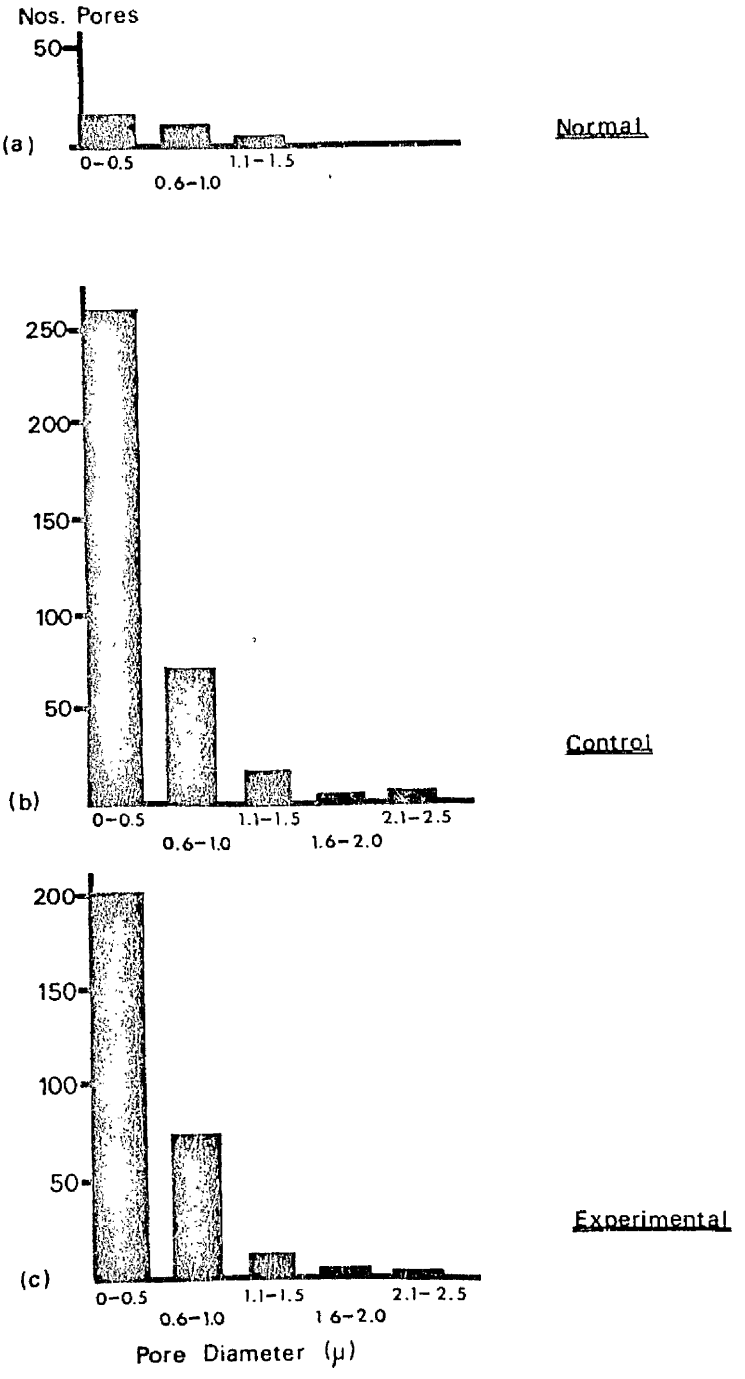

Figure 77: a),b),c). Histograms to show the size and frequency of the pore diameters in normal, control and experimental tissue as recorded in SEM study of the lining endothelium. (Not corrected for sample size).

	CONTROL n = 7	EXP n = 7
Area examined μ^2	495,000	384,000
Bulges, mean ± S.D.	5,216 ± 566	5,675 ± 817
Pores on bulges, mean ± S.D.	295 ± 215	294 ± 166
% Bulges with pores, mean ± S.D.	5.9 ± 4.3	5.1 ± 2.4
Other pores mean ± S.D.	382 ± 164	411 ± 214
Total pores mean ± S.D.	677 ± 348	706 ± 307

Table 11: Pooled data of group results (mean ± S.D.) of quantitative SEM study of the lining endothelium. Results expressed as features/mm^2.

nuclei or vacuoles.

ii) Pores on bulges.

iii) Non-bulge pores.

Pores were considered real if they had a smooth outline, while those with irregular edges were assumed to be artefacts and were ignored. The results from the group of prints in each eye were collected and expressed as results per square millimetre. A total of 352 prints were examined, 59 from normals, 165 from control eyes and 128 from experimentals.

In the normal eye there were around 5000 bulges/mm^2, but pores were rare and whenever found were three or four times more likely to be non-vacuolar. The pores were less than 1.5 μm in diameter (Fig 77).

Paired t-tests on the five matched pairs of eyes showed that there was no statistical difference in the numbers of each of the following: bulges, percentage bulges with pores, other pores and total pores. The pooled results of control and experimental groups are shown in Table 11. The area sampled in the experimental group was smaller (22%) than the control group. There was no statistical difference (t-test) in the numbers of bulges, bulge-pores and non-bulge pores between control and experimental groups. In both groups the mean number of total pores was approximately 700/mm^2, of which more than half were non-bulge pores.

The results of the pore size and frequency measurements in the normal, control and experimental groups are

diagrammatically represented in Fig 77). The numbers of pores shown are the actual counts, with no correction for sample size. Hence there appears to be slightly more pores in the control group than in the experimental. The frequency distribution of the pore diameters in all groups is skewed with the majority of pores being under 0.5 μm in size. Unfortunately, the data was not collected in a fashion which allowed the sizes of the vacuolar and non-vacuolar pores to be compared, however, from a qualitative impression it appeared that the non-vacuolar pores were smaller and probably contributed a substantial proportion of the smaller pores.

In the normal eyes (Mn 1) the percentage of bulges with pores was approximately 1%, whereas in both control and experimental groups it was 5-6%. A greater proportion of the total pores ($\simeq$ 40%) were situated on bulges in the control and experimental groups compared with about a quarter in normal eyes (although it has to be admitted that this is based on a small sample from normal eyes).

Despite the intrinsic sources of error in this study it is assumed that conditions were equal for both control and experimental groups of tissue. In summary the quantitative investigation did not reveal any difference in the numbers of bulges and pores in the lining endothelium between control and hyaluronidase treated eyes.

Incidence of patent and occluded collector channels

In this part of the investigation it was hoped to discover whether occlusion of collector channel openings

was commoner in control or experimental eyes. In the 193 semithin sections examined by light microscopy (from all 20 eyes) 68 possessed collector channels, ie 35.2%. In the 69 sections from seven control eyes, 20 had collector channels and of these 12 (60%) showed some form of occlusion by trabecular tissue. In the 69 sections from the seven experimental eyes 28 had collector channels and of these 15 (53·5%) were occluded to some extent.

This small sample of tissue suggests that collector channels are very numerous in the pig tailed macaque outflow system. A large percentage of these collector channels appeared to be either totally or partially occluded by distension of the cribriform layer. This was found to a similar extent in both control and experimental groups of eyes but was not found in normal unperfused eyes.

Assessment of colloidal iron staining in the trabecular meshwork

This section describes the results of the non-parametric technique which was carried out to discover if there was any obvious difference in the quantity of glycosaminoglycans, which was stained with colloidal iron, between control and experimental eyes.

A total of 29 sections from the five matched pairs of eyes were investigated. The results are shown in Table 12, and diagrammatically represented in Fig 78. In three of the five pairs (Mn 3, Mn 6, Mn 10) the score in the experimental eye was lower than the control eye. The reverse was true of the other two pairs (Mn 4, Mn 7). The

ANIMAL	No. of sections	Mean score per section	Total no. of vacuoles	% Vacuoles containing stain
Mn 3 CONTROL	4	18	26	69
Mn 3 EXPERIMENTAL	1	12	7	43
Mn 4 CONTROL	2	12.5	14	43
Mn 4 EXPERIMENTAL	2	14	6	33
Mn 6 CONTROL	4	16.7	51	63
Mn 6 EXPERIMENTAL	3	16	34	59
Mn 7 CONTROL	3	15.3	23	65
Mn 7 EXPERIMENTAL	3	18.3	10	50
Mn 10 CONTROL	4	18.3	29	52
Mn 10 EXPERIMENTAL	3	12.7	31	51
GROUP RESULT				
CONTROL	17	16.2	143	58
EXPERIMENTAL	12	14.6	88	47

Table 12: Table to show the results of the non-parametric study of the colloidal iron staining in the trabecular meshwork of the five paired pig tailed macaque eyes.

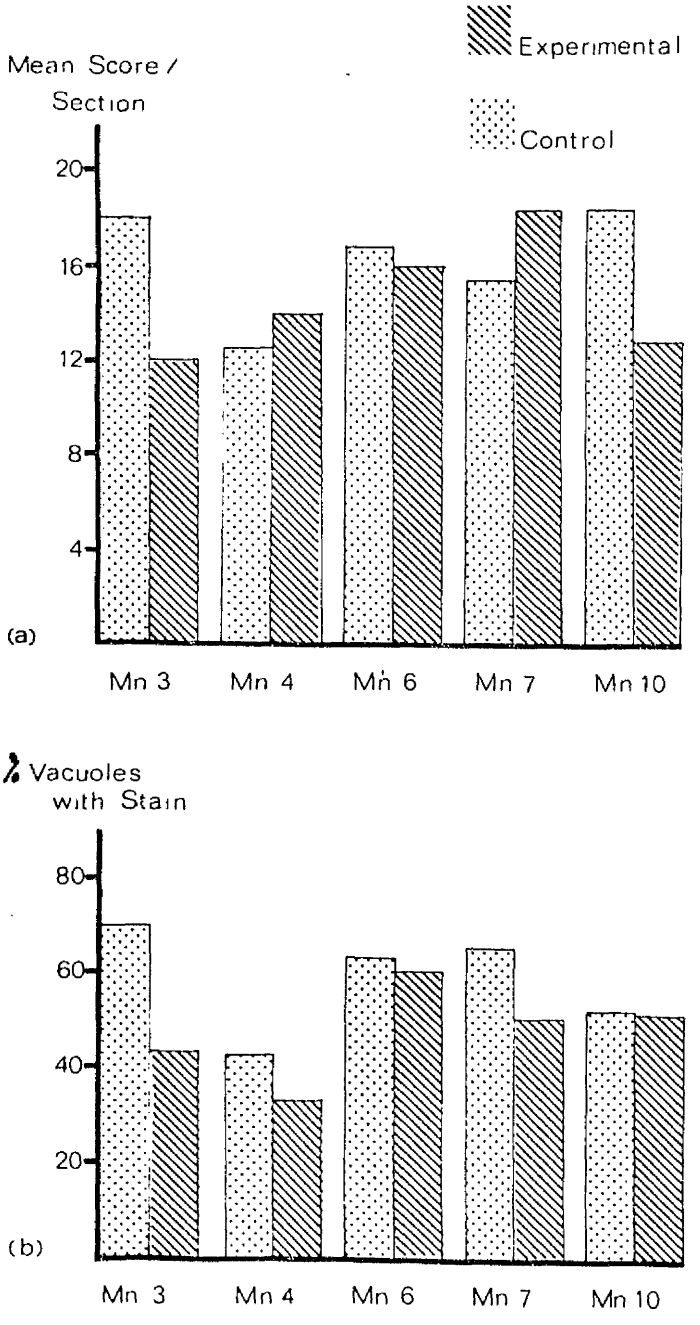

Figure 78: a) Diagrammatic representation of the mean score per section in the five pairs of control and experimental eyes in the non-parametric assessment of colloidal iron staining in the trabecular meshwork.

b) Diagrammatic representation of the percentage of 'giant vacuoles' seen with colloidal iron particles in their lumen in the five pairs of eyes.

guess as to which eye was experimental and which control, based on examination and scoring of the coded sections, was correct in three cases (Mn 3, Mn 6, Mn 10) but wrong in those two cases (Mn 4, Mn 7) in which scoring was higher in the experimental eye. The group data was tested using a Mann-Whitney U-test and no statistical difference was found (U=31.5).

The examination of 'giant vacuoles' in these sections revealed slightly fewer vacuoles per section (7.3) in experimental eyes than in control (8.4) as would have been expected from earlier results. The presence or absence of stain in the 'giant vacuoles' was noted and the total percentage of vacuoles in each eye was calculated (Table 12). The percentage was lower by varying extents in the experimental eye than in the control in all five pairs (Fig 78b). The group results revealed that 58% of vacuoles in control eyes and 47% in experimental eyes contained colloidal iron. This does not, however, reveal the approximate quantities of stain in each vacuole.

It is difficult to draw firm conclusions on a study of this nature, which may only have been capable of detecting gross changes in the GAG content of the tissues. Despite this it would seem reasonable to summarise that there was no gross difference in the GAG content between control and hyaluronidase treated eyes.

Inflammatory cell infiltration in the trabecular meshwork

Polymorphonuclear leucocytes were absent in the normal pig tailed macaque outflow apparatus. There was, however,

a large number of tissue histiocytes (total of 61 in 20 semithin sections $\simeq$ 3 per section). Sixty-nine semithin sections were examined from seven control eyes, and the same number was examined from seven experimental eyes. The results of the counts of polymorphonuclear leucocytes, (mean number of cells per section $\pm$ standard deviation) were as follows:

Control - 4.2 $\pm$ 1.9 cells/section

Experimental - 4.0 $\pm$ 2.2 cells/section

A t-test indicated that there was no statistical difference (t=0.57) in the incidence of this type of cell in the trabecular meshwork of control and experimental eyes.

The incidence of other non-endothelial cells (tissue histiocytes, macrophages, lymphocytes and plasma cells) were as follows:

Control - 1.2 $\pm$ 0.5 cells/section

Experimental - 1.7 $\pm$ 0.7 cells/section

The marginally higher incidence in experimental eyes was statistically significant (t=4.83, $p < 0.001$).

In summary there were only small numbers of inflammatory cells in the trabecular meshwork of both control and hyaluronidase treated eyes, which were mostly polymorphonuclear leucocytes. These were present in similar numbers in both groups and their presence was probably related to the invasive technique of the experiment. In both control and experimental groups the incidence of other non-endothelial cells, which included

the tissue histiocytes was lower than in normal unperfused tissue, which suggests that there has been a loss of tissue histiocytes in perfused eyes.

CORRELATION OF MORPHOLOGICAL AND PHYSIOLOGICAL RESULTS

In this section an attempt is made firstly to correlate the results of the quantitative morphological studies and secondly to correlate the physiological and morphological data.

The data is summarised in Table 13. Spearman's rank correlations were carried out on all the possible combinations (96) between the fourteen factors. Spearman's rank correlation involves ranking the data for each factor, before correlation. In some cases this may include data from sixteen eyes (eg, when correlating factors 7 to 12, Tables 13 and 14) or fourteen eyes (eg, factors 2 to 12) or only 10 eyes (factors 12 and 13 with all other factors). The results of the Spearman's rank correlations are summarised in Table 14. Due to the differing degrees of freedom the r-value necessary for significance at the 5% probability level also varies.

Correlation between morphological factors

Of the 28 Spearman's rank correlations calculated between the 8 morphological factors (7-14, block a in Table 14), 7 had significant r-values (8 and 9, 8 and 11, 8 and 12, 9 and 11, 9 and 12, 11 and 12, 12 and 14).

		Wt	IOP	F.18	F.22	C	TF	IWN	GV	% ES	B/mm^2	Pores	Total pores	GAG	GV GAG
Mn 1	L	12.0	–	–	–	–	–	12.5	16.1	36.9	4902	69	207	–	–
Mn 1	R	12.0	–	–	–	–	–	12.5	7.7	35.5	5476	19	86	–	–
Mn 2	EXP	11.5	10	1.90	2.96	0.27	61.1	9.2	27.0	57.9	6383	499	832	–	–
Mn 3	CON	14.0	4	0	0.04	0.01	1.1	7.9	7.6	52.2	4421	228	508	18.0	69
Mn 3	EXP	14.0	4	3.81	0.65	-0.79	46.6	9.1	9.1	45.5	5857	309	499	12.0	43
Mn 4	CON	12.0	10	1.73	2.20	0.12	46.7	10.2	28.1	50.1	5107	186	450	12.5	43
Mn 4	EXP	12.0	13	0	5.20	1.3	44.9	10.5	16.5	53.8	4583	187	425	14.0	33
Mn 5	CON	10.5	11	1.87	4.16	0.57	76.0	9.9	28.3	53.5	5315	491	789	–	–
Mn 6	CON	14.0	14	1.57	1.47	-0.03	41.4	10.4	36.4	51.0	4777	635	1365	16.7	63
Mn 6	EXP	14.0	20	1.39	3.20	0.45	69.8	11.4	27.9	52.8	6333	492	1317	16.0	59
Mn 7	CON	10.8	12	0	0.13	0.03	1.9	12.4	18.9	50.2	5249	166	582	15.3	65
Mn 7	EXP	10.8	16	0.68	0.71	0.01	13.8	14.9	6.0	45.8	4694	194	527	18.3	50
Mn 8	CON	12.3	12	0.15	3.07	0.73	36.5	8.3	13.8	39.8	6235	0	294	–	–
Mn 9	EXP	10.5	9	0.64	3.28	0.66	50.6	14.1	19.8	51.1	5333	333	773	–	–
Mn 10	CON	11.5	6	4.85	8.69	0.96	171.5	9.0	24.4	52.7	5407	358	753	18.3	52
Mn 10	EXP	11.5	6	11.85	14.65	0.70	348.6	7.7	10.8	49.6	6548	48	571	12.7	51

Table 13: Table summarising the physiological and morphological results in the normal, control and experimental eyes.
F.18 - flow 18 mm Hg. F.22 - flow 22 mm Hg. C - outflow facility. TF - total flow.
IWN - inner wall nuclei/section. GV - total vacuoles/section. % ES - % 'empty space'.
B/mm^2 - bulges/mm^2. Pores - pores on bulges. GAG - GAG score. GV GAG - % vacuoles with GAGs.

		Wt	IOP	F.18	F.22	C	TF	IWN	GV	% ES	B/mm^2	Pores	Total pores	GAG
		1	2	3	4	5	6	7	8	9	10	11	12	13
	2	-0.009												
	3	-0.058	-0.381											
	4	-0.327	0.002	-0.413										
	5	-0.323	0.030	0.020	0.862***									
	6	-0.258	-0.021	0.784***	0.807***	0.495								
	7	-0.358	0.658**	-0.422	-0.174	-0.169	-0.244							
	8	-0.054	0.298	0.241	0.266	0.092	0.424	0.093						
	9	-0.175	0.060	-0.007	0.349	0.341	0.345	-0.199	0.520*					
	10	-0.047	-0.172	0.616*	0.433	0.288	0.666**	-0.393	0.158	0.075				
	11	0.044	0.125	0.304	0.015	0.249	0.301	0.280	0.603*	0.708**	0.020			
	12	-0.164	0.234	0.298	0.116	-0.167	0.393	-0.052	0.594*	0.649**	0.328	0.849***		
	13	-0.215	0.297	-0.258	-0.085	0.027	-0.298	0.207	-0.116	0.377	-0.383	0.427	0.498	
GV GAG	14	0.108	-0.021	-0.271	-0.426	0.268	-0.401	-0.061	0.103	0.195	-0.061	0.257	0.669*	0.512

a)

b)

c)

Table 14: Table to show the results (r values) of the Spearman's rank correlation carried out on factors 1-14. The significance levels are indicated * $p < 0.05$, ** $p < 0.01$, *** $p < 0.001$.
F.18 - flow 18 mm Hg. F.22 - flow 22 mm Hg. C - outflow facility. TF - total flow.
IWN - inner wall nuclei/section. GV - total vacuoles/section. % ES - % 'empty space'.
B/mm^2 - bulges/mm^2. Pores - pores on bulges. GAG - GAG score. GV GAG - % vacuoles with GAGs.

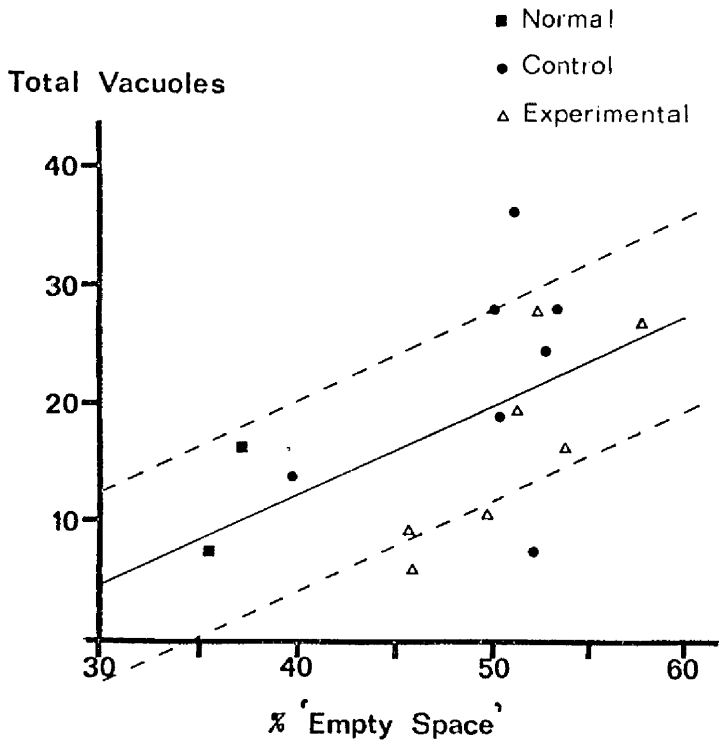

Figure 79: The total number of 'giant vacuoles' (mean per section) plotted against the percentage of 'empty space' in the cribriform layer in all the pig tailed macaque eyes investigated. The regression line is shown and can be expressed as $y = 0.77x - 18.9$, the standard deviation about the line is 8.1, and is indicated by the dotted line.

The first of these significant correlations was between total 'giant vacuoles'and percentage 'empty space' in the cribriform layer (factors 8 and 9, r=0.52, Fig 79). In broad terms this relationship suggested that an increase in distension from 35% to 55% 'empty space' would be paralleled by a doubling of vacuolar incidence.

'Giant vacuole' incidence was also correlated with both pores on bulges, (factors 8 and 11, r=0.60, Fig 80a) and the total number of pores (factors 8 and 12, r=0.59, Fig 80b). The pores on the bulges probably represent pores on the lumen aspect of 'giant vacuoles', and total pores consists of vacuolar and non-vacuolar pores both of which are transcellular channels. The slopes of both regression lines are very similar and suggest that with a doubling of vacuolar incidence from for example 15-30 vacuoles/section there is a 3 or 4 fold increase in both vacuolar and non-vacuolar pores to equal extents.

The percentage of 'empty space' in the cribriform layer correlated with both the pores on bulges (factors 9 and 11, r=0.708, Fig 81a) and total pores (factors 9 and 12, r=0.649, Fig 81b). It can be seen from Figure 81b that the slope of the line would have been greater and would have fitted better if it were not for the two points with over 1300 pores/mm^2 (Mn 6 - which had high resting intraocular pressures). The slope of the line without these two points would have meant that it would have crossed the ordinate at around 30% which is more realistic when one notes where the points for the two normal eyes lie (Mn 1). However, these

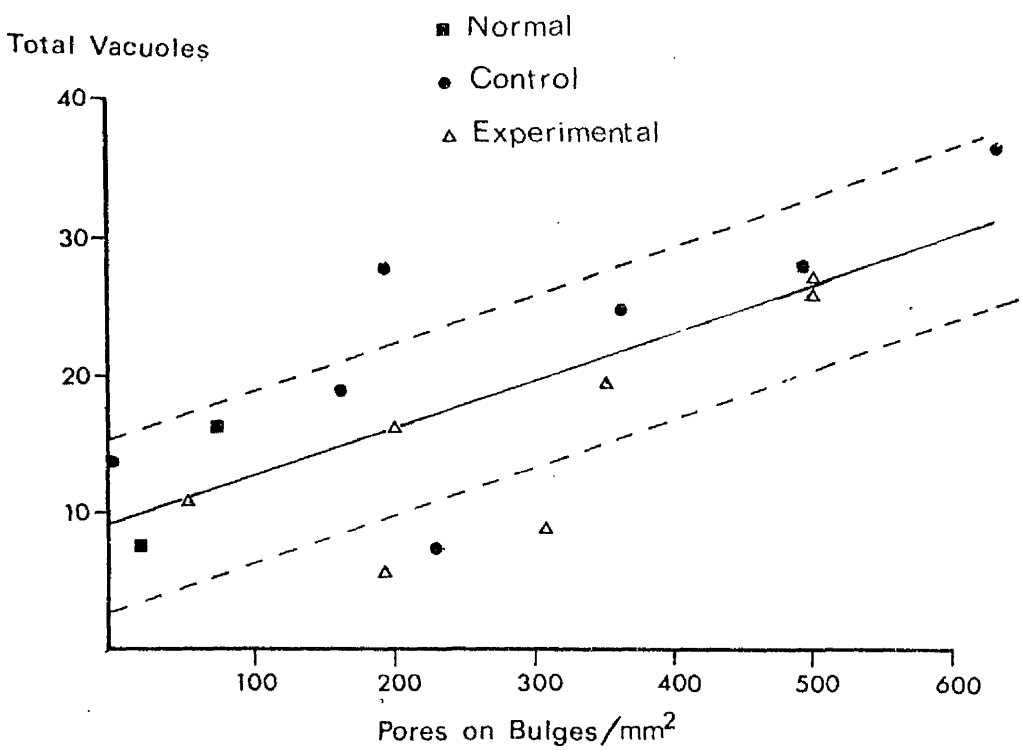

Figure 80: a) The relationship between the total number of vacuoles per section and the number of pores on bulges per mm^2 of the lining endothelium. The regression line (y= 0.04x +9.2) is indicated and the standard deviation about the line is 6.3.

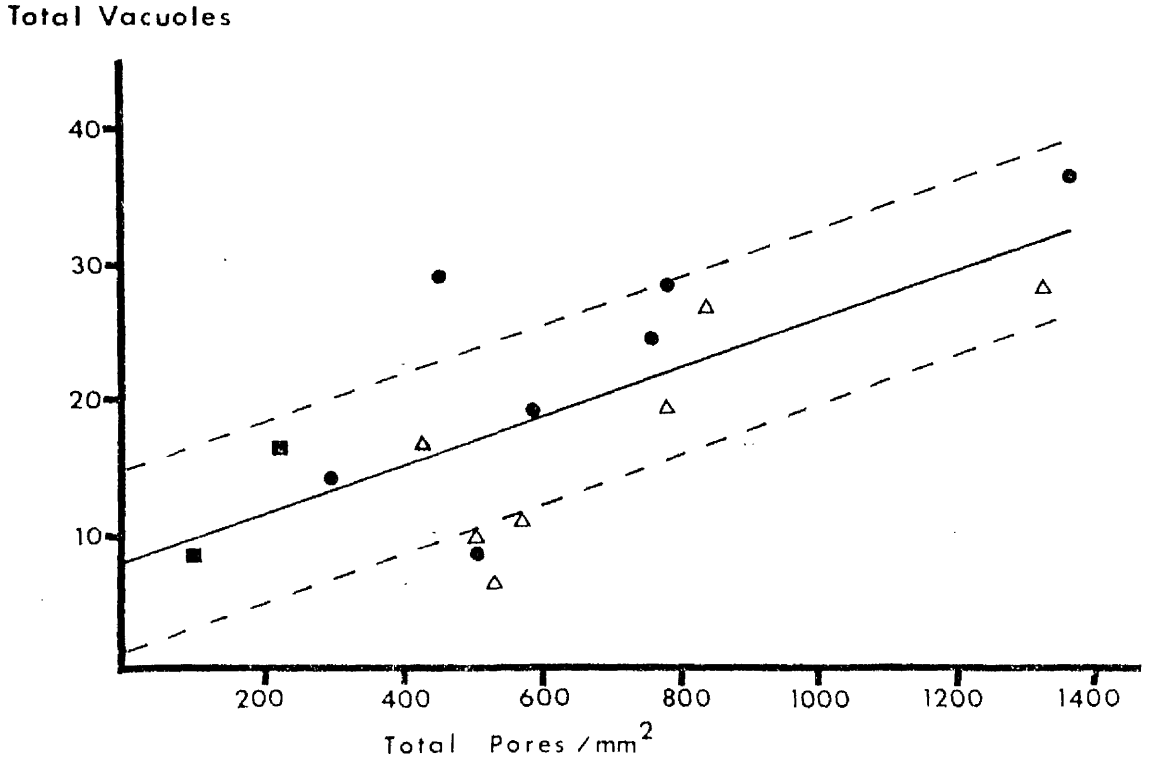

Figure 80: b) The relationship between the total number of vacuoles and the total pores per mm^2. The regression line (y= 0.018x +7.9) and standard deviation (6.9) about the line are indicated.

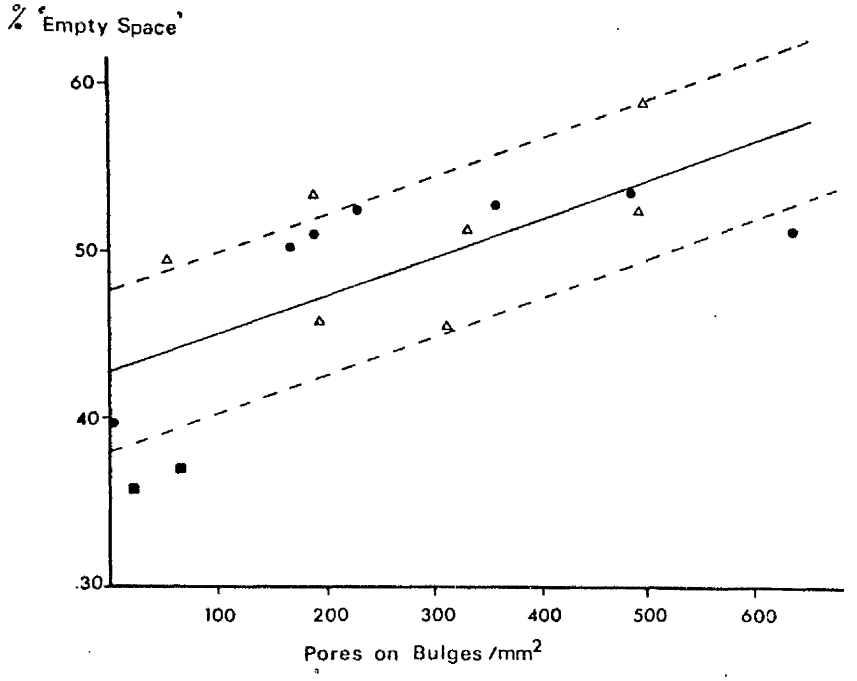

Figure 81: a) The relationship between the percentage of 'empty space' in the cribriform layer and the number of pores on bulges per mm^2 on the lining endothelium of normal, control and experimental pig tailed macaque eyes. The regression line (y= 0.02x +42.7) and standard deviation of the line (4.8) are indicated.

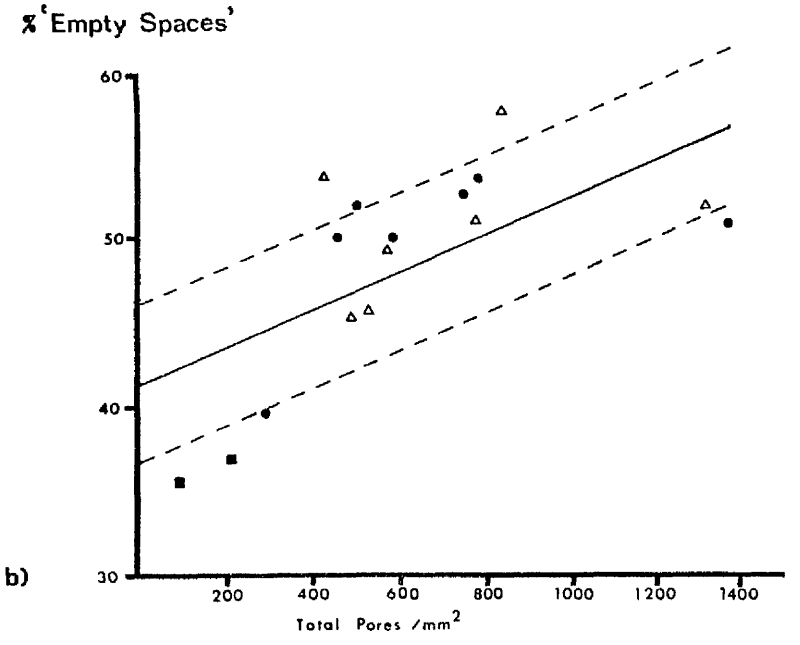

b)

Figure 81: b) Relationship between the % of 'empty space' in the cribriform layer and the total number of pores per mm^2. The regression line (y= 0.012x +41.5) and standard deviation (4.9) of the line are similar to that in Fig. 81a.

relationships may suggest the correlation is good up to a point (ie, a sharp rise between 35-50% 'empty space' will cause an increase in pores from 200-800/mm^2). It may be possible that either, any greater number of pores than this in the lining endothelium causes a loss of the distending effect due to the loss of resistance in the cribriform layer or the monolayer. Alternatively, it seems equally likely that distension has an upper limit of 55% due to the finite volume of the scleral sulcus.

It can be seen from all those above correlations that the incidence of 'giant vacuoles', the percentage of 'empty space' in the cribriform layer, vacuolar pores and non-vacuolar pores are all interrelated in every possible combination, which could be summarised by the following rule; "With increased distension in the cribriform layer there is an increase in vacuolation and the formation of transcellular channels".

Another positive correlation between morphological factors was that of the total number of pores and the percentage of vacuoles containing GAGs (factors 12 and 14, r=0.669). Although this could be interpreted as evidence of washout of GAGs, it was puzzling that no correlation existed between vacuolar pores and GAGs in vacuoles, therefore this may have to be interpreted with caution.

Correlation between physiological and morphological results

The correlations between the various physiological factors (block c - Table 14) were expected, and they will not be considered any further.

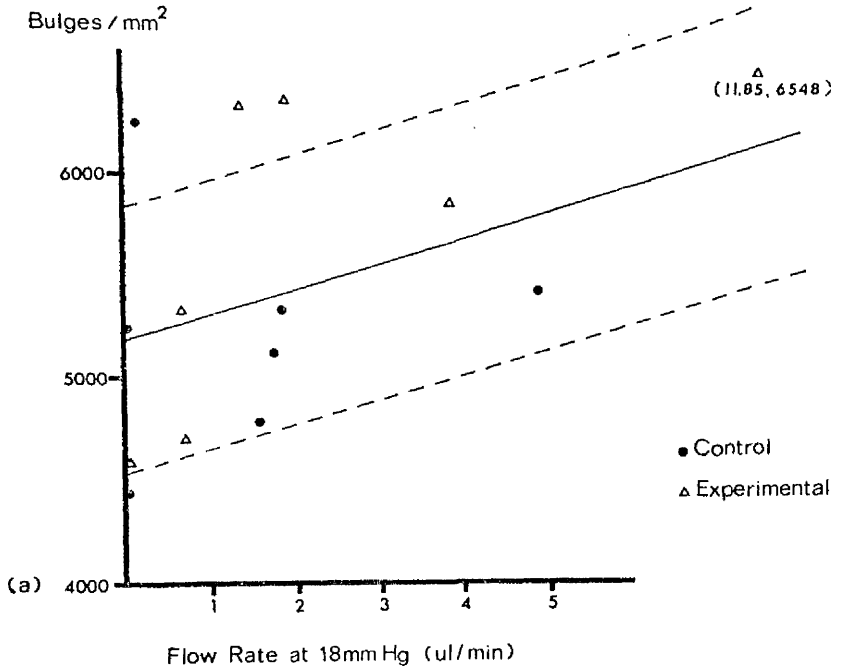

Figure 82: a) The relationship between the number of bulges per mm^2 the lining endothelium and the flow rate at 18mm Hg recorded in each of the control and experimental eyes. The regression line (y= 118x +5189) and standard deviation of the line (637) are indicated.

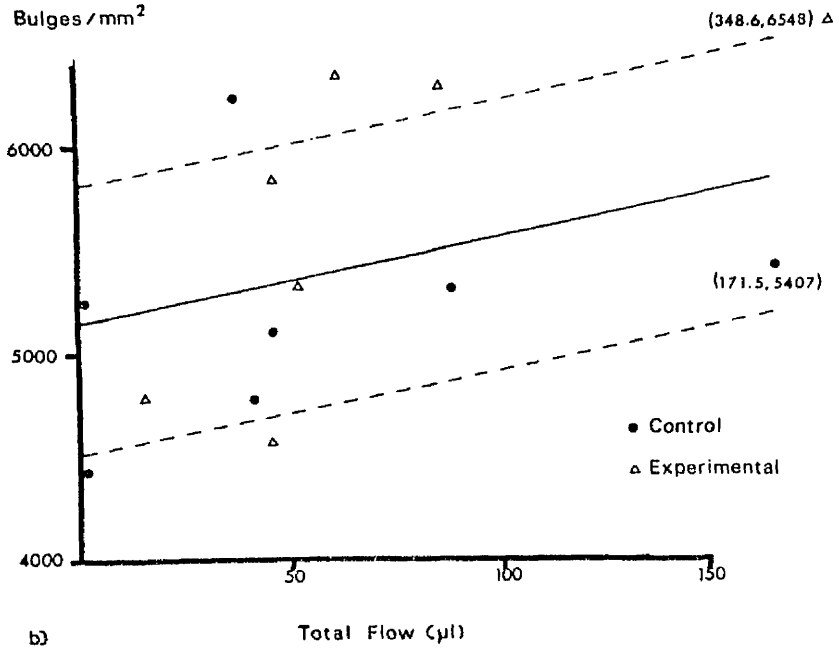

Figure 82: b) The relationship between the bulges per mm^2 and the total flow recorded throughout the physiological measurements. The regression line (y= 4.2x +5146) and standard deviation (636) are similar to Fig. 82a.

This section is concerned with the relationships between the phsyiological measurements (factors 1-6) and the morphological parameters (factors 7-14, block b - Table 14). Of the 48 Spearman's rank correlations only three were statistically significant (factors 2 and 7, 3 and 10, 6 and 10). The first of these correlations was between the number of nuclei in the inner wall of Schlemm's canal and the resting intraocular pressure. This was a rather puzzling result and is presumably a chance occurrence since it is unlikely that any such relationship could exist between these two factors.

The numbers of bulges per square millimetre correlated with both the flow rate at 18 mm Hg (factors 10 and 3, r=0.616, Fig 82a) and the total flow throughout the experiment (factors 10 and 6, r=0.666, Fig 82b). Although bulges in the lining endothelium consist of both nuclei and vacuoles, it is obvious that only the numbers of vacuoles can increase, therefore any change in the numbers of bulges seen by SEM must signify a change in vacuole numbers. Both regression lines cross the ordinates at almost identical points (Fig 82a and b). This suggested that with no inflow from the perfusion system there are around 5000 bulges. This is of similar dimension to the counts in the normal eyes (Mn 1 - 4902, 5476 bulges/mm^2). Therefore, although there is no inflow from the experimental system, it is likely that the animal's own aqueous production ($\simeq$ 3 μl/min) will maintain a population of vacuoles along with the constant population of nuclei.

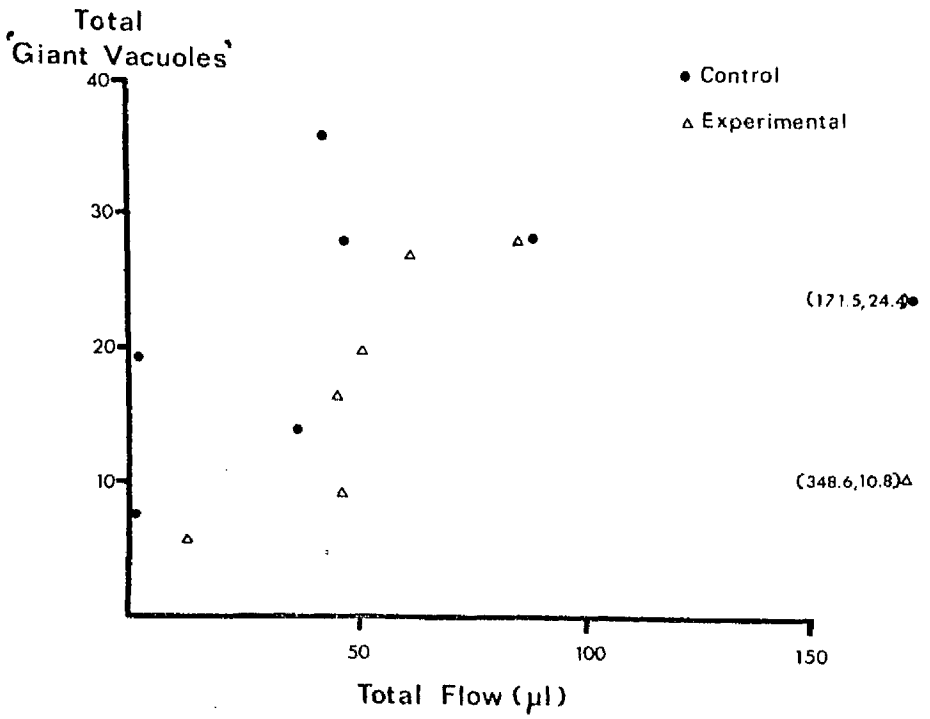

Figure 83: The total number of vacuoles per section and the total flow in control and experimental eyes are plotted to show the general positive correlation which is offset by the values of (Mn10) which had very high flows but few vacuoles.

The total flow throughout the experiment (factor 6) had high correlation coefficients (but below that required for statistical significance) with total 'giant vacuoles', the percentage 'empty space' and pores (Table 14). When total flow was plotted against 'giant vacuoles' (factors 6 and 8, $r=0.424$, $p < 0.1$) it was clear that the exceptionally high flows of both eyes in Mn 10 offset what would have otherwise been a statistically significant relationship.

On the basis of the above evidence it can be concluded that the numbers of 'giant vacuoles' (whether seen as bulges by SEM or true vacuoles by light microscopy) did increase with increased flow.

The correlations of both the GAG score (factor 13) and the percentage of vacuoles containing stain (factor 14) with the various physiological parameters (factors 3-6) although not statistically significant did show a trend towards negative correlations (Table 14). These may of course have been chance occurrences or else they may suggest that with increased flow through the outflow system there was decreased GAG content in the trabecular tissues and the 'giant vacuoles'.

If the eyes were considered separately as controls and experimentals then it was shown that with higher flow rates at 22 mmHg the experimental eyes of the matched pairs generally had fewer 'giant vacuoles' (Fig 84). This was not in keeping with the general trends previously described.

The results of the Spearman's rank correlation are

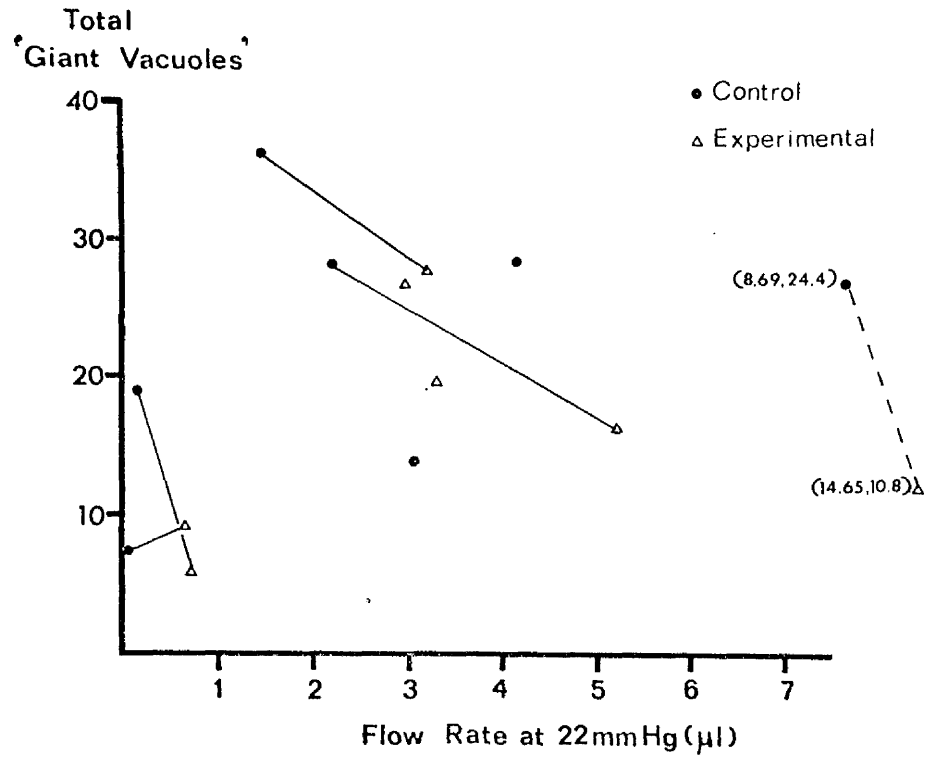

Figure 84: Diagram of the mean total number of 'giant vacuoles' per section plotted against the flow rate at 22mm Hg. The experimental eyes (•—▵) have in general fewer 'giant vacuoles' but greater flow rates than the control eyes.

summarised diagrammatically in Fig 85.

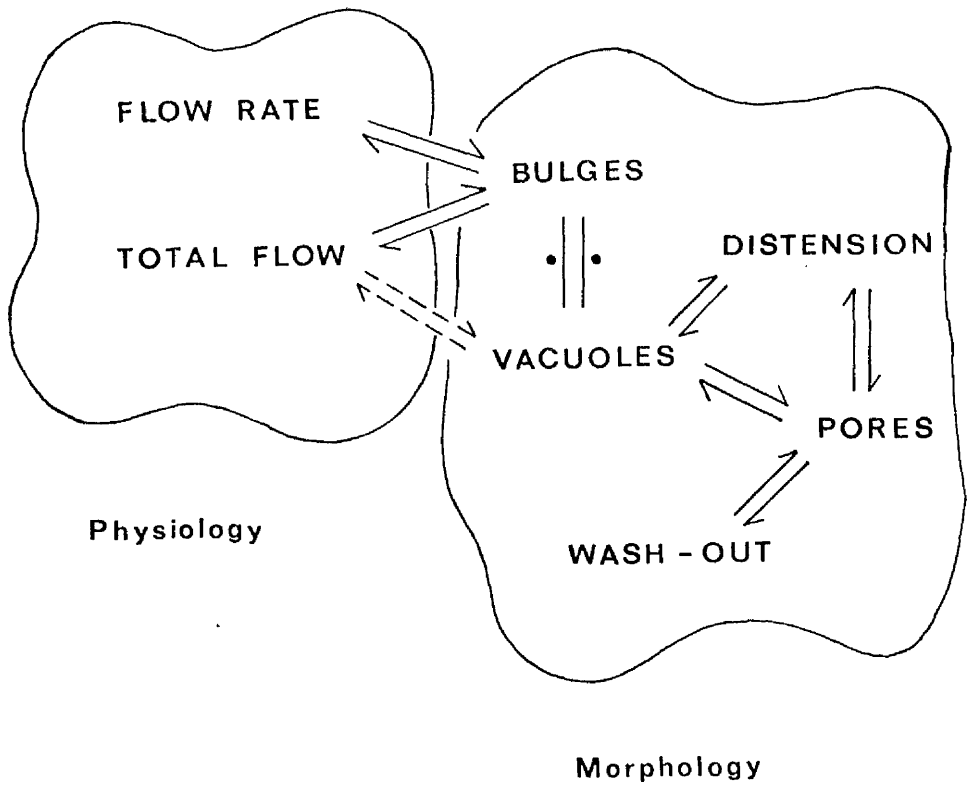

Figure 85: Diagram to summarise the relationships found in the Spearman's rank correlation of the physiological and morphological factors in the study of the pig tailed macaque outflow apparatus.

DISCUSSION

THE PHYSIOLOGICAL EFFECT OF HYALURONIDASE

The first major aim of the present investigation was to determine whether an intracameral injection of testicular hyaluronidase in the primate eye *in vivo* had any effect on aqueous outflow dynamics.

A significant difference in the flow rate at 18 mm Hg was found between the control and hyaluronidase treated eyes in three of the five matched pairs, and at 22 mm Hg in all five pairs. However, due to the extremely variable results between animals there was no difference in the group results of the two flow rates, the outflow facility and the total flow. It was evident that had there been less variation in the results between animals, a more noticeable trend of increased flow in the hyaluronidase treated eyes would have emerged. However, the magnitude of the difference between control and experiment eyes was not comparable in all the animals. As this is the first attempt to demonstrate the effects of hyaluronidase *in vivo* in the primate eye there were no directly comparable studies. However, similar variable results were found in human eyes *in vitro* (François, Rabaey and Neetens 1956, Pedlar 1956, Grant 1963) and in rhesus monkey eyes *in vitro* (Peterson and Jocson 1974). These results in primate eyes are in contrast to the consistent 50% decrease in resistance found in non-primate eyes *in vitro*, regardless of the species of animal, the type or the concentration of

hyaluronidase used (Table 3).

The variation in the physiological results between animals in the present study could to some extent be due to the fact that the experiment was carried out in vivo. There were several variables which could have altered measurement of flow rate during the experiment. These were mainly related to changes in anaesthesia. Firstly, halothane, which was used in the present experiment, has been shown to lower intraocular pressure (Krupin, Feitl, Roshe, Lee and Becker 1980). Secondly, alterations in the levels of blood pO_2 and pCO_2 may affect choroidal blood volume and blood flow through the capillary bed of the ciliary processes, which would lead to a drop in aqueous production (Gallin-Cohen, Podos and Yablonski 1980). Thirdly individual variations in response to anaesthetic agents such as thiopentone and ketamine hydrochloride may alter blood pressure and intraocular pressure to differing extents in individual animals.

Another source of variation may have been the technique used to determine aqueous outflow facility. The rise of 4 mm Hg between the two pressure levels used in this investigation (18 and 22 mm Hg) was chosen because it was hoped that it would be sufficient to produce an increase in inflow rates (to calculate gross outflow facility) without causing a drop in aqueous production or resorption, ie a "pseudofacility", which is about 5% of gross facility in normal monkeys (Bill 1977a). Similar or in some cases lower flow rates at 22 mm Hg than at 18 mm Hg suggested

either that the equipment used to determine flow rates was faulty or that there was a pressure dependent change in resistance (Moses 1977). This resulted in very low values or in some cases negative values for the facility of aqueous outflow. The equipment was thoroughly checked before and often during each experiment, in order to rule out the possibility of a blockage in the tubing. It was obvious therefore that the slight rise in pressure was somehow causing an increase in resistance. This was unexpected since several studies have shown a linear relationship between the inflow rates from a reservoir and the IOP in cynomolgous monkeys (Bill and Bárány 1966) and in rhesus monkeys (Brubaker and Worthen 1973) within the range of about 10 mm Hg above the spontaneous intraocular pressure. The mean resting intraocular pressure under anaesthesia was variable, with a mean of about 11 mm Hg, and in the undisturbed state was assumed to be similar to other primates, 15 mm Hg (Bito, Merrit and de Rousseau 1979) in which case one would not expect to find a decrease in resistance at 22 mm Hg.

One possible explanation for the variation of the hyaluronidase effect from one eye to another may be the presence of hyaluronidase inhibitors in secondary aqueous. In those experimental eyes which suffered more trauma than others, eg paracentesis or mechanical injury to iris or lens there may have been a breakdown of the blood-aqueous barrier at the ciliary processes, resulting in the release of plasma proteins into the aqueous humour (Eakins 1977).

Amongst those plasma proteins there would be hyaluronidase inhibitors. Although in most cases it was felt that due to the design of the cannula the trauma was minimal, the possibility that inhibitors may have been present in the aqueous in some of the experiments cannot be ignored. This was one of the problems with an *in vivo* experiment and emphasises the need for utmost care during cannulation procedures.

Other possible explanations of the physiological results will be discussed when considering the morphological effects of hyaluronidase (vide infra).

THE EXPERIMENTAL ANIMAL

The basic configuration of the angular region in the pig tailed macaque (*Macaca nemestrina*) was similar to most other sub-human primates which have been used in previous studies of this nature. There were a few morphological features of this animal which due to their possible effect on the experimental result require further discussion.

The function of the operculum is unknown but some authors have speculated that in some sub-human primates it may serve to protect the anterior part of the meshwork from excessive flow (Rohen, Lütjen, and Bárány 1967). However, the prominence of the operculum in the pig tailed macaque was variable, and when present it was frequently interrupted by large perforations. It could be predicted therefore that it would not protect the anterior meshwork

from high flows and indeed this was shown to be the case.

The canal of Schlemm in the pig tailed macaque appeared to be drained by a large number of collector channels. Moses (1979) using a mathematical model of the canal, suggested that pressure in the canal is greatest midpoint between two collector channels, and that the greatest pressure differential is at the opening of the collector channel and therefore the canal in this latter region will show a greater tendency to collapse. Since the pig tailed macaque had a large number of collector channels and therefore small distances between each opening, it could be predicted that there would be minimal resistance to circumferential flow in the canal at normal intraocular pressures and at raised pressures there would be frequent blockage of collector channel openings. The numerous cords in the canal of Schlemm of this species of monkey may when present prevent collapse of the canal, and therefore may have an important function in maintaining canal patency in this species with so many collector channels and no scleral spur (which helps prevent collapse at posterior part of canal - Moses (1977)).

The extracellular materials in the cribriform layer of the pig tailed macaque were similar to other sub-human primates and there was intense staining of the ground substance and the cell surfaces in colloidal iron preparations. On hindsight a weakness in the rationale of the present study was to have assumed on the basis of the morphological appearance that hyaluronate and choindroitin

sulphates were components of the cribriform layer in this species as seems likely in other species (see introduction to Part I). Preliminary enzyme digestion studies would have clarified this point.

The cells of the cribriform layer in the pig tailed macaque were very rich in cytoskeletal elements and had numerous contacts with the lining endothelium, and with each other. On this basis it would have been predicted that this tissue was as well equipped to withstand high flow situations as any other species of sub-human primate.

The complex nature of the inner wall of Schlemm's canal with its numerous folds and the connections with the long collagenous cords made the dissection of the trabecular wall for SEM studies very difficult, resulting in numerous areas of damage and large areas of endothelium hidden by cords. Therefore this species was not ideally suited to the detailed SEM investigations.

One of the most unexpected findings in the present investigation was the discovery of smooth muscle cells in the trabecular meshwork. Bundles of smooth muscle cells have been reported in rats and rabbits near the entrance to collector channels in the corneo-scleral tissue (Knepper, Farbman and Bondureff 1975, Tsukahara 1978, Sakimoto 1979). Gipson and Anderson (1979) using a histochemical marker for actin filaments found some intensely stained cells in the human trabecular meshwork and external to Schlemm's canal, which they suggested may be smooth muscle cells. The positive identification of smooth muscle cells in the

present study is the first definite report of these cells in the primate outflow apparatus. It is unlikely that this was a chance occurrence since they were seen to some extent in 11 of the 20 eyes investigated. They appeared to consist of anterior extensions of the longitudinal ciliary muscle which took on a more circumferential orientation in the meshwork, but did not however completely encircle the 360° of the meshwork. The close association of the smooth cells with unmyelated nerve fibres, and the fact that they had connections with both the lining endothelium and the cells of the cribriform and corneoscleral layers suggested that they may play a role in regulating the resistance to aqueous outflow in this species.

THE MORPHOLOGICAL EFFECTS OF HYALURONIDASE

The second aim of this investigation was to discover whether there was a morphological basis for the physiological effects of hyaluronidase. It was postulated on the basis of previous knowledge that the hyaluronidase would depolymerise GAGs in the cribriform layer, where it was believed these substances may not only help bind the tissue together, but also contribute to the resistance to aqueous outflow. It was postulated that any resistance lowering effect the enzyme may have would be manifest as a greater incidence of 'giant vacuoles' and transcellular channels along with a 'washout' of extracellular materials and greater distension of the cribriform layer.

The present investigation did not reveal any obvious difference between control and enzyme treated eyes in the nature or quantity of exracellular materials in the cribriform layer (both in conventional TEM and colloidal iron preparations). Both groups of eyes showed a depletion of these materials when compared to normal unperfused eyes, and this therefore seemed to be a general perfusion effect. Admittedly there may have been some alteration in the GAGs in the enzyme treated eyes which was not detectable by morphological techniques. Alternatively there may have been a small quantitative change in the GAGs which was not detected by the non-parametric technique used in this study. An obvious weak point of the study of colloidal iron treated tissue was the number of sections investigated, which was limited due to the availability of time. The amount of 'washout' of extracellular elements through 'giant vacuoles' did not seem any greater in the enzyme treated eyes than in the controls. In fact, in normal unperfused tissue 'washout' (or the presence of colloidal iron in the vacuole lumen) was equally prevalent. Due to the lack of serial sectioning evidence it was unclear whether those vacuoles devoid of stain were transcellular channels (in which case the material may have been washed through by the flow of aqueous), or blind invaginations. From the estimates available it would seem that at 18 mm Hg (fixation pressure in present study) the proportion of the vacuoles which would be transcellular channels would be 10% (Grierson and Lee 1978), 2% (Cole

and Tripathi 1971) and the higher estimates from SEM studies, 29% (Bill 1970) and 15% (Lee and Grierson 1975). Since in some cases around half of the vacuoles were devoid of stain it seems probable that some of these may be invaginations which do not contain GAGs, and indeed colloidal iron rich extracellular material was often seen on single sections to be present at the meshwork pore of an 'empty' vacuole.

Qualitative morphological examination did not reveal any major differences between the control and experimental group of eyes. It was only with the use of quantitative techniques that two differences could be detected, firstly in vacuolar incidence and secondly in the degree of distension ('empty space' in the cribriform layer).

The lower incidence of 'giant vacuoles' in the lining endothelium of Schlemm's canal in hyaluronidase treated eyes than in controls was an unexpected finding. This meant that enzyme treated eyes which had shown higher flows than their paired controls during the physiological procedures, had fewer vacuoles. The numbers of 'giant vacuoles' have been shown to depend, in a predictable fashion, on the fixation pressure (Johnstone and Grant 1973, Kayes 1975, Grierson and Lee 1975a, 1977a, Tripathi 1977a). This relationship did not seem to be true in the case of hyaluronidase treated eyes. The sizes of the 'giant vacuoles' although not quantitatively assessed did seem comparable in both groups. The only previous morphological study on the effects of intracameral hyaluronidase

injection (Grierson, Lee and Abraham 1979a), in contrast to the present study, showed a mean increase in vacuolar incidence of 48%. This previous study was similar to the present one in several respects, ie perfusate, type of enzyme, mode of injection, fixation pressure and many others, but did differ in the species of primate (Papio anubis), the concentration of enzyme (150 I.U.), the fact that no physiological determinations were carried out and the eyes were fixed two hours after the enzyme injection.

On morphological grounds it seems unlikely that the species of monkey would be an important difference between the two studies. It is equally unlikely that the different enzyme concentrations could account for the results since previous studies have shown little or no dose dependence relationship in the physiological effect (Bárány and Woodin 1954, van Buskirk and Brett 1978). The possible importance of physiological manipulations and the differences in time lapse between injection and fixation are subjects which will emerge later in this discussion.

In the present investigation both control and experimental groups of eyes showed marked distension of the cribriform layer which was marginally greater in experimentals, as indicated by image analysis. The study of Grierson and co-workers (Grierson, Lee and Abraham 1979a) described distension of the cribriform layer in hyaluronidase treated eyes, but this was not a feature of their controls, and therefore in this respect it differed from the present investigation.

In the present investigation the changes in trabecular meshwork of control and experimental eyes were more severe than would have been expected in eyes fixed at 18 mm Hg. They included; the rounding up of the trabecular endothelial cells on the uveal and corneoscleral trabeculae and their detachment from the core in some areas; frequent 'blow-outs' in the lining endothelium; prolapse of cribriform tissue into collector channel openings. Grierson and Lee (1975a) found similar changes to the above in rhesus monkey eyes exposed to 30 mm Hg for one hour. However, at this pressure level the cell to cell contact was maintained in most areas of the cribriform layer and in the corneoscleral meshwork the fine cytoplasmic processes were stretched but intact. In eyes maintained at 50 mm Hg for one hour the distension was similar to the more severe areas in the present study, with loss of cell to cell contact, only loosely dispersed cellular elements and almost complete loss of extracellular material in the cribriform layer. However, at this pressure there were frequent gaps in the lining endothelium which was not a feature of the present study. At 50 mm Hg there were still delicate processes crossing the intertrabecular spaces, which were lost in the present study, but in common with the present study they noted cells detaching from the trabeculae. The changes in cell ultrastructure and the disruption of the lining endothelium observed by Svedbergh (1974) in vervet monkeys maintained at elevated pressures of 33-48 mm Hg for 3-7 hours were not a feature of the

present study. Although Svedbergh (1974) claimed similar changes did not occur in control eyes exposed to the perfusate for equal periods of time, he failed to demonstrate this point.

It is therefore obvious that the changes in the trabecular meshwork in the present study were more severe than would be anticipated of eyes fixed at 18 mm Hg, and that some other factors must be involved. Bill, Lütjen-Drecoll and Svedbergh (1980) studied the morphological effects of eyes perfused at 20 µl/min for 80 minutes with ethylenediaminetetraacetic acid, disodium salt (Na_2EDTA), the chelating agent which binds calcium ions and affects cell junctions. Some of the changes in these eyes were similar to the present study, for example they frequently observed large "balloons" in the lining endothelium which also included the attached sub-endothelial layer of cells. These "balloons" are identical to the so-called 'blow-outs' in the present study. The loss of cell to cell contact in the cribriform layer was slightly more severe than the present study, but the loss of extracellular material seemed comparable. However, the severe effects of Na_2EDTA on the trabecular organisation, the corneal endothelium, the ciliary muscle and the iris sphincter were not features of the present investigation.

The similarities between the milder changes in Na_2EDTA perfused eyes and those observed in the present study particularly in the regions of high flow suggest the possibility that depletion of calcium ions from the cells

due to overlong exposure (over 4 hours) to mock aqueous may have led to weakening of cell to cell adhesions. Bárány's fluid, the mock aqueous used in the present study, reduces the spontaneous reduction in resistance ("washout effect") which is true of isotonic solutions of sodium chloride (Bárány 1964). This is believed to be due to the fact that Bárány's fluid is buffered, contains glucose, calcium and magnesium ions. However, in prolonged experiments mock aqueous tends to result in a fall in resistance to aqueous outflow compared with pooled aqueous humour (Gaasterland, Pederson and McLellan 1978).

If over-exposure to Bárány's fluid in the present study had weakened cell to cell associations, then it may be possible that the alterations in intraocular pressure involved during the facility determinations (eg suddenly opening the eye to 18 mm Hg - when it may have had a resting pressure of 9 mm Hg or less) could have led to the actual separation of weakened cell junctions. If this were the case then it would explain why the trabecular cells had lost their delicate processes and rounded up, also, why the changes in the cribriform layer and the lining endothelium were so marked. The loss of attachments between the lining endothelium and the underlying cellular and extracellular components of the cribriform layer would make vacuolation more difficult (Tripathi 1974, Johnstone 1979, Grierson and Lee 1975a). This would explain the occurrence of the 'blow-outs' in the present study, as areas of lining endothelium which are unable to vacuolate to relieve the

localised build up of aqueous and therefore balloon out into the canal lumen. Grierson and Lee (1975a) concluded from their pressure study that the response of the cribriform layer and lining endothelium to raised pressures was dependent more upon cell to cell contacts than the presence of extracellular materials wich were lost at higher pressures (Grierson and Lee 1977b).

There was no quantitative data on the incidences of 'blow-outs' in control and experimental eyes, however from qualitative impressions there did not appear to be any difference. The incidence of occlusion of collector channel openings by distended cribriform tissue was comparable in both controls and experimentals.

Scanning electron microscopy did not reveal any difference between controls and experiments in the incidence of bulges, vacuolar and non-vacuolar pores or in the sizes of the pores. It was expected that the numbers of bulges would have reflected the number of vacuoles and therefore been lower in experimental eyes, however, this was not the case. The discrepancy may be accounted for by the dissections, which besides being difficult in this species is made more difficult in perfused eyes due to the narrowing of Schlemm's canal. Therefore the already small samples may be an under-representation of high flow areas where vacuoles will be more frequent.

Similar difficulties were experienced by Lee and Grierson (1975) when trying to dissect tissue from rhesus monkey eyes which had been exposed to 22 and 30 mm Hg.

Svedbergh (1974) when dissecting tissue from vervet monkeys, encountered problems with the collagenous septae which were similar to the cords and septae in the pig tailed macaque.

If we assume for the present that hyaluronidase did decrease resistance to aqueous outflow by acting on the GAGs in the cribriform layer then this may explain the reason for the slightly greater distension and lower incidence of vacuoles in these eyes. It would be possible to envisage that the increased flow in the enzyme treated eyes may have caused greater perfusion effects, ie loss of cell to cell contact between the cribriform layer and the lining endothelium which would consequently make vacuolation more difficult.

The other alternatives as to why despite a physiological lowering of resistance the morphological data was so unequivocal (if one accepts that the SEM data does not agree with vacuolar incidence as seen by light microscopy, and that the difference in distension is very small) will be considered. They are as follows:

i) One possibility which it is felt can be discounted is that the enzyme had not reached the trabecular meshwork. There are two main reasons for discounting this suggestion. Firstly tracer studies in primate eyes have shown that material introduced into the anterior chamber can be detected in the 'giant vacuoles' within about 10-15 minutes (Feeney and Wissig 1965, Tripathi 1971, Bill and Smelser 1972). Secondly diffusion alone would have ensured that

the enzyme reached the meshwork, which was illustrated in the course of the present experiment when fixative containing fluorescein filled the anterior chamber within fifteen minutes.

ii) It seems possible that the maximum morphological effect may have been at the time of the physiological measurements, however, at time of fixation, a half hour later, the difference in the morphological appearance of both groups of eyes may have been less remarkable. Nevertheless it seems unlikely that the altered resistance in the experimental eyes could have re-established itself in such a short time.

iii) Although a TEM study of the lining endothelium did not detect any major disruptions in the lining endothelium of experiment eyes which would explain the higher flows in these eyes, this study was limited in the area of tissue examined. It would be theoretically possible for one or two large breaks in the lining endothelium to account for the higher flows seen in the experimental, and it is doubtful whether even detailed serial section studies could rule out the presence of such disruptions.

iv) From the morphological examination it appeared that both control and experimental groups had lost extracellular material particularly in high flow regions. It could be suggested that hyaluronidase by depolymerising the complex molecules of hyaluronate and proteoglycans would reduce the viscosity of the fluid passing through the transcellular channels. Mathematical models have been used to calculate

the theoretical resistance offered by the pores in the lining endothelium (Bill and Svedbergh 1972, Grierson, Lee, Moseley and Abraham 1979, Eriksson and Svedbergh 1980). These models have assumed that the Reynold's number of fluid passing through the transcellular channels is comparable with water. This may not be the case if large molecules of hyaluronate and proteoglycan were normally being washed through the system. Laurent (1981) recently estimated that the hyaluronate concentration in the aqueous humour of man is 1.1 µg/ml. If the rate of aqueous formation is about 3 µl/min this would mean that in an hour 0.2 µg of hyaluronate would leave through the outflow pathways. Admittedly this is a very small quantity but there may also be hyaluronate and proteoglycans, synthesised locally by the trabecular meshwork, which may also be being washed out constantly by aqueous. These large molecules (from both of the above mentioned sources) may contribute to the viscosity of the aqueous passing through the transcellular channels. If this were true in normal eyes and in the control eyes of the present study (where washout may be accelerated in the latter case) then on the basis of Poiseuille's formula, it is possible that flow through the same number and size of transcellular channels could be greater in hyaluronidase treated eyes in which the viscosity would be reduced (higher Reynold's number).

v) Another consideration is that outflow through the conventional pathways may have been similar in both control

and experimental groups but that hyaluronidase had increased the drainage through the unconventional routes. The two most likely suspects would be uveo-scleral and posteriorly through the vitreous.

The clefts between the ciliary muscle fibres often appeared dilated in the present study, however, this did not appear to be specific to hyaluronidase treated eyes. Hyaluronidase could have acted on the inter-cellular matrix between the muscle fibres and on the connective tissues around nerves and blood vessels which pierce the sclera. As a result posterior movement of fluid through this route, which has been estimated to contribute about 25% to aqueous outflow in monkeys (Bill and Hellsing 1965), could have been increased. A brief attempt was made to test this hypothesis in two baboons (Papio anubis) using fluorescein as a tracer in the anterior chamber, according to the technique of Sherman, Green and Laties (1978). Although fluorescein was seen to enter the ciliary muscle face, it was difficult to determine whether there had been greater penetration in the hyaluronidase eyes, and the results were inconclusive. This line of investigation is certainly a possibility for the future.

The second possible route which may have accounted for increased flows in the experimental eyes is posteriorly through the vitreous. If some of the hyaluronidase had diffused posteriorly through the pupil to the anterior vitreous face it may have depolymerised the hyaluronic acid. Indeed Melton and de Ville (1960) noted that after

perfusion for 130 minutes with "10 units" of hyaluronidase all of the eyes from cats, dogs, guinea pigs and rabbits showed liquifaction of the vitreous. Foulds, Moseley, Eadie and McNaught (1980) reported that injecting hyaluronidase into the vitreous of rabbits significantly increases the rate of removal of water by the choroid. The results suggested that hyaluronic acid in the vitreous impedes the diffusional movement of water. The concentration of hyaluronate is lower in rabbits (14-52 μg/ml) compared to man (140-338 μg/ml, Laurent 1981) presumably therefore this effect noted by Foulds et al (1980) would be greater in man and other primates. From the above evidence it seems possible that this route could have contributed to the greater fluid flows in the hyaluronidase treated eyes, but the importance of this contribution is unclear.

FUTURE INVESTIGATIONS

On the morphological evidence available it is probable that the outflow apparatus was exposed to Bárány's fluid for an excessive period. This in conjunction with the pressure alterations during physiological manipulations produced marked changes in the tissues which may have 'masked' the morphological effects of hyaluronidase. If the experiment were to be repeated it could be carried out in the following way. Firstly the whole experiment should be as short as reasonably possible (< 2 hours), in which

time a similar concentration of hyaluronidase could be injected using a smaller volume of the vehicle, Bárány's fluid, eg 10 µl. Flow rate would be perhaps better measured at only one pressure level, for example 5 mm Hg above the spontaneous intraocular pressure, one hour or less after the enzyme injection. Fixation could be carried out immediately after the flow rate determination at the same pressure, which would hopefully give a truer representation of the morphological configuration of the outflow apparatus at the time of enzyme action.

It has been suggested that enzymes introduced into the anterior chamber of patients with primary open angle glaucoma may be a useful "once-off" treatment to disperse the extracellular materials in the cribriform layer which may constitute the abnormally high resistance in the outflow pathways (Grierson, Lee and McMenamin 1981). Clearly it is necessary before any such mode of treatment be attempted that several facts be established. Firstly it would have to be reasonably certain that these materials in the cribriform layer were a primary factor in the increased resistance. Secondly it is vital that the true biochemical identity of these materials (see Part II for more details) be known, and how rapidly if at all they would be likely to be replaced by the native endothelial cells. Thirdly before any "pharmacological washout" using enzymes was attempted it would be necessary to carry out a similar study to that of the present, using for example human eyes immediately after enucleation (which would allow facility

determinations).

The developments of cell and tissue culture methods have allowed investigations into the metabolism of trabecular meshwork cells, however, this research is at an early stage. One topic which is already receiving attention is whether the cells are capable of the synthesis and degradation of the extracellular materials, particulary GAGs. It has already been reported that the cells from primate trabecular meshwork can synthesise GAGs, both hyaluronic acid and chondroitin sulphates, the latter of which are in proteoglycan complexes (Schachtschabel, Bigalke and Rohen 1977, Hassell, Newsome and Ballintine 1980). Evidence from the culture of primate meshwork cells that lysosomal enzymes are present is not yet available, but Hayasaka, Hara, Shiono and Mizuno (1980) have recently shown higher levels of lysosomal hyaluronidase in dissected preparations of the human "inner corneoscleral tissue" (which includes the trabecular meshwork) than in surrounding tissues.

It has been proposed that steroid-induced glaucoma in man may be the consequence of raised levels of GAGs in the outflow apparatus (Spaeth, Rodriques and Weinreb 1977). Raised levels of GAGs have been demonstrated biochemically (Knepper, Breen, Weinstein and Black 1978) and histochemically (Ticho, Lahav, Berkowicz and Yoffe 1979) in dexamethasone induced glaucoma in rabbits. François (1978) has postulated that corticosteroids may stabilise the lysosomal membranes which would cause a drop in GAG

degradation and a resulting excess of GAGs in the outflow tissues which could lead to raised intraocular pressure. Evidence of glucocorticoid affecting lysosomal enzymes is, however, lacking. Interestingly Polansky, Weinreb and Alvorado (1981) have reported that cultured trabecular meshwork cells have glucocorticoid receptors and beta adrenergic receptors which poses the question of whether this is true in vivo and if so could they be involved in regulating or monitoring the extracellular environment.

Once we understand what regulates the synthesis and polymerisation of the extracellular matrix in normal tissue, the techniques may be applied to the investigation of primary open angle glaucoma. It is possible that armed with the knowledge of the mechanisms which regulate the extracellular environment it may be feasible to use agents which for example would stimulate lysosomal enzyme secretion, consequently reducing resistance to aqueous outflow.

THE CORRELATION BETWEEN PHYSIOLOGICAL AND MORPHOLOGICAL RESULTS

The third major aim of this investigation was to correlate the physiological and morphological results and discuss them in relation to previus concepts of the functional morphology of the outflow apparatus. In this respect the application of rank correlation to all the quantitative results (from normals, controls and

experimentals) was successful (summarised in Fig 85) and confirmed previously held views on the morphological changes which the tissue undergoes in response to alterations in pressure and flow.

The unfortunate loss of pressure immediately prior to immerse fixation of the right eye in Mn 1 illustrated the very rapid response of the 'giant vacuoles' and transcellular channels, which were fewer in number than in the left eye, and at the same time reinforces the need for proper control of fixation pressures in any study of the outflow aparatus.

The change in configuration of the cribriform layer and lining endothelium, which was illustrated in Fig 9a and b in the general introduction, was quantitatively shown in the present study. The correlations between the distension of the cribriform layer, the numbers of 'giant vacuoles', the numbers of vacuolar and non-vacuolar transcellular channels were all positive (Fig 85) which means that they all increase or decrease together.

The correlation of the 'giant vacuole' incidence and the physiological results was hampered firstly by the fact that hyaluronidase eyes had higher flows but fewer vacuoles than the controls (vide supra) and secondly by the exceptionally high flows recorded in Mn 10 during the anaesthesia problems. Despite this the correlation between vacuoles and total flow was reasonably good. Grierson, Lee and Abraham (1979b) in an experimental study on the effects of topical pilocarpine in baboons found a good correlation

between the numbers of vacuoles and the final flow rates, but no scanning electron microscopy was carried out. The correlations in the present study between physiological parameters and the numbers of pores (transcellular channels) was weak. Lee and Grierson (1975) counted pores, in a similar fashion to the present study, in rhesus monkey tissue exposed for one hour to 8 and 15 mm Hg and found greater numbers of pores in the three eyes at 15 mm Hg. In the present study there was good correlation between the numbers of bulges seen by SEM and both the flow rates and final flows. This reinforces the evidence that vacuolar incidence increases with flow.

The numbers of pores per square millimeter in the lining endothelium as seen by SEM ($200/mm^2$ - normal; $700/mm^2$ in both controls and experimentals) were lower than previous workers. Bill (1970_a) reported $1200/mm^2$ in normotensive vervet and cynomolgous monkeys, Grierson, Lee, Moseley and Abraham (1979) found only $350/mm^2$ in normal human tissue (malignant melanomas). Segawa (1973) found $1000/mm^2$ in normal human eyes, while Bill and Svedbergh (1972) reported $1800/mm^2$ in normal human tissue. Svedbergh (1976) reported $1640/mm^2$ in cynomolgous eyes fixed at 12 mm Hg.

The lower incidences of pores in normal and perfuse fixed eyes of the present study than those reported in previous studies may be due to several factors. The complex nature of the trabecular wall of Schlemm's canal and the fact that the tissue is only viewed from one aspect

makes it seem likely that large numbers of pores may not be seen, leading to an undercount. The tissue in the present study was critical point dried while most previous quantitative studies have used freeze drying. It is unclear which technique is most suitable and there is need for a parallel study using both techniques on the same tissue to discover whether the number of pores is in any way affected by the preparation.

There were large numbers of non-bulge pores (non-vacuolar) recorded in the present study (60-70% of total pores) compared to previous studies. This may be due to both the under-representation of areas with large numbers of vacuoles in the sample (due to difficulty dissecting the narrowed canal) and also the fact that large numbers of vacuolar pores which do not appear on the apex of the vacuole may be missed during examination. Therefore there may have been a bias towards flat easily examined areas of lining endothelium where most non-bulge pores would be highly visible. A detailed serial section study by TEM would be required to clarify whether there were such large numbers of non-vacuolar pores.

Lütjen-Drecoll (1973) used rank correlation to study the relationships between physiological results and morphometric parameters in a similar fashion to the present study. In that study facility of aqueous outflow was measured in stumptail macaques (Macaca arctoides) after an intravenous injection of hexamethonium bromide and again after intracameral perfusion with pilocarpine. Only two

'giant vacuoles' were found in the 19 eyes studies which is hardly surprising since the anterior chamber was immerse fixed at atmospheric pressure after being dissected from the rest of the eye in situ. Lütjen-Drecoll did, however, observe a correlation between the amount of 'empty space' in immediate contact with the lining endothelium (but not with the remaining 'empty space' in the cribriform layer) with both facility after hexamethonium and pilocarpine. The author admitted that this was difficult to reconcile since facility decreased after hexamethonium but increased after pilocarpine. There was a weak negative correlation with the amount of sub-endothelial fibrillar ground substance and resistance. On this evidence Lütjen-Drecoll concluded that the area of sub-endothelial 'empty space' was an important determinant of resistance.

In the present investigation a weak negative correlation was found between the GAG score and total flow and all eyes showed a depletion of extracellular materials ('washout'). However, a more detailed morphometric study of the ground substance in the sub-endothelial region would be required to determine whether this correlated with resistance as in the study by Lütjen-Drecoll (1973).

PART II

AGE-RELATED CHANGES IN THE HUMAN OUTFLOW APPARATUS

INTRODUCTION TO PART II

The aging human eye undergoes many changes which are responsible for the gradual deterioration of vision, the best known of which are cataract formation and senile macular degeneration (Weale 1963).

As mentioned in the general introduction, primary open angle glaucoma is caused by increased resistance to aqueous outflow and occurs predominantly in individuals over 40-50 years of age.

It has been shown that there are many changes which take place in the aging eye which may affect aqueous outflow dynamics and the structures of the outflow system. The volume and depth of the anterior chamber decrease with age (Becker 1958, Brubaker, Nagataki et al 1981) probably as a consequence of the progressively increasing size of the lens (Syndacker 1956, Weale 1963). With age there is both a decrease in aqueous production (Becker 1958, Gaasterland, Kupfer, Milton et al 1978) and an increase in resistance to aqueous outflow (Becker 1958, Armaly and Sayegh 1970, Gaasterland, Kupfer et al 1978, Brubaker et al 1981). These two changes tend to counterbalance each other, but the intraocular pressure although maintained within normal limits, shows a tendency to rise with age according to some authorities(Kornweig, Feldstein and Schneider 1957, Gaasterland, Kupfer et al 1978, Brubaker et al 1981). Becker (1958) on the contrary found that intraocular pressure did not increase significantly with

age.

It seems likely that since episcleral venous pressure stays constant with age (Gaasterland, Kupfer et al 1978); and that the site of 75% of the resistance to aqueous outflow normally lies in the trabecular meshwork (see general introduction) that the increase in resistance with age is due to changes in this tissue. There has also been much speculation that the earliest pathological changes in primary open angle glaucoma which leads to increased resistance may similarly take place in the trabecular meshwork.

Several authors have noted in qualitative studies that there is an increase in the thickness of the trabeculae with age (Ashton, Brini and Smith 1956, Ashton 1960, Rohen 1969, Rohen and Lütjen-Drecoll 1971, Tripathi 1977a), and this has been described as being due to deposition of elastic-like fibres and 'curly collagen' (Rohen and Lütjen-Drecoll 1971, Tripathi 1977a). There have also been reports of changes in the nature and quantity of the extracellular elements in the cribriform layer (Vegge 1967, Rohen 1969, Rohen and Lütjen-Drecoll 1971, Fink, Felix and Fletcher 1972) but these have been limited qualitative studies on small numbers of specimens.

In morphological studies of primary open angle glaucoma most authors have stated that there is often difficulty in distinguishing between pathological changes and normal age-related changes (Ashton 1958, Fine 1964, Rohen 1969, Rohen and Witmer 1972, Nesterov and Batmanov 1974a, 1974b,

Tripathi 1977b and Fine, Yanoff and Stone 1981). Despite this difficulty and with the knowledge that the disease process is slow and subtle in nature, it is surprising that no attempts have been made to quantify the age-related changes in the normal human outflow apparatus.

THE AIMS OF PART II

i) To provide a qualitative description of the age-related changes in the human outflow apparatus.

ii) To provide a quantitative assessment of the changes which occur with age in -

a) trabecular thickness

b) the incidence of 'giant vacuoles'

c) the various components of the cribriform layer.

THE APPROACH TO PART II

The human eyes used in this investigation were enucleated in the treatment of various intraocular and orbital tumours and malformation of the posterior globe. The commonest reason for enucleation was the treatment of posterior choroidal melanoma, so there was a bias towards the older age groups. The material was collected during the period 1970-1981.

The investigation was carried out using the facilities afforded by light microscopy, transmission electron microscopy and scanning electron microscopy. Particular

attention was paid in this study to those features which were considered to be capable of altering the resistance to aqueous drainage, which as previously noted increases with age. When possible an attempt was made to provide an quantitative assessment of the relevant changes, since this would be valuable in the future assessment of the morphological changes observed in trabeculectomy specimens from patients with primary open angle glaucoma.

The measurement of trabecular thickness was carried out by means of a simple morphometric technique at the light microscopic level. This allowed more than one section per eye and a relatively large number of eyes to be investigated than would have been feasible with TEM.

The vacuolar incidence was assessed in an identical fashion to that previously described in Part I. This was carried out to investigate whether the changes in aqueous dynamics with age were reflected in the incidence of 'giant vacuoles' in the lining endothelium of Schlemm's canal.

The study of the age changes in the components of the cribriform layer required the use of TEM to distinguish the ultrastructural features of the materials present. The nature of the study did not lend itself to automated image analysis, therefore a well established morphometric technique which utilised a grid of random points on mapping electron micrographs was applied. It was chosen to study a very small sample from as many eyes from as wide an age range as possible. Alternatively, if one had wished to study the variation within individual eyes a large sample

from each eye could have been investigated.

MATERIALS AND METHODS

MATERIALS

The human eyes used in this study showed no clinical or histopathological evidence of abnormality in the anterior segment and intraocular pressure fell within normal limits. The eyes ranged from two months to 83 years of age. The age, sex, EM No and pathological diagnosis of each of the 43 specimens, along with details of which sections of the investigation they were used in, are provided in Appendix 11.

The eyes were immerse fixed in 2-4% gluteraldehyde after enucleation.

TISSUE DISSECTION

The calottes or anterior segments which were not required for routine histopathological diagnosis were dissected as follows. The anterior chamber was separated by division of the tissue at the ora serrata after any residual lens was removed.

Meridional slices of limbal tissue, 1-2 mm in thickness, were cut to provide a random representative sample of the available tissue. Depending on the amount of limbal tissue in the calottes, 10-20 slices were taken. Excess cornea, ciliary body and conunctiva were trimmed from each block. The tissue was then stored in 2-4% gluteraldehyde at $4^{o}C$ for 1-2 weeks prior to processing.

TISSUE PREPARATION

The procedures for tissue processing, sectioning, staining and examination for light microscopy (semithin sections) and conventional transmission electron microscopy were identical to those described in materials and methods in Part I of this presentation.

En bloc colloidal iron staining and scanning electron microscopy were applied to only a few of the eyes and procedures were identical to those described in Part I.

QUANTITATIVE ASSESSMENT OF TRABECULAR THICKNESS

Semithin sections (1 μm) stained with toluidine blue were examined by light microscopy. A simple technique was used to measure trabecular thickness. It utilised a calibrated eyepiece graticule in conjunction with the x100 objective (oil immersion) of a Leitz Orthoplan microscope. The graticule scale was orientated as shown in Fig 86, perpendicular to the long axis of the trabeculae and approximately in the centre of the meshwork. Values were obtained of the width of each of the trabeculae and intertrabecular spaces from the outermost to the innermost trabeculae. This was carried out once on each section, and on a total of five sections from each eye. From the measurements the following features were calculated for each eye.

a) The mean number of trabeculae per section.

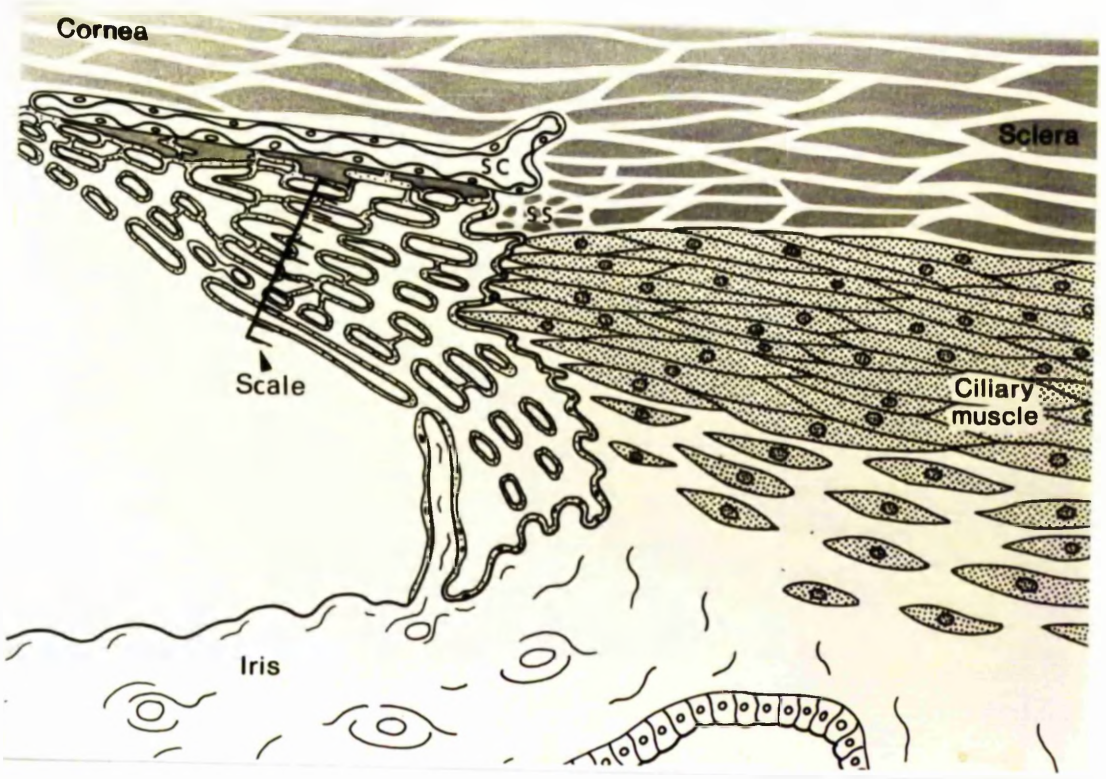

Figure 86: Diagram to show the positioning of the scale of the eyepiece graticule over the trabecular meshwork for the measurement of trabecular thickness.

b) The overall mean trabecular width per eye.

c) The mean number of intertrabecular spaces per section.

d) The mean width of the intertrabecular spaces per eye.

The specimens were coded throughout this procedure. Repeatability tests on the same sections in one eye gave a variation of approximately 2%. A total of 25 eyes (125 sections) between the ages of 2½ months to 83 years of age were investigated using this technique.

QUANTITATIVE ASSESSMENT OF VACUOLAR INCIDENCE

A total of twenty eyes (200 sections) between the age of 3 months to 83 years were investigated using the technique described in Part I.

MORPHOMETRIC ANALYSIS OF THE COMPONENTS IN THE CRIBRIFORM LAYER

A simple morphometric technique consisting of a grid of random points (Weibel 1969, Curtis 1960) was used to assess the percentage area occupied by the various components in mapping electron micrographs of the inner wall of Schlemm's canal. The technique which was applied consistently in all eyes was as follows. Ultrathin sections (60-90 nm) were cut and stained in the conventional fashion for TEM. Sequential photomicrographs at a magnification of x3400 were taken along the available length of the inner wall (Fig 87). These were enlarged to 20x25 cm prints, total

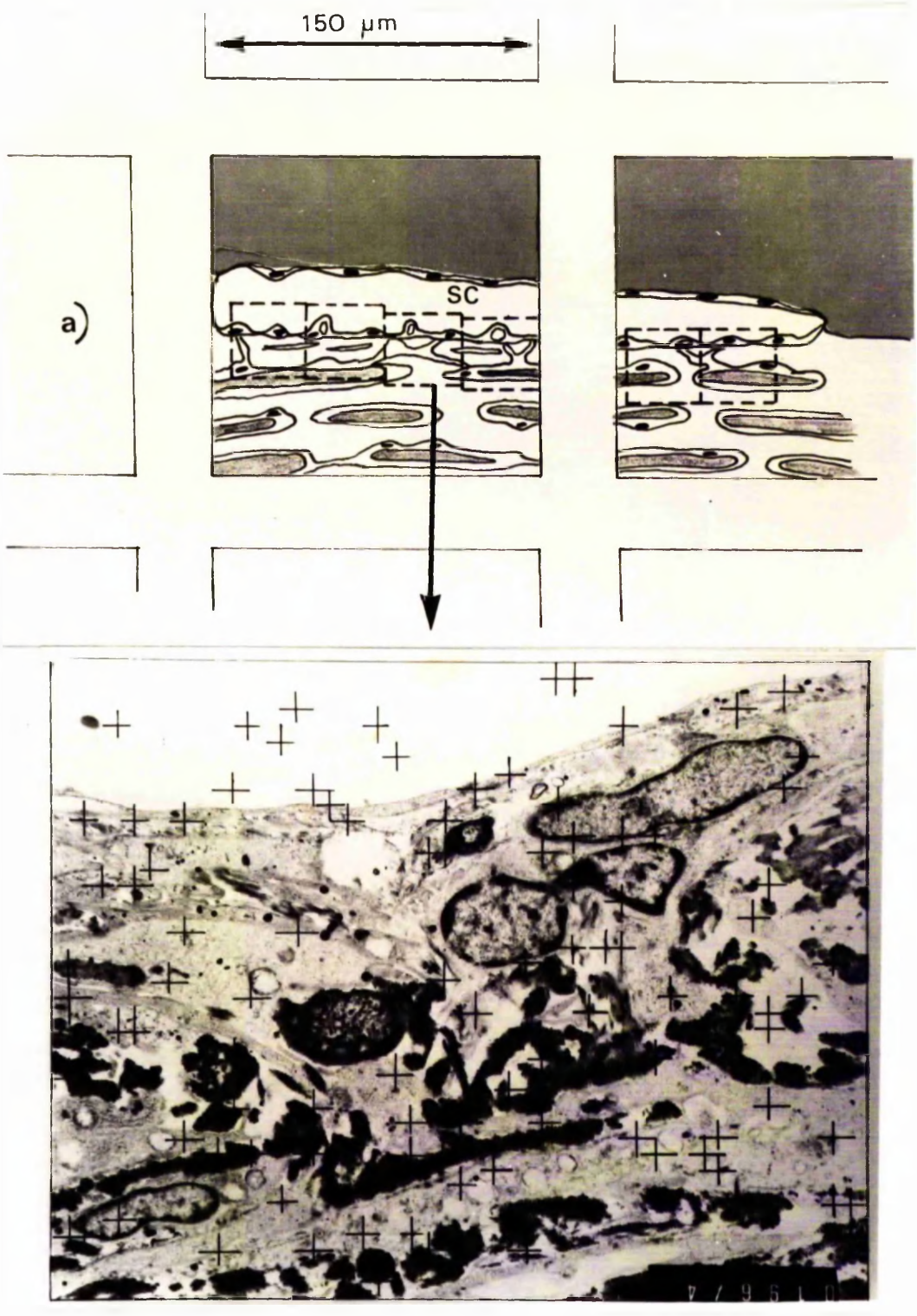

Figure 87: Diagram to show how serial photomicrographs were taken along the available length of the inner wall of Schlemm's canal in the human eye. Each photomicrograph was enlarged and a grid of random points was placed over this to assess the area of the components in the cribriform layer.

magnification of x8330, which corresponded to an area of approximately 600 square microns. A sheet of glass with 100 random points in an area of 20x25 cm was placed on top of the micrographs (Fig 87). The grid of points is in fact a modified Chalkley array (Chalkley 1943, Curtis 1960). The coordinates of the random points were plotted by allocating alternative random numbers to ordinate and abscissa, with a minimum separation distance of 0.5 cm.

The points which fell on the cribriform layer were counted and expressed as a percentage area of the print. The cribriform layer was defined as the area being bordered by the lining endothelium of Schlemm's canal and the outermost intertrabecular space ("trabeculum cribriforme" - Rohen and Lütjen-Drecoll 1971). This layer was considered for the purposes of morphometrics to consist of four main components: granular-fibrillar ground substance; electron dense plaques; basement membrane and cells. The points which fell on each component were recorded and calculated as a percentage area of the cribriform layer in each print. eg

$$\% \text{ component A} = \frac{P_A}{P_{cl}} \times 100\%$$

where P_A = points falling on component A

P_{cl} = points falling on cribriform layer.

The results from all the prints obtained from each eye were grouped and the mean and standard error was calculated. A total of 462 coded prints (51 sections) from 36 eyes were investigated by this technique. Increasing the number of points in the array to 400 resulted in a mean coefficient of variation of 8%. It is accepted that a greater number of points reduces the standard error for the components which only occupy a small area, eg basement membrane, as predicted by the Gauss equation (Curtis 1960). Despite this it was felt that the use of 100 points gave repeatable results within acceptable accuracy limits for the major components.

The theoretical minimum separation distance between the points (0.5 cm in the present study) rarely occurs in a random array. This distance should be less than the smallest discrete component being measured. However, this was not strictly applicable in the tissue under investigation in the present study since there were no discrete isolated components of a standard size. A random array of points, rather than a lattice, was used since one of the theoretical considerations of the latter is that the components are randomly orientated in the tissue or cell with regard to the plane of section (Weibel 1969). This is not the case in the present study, because the cribriform layer is an anisotropic tissue in meridional sections, therefore a random grid of points is more suitable.

Repeatability on one set of prints gave a variation of

less than 10% in the major components but the variation increased for components which occupied a small percentage area of the tissue, eg basement membrane (less than 5% of total area). Interobserver error was less than 5% for the major components.

RESULTS

QUALITATIVE DESCRIPTION OF AGE-RELATED CHANGES IN THE MORPHOLOGY OF THE HUMAN OUTFLOW APPARATUS

The under 10 year old age group

The outflow apparatus in the young eye had several distinguishing features. The trabecular meshwork was a long wedge shape in meridional sections, with a broad posterior face which merged with the ciliary muscle and iris base, and tapered anteriorly where it merged with the inner layers of the cornea (Fig 88 and 89). Schlemm's canal was long and narrow in infantile eyes (< 1 year) and the scleral sulcus was shallow. The scleral spur in the infant eye was usually diminuitive (Fig 88) but did occasionally seem more prominent (Fig 89). Due to the poorly developed spur the majority of the longtitudinal ciliary muscle fibres inserted directly into the posterior trabecular meshwork, but some innermost fibres did merge with the scleral spur particularly when it was better developed. The narrow canal of Schlemm occasionally seemed to be partly occluded due to opposition of the inner and outer walls (Fig 88) and was also clearly divided by collagenous septae in some areas (Fig 89 and 90).

In most eyes the iris root and meshwork merged in a very loose fashion (Fig 88) with iris processes which occasionally crossed from iris stromal tissue to the uveal meshwork. However, in a few areas in some eyes the iris root lay more anteriorly with little or no transition zone (Fig 89).

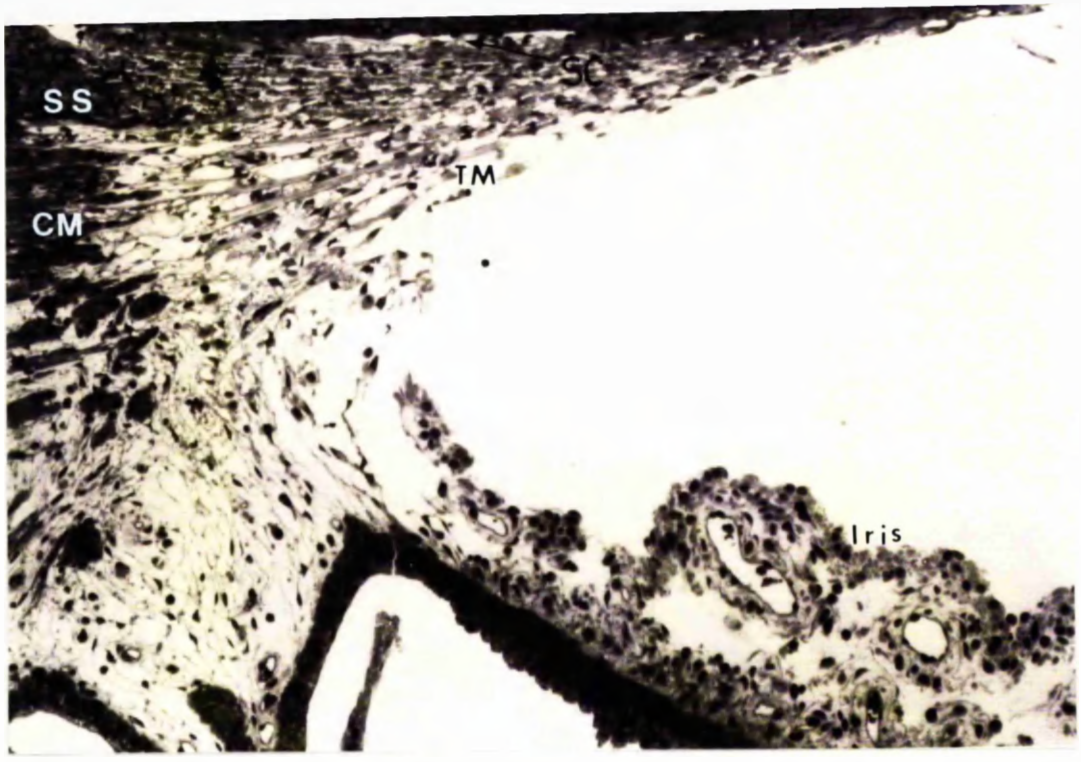

Figure 88: Light micrograph of angular structures in a 3 month old human eye (59/80). The canal of Schlemm is long and narrow and appears to be closed in a region of inner-outer wall contact (arrow). The scleral spur is diminuitive. (X 180).

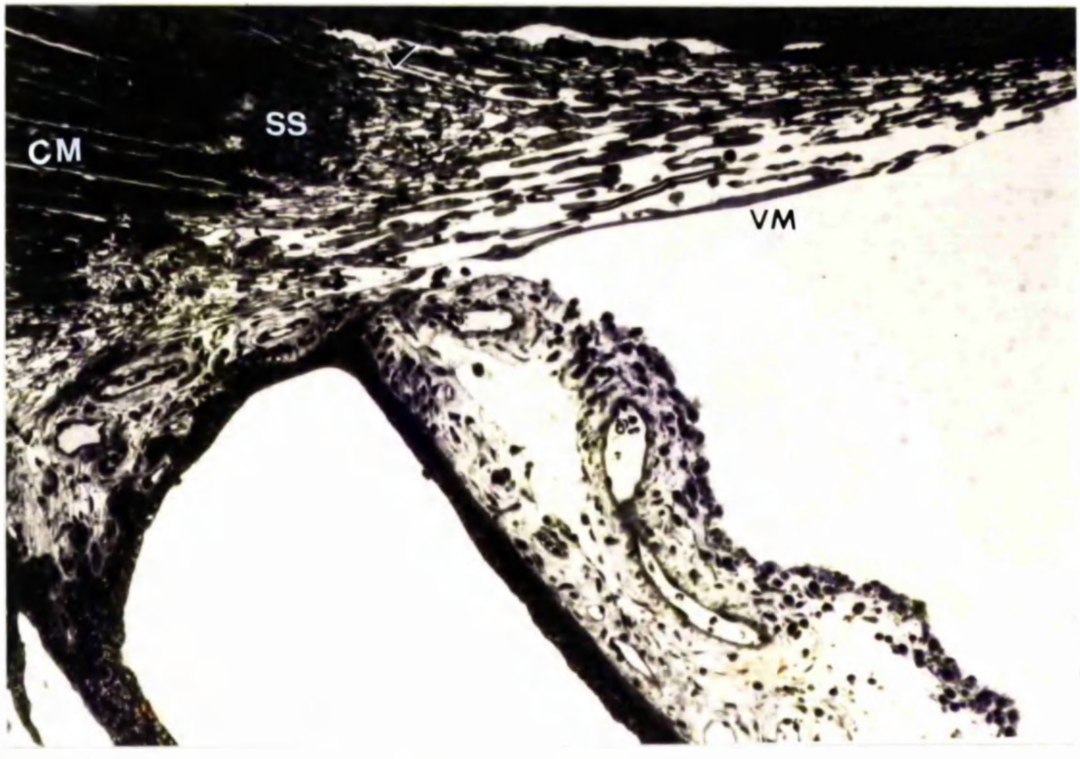

Figure 89: Light micrograph of the human outflow apparatus in a 4 month old human eye(049/79). In contrast to Fig. 88 the scleral spur is relatively well developed. The iris in this specimen seems more anteriorly positioned than in Fig. 88. Schlemm's canal is long and narrow and is bifurcated by a collagenous septum (arrow). (X 180).

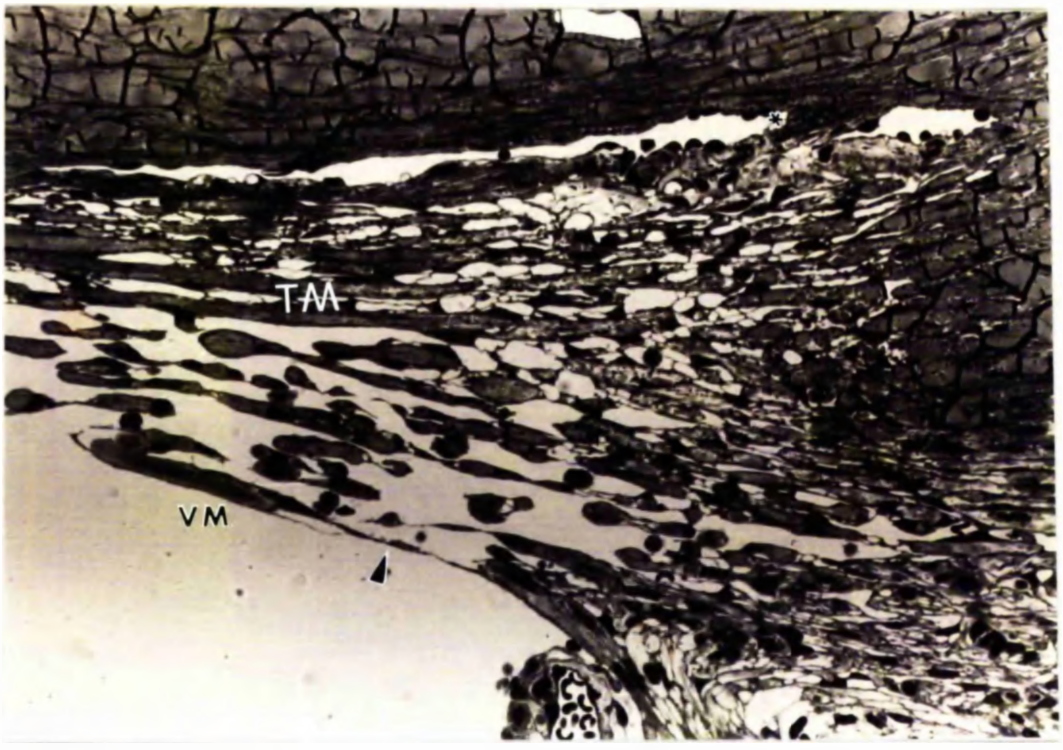

Figure 90: Light micrograph of the human outflow apparatus in 4 month old infant (049/79) to show a collagenous septum (*) in the canal and the large sheet-like uveal trabeculae with fine cell processes over the intratrabecular spaces(arrow). (X 340).

The uveal trabeculae in the infantile eyes were in some areas rope-like, but others had the appearance of perforated sheets and were similar to the layers of the corneoscleral meshwork (Fig 89 and 90). The intratrabecular spaces or perforations in isolated sections often appeared to be covered by endothelial cell processes (Fig 90). The basic configuration of the trabeculae was similar to that described in the general introduction (Fig 7), but in these young eyes the covering endothelial cells had relatively large numbers of pegs, invaginations and cytoplasmic condensations (Fig 91 and 92). The central collagenous core of the trabeculum was the largest component in these young eyes, with only a few elastic-like fibres and a narrow cortical region which was devoid of 'curly collagen'. The elastic-like fibres (Fig 92) were composed of an electron lucent homogeneous core and a fibrillar sheath (6-12 nm fibrils). The basement membrane was generally thin (Fig 91) or occasionally absent (Fig 91 and 92).

The cellular component and general arrangement of the cribriform layer was identical to the description in the general introduction. The extracellular component in these young eyes was comprised mainly of a granular ground substance intermingled with fine collagen fibrils (6-10 nm) and occasionally more mature collagen with 60 nm periodicity (henceforth this will be referred to as ground substance for brevity). Elastic-like material identical to those within the trabeculae were also occasionally seen in

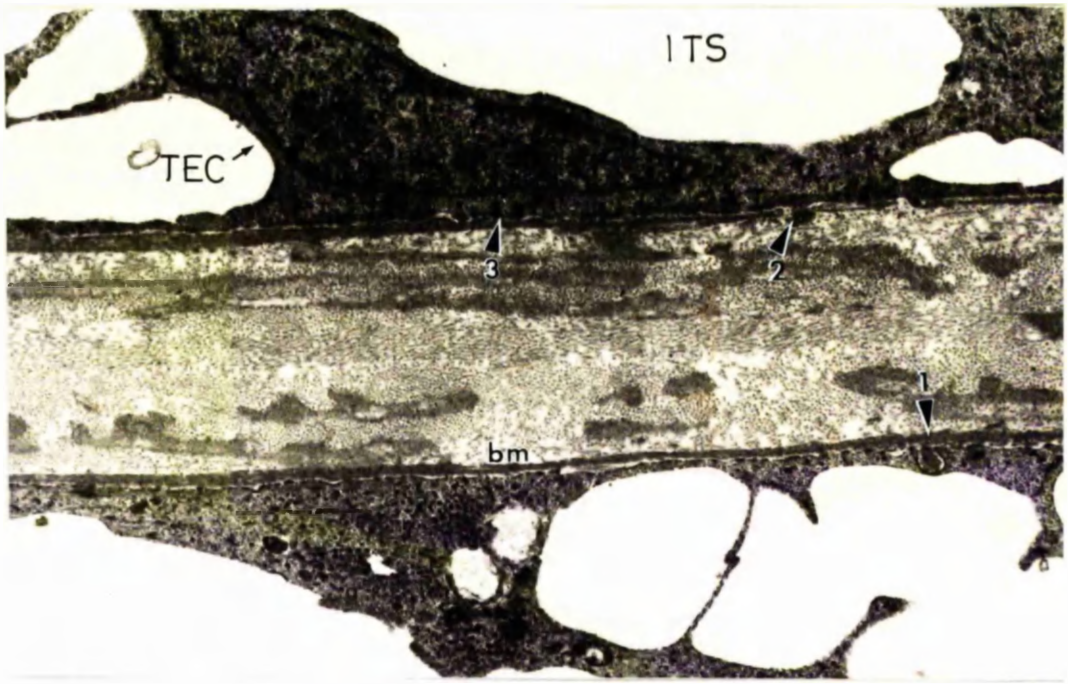

Figure 91: Transmission electron micrograph of a cross section of a corneoscleral trabeculae in a 1yr old human eye (346/78). Note the invagination in the trabecular endothelial cell containing basement membrane material (1), the cytoplasmic peg (2) and interdigitations of the cell membrane (3). (X 9200).

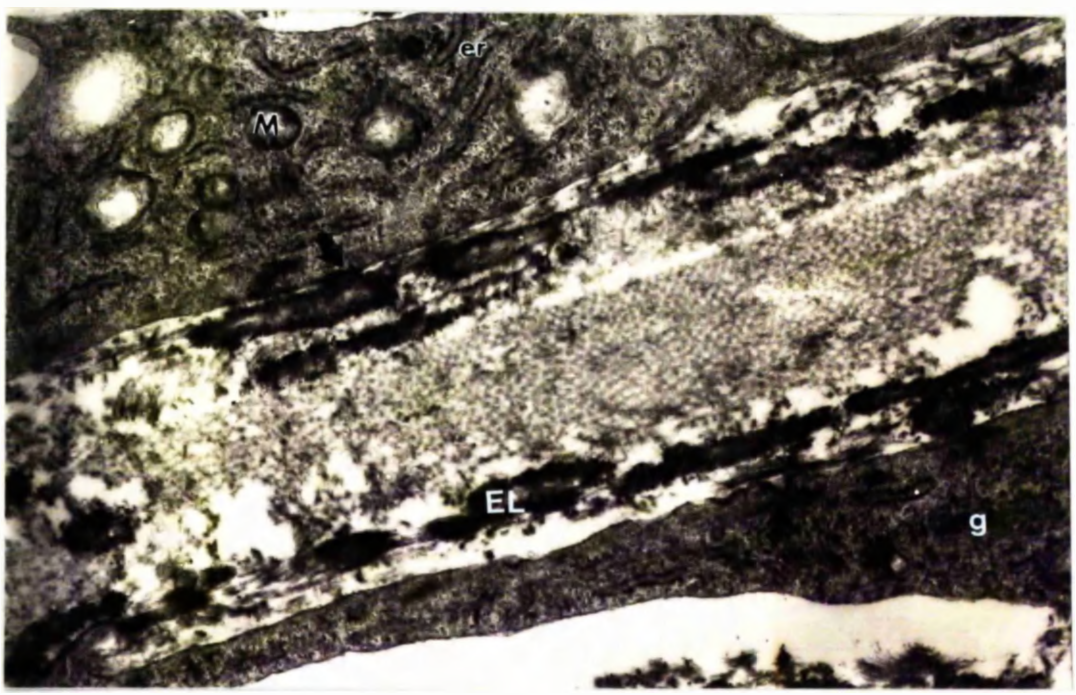

Figure 92: Transmission elctron micrograph of a corneoscleral trabeculae in a 2½ month old human eye(396/79). Note the collagenous core, elastic-like fibres and the absence of a basement membrane. The micrograph shows also, the ultrastructure of the trabecular endothelial cells, particularly condensations in the cytoplasm at the interdigitations of the cell membrane(arrows). (X 17,000).

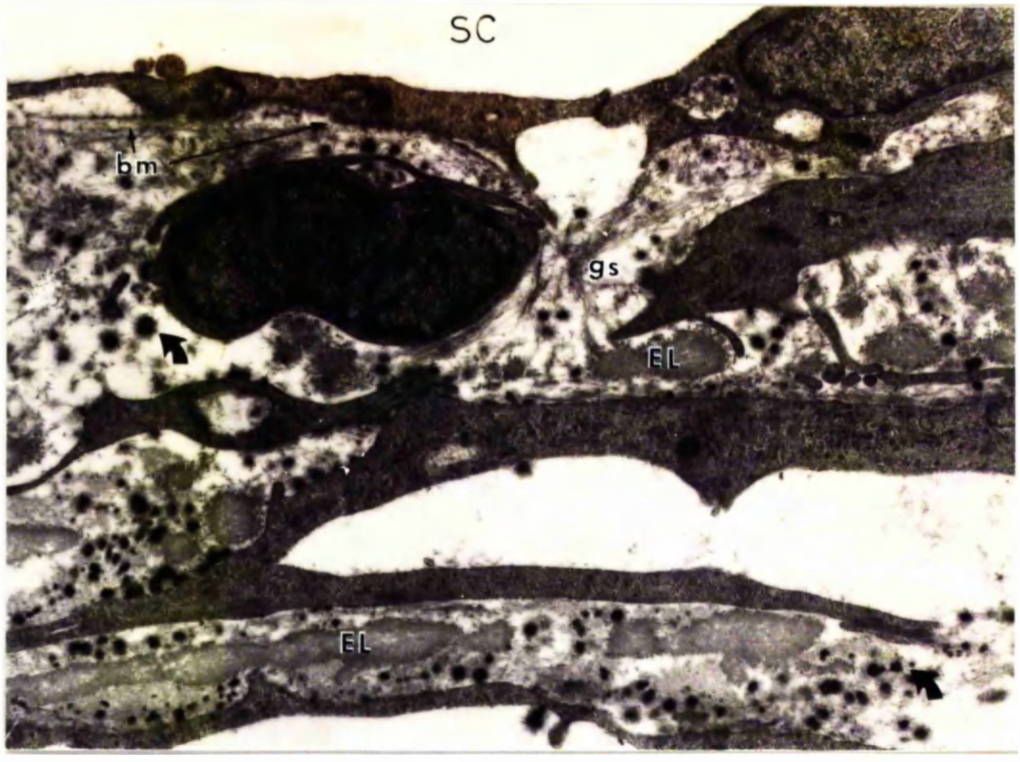

Figure 93: Transmission electron micrograph of the cribriform layer in the infant human eye(049/79). The small electron dense bodies (arrows) are probably DNA material released from the retinoblastoma. (X 12,500).

the cribriform layer (Fig 93). The amount of 'empty space' in the cribriform layer was variable. 'Giant vacuoles' were common in the lining endothelium of these young eyes (Fig 90).

Occasionally non-native cells such as erythrocytes and lymphocytes were seen in the trabecular meshwork. Tissue histiocytes were also found in the trabecular meshwork of this age group.

The 11-30 year old age group

The scleral spur in eyes of this age group was larger, more rounded and more prominent than in younger eyes. This had the effect of deepening the scleral sulcus. The trabecular meshwork could be divided into two portions by a theoretical line from the tip of the spur to Schwalbe's line (Fig 95) as is shown diagrammatically in Fig 3. The inner portion or uveal meshwork contained the rope-like trabeculae which are typical of the adult human eye (Fig 94). Schlemm's canal was generally shorter in the anteroposterior direction than in juvenile group and was usually of greater depth (Fig 94 and 95).

The trabeculae, both the uveal and corneoscleral, were slightly thicker than in younger eyes. There were more elastic-like fibres; these were composed of an electron dense core and a lighter staining sheath (Fig 96), which occasionally showed a banding pattern (40-80 nm). There were also deposits of 'curly collagen' in the cortical region. The elastic-like material, the 'curly collagen' and the basement membrane did not stain in the colloidal

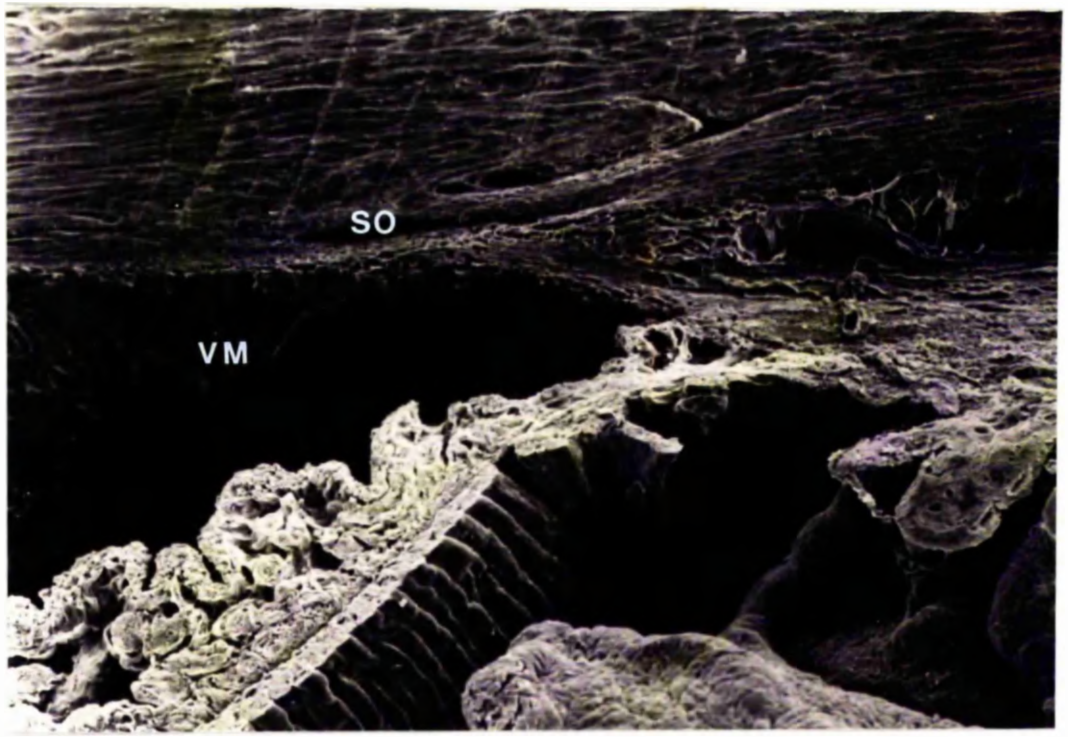

Figure 94: Scanning electron micrograph of the human outflow apparatus in an 18yr old patient(264/78). Note the configuration of the rope-like uveal trabeculae. (X 120).

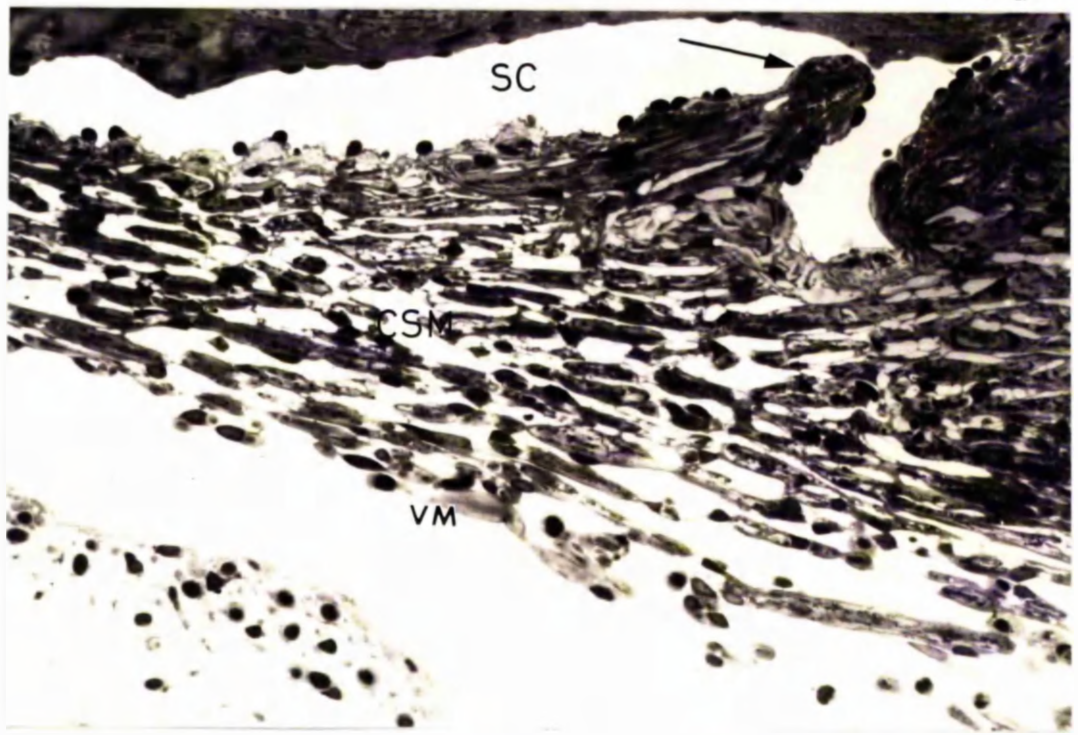

Figure 95: Light micrograph of the human outflow apparatus in a 22yr old eye(13/72). 'Giant vacuoles' are numerous in the lining endothelium. Schlemm's canal is almost divided by a septum(arrow). Note the large intertrabecular spaces in the uveal and corneoscleral meshwork. (X 380).

Figure 96: Transmission electron micrograph of colloidal iron stained tissue from a 20yr old human eye(381/80) to show the distribution of stain in a corneoscleral trabeculae. The basement membrane, curly collagen and elastic-like fibres were only stained at their peripheries. (X 11,700).

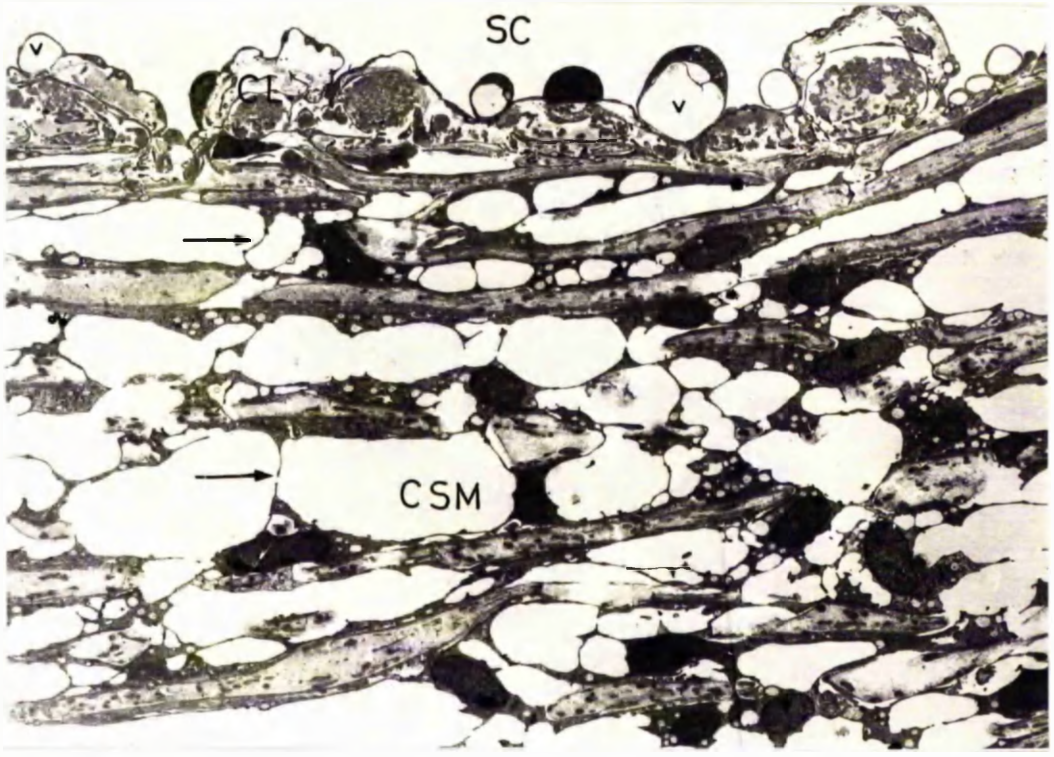

Figure 97: Transmission electron micrograph of the outflow apparatus from an 18yr old human(264/78). There were numerous fine cytoplasmic extensions of the trabecular endothelial cells (arrows) which crossed the intertrabecular spaces. There were abundant electron dense plaques in the cribriform layer and 'giant vacuoles' were numerous. (X 1400).

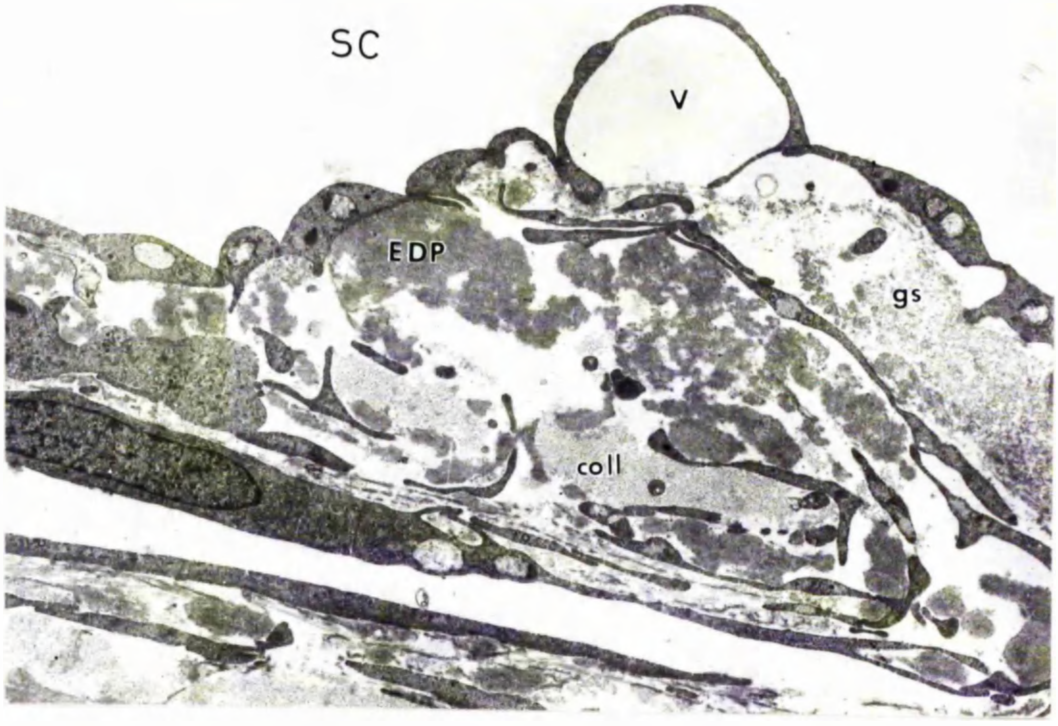

Figure 98: Higher power electron micrograph of the cribriform layer in the tissue shown in Fig. 97(264/78). The electron dense plaques were intermingled with collagen and ground substance. (X 6300).

Figure 99: Transmission electron micrograph of the cribriform layer in a 22yr old human eye(476/80) where the dominant type of extracellular material was ground substance. (X 8200).

iron preparation, however, the remainder of the trabeculae and the cell surfaces showed an affinity for this stain (Fig 96). The intertrabecular spaces were frequently crossed by fine cell processes (Fig 97).

The cribriform layer contained deposits of homogeneous plaques which were sparse in some areas and formed large aggregates in others (Fig 97). The majority of this material was neither typical 'curly collagen' nor typical elastic-like material (although these were present in small amounts) but shared some characteristics of both. Its appearance varied depending on section thickness and staining, but it usually showed some areas of banding, which were less distinctive than the 100 nm banding of 'curly collagen'. For convenience this material will be referred to as electron-dense plaques. As well as varying from section to section within one eye the amount of this material in the cribriform layer also varied between eyes of similar ages. In areas where it did not predominate the other major component, ground substance, was more prevalent (Fig 99).

'Giant vacuoles' were frequent in the lining endothelium of Schlemm's canal (Fig 95, 97 and 98).

The 31-50 year old age group

The trends that were beginning to emerge in the last age group become fully developed in the 31-50 year age range. Schlemm's canal was still open in most areas, but there were a few regions of canal closure due to inner and outer wall contact. The uveal meshwork was more compact

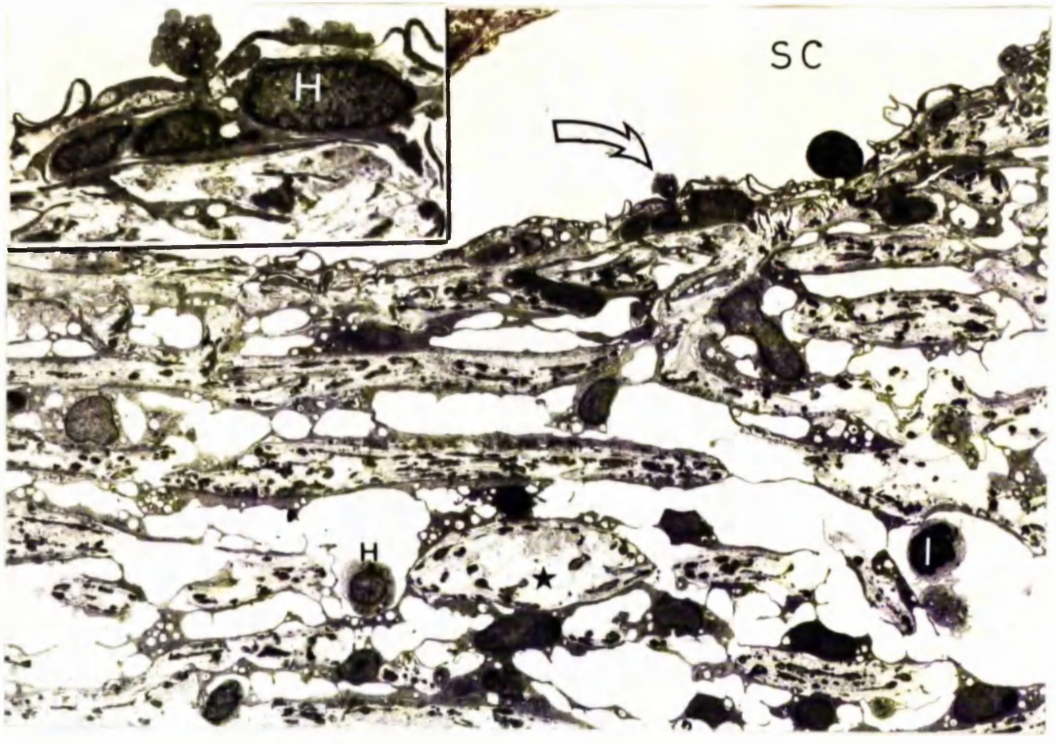

Figure 100: Transmission electron micrograph of the trabecular meshwork of a 46yr old eye(435/79). Note the thickened trabeculae (*) and the tissue histiocytes one of which was in the process of migrating through lining endothelium (see inset- X 3000). (X 1300).

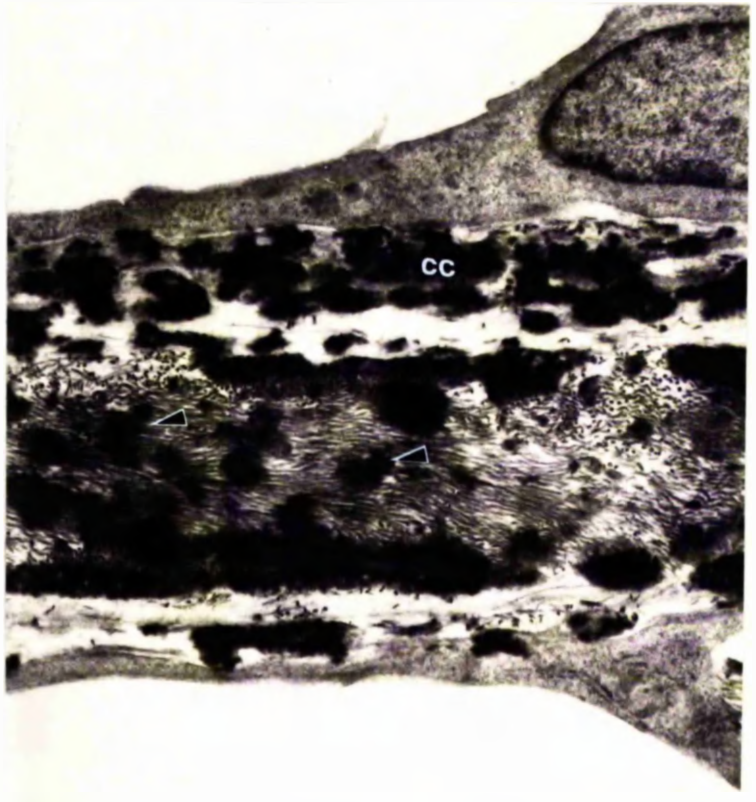

Figure 101: Transmission electron micrograph of a corneoscleral trabeculae in a 43yr old human eye(188/78). There were condensations in the control collagenous core(arrows), and increased deposits of curly collagen in the cortical region. (X 11,000).

with narrower intertrabecular spaces than in the two previous groups.

The trabecular endothelial cells were occasionally detached from their connective tissue cores (Fig 100). Although this was present to some extent in younger eyes, it seemed slightly more common in this age group. Undoubtedly some of the detachment may have been artefactually produced during the processing procedure, but in these areas the core materials seemed to be far more disorganised than would have been anticipated in an artefactual break which suggested they may in some cases have been real. The many specialisations of the trabecular endothelial cells which were assumed to be important in cell to trabeculae adhesion in younger eyes, were rarer in these older eyes (Fig 101 and 102). The trabeculae were thicker, firstly due to deposits of 'curly collagen' in the cortical region, secondly an increase in the diameter of the elastic-like material and lastly there were also condensations in the central collagenous core (Fig 101).

Tissue histiocytes were more prominent in the trabecular meshwork in this group of patients (Fig 100 and 102). The nature of the extracellular materials in the cribriform layer was variable, which is illustrated by comparison of tissue from two eyes of similar ages (of Fig 102 and Fig 103). In one, electron-dense plaques were predominent (Fig 102), while in the second, the extracellular space was packed with ground substance (Fig 103). In tissue stained with colloidal iron, the ground

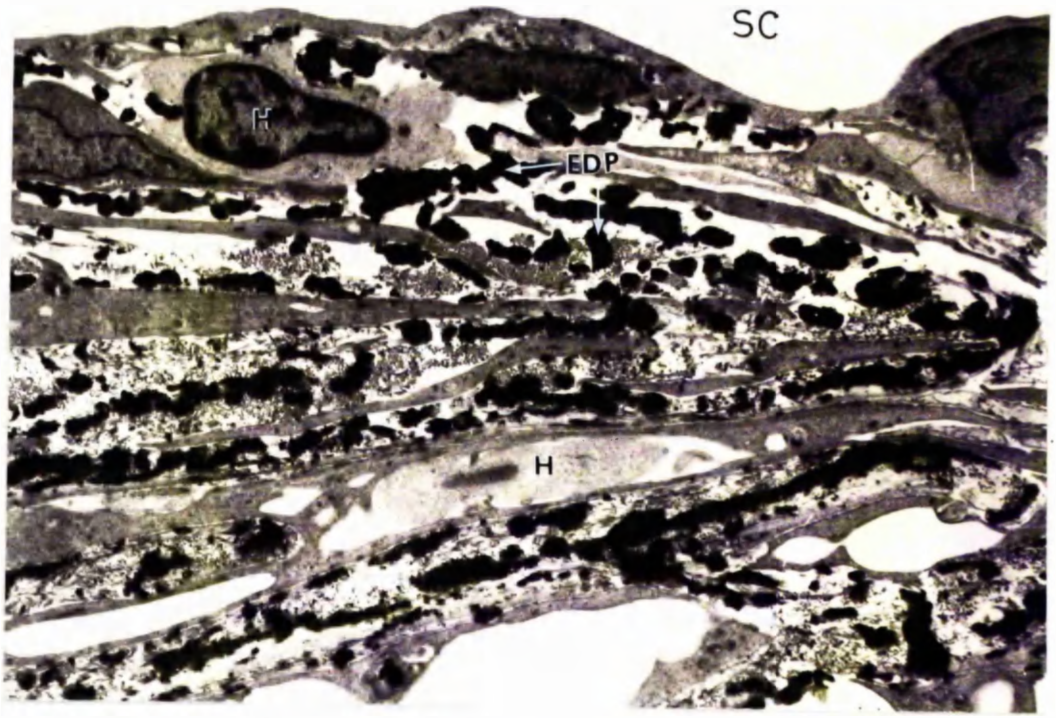

Figure 102: Transmission electron micrograph of the outer meshwork in a 43yr old human eye(188/78). In the cribriform layer there was very little ground substance but electron dense plaques were present. (X 4200).

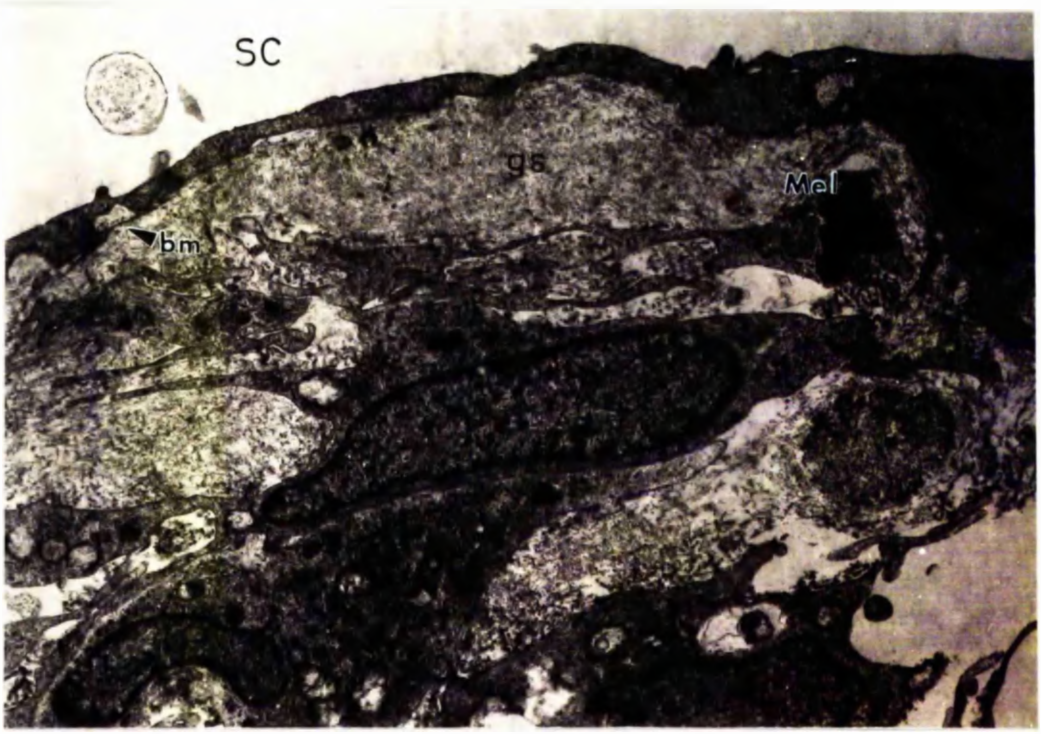

Figure 103: Transmission electron micrograph of the cribriform layer of a 38yr old human eye(76/75) in which the ground substance was the prdominant extracellular material. (X 6800).

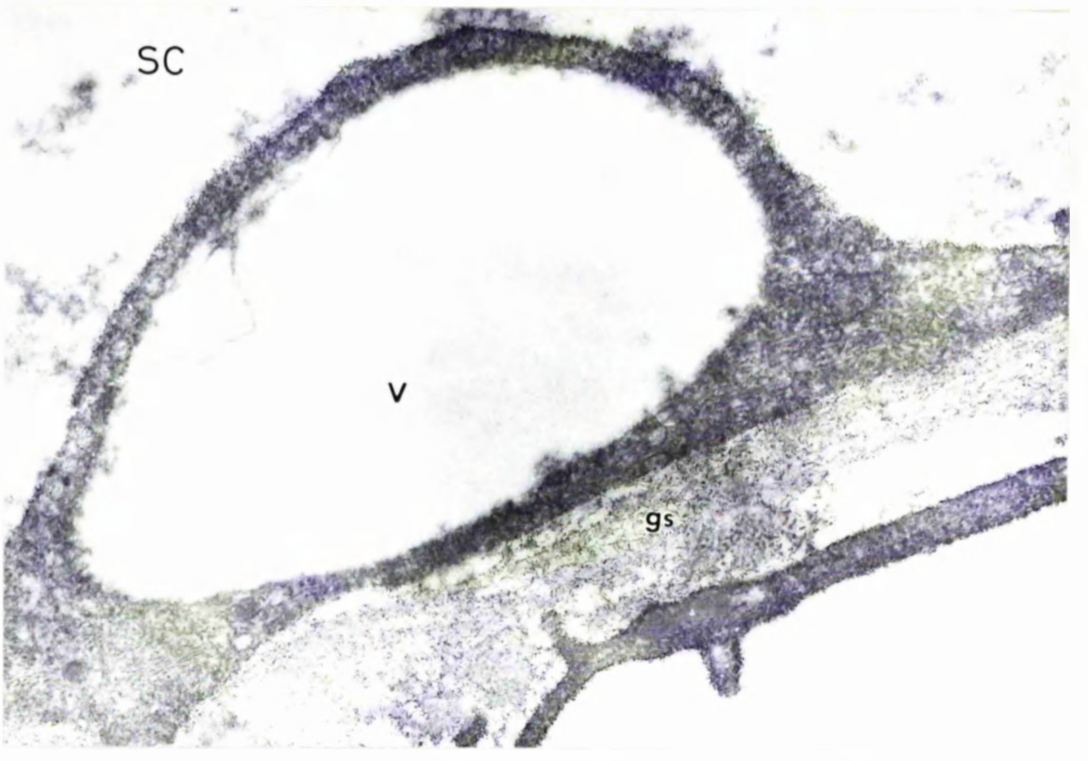

Figure 104: Transmission electron micrograph of colloidal iron stained human tissue(232/79 - 45yrs). The cell membranes and sub-endothelial ground substance are richly stained, but the 'giant vacuole' is devoid of any stain. (X 45,000).

substance showed a high affinity for this cationic dye (Fig 104). The surfaces of the cells in the cribriform layer and indeed throughout the trabecular meshwork, possessed a rich coat of colloidal iron particles. The only membranes which did not have an affinity for the particles, were found in some of the 'giant vacuoles' in the lining endothelium of Schlemm's canal (Fig 104). The most significant general trend in the aging process in the cribriform layer was that the electron dense plaques became more frequent while the incidence of 'giant vacuoles' remained the same as in previous groups (Fig 100 and 104).

The 51-70 year old age group

In this age group the trabecular meshwork by comparison with the long wedge shape of very young eyes, had a shorter rhomboidal form. The loose connective tissue which was present at the iris base and ciliary muscle face was atrophic (Fig 105). The uveal meshwork was often compact in the region of the prominent scleral spur (Fig 105) and the frequency of localised canal closure was greater in this age group (Fig 105).

There was an abundance of melanin granules in the trabecular endothelial cells, secondary lysosomes, residual bodies and lipid droplets, which may be indicative of increased phagocytic activity. Tissue histiocytes were also common in this age group.

The trend towards an increasing accumulation of electron-dense plaques in the cribriform layer continued (Fig 106). Ground substance was relatively rare in the

Figure 105: Light micrograph of the outflow apparatus in a 51yr old human eye(211/80). Note the prominant scleral spur, compact uveal meshwork and inner-outer wall contact in Schlemm's canal(arrow). (X 180).

Figure 106: Transmission electron micrograph of the cribriform layer in a 54 yr old human eye(03/71). Note the sub-endothelial ground substance and the electron dense plaques in this tissue. (X 9800).

inner part of the cribriform layer but still persisted directly under the lining endothelium (Fig 106). 'Giant vacuoles' were not as common in this age group as in previous groups and the distribution seemed patchy, some sections showed few if any, while in others 'giant vacuoles' were frequent.

The over 70 year old age group

In this age group there was a great deal of variation in the morphological appearance of the outflow apparatus. The changes which had occurred as part of the aging process in previous groups were increasingly obvious in the majority of these specimens. The uveal meshwork was tightly compacted with narrowed intertrabecular spaces (Fig 107, 108 and 109), particularly in the region of the scleral spur. The incidence of canal closure was higher in these senile eyes than in previous groups (Fig 108 and 109) and most of the regions of inner-outer wall apposition seemed to be well established.

The general appearance of the corneoscleral meshwork was also variable. In some regions there was obliteration of the intertrabecular spaces and fusion of the trabeculae. In other areas the morphology was more normal (Fig 108 and 109). The trabeculae were markedly thickened due to the focal deposition of 'curly collagen' in the cortical zone (Fig 110, 111 and 112). This was associated with thickening of the sheath region of the elastic fibre and condensations in the central collagenous core.

Intracytoplasmic melanin granules were also very common

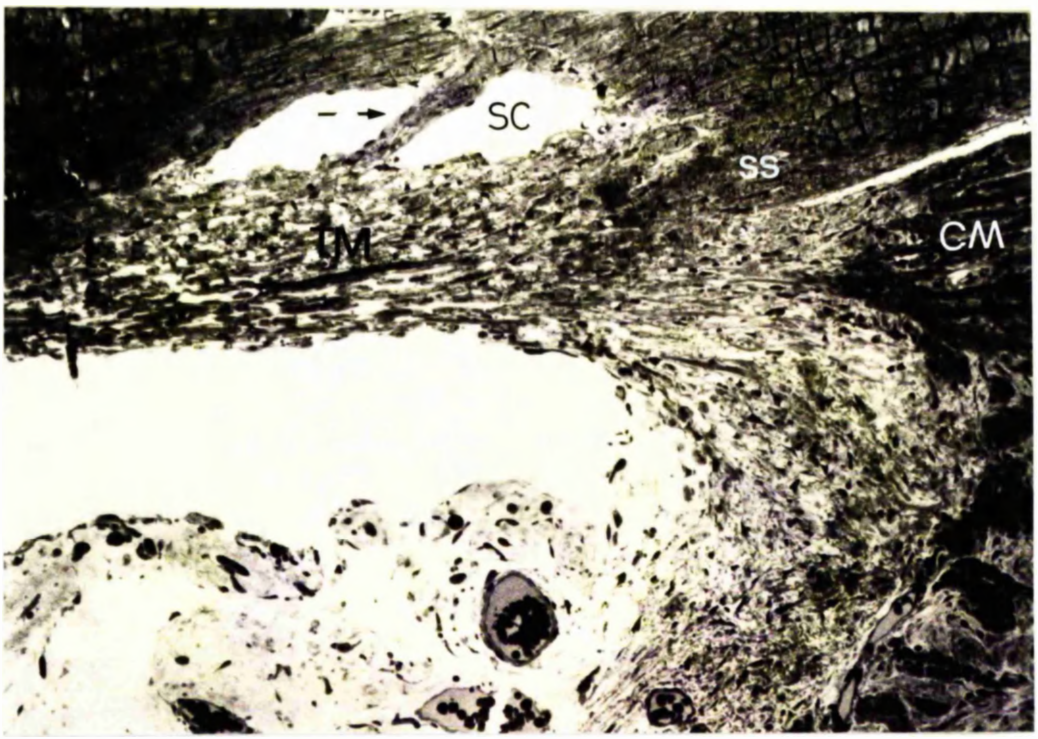

Figure 107: Light micrograph of the outflow apparatus in a 72yr old human patient(408/79) which shows a compact trabecular meshwork and open canal of Schlemm divided by a septum(arrow). The tissue is of a more rhomboidal form than in young eyes, (X 190).

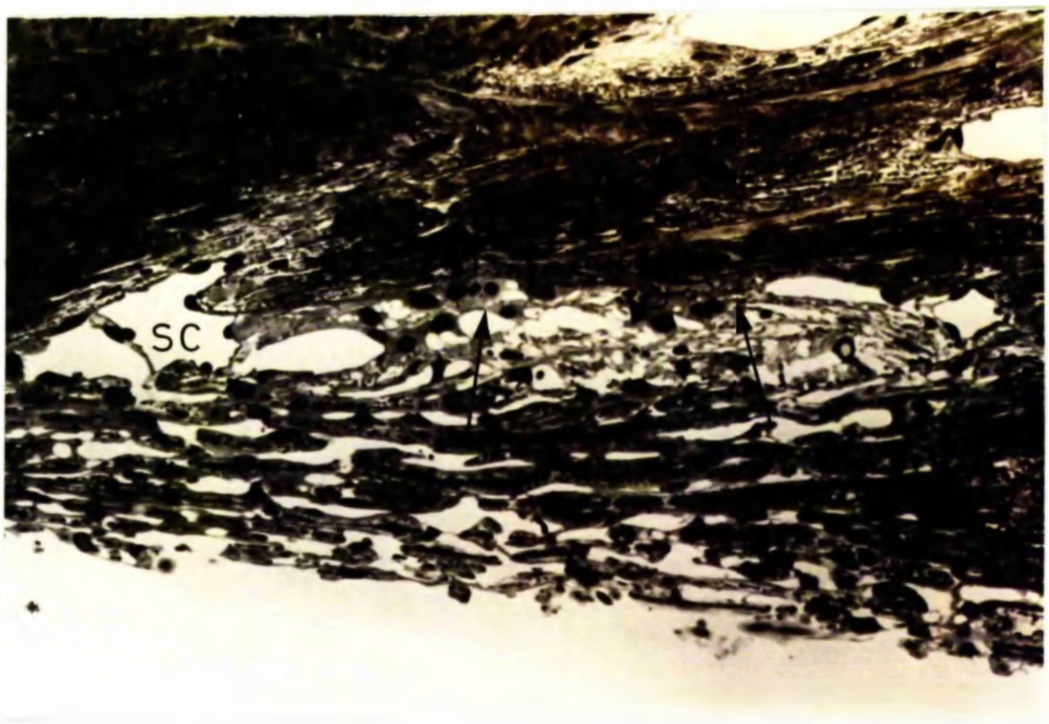

Figure 108: Light micrograph of the outflow apparatus in a 83yr old eye(19/79), which shows large areas of established inner-outer wall contact with subsequent closure of th lumen of Schlemm's canal(arrows), (350).

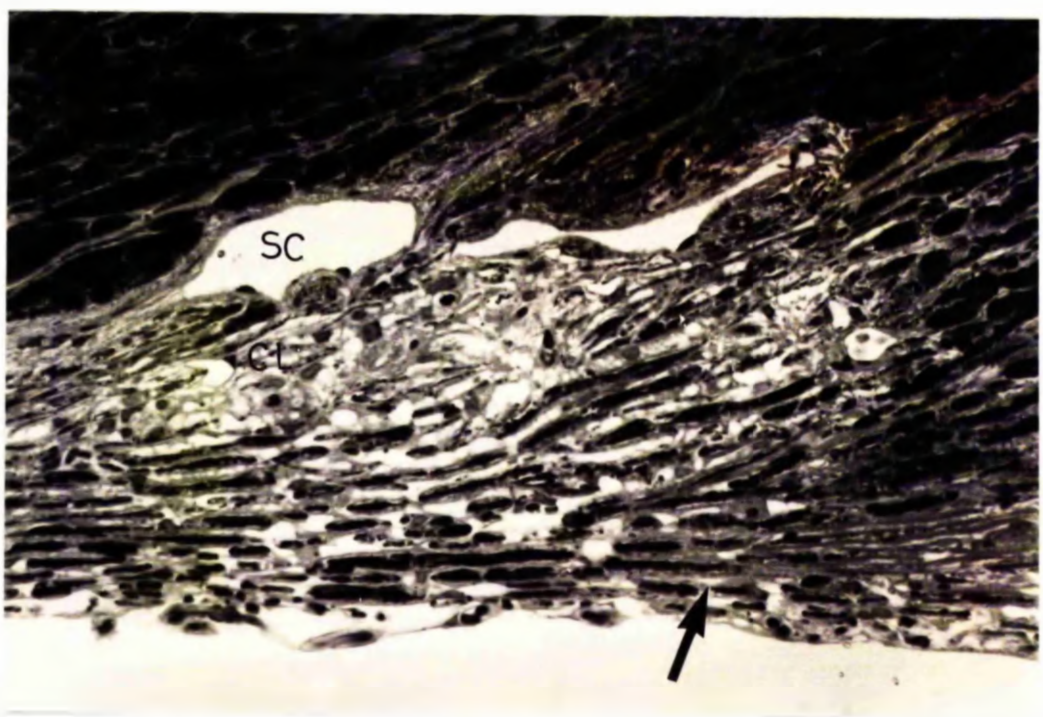

Figure 109: Light micrograph showing another region of the same eye as in Fig. 108 (19/79), with less canal closure. Note the compact uveal meshwork with obliteration of almost all the inter-trabecular spaces (arrow), (X 350).

in the trabecular endothelial cells of most eyes (Fig 110 and 113). There appeared to be a reduction in the numbers of trabecular endothelial cells compared to younger eyes, in some regions the cellular cover on the trabeculae was very thin and there were very few fine cytoplasmic processes crossing the intertrabecular spaces (Fig 110, 111, 112 and 113). There were many regions of the corneoscleral trabeculae which were denuded of endothelial cover altogether. The denuded trabeculae were disorganised and the appearance suggested that there was release of the connective tissue elements into the intertrabecular spaces and outer meshwork (Fig 110).

The cribriform layer in the majority of eyes contained large deposits of electron-dense plaques (Fig 110, 111 and 113) but there were occasional areas which were free from this accumulation (Fig 112), in the latter situation ground substance was predominent. Strands of loose basement membrane material were common in these eyes (Fig 112 and 113). There were fewer cell layers in the cribriform region than in young eyes (Fig 113). In colloidal iron stained preparations there was less staining than in younger eyes, presumably this was a consequence of the reduction in ground substance. The electron-dense plaques were stained only at the periphery (Fig 114). Cell membrane staining, however, was comparable to that observed in young eyes; the luminal aspect of the lining endothelium was lined by a very intense coat of colloidal iron particles. 'Giant vacuoles' in the lining endothelium of

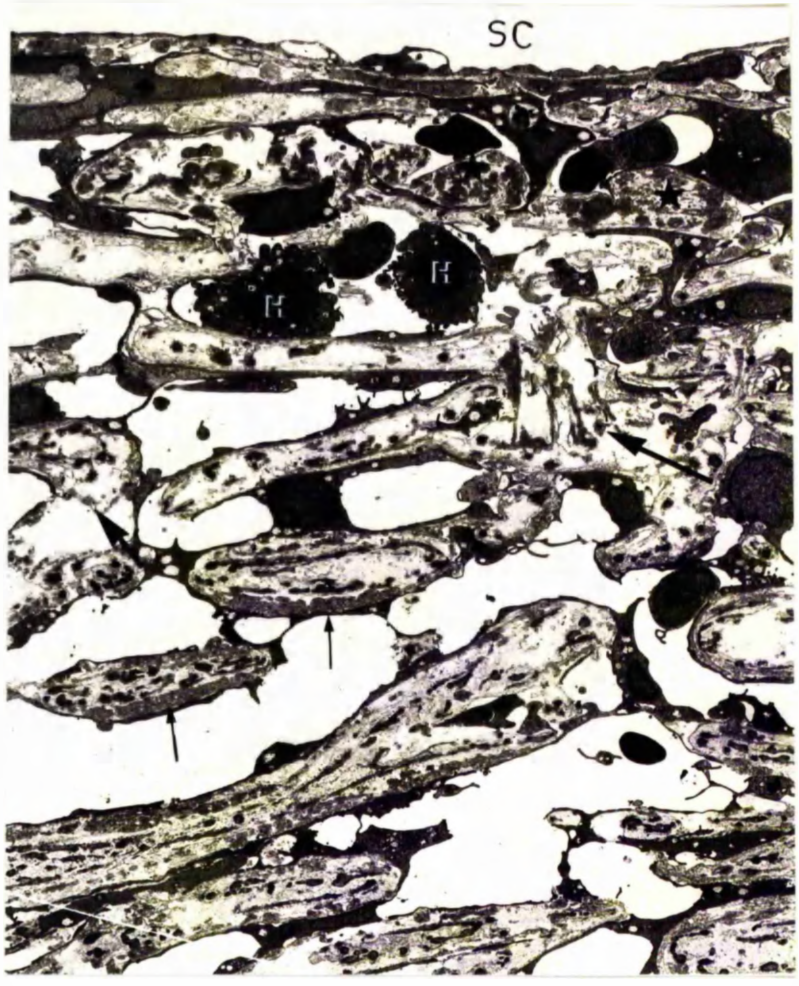

Figure 110: Transmission electron micrograph of the trabecular meshwork of a 72yr old human eye(32/75). Note the localised deposition of extracellular material in the cortical region of the trabeculae (small arrows) and the apparent degeneration of the denuded trabeculae (large arrows), with release of core material into the outer meshwork where it appeared to have accumulated (*). There seemed to be very few trabecular endothelial cell nuclei and there were very few fine cell processes, with the cell cover on most trabeculae being very thin. (X1700).

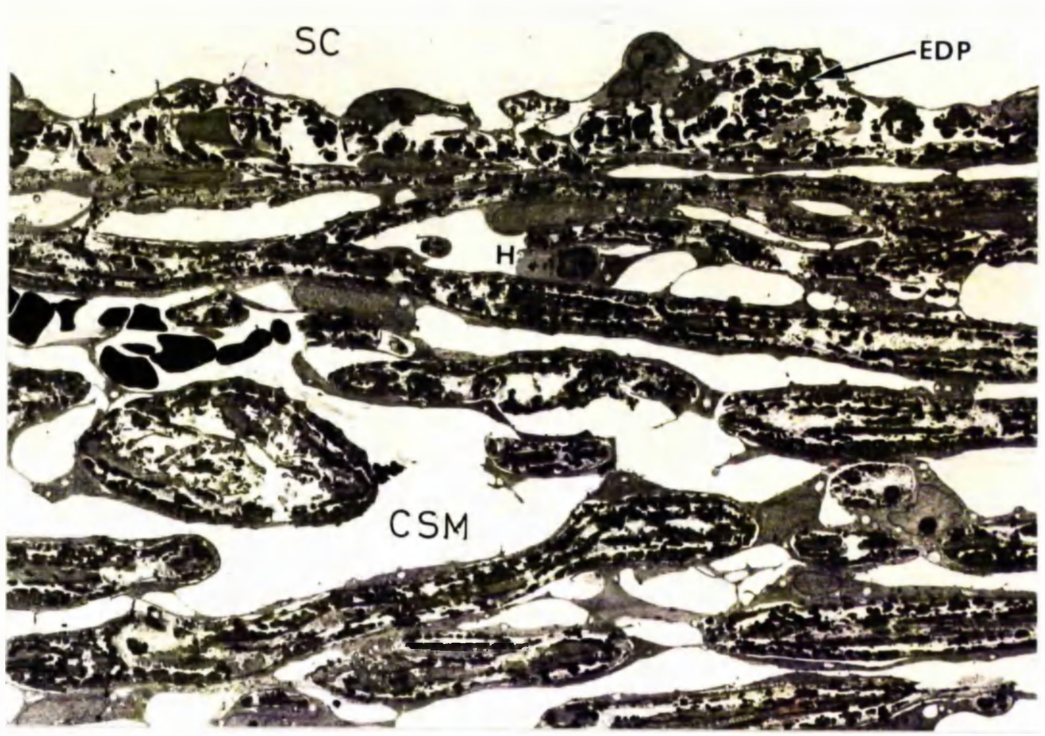

Figure 111: Transmission electron micrograph of the trabecular meshwork in a 76yr old eye(264/78). Note the thickened trabeculae, the accumulations of electron dense plaques in the cribriform layer and the scarcity of 'giant vacuoles'. (X 1300).

Figure 112: Transmission electron micrograph of an 80yr old eye (185/76) which in comparison to Fig. 111 does not have electron dense plaques in the cribriform layer, but only a little ground substance. (X 1300).

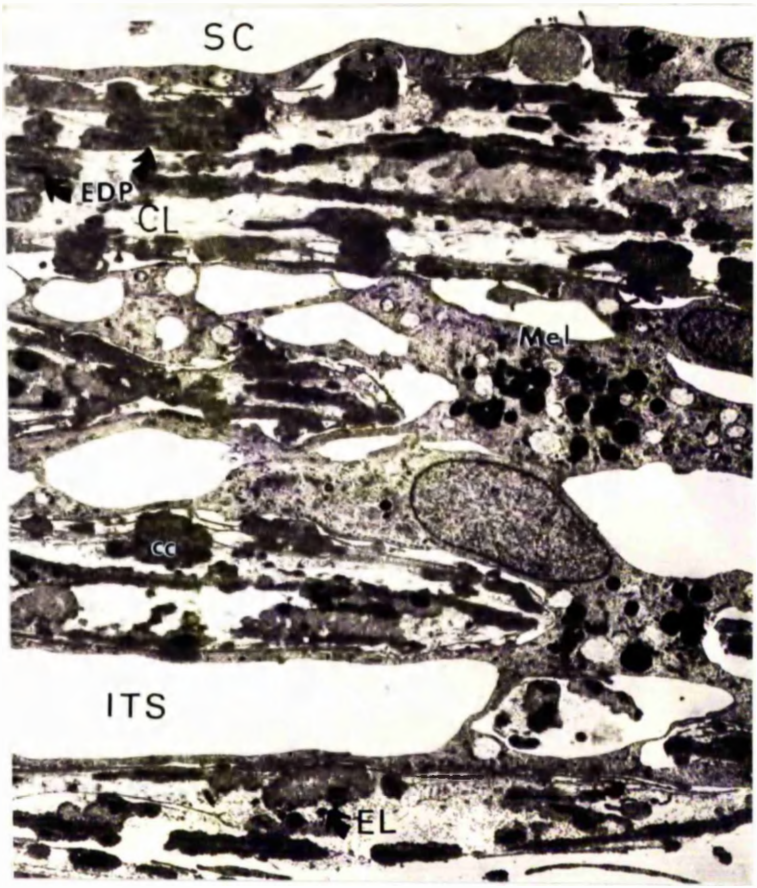

Figure 113: Transmission electron micrograph of the outer meshwork in a 74yr old eye(111/78). Note the accumulations of electron dense plaques which in this case are clearly similar to the curly collagen in the trabeculae. (X 40000).

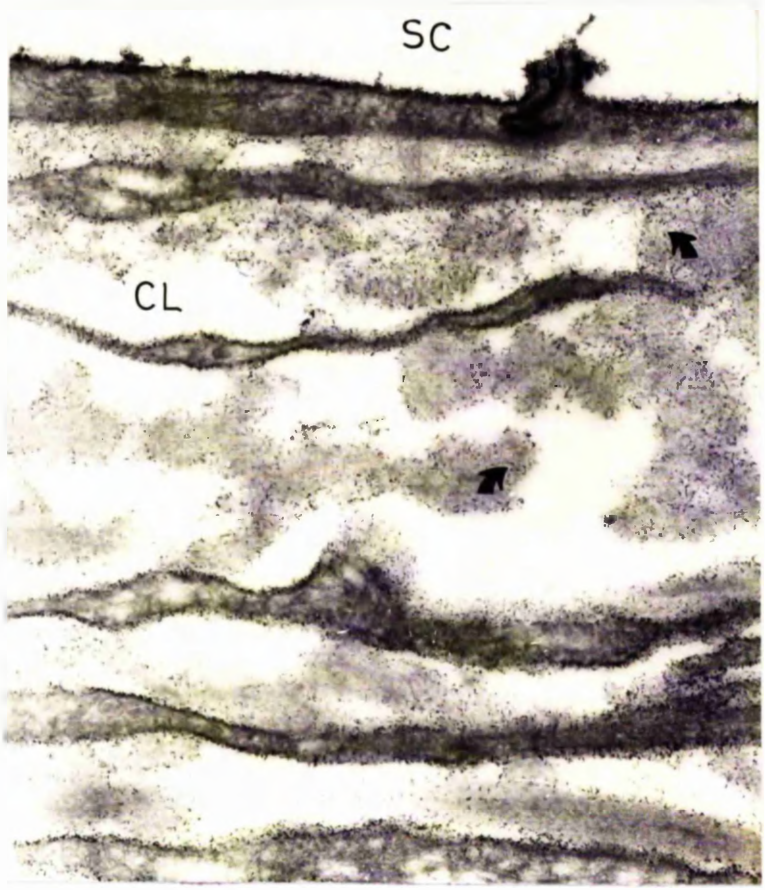

Figure 114: Transmission electron micrograph of colloidal iron stained tissue from an 83yr old eye(19/79). The plaques of extracellular material in the cribriform layer are only stained at their periphery(arrows). The staining on the lumen aspect of the lining endothelium of Schlemm's canal is particularly rich. (X 34,000).

Schlemm's canal were infrequent in this group.

QUANTITATIVE CHANGES WITH AGE IN THE HUMAN OUTFLOW APPARATUS

Trabecular thickness

The results obtained from 25 eyes are summarised in Table 15. The age-frequency distribution of the specimens (Fig 115) demonstrates the wide age range investigated but also that there was at least one specimen from each decade and up to four or five in others.

There was no change with age in the mean number of trabeculae or intertrabecular spaces per section (Table 15). The overall mean width of the trabeculae showed a definite increase with age (Fig 116) which was shown by regression analysis to be statistically significant ($r = 0.802$, $p < 0.001$). There was also an increase in the variance of the measurements with age, which is to be expected in a morphometric technique of this nature where not all trabeculae will be cut in the region of maximum thickness.

The results, rather surprisingly, showed that there was no change in the width of the intertrabecular spaces (Table 15).

Vacuolar incidence

The criteria used to identify a 'giant vacuole' for the purposes of quantitative assessment were identical to those

Patient EM No.	Age (yrs)	No. of trabeculae per section (x ± S.D.)	Trabecular width (x ± S.D.)	No. of spaces per section (x ± S.D.)	Width of spaces (x ± S.D.)
R.J. 396/79	0.2	8.8 ± 1.8	3.7 ± 1.4	5.8 ± 3.3	3.5 ± 3.7
A.McI. 59/80	0.25	9.0 ± 3.0	5.1 ± 1.6	8.0 ± 2.5	5.1 ± 4.4
G.C. 049/79	0.3	10.4 ± 1.0	5.2 ± 2.4	10.2 ± 2.3	6.4 ± 5.0
S.R. 346/78	1	9.8 ± 1.3	4.4 ± 1.5	7.4 ± 1.5	4.3 ± 2.4
M.H. 449/79	6	10.2 ± 1.8	4.7 ± 1.7	7.0 ± 1.7	4.1 ± 1.7
I.P. 264/78	18	9.8 ± 1.9	5.0 ± 1.6	7.6 ± 2.8	5.6 ± 3.2
M.O'H. 381/78	20	9.4 ± 2.8	5.0 ± 1.9	5.0 ± 1.7	3.6 ± 2.2
S.C. 13/72	22	9.0 ± 0.8	6.0 ± 2.1	6.5 ± 2.6	4.6 ± 3.7
J.O. 476/80	22	9.4 ± 0.5	5.0 ± 1.8	7.8 ± 1.6	4.8 ± 3.7
S.D. 157/80	24	7.8 ± 1.8	5.1 ± 2.1	5.4 ± 2.1	2.9 ± 1.8
A.M. 63/77	30	10.0 ± 1.0	4.7 ± 1.6	8.0 ± 1.6	4.4 ± 3.1
G.B. 76/75	38	7.6 ± 1.5	5.5 ± 2.0	4.0 ± 1.2	5.5 ± 4.4
L.B. 188/78	43	10.8 ± 1.6	5.6 ± 1.9	6.0 ± 1.0	5.0 ± 3.8
F.S. 232/79	45	7.8 ± 3.0	6.1 ± 1.8	7.4 ± 2.3	6.2 ± 4.8
M.M. 435/79	46	11.6 ± 1.1	6.0 ± 3.0	8.4 ± 1.9	3.9 ± 2.4
R.A. 617/79	51	9.8 ± 0.8	5.6 ± 2.4	7.2 ± 1.3	4.5 ± 3.5
E.M. 211/80	51	9.0 ± 2.0	5.5 ± 2.0	5.6 ± 2.9	3.5 ± 2.4
T.H. 212/80	51	11.6 ± 1.5	5.8 ± 2.1	8.2 ± 2.9	4.1 ± 3.8
W.M. 272/80	55	8.4 ± 2.3	6.7 ± 3.0	5.6 ± 2.7	6.5 ± 5.8
A.E. 325/80	60	7.8 ± 1.1	6.8 ± 2.0	5.4 ± 1.3	4.5 ± 3.4
M.H. 280/80	61	9.6 ± 1.5	5.7 ± 2.0	6.6 ± 1.1	5.8 ± 4.8
C.M. 214/80	65	8.4 ± 1.1	5.8 ± 2.1	7.0 ± 1.4	5.4 ± 2.9
M.C. 408/79	72	9.8 ± 1.1	6.3 ± 2.6	6.6 ± 0.9	3.5 ± 2.1
J.C. 19/79	83	9.4 ± 2.4	6.4 ± 2.4	6.0 ± 1.9	4.0 ± 3.8
I.M. 13/80	83	11.4 ± 3.5	6.7 ± 2.7	5.0 ± 0.7	4.9 ± 5.3

Table 15: Table summarising the results of the study of trabecular thickness in 25 human eyes of various ages. Measurements are in microns.

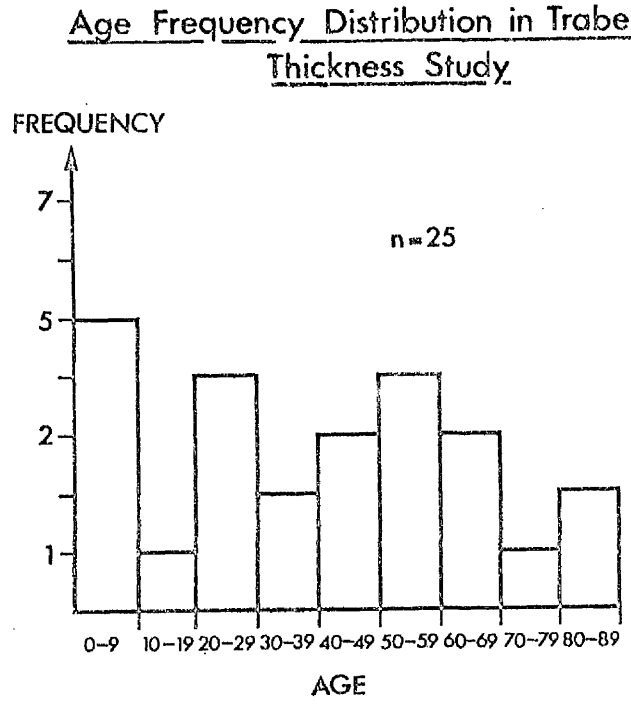

Figure 115: Age frequency distribution of the 25 human eyes used in the trabecular thickness study.

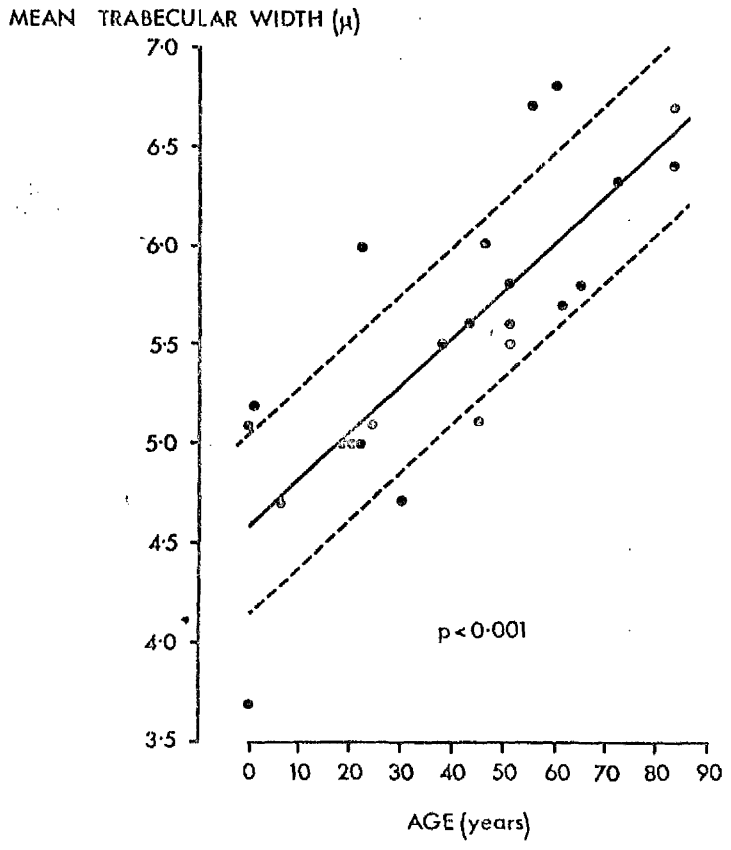

Figure 116: The results of the trabecular thickness study. The regression line (y= 0.024x +4.59) and standard deviation about the line(0.47)are indicated.

Age Frequency Distribution in Vacuole Count Study

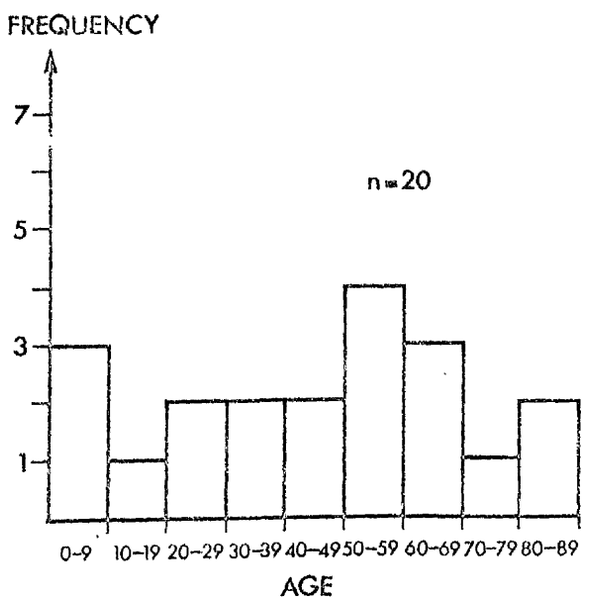

Figure 117: Age frequency distribution of the 20 human eyes used in the study of vacuolar incidence.

described in Part I. The age-frequency distribution of the twenty eyes (Fig 117) used in this investigation showed that except for the second decade, relatively even samples were taken.

The results of the counts of endothelial cell nuclei and 'giant vacuoles' are shown in Table 16. The value for the number of inner wall nuclei did not change with age, which indicated that there were equivalent numbers of cells in the endothelial monolayer of the canal of Schlemm throughout the age range. The mean number of 'giant vacuoles' per section (both inner wall and total vacuoles) in the lining endothelium of Schlemm's canal was very variable in the first five decades (between 5-15 per section), however, in the over fifties group there were very few vacuoles (less than a mean of 5 per section) - Fig 118 and 119. Regression analysis with age was statistically signficant ($r = -0.62$, $0.001 < p < 0.01$, both inner wall and total vacuoles). The coefficient of variation ($\frac{SD}{\bar{x}} \times 100\%$) was calculated for each eye, and is an indication of the variation in vacuole counts between the sections (Table 16). When this value was plotted against age there was a significant increase (Fig 120, $r = 0.57$, $0.001 < p < 0.01$). This provided evidence that with age the 'giant vacuoles' not only decrease in number but tend to become more clustered in some areas of the canal.

Components of the cribriform layer

A total of 36 eyes were used in this part of the investigation. The age-frequency distribution of the

Patient	EM No.	Age (Years)	Inner wall nuclei (x ± S.D.)	Inner wall vacuoles (x ± S.D.)	Other vacuoles (x ± S.D.)	Total vacuoles (x ± S.D.)	Coefficient of variation of total vacuoles
A.McI.	59/80	0.25	5.9 ± 2.2	8.5 ± 3.5	0.3 ± 0.9	8.8 ± 3.9	43.3
G.C.	049/79	0.30	7.9 ± 3.2	12.0 ± 4.5	1.2 ± 1.4	13.2 ± 5.7	43.2
M.H.	449/78	6	9.4 ± 3.5	4.2 ± 2.4	0.8 ± 1.0	5.0 ± 2.8	56.0
I.P.	264/78	18	8.8 ± 5.1	14.0 ± 4.0	2.4 ± 1.3	16.4 ± 4.6	28.0
G.O.	476/80	22	6.4 ± 2.6	5.1 ± 4.5	0.4 ± 1.3	5.5 ± 4.6	83.6
S.T.	157/80	24	8.6 ± 3.6	10.0 ± 5.2	2.0 ± 2.5	12.0 ± 5.4	45.0
A.N.	63/77	30	6.0 ± 2.8	8.4 ± 4.6	1.2 ± 1.6	9.6 ± 5.9	61.5
G.B.	76/75	38	6.3 ± 2.5	5.1 ± 2.9	0.5 ± 0.7	5.7 ± 3.2	57.1
F.S.	232/79	45	7.2 ± 3.6	7.1 ± 2.1	0.8 ± 1.1	7.8 ± 2.1	26.9
M.M.	435/79	46	8.2 ± 2.7	10.7 ± 4.5	1.6 ± 1.2	13.3 ± 4.8	36.1
R.A.	617/79	51	5.0 ± 3.7	10.8 ± 7.0	1.6 ± 2.2	12.5 ± 8.5	68.0
E.M.	211/80	51	6.7 ± 1.3	0.8 ± 1.3	1.1 ± 1.5	1.9 ± 2.0	105.3
T.H.	212/80	51	5.5 ± 2.5	0.1 ± 0.3	0.2 ± 0.6	0.3 ± 0.7	233.3
W.M.	272/80	55	5.5 ± 2.3	0.8 ± 1.0	0.3 ± 0.9	1.2 ± 1.4	116.6
A.E.	325/80	60	7.4 ± 1.2	5.2 ± 3.3	0.3 ± 0.6	5.5 ± 3.3	60.0
M.H.	280/80	61	7.0 ± 3.4	0.8 ± 1.0	0	1.2 ± 1.3	108.0
C.M.	214/80	65	4.2 ± 1.9	1.3 ± 2.2	0	1.3 ± 2.2	169.2
M.C.	408/79	72	4.0 ± 2.3	0.4 ± 0.8	0	0.5 ± 0.8	160.0
J.C.	19/79	83	3.9 ± 1.5	0.4 ± 1.0	0.1 ± 0.3	0.5 ± 0.1	200.0
I.M.	13/80	83	7.3 ± 2.8	4.2 ± 2.5	0.1 ± 0.3	4.3 ± 2.7	62.8

Table 16: Table summarising the results of the quantitative assessment of the incidence of 'giant vacuoles' in the lining endothelium of Schlemm's canal in 20 human eyes. The results are expressed as mean number of features per section in each eye.

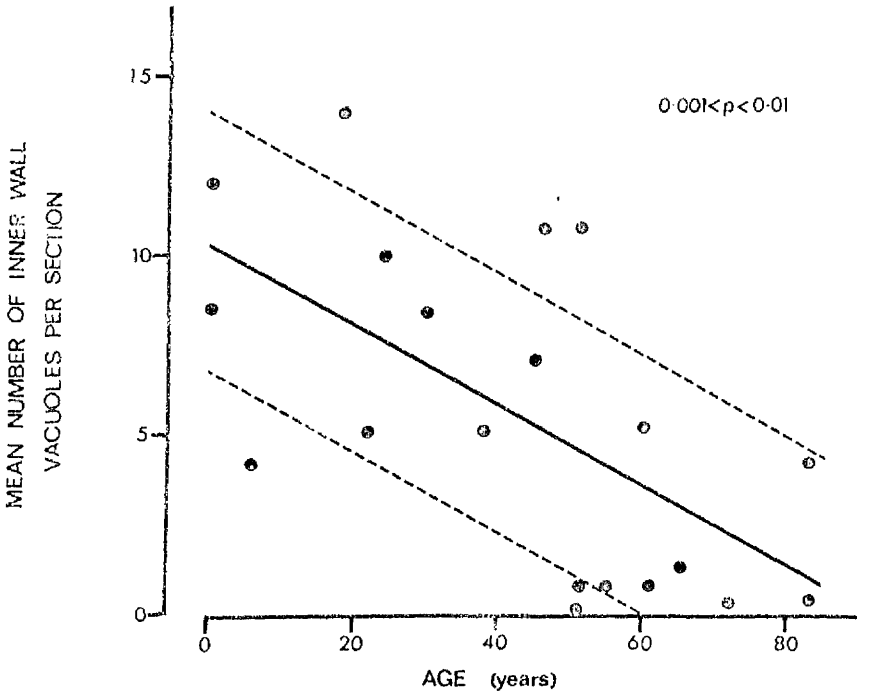

Figure 118: Results of the vacuolar incidence study, showing the mean number of vacuoles on the inner wall of Schlemm's canal per section in each eye. The regression line ($y = -0.123x + 10.4$) and standard deviation (3.6) are indicated.

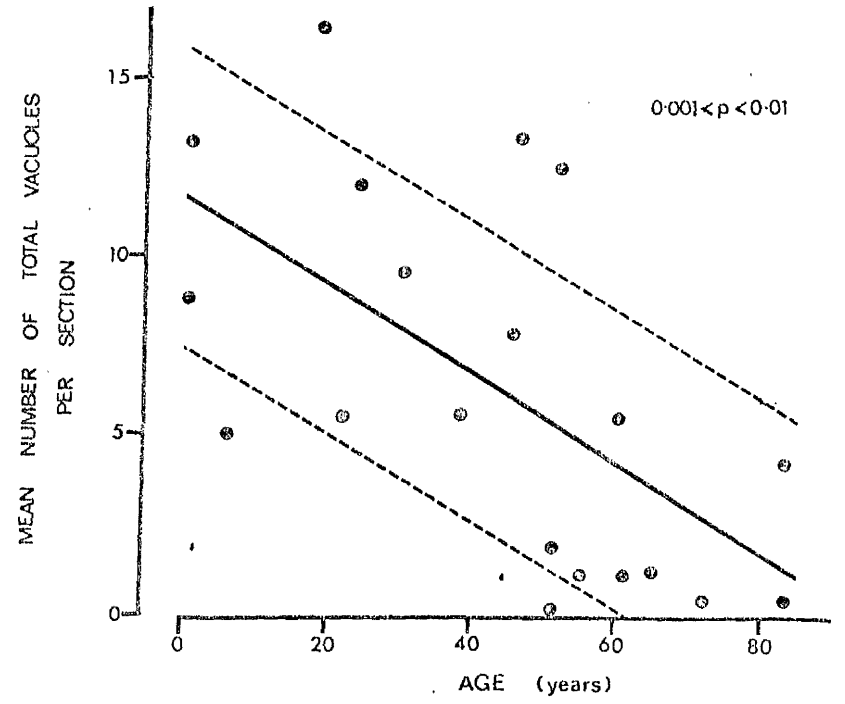

Figure 119: The mean number of 'giant vacuoles' in the lining endothelium is plotted against age of the eye The regression line ($y = -0.123x + 11.7$) and standard deviation about the line (4.1) are almost identical to Fig 118.

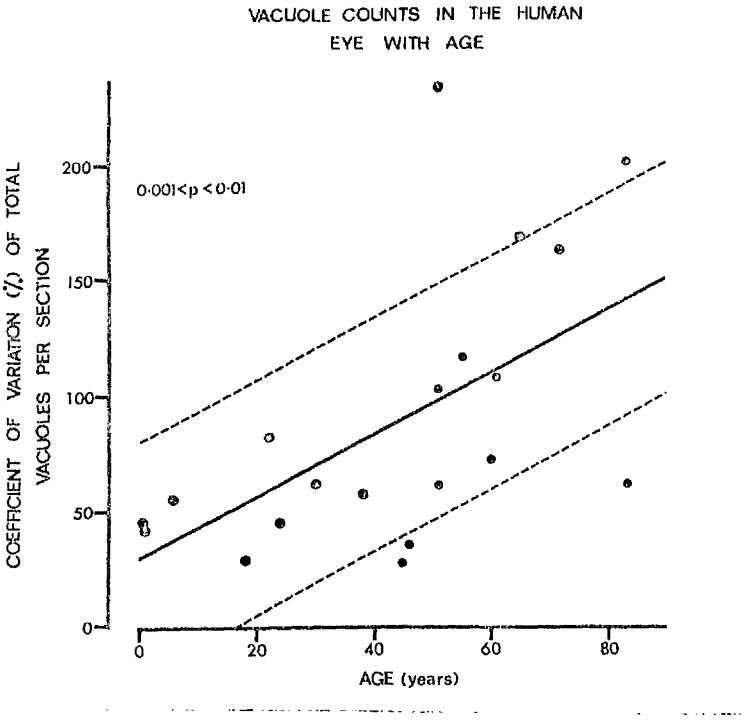

Figure 120: The coefficient of variation of the total number of vacuoles in each eye is plotted against age. The regression line (y= 1.19x +27.8) and standard deviation about the line (42.4) are indicated.

number of eyes and area of tissue (ie number of prints) (Fig 121 and 122) shows that apart from the high incidence of 61-70 year olds the distribution in the age groups was even throughout the range. A mean of 12.5 prints were examined in each eye.

The mean percentage area occupied by the cribriform layer (Table 17) was extremely variable between eyes but did not show any overall change with age.

i) The ground substance component of the cribriform layer consisted of both granular ground substance and unit collagen fibrils. The results of the morphometric study revealed that in eyes under forty years of age this component occupied between 20-40% of the total area of the cribriform layer while in older eyes it occupied only 10-20%. Regression analysis confirmed that this downward trend with age was significant (Fig 123, $r = -0.567$ $p < 0.001$). The distribution of this material within one eye was extremely variable, even along the length of the inner wall within one section. There was also a great deal of variation between eyes of similar ages (Fig 123).

ii) Electron dense plaques occupied only a minor part of the total of the cribriform layer in eyes below the age of forty, but over this age this material generally occupied between 10-25% of the area (Table 18, Fig 124). Regression analysis confirmed the positive correlation with age (Fig 124, $r = 0.779$, $p < 0.001$).

iii) Basement membrane material in the cribriform layer included both the discontinuous layer under the lining

Patient's initials EM No.	AGE (yrs)	No. of sections	No. of prints	% area cribriform layer ± S.D.
RS 396/79	0.2	1	8	46.3 ± 3.8
GC 049/79	0.3	2	11	40.0 ± 10.5
SR 346/78	1.0	1	5	61.0 ± 12.3
MH 449/78	6.0	2	28	58.3 ± 10.0
IP 264/78	18.0	1	12	61.4 ± 16.1
HON 381/78	20.0	2	20	44.4 ± 15.8
SC 13/72	21.0	1	14	45.0 ± 13.8
JO 476/80	22.0	2	10	47.1 ± 20.4
ST 151/80	24.0	1	5	85.0 ± 6.1
AM 63/77	30.0	2	22	44.7 ± 17.8
GB 76/75	38.0	1	12	33.0 ± 17.0
LB 188/78	43.0	1	8	39.9 ± 13.1
FS 232/79	45.0	1	9	51.5 ± 13.7
MM 435/79	46.0	1	10	26.8 ± 12.6
MH 450/78	50.0	1	9	67.6 ± 8.7
WC 64/77	50.0	1	19	37.7 ± 13.8
PG 03/71	54.0	1	12	45.7 ± 11.5
SB 111/76	58.0	1	9	57.0 ± 7.2
JH 442/78	59.0	1	8	70.6 ± 17.7
MA 54/74	63.0	1	9	46.7 ± 13.8
AMcC 349/75	63.0	2	11	45.6 ± 12.3
JK 582/76	63.0	2	28	41.6 ± 13.7
AM 344/78	64.0	2	13	68.5 ± 11.4
RF 245/77	66.0	1	7	43.4 ± 21.8
AD 444/76	68.0	1	5	51.4 ± 14.4
AP 285/79	68.0	2	16	53.2 ± 15.1
MG 79/73	68.0	2	19	60.2 ± 11.5
JD 42/76	70.0	1	13	44.2 ± 9.7
MC 408/79	70.0	2	14	70.9 ± 15.7
DS 287/79	72.0	1	12	55.2 ± 14.7
MMcL 111/78	74.0	1	5	54.8 ± 19.4
JH 32/75	75.0	1	7	37.0 ± 16.0
MW 269/78	76.0	1	8	48.5 ± 14.5
AMcC 185/76	80.0	3	27	31.3 ± 10.4
JC 19/79	83.0	2	11	87.7 ± 5.7
IM 13/80	83.0	2	16	65.6 ± 9.5

Table 17: Table showing the details of number of sections, number of prints and the mean percentage area occupied by the cribriform layer in the 38 human eyes used in this part of the investigation.

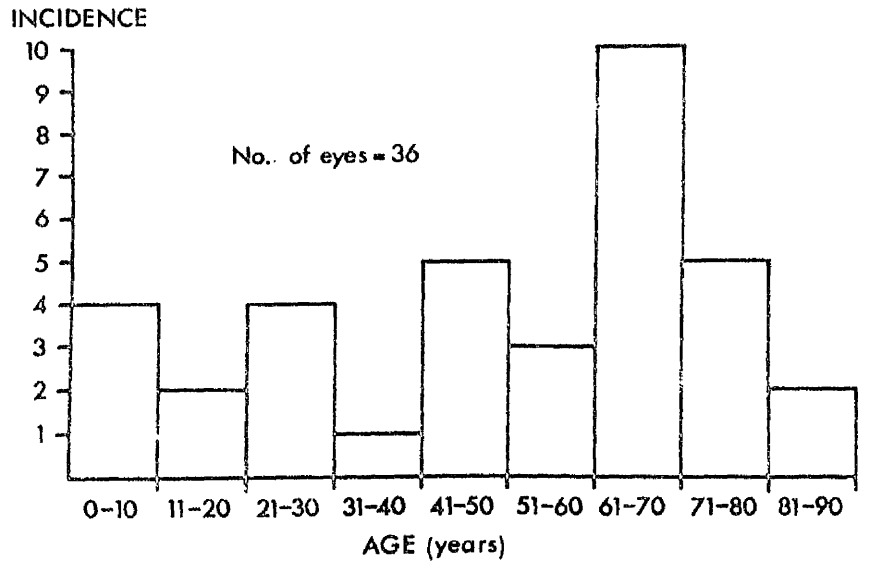

Figure 121: Age frequency distribution of the 36 human eyes used in the study of the components of the cribriform layer.

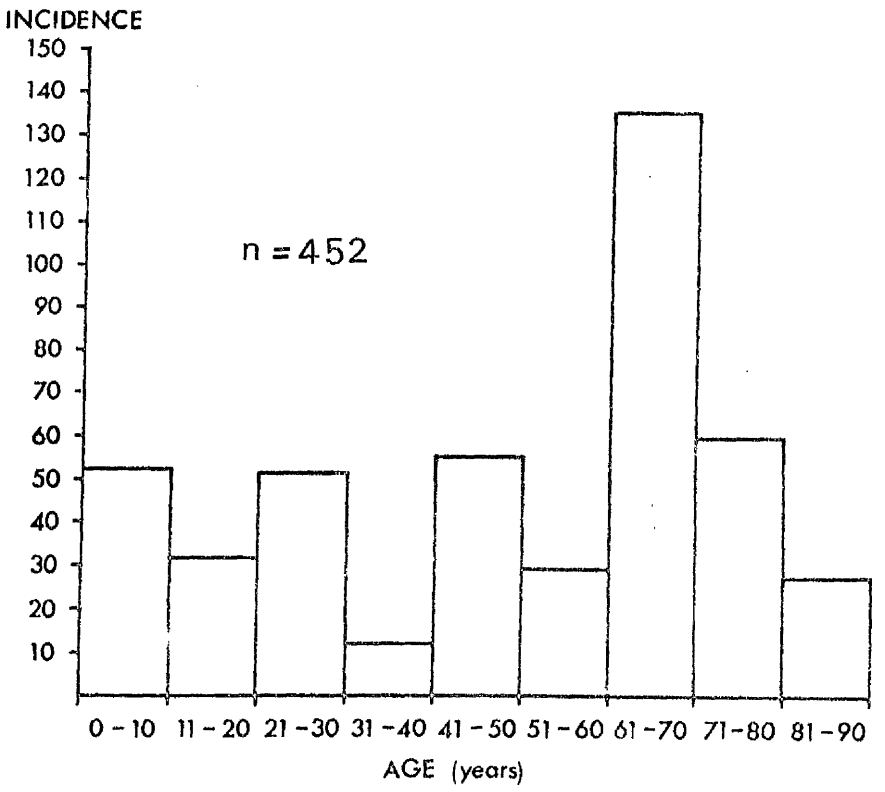

Figure 122: The age frequency distribution of the numbers of prints used in the study of the components of the cribriform layer.

PATIENT	EM No.	AGE (yrs)	% AREA gs (± SE)	% AREA EDP (± SE)	% AREA bm (± SE)	% AREA cells (± SE)
RS	396/79	0.2	24.5 ± 2.1	6.7 ± 1.5	0.6 ± 0.4	39.4 ± 4.0
GC	049/79	0.3	38.8 ± 4.5	0.4 ± 0.4	1.0 ± 0.4	34.6 ± 3.7
SR	346/78	1.0	23.3 ± 4.2	3.0 ± 1.7	2.3 ± 1.0	40.9 ± 3.0
MH	449/78	6.0	31.3 ± 1.7	3.5 ± 0.7	1.9 ± 0.3	46.3 ± 2.2
IP	264/78	18.0	19.7 ± 2.4	13.4 ± 1.4	1.5 ± 0.5	28.5 ± 2.2
HON	381/78	20.0	24.0 ± 2.5	0.9 ± 0.4	2.5 ± 0.9	41.6 ± 3.5
SC	13/72	21.0	37.0 ± 2.4	3.3 ± 0.8	1.3 ± 0.5	37.8 ± 3.1
JO	476/80	22.0	24.9 ± 3.7	6.6 ± 1.8	3.7 ± 1.0	38.7 ± 3.0
ST	157/80	24.0	21.6 ± 1.9	3.1 ± 1.8	0.5 ± 0.3	31.0 ± 1.7
AM	63/77	30.0	32.8 ± 2.0	5.6 ± 1.2	2.4 ± 0.8	38.7 ± 2.7
GB	76/75	38.0	29.0 ± 5.5	5.3 ± 1.5	2.3 ± 0.5	44.7 ± 6.0
LB	188/78	43.0	15.7 ± 3.8	17.9 ± 6.3	0.6 ± 0.5	29.7 ± 6.1
FS	232/79	45.0	44.6 ± 4.9	2.4 ± 1.0	0	22.8 ± 2.5
MM	435/79	46.0	21.3 ± 2.8	14.3 ± 2.1	3.6 ± 0.8	26.8 ± 4.0
MH	450/78	50.0	14.5 ± 2.1	13.8 ± 2.0	1.9 ± 0.3	32.5 ± 3.3
WC	64/77	50.0	17.2 ± 2.8	18.4 ± 2.1	2.0 ± 0.6	42.4 ± 2.5
PG	03/71	54.0	18.0 ± 3.7	21.7 ± 1.7	1.1 ± 0.8	25.7 ± 2.2
SB	111/76	58.0	13.8 ± 2.7	22.4 ± 2.0	1.4 ± 0.6	35.0 ± 2.8
JH	442/78	59.0	15.2 ± 2.2	21.1 ± 2.6	1.6 ± 1.0	36.5 ± 3.1
MA	54/74	63.0	15.4 ± 1.9	18.8 ± 2.1	3.8 ± 1.1	39.7 ± 3.9
MC	349/75	63.0	14.2 ± 1.7	12.2 ± 1.7	4.5 ± 1.6	38.2 ± 4.6
JK	582/76	63.0	25.3 ± 2.8	18.1 ± 3.1	1.8 ± 0.5	35.2 ± 2.4
AM	344/78	64.0	21.7 ± 1.2	12.1 ± 1.3	5.4 ± 0.8	32.6 ± 1.8
RF	245/77	66.0	27.6 ± 4.5	11.2 ± 2.2	4.6 ± 1.6	21.4 ± 2.5
AD	444/76	68.0	17.9 ± 3.3	22.6 ± 2.3	3.5 ± 1.7	20.6 ± 3.1
AP	285/79	68.0	10.2 ± 1.2	24.6 ± 2.9	2.7 ± 0.8	32.8 ± 2.7
MG	79/73	68.0	12.1 ± 1.8	21.4 ± 1.2	2.3 ± 0.5	37.3 ± 1.9
JD	42/76	70.0	28.7 ± 3.5	10.6 ± 1.6	1.7 ± 0.6	45.0 ± 4.3
MC	408/79	70.0	15.1 ± 1.4	20.3 ± 1.4	2.3 ± 0.6	24.6 ± 2.5
DS	287/79	72.0	17.8 ± 2.4	11.3 ± 1.6	3.9 ± 1.0	41.4 ± 1.7
MMcL	111/78	74.0	5.1 ± 1.0	20.4 ± 3.3	8.0 ± 2.3	26.3 ± 6.2
JH	32/75	75.0	20.0 ± 4.0	22.0 ± 3.8	2.3 ± 1.4	38.6 ± 4.7
MW	269/78	76.0	7.9 ± 1.3	29.0 ± 2.3	1.7 ± 0.6	35.3 ± 4.0
AMcC	185/76	80.0	26.0 ± 2.7	15.9 ± 2.4	4.4 ± 1.1	38.5 ± 3.8
JC	19/79	83.0	8.3 ± 1.1	23.2 ± 2.2	1.1 ± 0.4	41.9 ± 2.7
IM	13/80	83.0	14.3 ± 1.2	20.0 ± 1.9	1.0 ± 0.4	27.6 ± 2.8

Table 18: Summary of the results in the morphometric assessment of the components in the cribriform layer in 38 human eyes.

gs - ground substance

EDP - electron dense plaques

bm - basement membrane

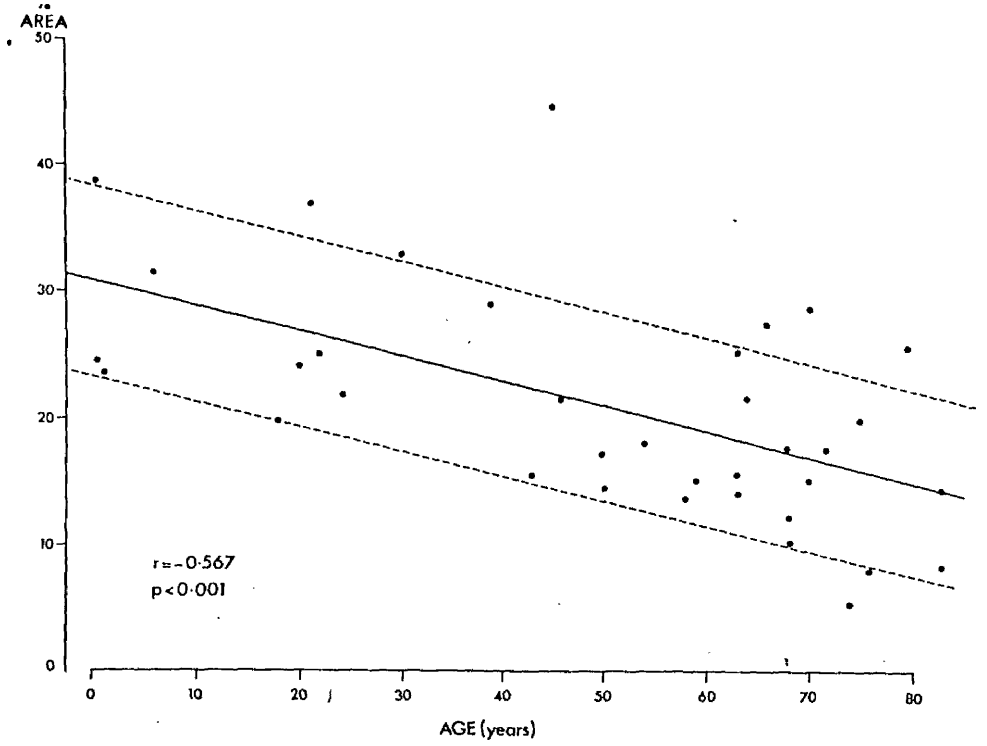

Figure 123: Results of the percentage area occupied by the ground substance component in the cribriform layer in the 36 eyes of various ages. The regression line ($y = -0.199x + 30.9$) and standard deviation about the line (7.4) are indicated.

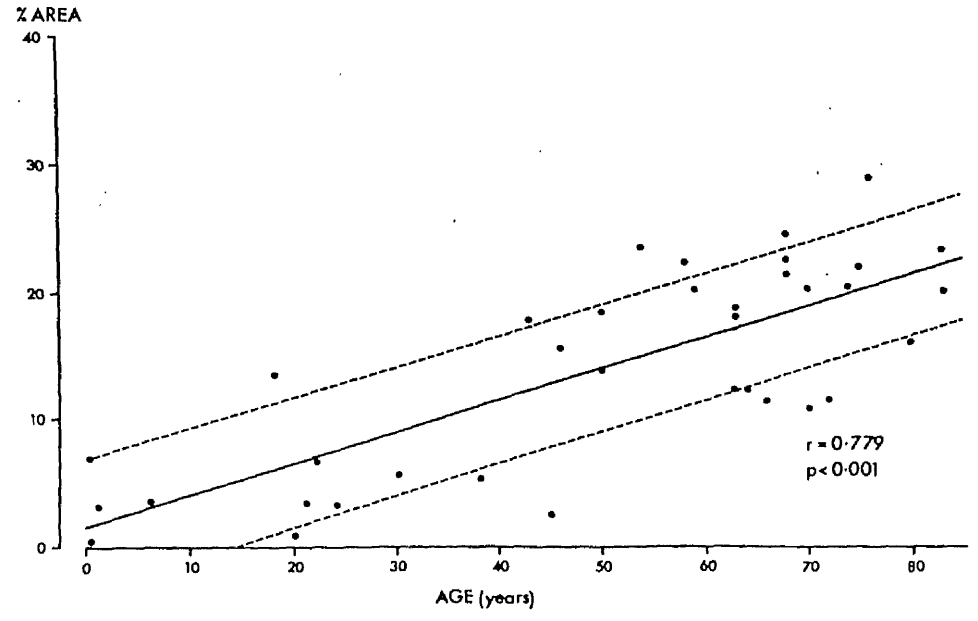

Figure 124: Results of the percentage area occupied by electron dense plaques in the cribriform layer. The regression line($y = 0.245x + 1.61$) and standard deviation (5.1) are indicated.

endothelium and other more randomly dispersed clumps. Although this technique is inadequate for the measurement of small components [See Methods], it was interesting to note that there was more variation in the area occupied by basement membrane in older eyes (Fig 125), this suggested that there may be a thickening of the material already present or increased deposition of the material in the cribriform layer with age.

iv) The cellular component consisted of both native endothelial cells and tissue histiocytes. The latter cell type was included because it was often difficult to discriminate between the cell types when only small areas of cytoplasm were present in the section being examined. Erythrocytes were not considered as a cellular component. The results (Table 18, Fig 126) indicated that this component occupied between 20-50% of the area of the cribriform layer and showed no change with age (Table 18, Fig 126).

It was evident from the results that there an inverse relationship between two of the components, ie ground substance and electron-dense plaques. When the results of each of these components were plotted (Fig 127) it was clear that when ground substance occupied a large area of the cribriform layer electron-dense plaques were less evident and vice versa. Regression analysis confirmed the strong negative correlation ($r = -0.797$, $p < 0.001$). It appears therefore that the two major extra-cellular components of the cribriform layer are mutually exclusive

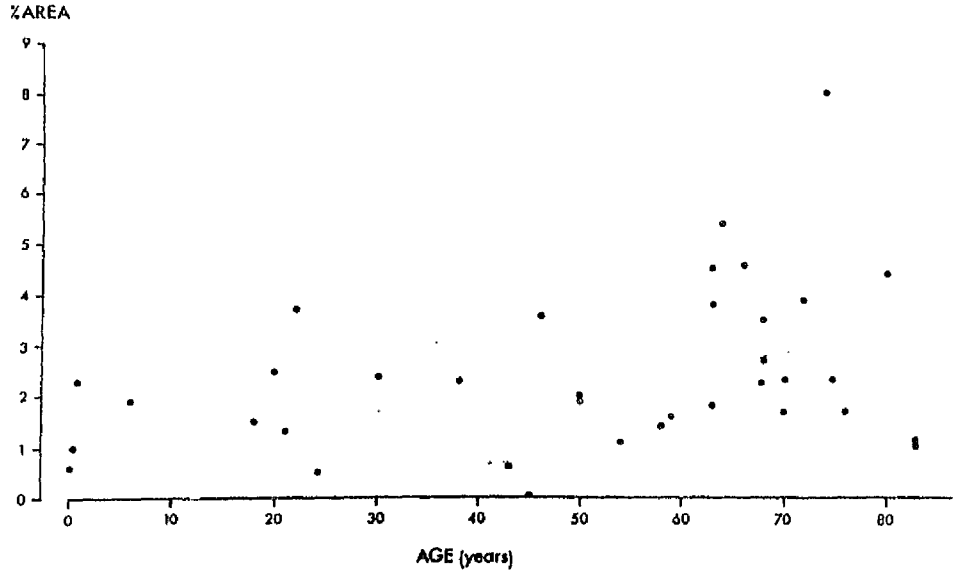

Figure 125: The percentage area of basement membrane component in the cribriform layer is plotted against age in each of the 36 eyes.

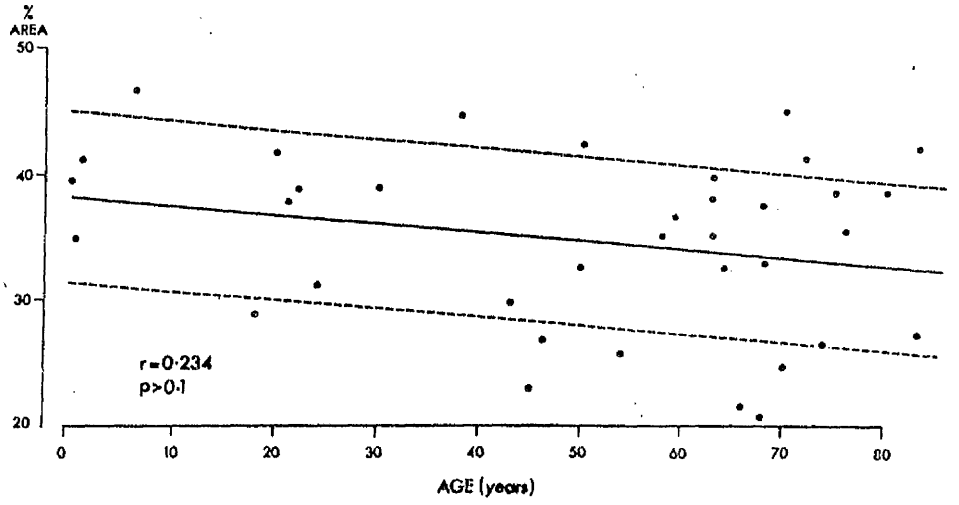

Figure 126: The results of the percentage area occupied by the cellular component in the 36 eyes.

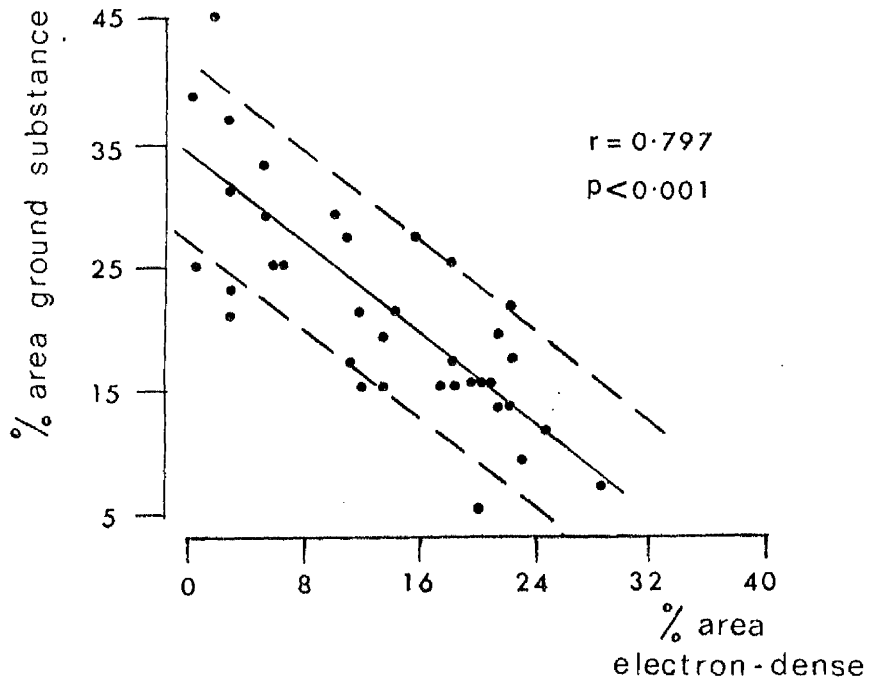

Figure 127: Graphic representation of the relationship between the percentage area occupied by the two main extracellular components of the cribriform layer, ie. ground substance and electron dense plaques. The regression line (y= 0.89x +33.2) and standard deviation (6.1) are indicated.

viz with age the ground substance was gradually replaced by more electron-dense plaques. There was no correlation between the increase in electron-dense plaques and the thickness of the cribriform layer.

SUMMARY OF AGE-RELATED CHANGES

The age related changes in the morphology of the human outflow apparatus, summarised diagrammatically in Fig 128a and b, were as follows.

i) The scleral spur was diminuitive in very young eyes ($<$ 1 year) but became more prominent with age.

ii) The uveal meshwork became more compact in older eyes, particularly in the region of the scleral spur.

iii) The configuration of the meshwork showed a gradual change from a long wedge shape to a shorter more rhomboidal form.

iv) The trabeculae thickened with age mainly due to the accumulation of 'curly collagen' and elastic-like fibres (B in Fib 128b).

v) The trabecular endothelial cells became more phagocytically active, lost their fine cytoplasmic processes (C in Fig 128a) and in some areas became detached from the trabecular core which appeared to result in an erosion of the extracellular elements.

vi) In the cribriform layer there was an increased accumulation of electron-dense plaques with age and this was associated with a corresponding decrease in the ground

substance.

vii) 'Giant vacuoles' in the lining endothelium were rare in older eyes.

viii) Tissue histiocytes were commoner in the trabecular meshwork of older specimens.

ix) There were atrophic changes in the region of the iris base and ciliary muscle face (A in Fig 128b).

x) Localised regions of canal closure were commoner in older eyes (D in Fig 128b).

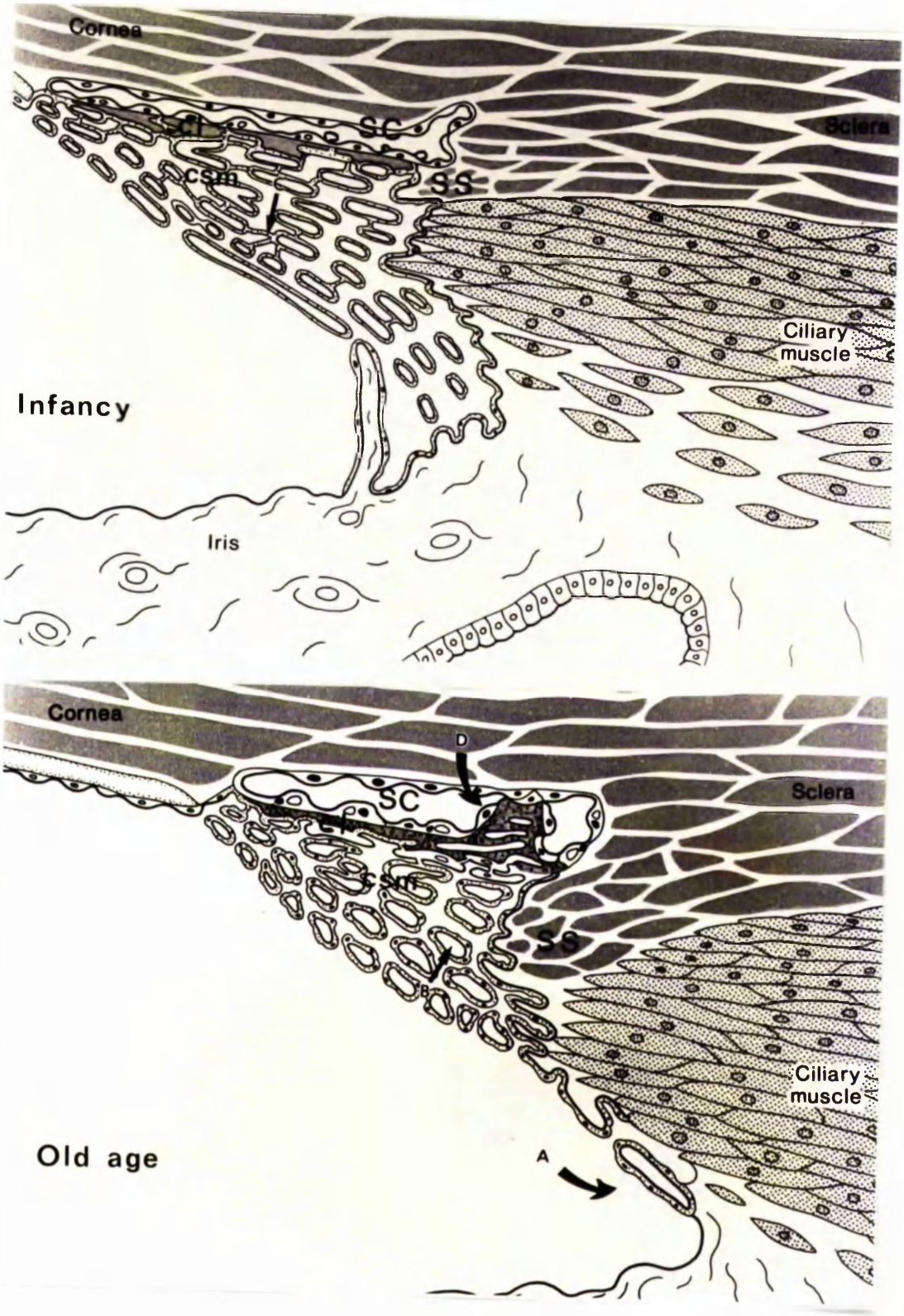

Figure 128: Schematic diagrams of the human outflow apparatus in an infant and in old age to summarise the main age related changes.

DISCUSSION

The age-related changes in the morphology of the human outflow apparatus shown in the present investigation were variable, both between eyes of similar ages and within one eye. Due to the extremely variable appearance it was necessary to quantify the changes as far as possible. This may be particularly relevant in the comparison of age changes to the changes in primary open angle glaucoma some of which in isolated sections may be indistinguishable but on quantitative examination of larger samples a real difference may be more obvious.

The numbers of tissue histiocytes, although not quantitatively assessed, did appear to be greater in the outflow apparatus of older eyes. These monocytic cells, often called tissue macrophages, are found in most connective tissues where they similarly increase in number with age (Hall 1976). Tissue histiocytes in other connective tissues play an important part in clearing debris particularly after mild trauma, and in re-cycling degraded proteins (Hall 1976). In the trabecular meshwork these cells along with the native endothelial cells are essential to the role of the meshwork as a biological filter. An increase in the number of histiocytes along with the increase in intracytoplasmic melanin, secondary lysosomes and residual bodies in the endothelial cells in older eyes suggests that there are greater amounts of debris entering the meshwork. Some debris is almost certainly derived from the lens, the iris and ciliary processes which show degenerative and atrophic changes with

age (Hogan and Zimmerman 1962). Undoubtedly the presence of some of the inflammatory cells in the meshwork, which included macrophages, lymphocytes and polymorphonuclear leucocytes, could be attributed to the pre-existing pathological disorders in the eye, but this would not explain the increased frequency of histiocytes with age.

The qualitative impressions of previous workers that the trabeculae thicken with age (Ashton 1960, Holmberg 1965, Rohen and Lütjen-Drecoll 1971) has been confirmed by the present quantitative study. In agreement with previous studies this increased width was found to be the result of deposition of 'curly collagen' in the cortical region of the trabeculae. This deposition was accompanied by a thickening of the elastic fibre sheath. This form of degeneration appears to be widespread in the eye and similar deposits have been seen in Descemet's membrane (Jakus 1961) and Bruch's membrane (Hogan, Alvorado and Weddell 1971).

The measurement of the age changes in the mean width of intertrabecular spaces was not an entirely suitable assessment of space available for aqueous movement for two mean reasons. Firstly the space in the meshwork would vary depending on the state of contraction of the ciliary muscle at the time of enucleation.

Secondly a measurement of mean width of the intertrabecular spaces did not seem to truly represent the area or volume of the spaces in the meshwork. The finding of no change in the width of the spaces with age may have

been observed since in young eyes the spaces were subdivided by the cytoplasmic processes which were greatly decreased in the old eye. Therefore despite the quantitative results it was felt from qualitative observations that the spaces did decrease with age, however, this was more severe in some areas than in others, particularly in regions of trabecular fusion. Similar narrowing of the spaces with age was observed by other authors (Rohen and Lütjen-Drecoll 1971, Tripathi 1977a).

Incomplete cellular cover of the trabeculae was to some extent a feature of all ages, but was more prevalent in older eyes (over 50 years). With the loss of the protective cell cover and exposure to the action of aqueous humour there was a disorganisation of the core materials, some of which appeared to be washed into the outer meshwork where there was an accumulation between the compact layers of cells. The possible contribution that these materials may have on resistance to aqueous flow through the cribriform layer will be discussed later, however, it is important that the factors which may cause this breakdown of trabeculae be considered.

i) In view of both the recent report of a quantitative decrease in cellularity in the trabecular meshwork with age (Alvorado, Murphy and Polansky 1980) and the present finding of increased trabecular thickness it would seem that in the older eye fewer cells are available to cover a larger surface area of trabeculae. It is not surprising therefore that there is a general thinning of the cell

cover and fewer fine cytoplasmic extensions in older specimens.

One criticism of the present study is that age-related changes in the cell density of the trabecular meshwork was not assessed, however, this is one aspect of the present study which could be extended in the future.

ii) The surface specialisations between the trabecular endothelial cells and the connective tissue core observed in the present study and by previous workers (Spelsberg and Chapman 1962, Tripathi 1977a) appeared scarcer in older eyes. If these structures are important in adhesion of the cells to the core then a decrease in their frequency may be an important predisposing factor to cell detachment. It is possible that the cells may have lost the ability to form such specialisations or alternatively it may imply that due to the cell loss the cells which have to extend to cover the denuded areas of trabeculae do not form new specialisations (eg pegs).

iii) It may be possible that after 60 or 70 years of ciliary muscle action during accomodation, that the change in configuration of the trabecular meshwork that this will produce, may lead to alterations in the trabecular endothelial cells. The continual stretching and recoiling may ultimately affect the pliability of the cells. Lütjen-Drecoll and Kaufman (1979) studied the effects of prolonged use of the powerful miotic, echothiophate (phospholine iodide) on the morphology of the outflow apparatus in young cynomolgous monkeys. After treatment

with this drug, the trabecular endothelial cells showed signs of degenerative changes including mitochondrial swelling, cytoplasmic vacuolisation and frequent detachment from the trabeculae.

These changes which were presumed to be the result of ciliary muscle contraction which caused increased tension on the meshwork were apparent in eyes treated twice daily for 54 days but were more severe in 138 and 155 day treated animals. In this species of monkey which has a diminuitive scleral spur the muscle inserts directly into the meshwork. In man it has been shown that the muscle exerts its effect on the meshwork by the backward displacement of the scleral spur to which the corneoscleral trabeculae are attached (Grierson, Lee and Abraham 1978).

The detachment of cells from the core noted by Lütjen-Drecoll and Kaufman (1979) were thought to be due to the tension on the meshwork. Although this is a very severe example it lends support to the contention that a lifetime's 'wear and tear' due to changing configuration of the meshwork may cause changes in the trabecular endothelial cells such as loss of cell to cell contact which may lead to cells detaching from the cores.

One alteration which the cells may undergo with age which may precipitate the loss of cell to cell contact is in the nature of the microfilaments. The trabecular endothelial cells in the human trabecular meshwork have been shown to contain actin-like filaments and intermediate filaments (Gipson and Anderson 1979, Grierson and Rahi

1979). These microfilaments were suggested by the above authors as possibly having a role in the following; maintenance of cell to cell contact; cell to trabeculae contact and cell pliability. Recent studies of the morphological and physiological effects of cytochalasin B (a fungal metabolite which disrupts contractile microfilaments) have supported the suggestions that the microfilaments are important in the maintenance of tissue integrity and resistance to aqueous outflow (Kaufman and Bárány 1977, Kaufman, Bill and Bárány 1977, Svedbergh, Lütjen-Drecoll, Ober and Kaufman 1978, Johnstone, Tanner, Chau and Kopecky 1980).

As yet there is no information on the changes with age in the microfilaments and this would certainly be a potentially profitable line of future research.

iv) It is generally accepted that with age there is a reduction in aqueous production and drainage in the human eye (see introduction). It has become apparent recently that localised underperfusion of the meshwork may have deleterious effects on the tissue in several respects. It has been shown that the non-operated areas of the trabecular meshwork, in cynomolgous monkeys which had undergone trabeculectomies three months previously showed thickened trabeculae similar to those observed in the aging process (Lütjen-Drecoll and Bárány 1974). It is possible that these areas were in fact underperfused due to the creation of the fistula. Underperfusion may, due to the poor removal of toxic metabolic waste products, disturb

cell function which is perhaps manifest as an increasing deposition of extracellular elements in the trabeculae. In the aging eye localised underperfusion may be an important factor in leading to the accumulation of 'curly collagen' in the trabeculae.

Which, if any, of the above four factors may be the more important in the age-related changes in the uveal and corneoscleral meshwork, is unknown. It seems likely that only when there is obliteration of the intratrabecular spaces due to adhesion of several layers of trabeculae that the resistance to aqueous passage in these regions of the meshwork will be altered. What may be of more relevance to the increased resistance to outflow with age, is not the narrowing of spaces in the uveal and corneoscleral meshwork, but the material which is released during the breakdown of trabeculae and subsequently may accumulate in the cribriform layer. As this layer is suspected as being the locus of resistance to aqueous outflow (Bill and Svedbergh 1972, Tripathi 1977a, Grierson, Lee, Moseley and Abraham 1979) any material deposited in this region may further obliterate the available spaces for aqueous passage and cause an increase in resistance.

Rohen and Lütjen-Drecoll (1971) suggested that the overall thickness of the cribriform layer decreased with age and also that the number of cell layers decreased. The present study did not support the first of these observations, however, from qualitative impressions it appeared that the number of cell layers may have decreased

marginally. This was not confirmed by quantitative investigations, the discrepancy possibly being accounted for by the increase in tissue histiocytes in older specimens.

The finding of a quantitative increase in the electron-dense plaques in the cribriform layer with age confirms the impressions of previous workers (Rohen and Lütjen-Drecoll 1971, Fink, Felix and Fletcher 1972, Tripathi 1977a). There has been some confusion in the past regarding the description and nomenclature of these materials in the cribriform layer. In some cases both 'curly collagen' and elastic-like material have been described (Vegge 1967, Vegge and Ringvold 1971, Tripathi 1977a) while others have not made any distinction (Rohen and Lütjen-Drecoll 1971, Segawa 1975). The variable appearance of the electron-dense plaques may be due in part to the different forms of fixation, osmication, embedding media, section thickness and section staining employed by different workers.

Although some of the extracellular materials are probably synthesised locally in the cribriform layer, it seems likely from the present study, that the increasing accumulation with age of electron-dense plaques is partly the consequence of breakdown of trabeculae. 'Curly collagen', elastic-like material, basement membrane, collagen and ground substance could be washed from the trabeculae into the cribriform layer. Some of the finer material may be 'washed-out', leaving larger more complex elements such as 'curly collagen' and elastic-like fibres

trapped in this layer. It seems likely that any such material exposed to the action of aqueous, for many years, may change its morphological appearance such that it is unrecognisable from its original form. This may have led to confusion in the past since material recently deposited in this area may be identified as 'curly collagen' or the banded sheath of the elastic-like fibres.

Lütjen-Drecoll and Bárány (1974) in their study on non-operated areas of the meshwork in monkey eyes which had previously undergone trabeculectomy procedures found that there was a good correlation between the amounts of 'subendothelial deposits' (assessed by morphometrics) and the post-operative outflow facility. The underperfusion caused by the fistula had resulted in a build up of this material in the cribriform layer which was similar to advanced aging changes or some reports of changes in primary open angle glaucoma (vide infra).

The decrease in 'giant vacuole' incidence found in the present study correlates very well with the physiological evidence of decreased aqueous production and outflow with age (Becker 1958, Gaasterland, Kupfer et al 1978, Brubaker et al 1981). The question arises as to whether the change in the extracellular materials of the cribriform layer increases the resistance to aqueous outflow (reflected by fewer vacuoles) which is then counterbalanced by decreased aqueous production. Alternatively it is possible that aging changes in the ciliary processes lead to a decrease in aqueous production, which due to the effects of

localised underperfusion and less 'washout' lead to the accumulation of extracellular materials in the cribriform layer, which then causes increased resistance. This problem at the present time is unresolved.

Age-related changes in the uveal meshwork and scleral spur similar to those in the present study have been noted by other authors (Fine 1964, Nesterov 1977, Nesterov and Batmanov 1972, 1974a). The increasing frequency with age of regions of canal closure confirms the work of Teng, Katzin and Chi (1955, 1957); this was disputed by Ashton et al (1956) who believed that these were post-mortem changes. It is clear from the present work, however, that canal closure in older eyes is not a post-mortem artefact. Several factors may predispose the older outflow system to focal canal closure.

i) Clinical evidence suggests that intraocular pressure increases with age (Kornzweig et al 1957, Gaasterland, Kupfer et al 1978, Brubaker et al 1981). Although in experimental studies it takes a much higher than normal pressure to cause canal closure, it seems possible that older eyes may be more at risk since the changes in the cribriform layer may alter the ability of this tissue to distend in the normal fashion in response to raised pressure or flow. If there were regions which offered abnormally high resistance and were unyielding these could be forced outwards to come in contact with the outer wall of Schlemm's canal.

ii) In relation to the previous point there may be a

change with age in the elasticity of the trabecular meshwork. If the corneoscleral meshwork became more flaccid with age as suggested by Moses and Arnzen (1980), then it may become more easily bowed outwards thus increasing the likelihood of canal closure. Moses and Arnzen (1980) stated "Tension on the trabecular mesh is primarily due to the elastic choroid. The tension is increased during contraction of the meridional portion of the ciliary muscle. Therefore it is to be anticipated that the mesh will become less tense and the canal more easily collapsed if the choroid becomes less elastic and the ciliary muscle less active, as perhaps occurs with age or as the result of cycloplegic drugs".

It is not difficult to envisage that the structural changes which the trabeculae undergo with age could alter their elasticity. In other connective tissues such as skin there is a loss of elasticity with age, which is probably due to biochemical changes in the collagen (increased intermolecular cross linking) and elastin which affects their physical properties (Hall 1976). Reduced tension on the corneoscleral meshwork would alter its ability to recoil to the normal configuration after a period of high flow or pressure. As a consequence any inner-outer wall contact which may have occurred, perhaps during a period of elevated pressure, would not be separated and may become established. Any alteration in the pliability of the cells in the cribriform layer with age, would also affect the tissues susceptability to canal closure.

The suggestion by some authors that regions of inner and outer wall contact are characterised by endothelial proliferation was not confirmed by the present study (Teng et al 1955, 1957, Fine 1964, Fine, Yanoff and Stone 1980).

The mean features of age-related changes in the outflow apparatus and the factors which may be involved are summarised in Fig 129.

The pathogenesis of primary open angle glaucoma is still unknown, but one factor which has been strongly implicated is that this is a pathological extreme of the normal aging process (Kolker and Hethington 1976, Lee and Grierson 1981). The study of this disease has been severely hampered by the nature and availability of suitable specimens. The two main sources of tissue, post-mortem eyes and trabeculectomy specimens are of limited value for several reasons. The first is that post-mortem changes render tissue from this source inappropriate for ultrastructural studies, while trabeculectomy specimens suffer damage during surgery and fixation is at atmospheric pressure (which is not wholly suited to studies of the outflow apparatus). The second limitation is that the disease process is usually well advanced and any morphological changes may be attributable to either pressure or drug induced effects or both. The pathological changes which have been reported in this disease are summarised below, and it is evident that features i) to v) are not only present to some extent in advanced age but could be attributed to longterm drug schedules and

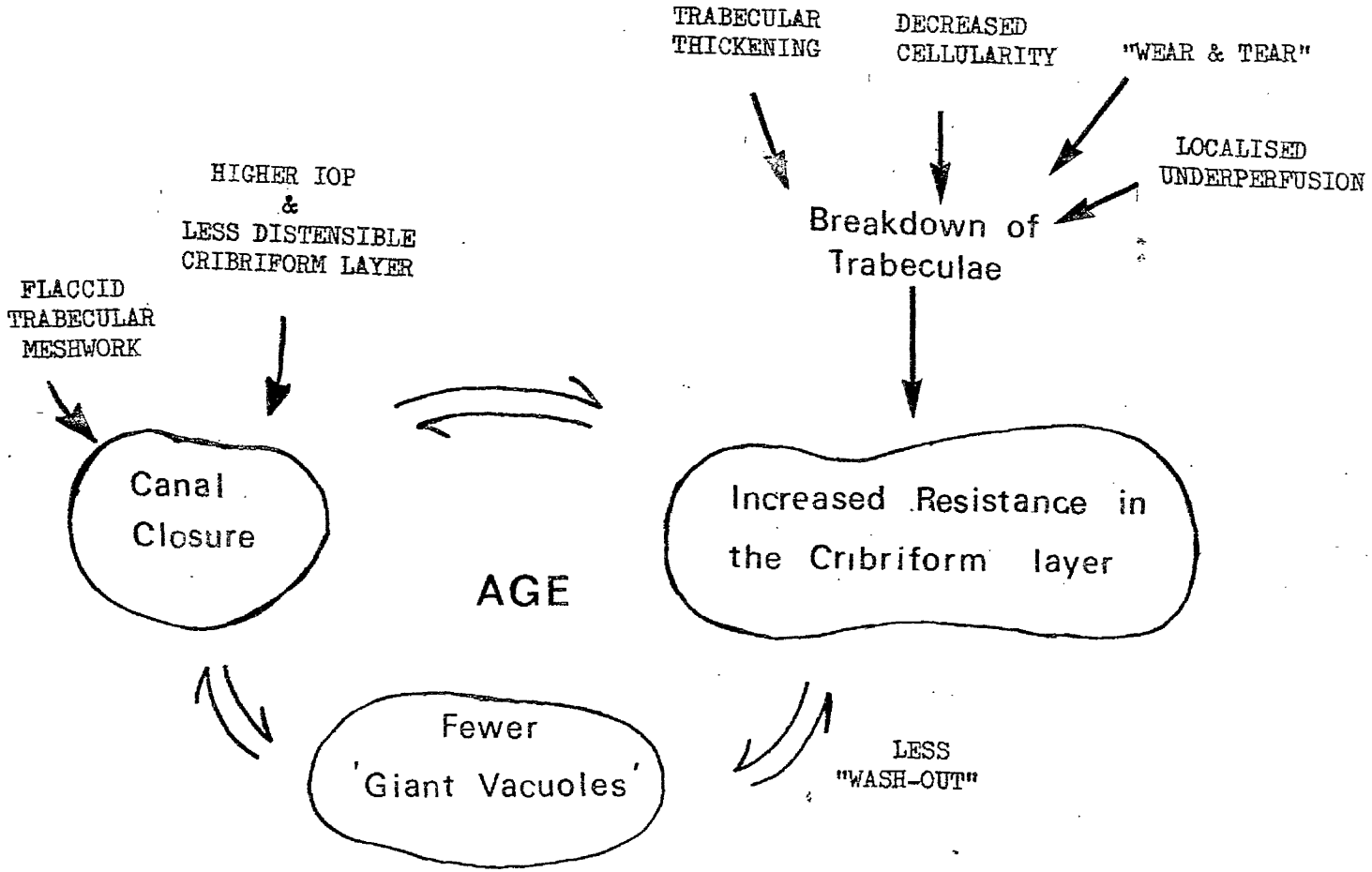

Figure 129: Diagram to summarise the important age related changes and factors which may contribute to these changes.

underperfusion.

i) Thickening of trabeculae and occlusion of intertrabecular spaces (Teng et al 1957, Kolker and Hetherington 1976, Tripathi 1977b).

ii) Accumulation of extracellular materials in the cribriform layer (Rohen and Witmer 1972, Lee and Grierson 1974, Segawa 1975, Rodrigues et al 1976, 1980, Tripathi 1977b). Segawa described "amorphous materials" which he suggested was a "chondroitin-sulphate protein complex and glycoprotein". Most other workers have described material which is similar to the electron-dense plaques of the present study. The recent study by Rodrigues et al 1980, while admitting that glycosaminoglycans may also be present, found by the use of immunofluorescence and immunoperoxidase that the plaques in the cribriform layer contained type IV collagen, laminin and fibronectin. This was true of normals but to a greater extent in glaucomatous specimens.

iii) Most studies of the outflow system in glaucomatous eyes have reported a scarcity of 'giant vacuoles' (Rohen and Witmer 1972, Tripathi 1972, 1977b, Lee and Grierson 1974), but this has been disputed (Fink, Felix and Fletcher 1972). Tripathi (1977b) put forward the suggestion that the primary defect in glaucoma may lie in the vacuolation process, and more recently Tripathi and Tripathi (1980) have briefly reported that there are fewer contractile proteins in cultured trabecular meshwork cells from glaucoma patients in comparison with their controls. Care

must be taken not to over-interpret this important finding, since it may be a secondary effect of previous drug schedules.

iv) Another school of thought proposes that closure of Schlemm's canal may be the cause of increased resistance to aqueous outflow, particularly in the region of collector channel ostia (Moses 1977, Moses et al 1981, Nesterov 1977, Nesterov and Batmanov 1972, 1974a). Nesterov (1977) postulated on the basis of histological evidence that certain factors predispose eyes to canal closure and subsequent open angle glaucoma, these include; a small scleral spur, a more posterior attachment of ciliary muscle, an anteriorly situated Schlemm's canal and a smaller angle between the canal and the anterior chamber.

v) Recently Fine and co-workers (1981) on the basis of a study of post-mortem tissue from four patients with bilateral open angle glaucoma postulated that the earliest changes in the disease may be compaction of the uveal meshwork against the scleral spur, hyalinisation of the ciliary muscle and atrophy of the iris root. These changes they suggest would interfere with uveo-scleral drainage and lead to further pathological changes in deeper layers of the meshwork.

vi) Becker and co-workers (1962, 1963) reported deposition of gammaglobulins, lymphocytes and plasma cells in the trabecular meshwork of open angle glaucoma patients, implying that primary open angle glaucoma was an autoimmune disease. However, this has not been substantiated by other

workers (Shields, McCoy and Shelburne 1976, Felberg, Leon and Gasparini 1977, Rodrigues et al 1980).

It is hoped that the present study of the aging changes in the human outflow apparatus will allow a more thorough evaluation of the morphological changes in primary open angle glaucoma in future studies of this disease. Detailed qualitative and quantitative studies of glaucomatous tissue are required, with similar morphometric techniques to those used in the present study being applied to assess the trabecular thickness and the extracellular components of the cribriform layer. It would then be theoretically possible to compare such results to those which would be predicted on the basis of the patient's age. A study of this nature should ideally be carried out on eyes which have received no previous drug therapy, since these may induce morphological changes which 'mimic' age changes. Future investigations of normal aging changes and glaucomatous changes should be directed towards the question of variation in the morphological appearance within one eye. Since the difference between the normal and diseased state may be quantitative in nature, detailed studies of large samples of the outflow apparatus from the whole 360^{o} circumference are required.

Potentially interesting features worthy of quantitative assessment may be

a) the components of the cribriform layer (including 'empty space')

b) the trabecular thickness

c) the area of intertrabecular spaces

d) the incidence of 'giant vacuoles'

e) the cellularity of the trabecular meshwork

f) the frequency of canal closure.

FINAL COMMENTS

The experimental studies of Part I of the present investigation illustrated the problems of trying to carry out combined physiological and morphological studies of the outflow apparatus. From the evidence of the present study it seems probable that GAGs do contribute to the resistance to aqueous outflow *in vivo* in the primate eye, but further studies are required. In future combined physiological and morphological studies it would be advisable to prevent excessive physiological manipulation and to limit the period to which the eye is exposed to mock aqueous solutions. In the present study it was felt that the morphological effects of over-perfusion may have 'masked' any morphological effect attributable to the action of hyaluronidase.

The present experimental study quantitatively reinforced previous impressions on the response of the outflow apparatus to increased flow. It was shown that with increased flow there was an increase in the amount of 'empty space' in the cribriform layer (measure of the degree of distension) which was associated with increased incidence of 'giant vacuoles' and transcellular channels in the lining endothelium of Schlemm's canal.

Extracellular materials, similar to those seen to increase with age in the present study, have been suggested as perhaps being the primary cause of increased resistance in primary open angle glaucoma (Rohen and Witmer 1972, Lee and Grierson 1974, Segawa 1975, Rodrigues et al 1976, Tripathi 1977b). The nature of this material is still

unknown, but recent evidence (Rodrigues et al 1980) suggests that as well as GAGs a variety of other materials such as type IV collagen, laminin and fibronectin may be present. If and when the exact make-up of the materials in the cribriform layer is known then it may still be feasible to use various enzymes capable of degrading such substances and study their effects on resistance. Such studies could be performed on fresh post-mortem eyes or eyes enucleated in the treatment of posterior pole malformations. Older specimens would be preferable in a study of this nature.

One of the main problems in studying primary open angle glaucoma is obtaining specimens at the early stages of the disease. Whether the use of dogs (mainly Beagles) with inherited open angle glaucoma may provide a potential model for the study of primary open angle glaucoma in humans is still unclear. The disease in dogs has been proposed by Bedford (1980) to be age-related, and Peiffer, Gum, Grimson and Gelatt (1980) have found significantly lower values for facility of aqueous outflow in glaucomatous beagles compared to normal dogs in an experimental study. However, species differences in the anatomy of the outflow system and aqueous dynamics must be fully appreciated in any comparison of the disease to that in the human. One possible line of future investigation would be combined physiological and morphological studies in glaucomatous dogs.

REFERENCES

Agarwal, L.P., Singh, V.N., Mishra, R.K. & Khosla, P.K. (1972).
Light and electron microscopy of the "presumed elastic" component of the trabeculae and scleral spur of the human eye. Orient. Arch. Ophthal., 10, 151-161.

Alvorado, J.A., Murphy, C.G. & Polansky, J.R. (1980).
Age related changes in trabecular meshwork cellularity. Invest. Ophthal. Arvo abstract (Suppl), 19, 273.

Anderson, P.J., Wang, J. & Epstein, D.L. (1980).
Metabolism of calf trabecular (reticular) meshwork. Invest. Ophthal., 19, 13-20.

Armaly, M.F. (1970).
Water drinking test, I. Arch. Ophthal., 83, 169-175.

Armaly, M.F. & Sayegh, R.F. (1970).
Water drinking test, II. The effect of age on tonometric and tonographic measures. Arch. Ophthal., 83, 176-181.

Armaly, M.F. & Wang, Y. (1975).
Demonstration of acid mucopolysaccharides in the trabecular meshwork of the rhesus monkey. Invest. Ophthal., 14, 507-516.

Ascher, K.W. (1942).
Aqueous veins. Am. J. Ophthal., 25, 31-38.

Ashton, N. (1951).
Anatomical study of Schlemm's canal and aqueous veins by means of neoprene casts. Part I. Aqueous veins. Brit. J. Ophthal., 35, 291-303.

Ashton, N. (1958).
Discussion on the trabecular structure in relation to the problem of glaucoma. Proc. R. Soc. Med., 52, 69-74.

Ashton, N. (1960).
The exit pathway of the aqueous. Trans. Ophthal. Soc. U.K., 80, 397-420.

Ashton, N., Brini, A. & Smith, R. (1956).
Anatomical studies of the trabecular meshwork of the normal human eye. Brit. J. Ophthal., 36, 257-282.

Balazs, E.A. (1965).
Amino sugar containing macromolecules in the tissues of the eye and the ear. In The Amino Sugars, ed. Balazs, E.A. and Jeanloz, R.W. Vol. IIA, pp. 401-460. New York and London : Academic Press.

Bárány, E.H. (1947).
The recovery of intraocular pressure, arterial blood pressure, and heat dissipation by the external ear after unilateral carotid ligation. Acta. Ophthal., 25, 81-94.

Bárány, E.H. (1953).
In vitro studies of the resistance to flow through the angle of the anterior chamber. Acta. Soc. Med. Ups., 59, 260-270.

Bárány, E.H. (1956)a.
Physiological and pharmacological factors influencing the resistance to aqueous outflow. In Glaucoma, Trans. 1st Josiah Macy Foundation, ed. Newell, F.W. pp. 123-221.

Bárány, E.H. (1956)b.
The action of different kinds of hyaluronidase on the resistance to flow through the angle of the anterior chamber. Acta. Ophthal., 34, 397-402.

Bárány, E.H. (1964).
Simultaneous measurement of changing intraocular pressure and outflow facility in the vervet monkey by constant pressure infusion. Invest. Ophthal., 3, 135-143.

Bárány, E.H. & Scotchbrook, S. (1954).
Influence of testicular hyaluronidase on the resistance to flow through the angle of the anterior chamber. Acta. Physiol. Scand., 30, 240-248.

Bárány, E.H. & Woodin, A.M. (1954).
Hyaluronic acid and hyaluronidase in the aqueous humor and the angle of the anterior chamber. Acta. Physiol. Scand., 33, 257-290.

Barrett, A.J. (1969).
Properties of lysosomal enzymes. In Lysosomes in Biology and Pathology, ed. Dingle, J.T. and Dean, R.T. Vol. 2. Ch. 10. pp. 292-312. Amsterdam and London : North Holland Publishing Co.

Bartels, S.P., Pederson, J.E., Gaasterland, D.E. & Armaly, M.F. (1979).
Sites of breakdown of the blood-aqueous barrier after paracentesis of the rhesus monkey eye. Invest. Ophthal., 18, 1050-1060.

Becker, B. (1958).
Decline in aqueous secretion and outflow facility with age. Am. J. Ophthal., 46, 731-736.

Becker, B. & Constant, M.A. (1956)a.
The facility of aqueous outflow : a comparison of tonography and perfusion measurements in vivo and in vitro. Arch. Ophthal., 55, 305-312.

Becker, B. & Constant, M.A. (1956)b.
Species variation in facility of aqueous outflow. Am. J. Ophthal., 42, 189-194.

Becker, B., Keates, E.U. & Coleman, S.L. (1962).
Gammaglobulin in the trabecular meshwork of glaucomatous eyes. Arch. Ophthal., 68, 643-647.

Becker, B., Unger, H.H., Coleman, S.L. & Keates, E.U. (1963).
Plasma cells and gammaglobulin in the trabecular meshwork of eyes with primary open angle glaucoma. Arch. Ophthal., 70, 38-44.

Bedford, P.G. (1980).
The aetiology of canine glaucoma. Vet. Rec., 107, 76-82.

Berggren, L. & Vrabec, F. (1957).
Demonstration of a coating substance in the trabecular meshwork of the eye. Am. J. Ophthal., 44, 200-208.

Bill, A. (1965).
The aqueous humor drainage mechanism in cynomologous monkey (Macaca irus) with evidence for unconventional routes (Invest. Ophthal., 4, 911-919.

Bill, A. (1970)a.
Scanning electron microscope studies of the canal of Schlemm. Exp. Eye. Res., 10, 214-218.

Bill, A. (1970)b.
The effect of changes in arterial blood pressure on the rate of formation of aqueous humour in a primate (Cercopithecus ethiops). Ophthal. Res., 1, 193-200.

Bill, A. (1971).
Aqueous humour dynamics in monkeys (Macaca irus and Cercopithecus ethiops). Exp. Eye Res., 11, 195-206.

Bill, A. (1974).
The role of iris vessels in aqueous humor dynamics. Jap. J. Ophthal., 18, 30-36.

Bill, A. (1975).
The drainage of aqueous humour. Invest. Ophthal., 14, 1-3.

Bill, A. (1977)a.
Basic physiology of the drainage of aqueous humour. Exp. Eye Res., 25, 291-304.

Bill, A. (1977)b.
A reply to R. Tripathi : Uveoscleral drainage of aqueous humour. Exp. Eye Res., 25, 309-310.

Bill, A. & Bárány, E.H. (1966).
Gross facility, facility of conventional routes and pseudofacility of aqueous humour outflow in the cynomolgous monkey. Archs. Ophthal., 75, 665-673.

Bill, A. & Hellsing, K. (1965).
Production and drainage of aqueous humor in the cynomolgous monkey (Macaca Irus). Invest. Ophthal., 4, 920-926.

Bill, A., Lütjen-Drecoll, E. & Svedbergh, B. (1980).
Effects of intracameral Na_2 EDTA and EDTA on aqueous outflow routes in the monkey eye. Invest. Ophthal., 19, 492-503.

Bill, A. & Phillips, C.I. (1971).
Uveoscleral drainage of aqueous humor in human eyes. Exp. Eye Res., 12, 275-281.

Bill, A. & Svedbergh, B. (1972).
Scanning electron microscopic studies of the trabecular meshwork and the canal of Schlemm - an attempt to localise the main resistance to outflow of aqueous humour in man. Acta Ophthal., 50, 295-320.

Bito, L.Z., Merrit, S.Q. & De Rousseau, C.J. (1979).
Intraocular pressure of rhesus monkeys (Macaca mulatta). An initial survey of two free-breeding colonies. Invest. Ophthal., 18, 785-793.

Boyde, A. (1978).
Pros and cons of critical point drying and freeze drying for SEM. SEM, II, 303-313.

Bradbury, S. (1979).
Microscopical image analysis problems and approaches. Journal of Microscopy, 115, 137-150.

Brubaker, R.F. (1967).
Determination of episcleral venous pressure in the eye. Arch. Ophthal., 77, 110-114.

Brubaker, R.F. Nagataki, S., Townsend, D.J., Burns, R.R., Higgens, R.G. & Wentworth, W. (1981).
The effect of age on aqueous humour formation in man. Ophthalmology, 88, 283-288.

Brubaker, R.F. & Worthen, D.M. (1973).
The filtration coefficient of the intraocular vasculature as measured by low-pressure perfusion in a primate eye. Invest. Ophthal., 12, 321-326.

Buddeche, E. & Kresse, H. (1974).
Mammalian enzymes degrading glycosaminoglycans. In Connective Tissues : Biochemistry and Pathophysiology, ed. Frick, R. and Hartmann, F. pp. 131-145. Berlin : Springer-Verlag.

Chalkley, H.W. (1943).
Method for the quantitative morphological analysis of tissues. J. Nat. Cancer Inst., 4, 47-53.

Cole, D.F. (1974).
Comparative aspects of the intraocular fluids. In The Eye ed. Davson, H., Vol. 5, p. 71. New York, San Fransisco, London : Academic Press.

Cole, D.F. (1977).
Secretion of aqueous humour. Exp. Eye Res., 25, 161-176.

Cole, D.F. & Munro, P.A.G. (1976).
The use of fluorescein-labelled dextrans in investigations of aqueous humour outflow in rabbit. Exp. Eye Res., 23, 571-585.

Cole, D.F. & Tripathi, R.C. (1971).
Theoretical consideration on the mechanism of aqueous outflow. Exp. Eye Res., 12, 25-32.

Comper, W.D. & Laurent, T.C. (1978).
Physiological function of connective tissue polysaccharides. Phsyiol. Review, 58, 255-315.

Curtis, A.S.G. (1960).
Area and volume measurements by random sampling methods. Med. Biol. Illust., 10, 261-266.

Duke, J.R. & Seigelman, S. (1961).
Acid mucopolysaccharides in the trabecular meshwork of the chamber angle. Arch. Ophthal., 66, 399, 404.

Eakins, K.E. (1977).
Prostaglandin and non-prostaglandin mediated breakdown of blood aqueous barrier. Exp. Eye Res., 25, 483-498.

Ellingsen, B.A. & Grant, W.M. (1971)a.
Trabeculotomy and sinusotomy in enucleated human eyes. Invest. Ophthal., 10, 430-437.

Ellingsen, B.A. & Grant W.M. (1971)b.
Influence of intraocular pressure and trabeculectomy on aqueous outflow in enucleated monkey eyes. Invest. Ophthal., 10, 705-709.

Eriksson, A. & Svedbergh, B. (1980).
Transcellular aqueous humour outflow : A theoretical and experimental study. Albrecht v. Graefes Arch. klin. exp. Ophthal., 212, 53-63.

Feeney, M.L. & Wissig, S. (1966).
Outflow studies using an electron dense tracer. Trans. Amer. Acad. Ophthal. Otolar., 70, 791-798.

Felberg, N.T., Leon, J.A., Gasparini, J. & Spaeth, G.L. (1977).
A comparison of antinuclear antibodies and DNA binding antibodies in chronic open angle glaucoma. Invest. Ophthal., 16, 757-760.

Fine, B.S. (1964).
Observations on the drainage angle in man and rhesus monkeys : a concept of the pathogenesis of chronic simple glaucoma. Invest. Ophthal., 3, 609-646.

Fine, B.S. (1966).
Structures of the trabecular meshwork and the canal of Schlemm. Trans. Amer. Acad. Ophth. Otolar., 70, 777-790.

Fine, B.S., Yanoff, M. & Stone, R.A. (1981).
A clinicopathologic study of four cases of primary open angle glaucoma compared to normal eyes. Am. J. Ophthal., 91, 88-105.

Fink, A.I., Felix, M.D. & Fletcher, R.C. (1972).
Schlemm's canal and adjacent structures in glaucomatous patients. Am. J. Ophthal., 74, 893-905.

Flocks, M. (1956).
The anatomy of the trabecular meshwork as seen in tangential sections. Arch. Ophthal., 56, 708-718.

Foulds, W.S., Moseley, H., Eadie, A. & McNaught, E. (1980).
Vitreal, retinal and pigment epithelial contributions to the posterior blood-ocular barrier. Trans. Ophthal. Soc. U.K., 100, 341-342.

François, J. (1978).
Corticosteroid glaucoma. Met. Ophthal., 2, 3-11.

François, J., Rabaey, M. & Neetens, A. (1956).
Perfusion studies on the outflow of aqueous humor in human eyes. Arch. Ophthal., 55, 193-204.

Gaasterland, D.E., Kupfer, C., Milton, R., Ross, K., McCain, L. & McLellan, H. (1978).
Studies of aqueous humour dynamics in man. IV. Effect of age upon parameters of IOP in normal eyes. Exp. Eye Res., 26, 651-656.

Gaasterland, D.E., Pederson, J.E. & McLellan, H.M. (1978).
Perfusate effects upon resistance to aqueous humour outflow in rhesus monkey eyes. Invest. Ophthal., 17, 391-397.

Gallin-Cohen, P.E., Podos, S.M. & Yablonski, M.E. (1980).
Oxygen lowers intraocular pressure. Invest. Ophthal., 19, 43-48.

Garron, L.K. (1959).
The fine structure of the normal trabecular apparatus in man. In Proceedings of the 4th Macy Conference on Glaucoma, ed. Newell, F.W. pp. 11-20, Princeton, N.J.

Garron, L.K. & Feeney, M.L. (1959).
Electron microscope studies of the human eye. II. Study of the trabeculae by light and electron microscopy. Arch. Ophthal., 62, 966-973.

Gasic, G. & Berwick, L. (1963).
Hale's stain for sialic acid containing mucins. Adaptation to electron microscopy. J. Cell. Biol., 19, 223-228.

Gipson, I.K. & Anderson, R.A. (1979).
Actin filaments in cells of human trabecular meshwork and Schlemm's canal. Invest. Ophthal., 18, 547-561.

Grant, W.M. (1958).
Further studies on facility of flow through trabecular meshwork. Arch. Ophthal, 60, 523-533.

Grant, W.M. (1963).
Experimental aqueous perfusion in enucleated human eyes. Arch. Ophthal., 69, 783-801.

Green, K. & Pederson, J.E. (1972).
Contribution of secretion and filtration to aqueous humour formation. Am. J. Physiol., 222, 1218-1226.

Grierson, I. (1976).
The morphology of the outflow apparatus of the eye with particular reference to its structural appearance at various levels of intraocular pressure. Ph.D. Thesis. University of Glasgow.

Grierson, I. & Johnson, N.F. (1981).
The post-mortem vacuoles of Schlemm's canal. Albrecht v. Graefes Arch. klin. exp. Ophth. supplement. Current research in Ophthalmic Electron Microscopy, 213, 41-56.

Grierson, I. & Lee, W.R. (1973).
Erythrocyte phagocytosis in the human trabecular meshwork. Brit. J. Ophthal., 57, 400-415.

Grierson, I. & Lee W.R. (1974)a.
Junctions between the cells of the trabecular meshwork. Albrecht v. Graefes Arch. klin. exp. Ophthal., 192, 89-104.

Grierson, I. & Lee, W.R. (1974)b.
Changes in the monkey outflow apparatus at graded levels of intraocular pressure : a qualitative analysis by light microscopy and scanning electron microscopy. Exp. Eye Res., 19, 21-33.

Grierson, I. & Lee, W.R. (1975)a.
The fine structure of the trabecular meshwork at graded levels of intraocular pressure.
(1) Pressure effects within the near physiological range (8-30 mm Hg).
(2) Pressure outside the physiological range (0 and 50 mm Hg).
Exp. Eye Res., (1) 20, 505-521.
(2) 20, 223-530.

Grierson, I. & Lee, W.R. (1975)b.
Pressure-induced changes in the ultrastructure of the endothelium lining Schlemm's canal. Am. J. Ophthal., 80, 863-884.

Grierson, I. & Lee, W.R. (1975)c.
Acid mucopolysaccharides in the outflow apparatus. Exp. Eye Res., 21, 417-431.

Grierson, I. & Lee, W.R. (1977)a.
Light microscopic quantitation of the endothelial vacuoles in Schlemm's canal. Am. J. Ophthal., 84, 234-246.

Grierson, I. & Lee, W.R. (1977)b.
Pressure effects on the distribution of extracellular materials in the rhesus monkey outflow apparatus. Albrecht v. Graefes Arch. klin. exp. Ophhal., 203, 155-168.

Grierson, I. & Lee, W.R. (1978).
Pressure effects on flow channels in the lining endothelium of Schlemm's canal. Acta Ophthal., 56, 935-952.

Grierson, I., Lee, W.R. & Abraham, S. (1977)a.
Pathways for the drainage of aqueous humour into Schlemm's canal. Trans. Ophthal. Soc. U.K., 97, 719-725.

Grierson, I., Lee, W.R. & Abraham, (1977)b.
The distribution and significance of hyaluronidase-sensitive materials in the trabecular wall of Schlemm's canal. Trans. Ophthal. Soc. U.K., 97, 739-745.

Grierson, I., Lee, W.R. & Abraham, S. (1977)c.
The appearance of the outflow apparatus of the eye after staining with ruthenium red. Acta. Ophthal., 55, 827-835.

Grierson, I., Lee, W.R. & Abraham, S. (1978).
The effects of Pilocarpine on the morphology of the human outflow apparatus. Brit. J. Ophthal., 62, 302-313.

Grierson, I., Lee, W.R. & Abraham, S. (1979)a.
A light microscopic study of the effects of testicular hyaluronidase on the outflow system of a baboon (Papio cynocephalus). Invest. Ophthal., 18, 356-360.

Grierson, I., Lee, W.R. & Abraham, S. (1979)b.
The effects of topical pilocarpine on the morphology of the outflow apparatus of the baboon (Papio cynocephalus). Invest. Ophthal., 18, 346-355.

Grierson, I., Lee, W.R. & Abraham, S. and Howes, R.L. (1978).
Associations between the cells of the walls of Schlemm's canal. Cur. Res. Ophthal. E.M., 2, 33-47.

Grierson, I., Lee, W.R., Moseley, H. & Abraham, S. (1979)c.
The trabcular wall of Schlemm's canal. A study of the effect of pilocarpine by scanning electron microscopy. Brit. J. Ophthal., 63, 9-16.

Grierson, I., Lee, W.R. & McMenamin, P.G. (1981).
The morphological basis of drug action on the outflow system of the eye. In Glaucoma, Recent Advances, Research and Clinical Forums, ed. Phillips, C. In press.

Grierson, I., & Rahi, A.H.S. (1979).
Microfilaments in the cells of the human trabecular meshwork. Brit. J. Ophthal., 63, 3-8.

Hall, D.A. (1976).
The aging of connective tissue. London : Academic Press.

Harnisch, J.P. (1976).
Electron microscopical delineation of acid mucopolysaccharides in the trabecular meshwork. Klin. Monatsbl. Augenheilk., 169, 90-94.

Hassell, J.R., Newsome, D.A. & Ballantine, J.R. (1980).
Synthesis of extracellular matrix components by trabecular meshwork in organ culture. Invest. Ophthal., 19, 273.

Hayasaka, S., Hara, S., Shiono, T. & Mizuno, K. (1980).
Presence of lysosomal hyaluronidase in human corneoscleral tissue. Albrecht v. Graefes Arch. klin. exp. Ophthal., 213, 235-238.

Hayasaka, S. & Sears, M.L. (1978).
Distribution of acid phosphatase β-glucuronidase and lysosomal hyaluronidase in the anterior segment of the rabbit eye. Invest. Ophthal., 17, 982-987.

Hayreh, S.S. (1966).
Posterior drainage of the intraocular fluid from the vitreous. Exp. Eye Res., 5, 123-144.

Hogan, J.J., Alvorado, J.A. & Weddell, J.E. (1971).
Histology of the Human Eye. Philadelphia, Toronto and London : W.B. Saunders.

Holmberg, A.S. (1959).
The fine structure of the inner wall of Schlemm's canal. Arch. Ophthal., 62, 956-958.

Holmberg, A.S. (1965).
Schlemm's canal and the trabecular meshwork. An electron microscopic study of the normal structure in man and monkey (Cercopithecus ethiops). Docum. Ophthal., 19, 339-373.

Inomata, H. & Bill, A. (1977).
Exit sites of uveoscleral flow of aqueous humour in cynomolgous monkey eyes. Exp. Eye Res., 25, 113-118.

Inomata, H., Bill, A. & Smelser, G.K. (1972)a.
Aqueous humour pathways through the trabecular meshwork and into Schlemm's canal in the cynomolgous monkey (Macaca irus). An electron microscopic study. Am. J. Ophthal., 73, 760-789.

Inomata, H., Bill, A. & Smelser, G.K. (1972)b.
Unconventional routes of aqueous humour outflow in cynomolgous monkeys (Macaca irus). Am. J. Ophthal., 73, 893-907.

Iwamoto, T. (1964).
Light and electron microscopy of the presumed elastic components of the trabeculae and scleral spur of the human eye. Invest. Ophthal., 3, 144-156.

Iwamoto, T. (1967).
Light and elecron microscopy of Sonderman's channels in the human trabecular meshwork. Albrecht v. Graefes Arch. klin. exp. Ophthal., 172, 197-212.

Jakus, M.A. (1961).
The fine structure of the human cornea. In The Structure of the Eye, ed. Smelser, G.K. pp. 343-366. New York : Academic Press.

Jensen, O.A., Prause, J.U. & Laursen, H. (1981).
Shrinkage in preparatory steps for scanning electron microscopy. Albrecht v. Graefes Arch. klin. exp. Ophthal., 213, 1-10.

Johnstone, M.A. (1979).
Pressure-dependent changes in nuclei and process origins of the endothelial cells lining Schlemm's canal. Invest. Ophthal, 18, 44-51.

Johnstone, M.A. & Grant. W.M. (1973).
Pressure-dependent changes in stuctures of the aqueous outflow system of human and monkey eyes. Am. J. Ophthal., 75, 365-383.

Johnstone, M.A., Tanner, D., Chau, B. & Kopecky, K. (1980).
Concentration-dependent morphologic effects of cytochalasin B in the aqueous outflow system. Invest. Ophthal., 19, 835-841.

Kaufman, P.L. & Bárány, E.H. (1977).
Cytochalasin B reversibly increases outflow facility in the eye of the cynomolgous monkey. Invest. Ophthal., 16, 47-53.

Kaufman, P.L., Bill, A. & Bárány, E.H. (1977).
Effect of cytochalasin B on conventional drainage of aqueous humour in cynomolgous monkeys. Exp. Eye Res., 25, 411-414.

Kayes, J. (1967).
Pore structure of the inner wall of Schlemm's canal. Invest. Ophthal., 6, 381-394.

Kayes, J. (1975).
Pressure gradient changes on the trabecular meshwork of monkeys. Am. J. Ophthal., 79, 549-556.

Kinsey, V.R. & Reddy, D.V.N. (1964).
Chemistry and dynamics of aqueous humor. In The Rabbit in Eye Research, ed. Prince, J.H. Ch.9, pp. 218-319. Illinois : Thomas.

Knepper, P.A., Breen, M., Weinstein, H.G. & Black, L.J. (1978).
Intraocular pressure and glycosaminoglycan distribution in the rabbit eye. Effect of age and dexamethasone. Exp. Eye Res., 27, 567-575.

Knepper, P.A., Farbman, A.I. & Bondareff, W. (1975).
A smooth muscle plexus associated with the aqueous outflow pathway of the rabbit eye. Anat. Rec., 182, 41-52.

Knepper, P.A., Farbman, A.J. & Telser, A.G. (1981).
Aqueous outflow pathway of glycosaminoglycans. Exp. Eye Res., 32, 265-277.

Kolker, A.E. & Hetherington, J. (1976).
Becker-Shaffer's Diagnosis and Therapy of the Glaucomas, 4th edition. St. Louis : C.V. Mosby.

Kornzweig, A.L., Feldstein, M. & Schneider, J. (1957).
The eye in old age. IV. Ocular survey of over one thousand aged persons with special reference to normal and disturbed functions. Am. J. Ophthal., 44, 29-38.

Krupin, T., Feitl, M., Roshe, R., Lee, S. & Becker, B. (1980).
Halothane anaesthesia and aqueous humour dynamics in laboratory animals. Invest. Ophthal., 19, 518-521.

Kupfer, C. & Ross, K. (1971).
Studies of aqueous humour dynamics in man. I. Measurements in young normal subjects. Invest. Ophthal., 10, 518-522.

Lamble, J.W. (1974).
Some respnonses of the rabbit eye to topically administered adrenaline bitartrate. Exp. Eye Res., 19, 419-434.

Laurent, U.B.G. (1981).
Hyaluronate in aqueous humour. Exp. Eye Res., 33, 147-155.

Lee, W.R. (1971).
The study of the passage of particles through the endothelium of the outflow apparatus of the monkey eye by scanning and transmission electron microscopy. Trans. Ophthal. Soc. U.K., 91, 687-705.

Lee, W.R. & Grierson, I. (1974).
Relationships between intraocular pressure and the morphology of the outflow apparatus. Trans. Ophthal. Soc. U.K., 94, 430-449.

Lee, W.R. & Grierson, I. (1981).
Anterior segment changes in glaucoma. In Pathobiology of Ocular Disease, ed. Klintworth, G. and Garner, A. Ch.17. New York : Marcel Dekker. In press.

Leeson, T.S. & Speakman, J.S. (1961).
The fine structure of extracellular material in the pectinate ligament. Acta. Anat., 46, 363-379.

Leydhecker, W., Akiyama, K. & Neumann, H.G. (1958).
Der intraoculare Druck ges under menschlicher Augen. Klin. Monatsbl. Augenheilk., 133, 662-670.

Lütjen-Drecoll, E. (1973).
Structural factors influencing outflow facility and its changeability under drugs. Invest. Ophthal., 12, 280-294.

Lütjen-Drecoll, E. & Bárány, E.H. (1974).
Functional and electron microscopic changes in the trabecular meshwork remaining after trabeculectomy in cynomolgous monkeys. Invest. Ophthal., 13, 511-524.

Lütjen-Drecoll, E. & Kaufman, P.L. (1979).
Echothiophate-induced structural alterations in the anterior chamber angle of the cynomolgous monkey. Invest. Ophthal., 18, 918- 929.

Macri, F.J. (1961).
Interdependence of venous and eye pressure. Arch. Ophthal., 65, 442-449.

Masuda, K. (1974).
Pressure dependance of the aqueous humour formation in rabbit and cynomolgous monkey eyes. Jap. J. Ophthal., 16, 190-209.

Melton, C.E. & de Ville, W.B. (1960).
Perfusion studies on the eyes of four species. Am. J. Ophthal., 50, 302-308.

Meyer, K. (1947).
The biological significance of hyaluronic acid and hyaluronidase. Physiol. Rev., 3, 335-359.

Meyer, K. & Palmer, J.W. (1934).
The polysaccharide content of the vitreous. J. Biol. Chem., 197, 629-534.

Mizokami, K. (1977).
Demonstration of masked acidic glycosaminoglycans in the normal trabecular meshwork. Jap. J. Ophthal., 21, 57-71.

Morton, D.B. (1976).
Lysosomal enzymes in mammalian spermatozoa. In Lysosomes in Biology and Pathology, ed. Dingle, J.T. and Dean, R.T. Vol. 5, 205-255. Amsterdam and London : North Holland Publishing Co.

Moses, R.A. (1977).
The effect of intraocular pressure on resistance to outflow. Surv. Ophthal., 22, 88-100.

Moses, R.A. (1979).
Circumferential flow in Schlemm's canal. Am. J. Ophthal., 88, 585-591.

Moses, R.A. & Arnzen, R.J. (1980).
The trabecular meshwork - a mathematical analysis. Invest. Ophthal., 19, 1490-97.

Moses, R.A., Grodzki, W.J., Etheridge, E.H. & Wilson, C.D. (1981).
Schlemm's canal : The effect of intraocular pressure. Invest. Ophthal., 20, 61-68.

Nagasubramanian, S. (1977).
Role of pituitary vasopressin in the formation and dynamics of aqueous humour. Trans. Ophthal. Soc, U.K., 97, 686-701.

Napier, J.R. & Napier, P.H. (1967).
A Handbook of Living Primates. London, New York : Academic press.

Nesterov, A.P. & Batmanov, Y.E. (1972).
Study of morphology and function of the drainage area of the eye. Acta. Ophthal., 50, 337-350.

Nesterov, A.P. & Batmanov, Y.E. (1974)a.
Schlemm's canal and scleral spur in normal and glaucomatous eyes. Am. J. Ophthal., 78, 634-638.

Nesterov, A.P. & Batmanov, Y.E. (1974)b.
Trabecular wall of Schlemm's canal in the early stage of primary open angle glaucoma. Am. J. Ophthal., 78, 639-647.

Nesterov, A.P. (1977).
Role of Schlemm's canal in aqueous resistance in normal and glaucomatous eyes. In International Glaucoma Symposium. Recent Advances in Glaucoma, ed. Rehak, S., Krasnor, M.M. and Paterson, G. pp. 31-37. Berlin : Springer.

Ogston, A.G. (1970).
The biological function of the glycosaminoglycans. In Chemistry and Molecular Biology of the Intercellular Matrix, ed. Balazs, E.A. pp. 1231-1240. London : Academic press.

Pederson, J.E. & Green, K. (1975).
Solute permeability of the normal and prostaglandin stimulated ciliary epithelium and the effect of ultrafiltration on active transport. Exp. Eye Res., 21, 569-580.

Pedlar, C. (1956).
The relationship of hyaluronidase to aqueous outflow resistance. Trans. Ophthal. Soc. U.K., 76, 51-63.

Peiffer, R.L., Gum, G.G., Grimson, R.C. & Gelatt, K.N. (1980).
Aqueous humour outflow in beagles with inherited glaucoma, constant pressure perfusion. Am. J. Vet. Res., 11, 1808-1813.

Perkins, E.S. (1955).
Pressure in the canal of Schlemm. Brit. J. Ophthal., 39, 215-219.

Peterson, W.S. & Jocson, V.L. (1974).
Hyaluronidase effects on aqueous outflow resistance. Am. J. Ophthal., 77, 573-577.

Polanksy, J., Gospodarowicz, D., Weinreb, R. & Alvarado, J. (1978).
Human trabecular meshwork cell culture and glycosaminoglycan synthesis. Invest. Ophthal., 17, 207.

Raviola, G. (1977).
The structural basis of the blood ocular barriers. Exp. Eye Res., 25, 27-63.

Reddy, V.N. (1979).
Dynamics of transport system in the eye. Invest. Ophthal., 18, 1000-1018.

Ringvold, A. (1978).
Actin filaments in trabecular endothelial cells in eyes of the vervet monkey. Acta. Ophthal., 56, 217-225.

Ringvold, A. & Vegge, T. (1971).
Electron microscopy of the trabecular meshwork in eyes with exfoliation syndrome. Virchows Arch. Abt. A. Path. Anat., 353, 110-127.

Rodrigues, M.M., Katz, S.I., Foidart, J.M. & Spaeth, G.L. (1980).
Collagen, factor VIII antigen and immunoglobulins in the aqueous drainage channels. Ophthalmology, 87, 337-343.

Rodrigues, M.M., Spaeth, G.L., Silalingam, E. & Weinreb, S. (1976).
Histology of one hundred and fifty trabeculectomy specimens in glaucoma. Trans. Ophthal. Soc. U.K., 96, 245-255.

Rohen, J.W. (1969).
New studies of the functional morphology of the trabecular meshwork and the outflow channels. Trans. Ophthal. Soc. U.K., 89, 431-447.

Rohen, J.W., Linner, E. & Witmer, R. (1973).
Electron microscopic studies of the trabecular meshwork in two cases of corticosteroid glaucoma. Exp. Eye Res., 17, 19-31.

Rohen, J.W. & Lütjen-Drecoll, E. (1971).
Age changes of the trabecular meshwork in human and monkey eyes. In Altern und Entwicklung, ed. Schattaner, F.K., pp. 1-36. Stuttgart, New York : Verlag.

Rohen, J.W., Lütjen-Drecoll, E. & Bárány, E.H. (1967).
The relationship between the ciliary muscle and the trabecular meshwork and its importance for the effects of miotics on outflow resistance. Albrecht v. Graefes Arch. klin. exp. Ophthal., 172, 23-47.

Rohen, J.W. & van der Zypen, E. (1968).
The phagocytic activity of the trabecular meshwork endothelium. Albrecht v. Graefes Arch. klin. exp. Ophthal., 175, 251-266.

Sakimoto, G. (1979).
Smooth muscle cells associated with the aqueous drainage channel of the rabbit. Jap. J. Ophthal., 23, 162-173.

Salzmann, M. (1912).
The Anatomy and Histology of the Human eyeball.

Schachtschabel, D.O., Bigalke, B. & Rohen, J.W. (1977).
Production of glycosaminoglycans by cell cultures of the trabecular meshwork of the primate eye. Exp. Eye Res., 24, 71-80.

Sears, M.L. (1960).
Outflow resistance of the rabbit eye : techniques and effects of acetazolomide. Arch. Ophthal., 64, 823-838.

Sears, M.L. (1966).
The mechanism of action of adrenergic drugs in glaucoma. Invest. Ophthal., 5, 115-119.

Segawa, K. (1970).
Localisation of acid mucopolysaccharides in the human trabecular meshwork. Jap. J. Clin. Ophthal., 24, 363-367.

Segawa, K. (1971).
Concerning the giant vacuoles of the trabecular wall of Schlemm's canal. Jap. J. Ophthal., 15, 204-214.

Segawa, K. (1973).
Pore structures of the endothelial cells of the aqueous outflow pathway. Scanning electron microscopy. Jap. J. Ophthal., 17, 133-139.

Segawa, K. (1975).
Ultrastructural changes of the trabecular tissue in primary open angle glaucoma. Jap. J. Ophthal., 19, 317-338.

Segawa, K. (1979).
Electron microscopic changes of the trabecular tissue in primary open angle glaucoma. Ann. Ophthalmol., 11, 49-54.

Serafini-Fracassini, A. & Smith, J.W. (1974).
The Structure and Biochemistry of Cartilage. Edinburgh and London : Churchill Livingston.

Shabo, A.L., Reese, T.S. & Gaasterland, D. (1973).
Post-mortem formation of giant vacuoles in Schlemm's canal of the monkey. Am. J. Ophthal., 76, No.6, 896-905.

Sherman, S.H., Green, K. & Laties, A.M. (1978).
The fate of anterior chamber fluorescein in the monkey eye. 1. The anterior chamber outflow pathways. Exp. Eye Res., 27, 159-173.

Shields, N., McCoy, R.C. & Shelburne, J.D (1976).
Immunofluorescent studies on the trabecular meshwork of eyes with open angle glaucoma. Invest. Ophthal., 15, 1014-1017.

Snydacker, D. (1956).
The relation of the volume of the crystalline lens to the depth of the anterior chamber. Trans. Am. Ophthal. Soc., 54, 675-685.

Sonderman, R. (1933).
Ulber entstenung morphologie und funcktion des Schlemmschen kanals. Arch. Ophthal., 11, 280-301.

Spaeth, G.L., Rodrigues, M.M. & Weinreb, S. (1977).
Steroid induced glaucomas. Trans. Am. Ophthal. Soc., 75, 353-381.

Speakman, J.S. (1960).
Drainage channels in the trabecular wall of Schlemm's canal. Brit. J. Ophthal., 44, 513-523.

Spelsberg, W.W. & Chapman, C.B. (1962).
Fine structure of human trabeculae. Arch. Ophthal., 67, 773-784.

Stanworth, A. (1966).
The ocular effects of local corticosteroids and hyaluronidase. In Drug Mechanisms in Glaucoma, ed. Paterson, G., Miller, S.J.H. and Paterson, G. pp. 231-248. London : J.A. Churchill Ltd.

Strang, R., Wilson, T.M. & MacKenzie, E.T. (1977).
Choroidal and cerebral blood flow in baboons measured by the external monitoring of radioactive inert gases. Invest. Ophthal., 16, 571-576.

Svedbergh, B. (1974).
Effects of artificial intraocular pressure elevation on the outflow facility and the ultrastructure of the chamber angle in the vervet monkey (Cercopithecus ethiops). Acta. Ophthal., 52, 829-846.

Svedbergh, B. (1976).
Aspects of the aqueous humour drainage. Acta. Univ. Upssal., 256, 1-71.

Svedbergh, B., Lütjen-Drecoll, E., Ober, M. & Kaufman, P.L. (1978).
Cytochalasin B induced structural changes in the anterior ocular segment of the cynomolgous monkey. Invest. Ophthal., 17, 718-734.

Tappel, A.L. (1976).
Lysosomal enzymes and other components. In Lysosomes in Biology and Pathology, ed. Dingle, J.T. and Dean, R.T., Vol.2, Ch.9, pp. 286-291.

Teng, C.C., Katzin, H.M. & Chi, H.H. (1955).
Primary degeneration in the vicinity of the chamber angle. As an aetiological factor in wide angle glaucoma. Am. J. Ophthal., 40, 619-631.

Teng, C.C., Katzin, H.M. & Chi, H.H. (1957).
Primary degeneration of the chamber angle. As an aetiological factor in wide angle glaucoma. Part II. Am. J. Ophthal., 43, 193-203.

Ticho, U., Lahav, M. Berkowicz, S. & Yoffe, P. (1979).
Ocular changes in rabbits with corticosteroid induced ocular hypertension. Brit. J. Ophthal., 63, 646-650.

Tokoro, T. (1972).
Relationship between the blood velocity in the ciliary body and intraocular pressure of rabbit eyes. Invest. Ophthal., 11, 945-954.

Tripathi, R.C. (1968).
Ultrastructure of Schlemm's canal in relation to aqueous outflow. Exp. Eye Res., 7, 335-341.

Tripathi, R.C. (1969).
Ultrastructure of the trabecular wall of Schlemm's canal. Trans. Ophthal. Soc. U.K., 89, 449-465.

Tripathi, R.C. (1971).
Mechanism of the aqueous outflow across the trabecular wall of Schlemm's canal. Exp. Eye Res., 11, 116-121.

Tripathi, R.C. (1972).
Aqueous outflow pathway in normal and glaucomatous eyes. Brit. J. Ophthal., 56, 157-174.

Tripathi, R.C. (1974).
Comparative physiology and anatomy of the aqueous outflow pathway. In The Eye, ed. Davson, H., Vol.5, Ch.3. New York, London : Academic Press.

Tripathi, R.C. (1977)a.
The functional morphology of the outflow systems of ocular and cerebrospinal fluids. Exp. Eye Res., 25, 65-116.

Tripathi, R.C. (1977)b.
Pathological anatomy in the outflow pathway of aqueous humour in chronic simple glaucoma. Exp. Eye Res., 25, 403-407.

Tripathi, R.C. & Tripathi, B.J. (1980).
Contractile protein alterations in trabecular endothelium in primary open angle glaucoma. Exp. Eye Res., 31, 721-725.

Tsukahara, S. (1978).
The existence of smooth muscle adjacent to the Schlemm's canal of the normal albino rat eye. Acta. Ophthal., 56, 735-741.

Van Buskirk, E.M. & Brett, J. (1978).
The canine eye : In vitro dissolution of the barriers to aqueous flow. Invest. Ophthal., 17, 258-263.

Van Buskirk, E.M. & Grant, W.M. (1974).
Influence of temperature and the question of involvement of cellular metabolism in aqueous outflow. Am. J. Ophthal., 77, 565-572.

Vegge, T. (1963).
Ultrastructure of normal human trabecular endothelium. Acta. Ophthal., 41, 193-199.

Vegge, T. (1967).
The fine structure of the trabeculum cribriforme and the inner wall of Schlemm's canal in the normal human eye. Z. Zellforsch., 77, 267-281.

Vegge, T. & Ringvold, A. (1971).
The ultrastructure of the extracellular components of the trabecular meshwork in the human eye. Z. Zellforsch., 115, 361-376.

Vrabec, F. (1957).
The amorphous substance in the trabecular meshwork. Brit. J. Ophthal., 41, 20-24.

Watson, P.G., & Grierson, I. (1981).
The place of trabeculectomy in the treatment of glaucoma. Ophthalmology, 88, 175-196.

Weale, R.A. (1963).
The Aging Eye. London : H.K. Lewis.

Weekers, R., Watillon, M. & de Rudder, M. (1956).
Experimental and clinical investigation into the resistance of outflow of aqueous humour in normal subjects. Brit. J. Ophthal., 40, 225-233.

Weibel, E.R. (1969).
Stereological principles for morphometry in electron microscopic cytology. Int. Rev. Cytol., 20, 235-302.

Wells, O.C. (1974).
Scanning Electron Microscopy. New York : McGraw Hill Book Co.

Wolff, E. (1954).
The Anatomy of the Eye. 4th Edition. London : H.K. Lewis.

Zimmerman, L.E. (1957).
Demonstration of hyaluronidase sensitive acid mucopolysaccharides in trabecula and iris in routine paraffin sections of adult human eyes. Am. J. Ophthal., 44, 1-4.